



TALLINN UNIVERSITY OF TECHNOLOGY
SCHOOL OF ENGINEERING
Department of Mechanical and Industrial Engineering

**TWO DEGREES OF FREEDOM MOBILE LANDING
PLATFORM TO A SHIP PVL101 "KINDRAL
KURVITS"**

**KAHE VABADUSASTMEGA MOBIILNE
MAANDUMISPLATVORM LAEVALE PVL101 "KINDRAL
KURVITS"**

MASTER THESIS

Student: .Jaanus Urb. /name/

Student code: 183767MATM

Supervisor: PhD Andres Petritšenko
/name, position/

Tallinn 2021..

(On the reverse side of title page)

AUTHOR'S DECLARATION

Hereby I declare, that I have written this thesis independently.
No academic degree has been applied for based on this material. All works, major viewpoints and data of the other authors used in this thesis have been referenced.

"4" January 2021

Author: Jaanus Urb

/digitally signed /

Thesis is in accordance with terms and requirements

"4" January 2021

Supervisor: PhD Andres Petrišenko.

/signature/

Accepted for defence

".....".....20... .

Chairman of theses defence commission:

/name and signature/

Non-exclusive Licence for Publication and Reproduction of Graduation Thesis¹

I, _____ (name of the author) (date of birth:)
hereby

1. grant Tallinn University of Technology (TalTech) a non-exclusive license for my thesis

(title of the graduation thesis)

supervised by

(Supervisor's name)

1.1 reproduced for the purposes of preservation and electronic publication, incl. to be entered in the digital collection of TalTech library until expiry of the term of copyright;

1.2 published via the web of TalTech, incl. to be entered in the digital collection of TalTech library until expiry of the term of copyright.

1.3 I am aware that the author also retains the rights specified in clause 1 of this license.

2. I confirm that granting the non-exclusive license does not infringe third persons' intellectual property rights, the rights arising from the Personal Data Protection Act or rights arising from other legislation.

¹ Non-exclusive Licence for Publication and Reproduction of Graduation Thesis is not valid during the validity period of restriction on access, except the university's right to reproduce the thesis only for preservation purposes.

_____ *(signature)*

_____ *(date)*

THESIS TASK

Student: Jaanus Urb, 183767MATM .(name, student code)
Study programme, MATM02/18, Product Development (code and title) main speciality:

Supervisor(s):

1. Tallinna Tehnikaülikool, Inseneriteaduskond, Mehaanika ja tööstustehnika instituut , insener Andres Petritšenko, 5076055 (position, name, phone)
2. Tallinna Tehnikaülikool, Inseneriteaduskond: Ehituse ja arhitektuuri instituut: Konstruktsiooni- ja vedelikumehaanika uurimisrühm; vanemteadur ja programmijuht Kristjan Tabri, 5092585 (position, name, phone)

Consultants:

1. Jaanus Kaugerand, doktorant-nooremteadur (name, position) Tallinna Tehnikaülikool, IT teaduskond, Tarkvarateaduse instituut, 6202109, jaanus.kaugerand@taltech.ee (company, phone, e-mail)

Thesis topic:

(in English) **Two** degrees of Freedom mobile landing platform to a ship PVL101 "Kindral Kurvits"

(in Estonian) Kahe vabadusastmega mobiilne maandumisplatvorm laevale PVL101 "Kindral Kurvits"

Thesis main objectives:

| |
|---|
| 1. Study of the ship PVL101 "Kindral Kurvits" roll, pitch and heave motions and solve the differential equations. |
| 2. Study parallel mechanism and select optimum kinematic solution. |
| 3. Per-project of the two degrees of freedom platvorm. |

Thesis tasks and time schedule:

| No | Task description | Deadline |
|-----------|--|-----------------|
| 1. | Ships differential equations solving. | 1.10.2020 |
| 2. | Selecting and solving the kinematics of the mechanism. | 5.11.2020 |
| 3. | Per-project calculations and drawings. | 31.12.2020 |

Language: English Deadline for submission of thesis: "4" January 2021.a

Student: Jaanus Urb. "4" January 2021.a

/signature/

Supervisor: Phd Andres Petritšenko "....."201....a

/signature/

Consultant: "....."201....a

/signature/

Head of study programme: Martin Eerme

"....."201.a

/signature/

Terms of thesis closed defence and/or restricted access conditions to be formulated on the reverse side

Contents

| | |
|---|-----------|
| Abstract | 5 |
| 1. INTRODUCTION | 9 |
| 1.1. Overview | 9 |
| 1.2. The landing and take-off deck | 10 |
| 1.3. The mechanical design | 10 |
| 1.4. The thesis structure | 11 |
| 2. Ship motions | 13 |
| 2.1. Overview | 13 |
| 2.1.1. PVL-101 main dimensions | 13 |
| 2.2. Heaving | 14 |
| 2.2.1. Inertial force | 15 |
| 2.2.2. Damping force | 16 |
| 2.2.3. Restoring force | 17 |
| 2.2.4. Free, damped Heaving Motion ($F_0 = 0$) | 18 |
| 2.2.5. Exciting force | 19 |
| 2.2.6. Forced heaving Motion | 21 |
| 2.2.7. Forced damped PVL-101 heaving differential equation and its solution | 22 |
| 2.2.8. State-space ODE model | 22 |
| 2.3. Accelerated rotational motion | 25 |
| 2.4. Pitching | 26 |
| 2.4.1. Inertial moment | 27 |
| 2.4.2. Damping moment | 29 |
| 2.4.3. Restoring moment coefficient | 29 |
| 2.4.4. Free, damped Pitching Motion ($M_0 = 0$) | 29 |
| 2.4.5. Exciting moment | 30 |
| 2.4.6. Forced damped PVL-101 pitching differential equation and its solution | 30 |
| 2.5. Rolling | 31 |
| 2.5.1. Inertial moment | 32 |
| 2.5.2. Damping moment | 33 |
| 2.5.3. Restoring moment coefficient | 35 |
| 2.5.4. Free, damped Rolling Motion ($M_0 = 0$) | 38 |

| | |
|--|------------|
| 2.5.5. Exciting moment and linear forced rolling motion with damp- ing | 39 |
| 3. Two Degrees of Freedom Spherical parallel mechanism | 43 |
| 3.1. Overview and problem statement | 43 |
| 3.1.1. Two degrees of freedom mechanisms design and comparison . . | 43 |
| 3.2. Description of the Spherical Parallel Manipulator | 46 |
| 3.2.1. Kinematics | 47 |
| 3.2.2. Analysis of Velocity and Acceleration | 48 |
| 4. Per-project of the 2 DOF SPM design and construction calculations | 51 |
| 4.1. Overview | 51 |
| 4.2. The mechanical concept, constraints and design steps | 51 |
| 4.2.1. Mechanical Design steps | 52 |
| 4.3. Preliminary model | 53 |
| 4.4. Preliminary model for motion simulation | 58 |
| 4.5. Analysis of the preliminary model | 58 |
| 4.6. Drive and gearbox | 59 |
| 4.7. Conclusion | 60 |
| Acknowledgments | 65 |
| A. : Appendix 1: Heaving Calculations | 67 |
| A.1. Heaving - Calculation of added Mass a_z | 70 |
| A.2. Heaving - Calculation of damping coefficient | 71 |
| A.3. Heaving - Calculation of restoring coefficient | 71 |
| A.4. Heaving - Calculation of Free damped Heaving equation solution . . . | 73 |
| A.5. Heaving - Calculation of exciting coefficient | 76 |
| A.6. Heaving - PVL-101 differential equation calculation and its solution" . | 76 |
| B. : Appendix 2: Pitching Calculation of coefficients | 89 |
| B.1. Pitching - Calculation of the virtual mass moment of inertia a_θ | 89 |
| B.2. Pitching - Calculation of damping coefficient | 92 |
| B.3. Pitching - Calculation of restoring coefficient | 93 |
| B.4. Pitching - Calculation of Free damped Pitching equation solution . . | 93 |
| B.5. Pitching - Calculation of Exciting moment | 97 |
| B.6. 5.Pitching - PVL-101 differential equation calculation and its solution" | 97 |
| C. : Appendix 3: Rolling Calculation of coefficients | 105 |
| C.1. Rolling - Calculation of the virtual mass moment of inertia a_ϕ | 105 |
| C.2. Rolling - Calculation of damping coefficient b_ϕ | 106 |
| C.3. Rolling - Calculation of restoring coefficient c_ϕ | 106 |
| C.4. Rolling - Calculation of Free damped rolling equation solution | 108 |
| C.5. Rolling - Calculation of Exciting moment | 111 |
| C.6. Rolling - PVL-101 differential equation calculation and its solution" . | 113 |

D. : Appendix 4: 2 DOF mechanisms comparison and SPM calculations 123

D.1. Two Degrees of Freedom parallel mechanisms comparison 123

D.2. SPM calculations 123

D.3. SPM kinematic schematic 133

E. : Appendix 5: 2 DOF SPM Assembly calculations 139

E.1. Top Plate 3 FEM 139

E.2. Link 1 Assembly FEM 151

E.3. Link 2 Assembly FEM 157

E.4. Link 4 Assembly FEM 163

E.5. Link 5 Assembly FEM 169

F. Appendix 6: Preliminary- project drawings 175

| | |
|--|------------|
| F.1. SPERICAL PARALLEL MANIPULATOR ASSEMBLY DWG NR-SPM0000 | 176 |
| F.2. LINK 1 ASSEMBLY & LINK 5 ASSEMBLY DWG NR-SPM1000 | 177 |
| F.3. BEND LINK DWG NR-SPM1100 | 178 |
| F.4. MIDDLE BUSHING DWG SPM1200 | 179 |
| F.5. LINK 2 ASSEMBLY & LINK 4 ASSEMBLY DWG NR-SPM2000 | 180 |
| F.6. SHAFT DWG NR SPM2100 | 181 |
| F.7. 2 LINK 2 BEND & 4 LINK 4 BEND DWG NR-SPM2200 | 182 |
| F.8. 6 Base Plate Assembly DWG SPM6000 | 183 |
| F.9. 6 Base Plate DWG SPM6100 | 184 |
| F.10. CENTRE POST DWG SPM6200 | 185 |
| F.11. Fixed yoke - N/A | 186 |
| F.12. Motor Stand Leg 1 DWG SPM 6400 | 187 |
| F.13. MOTOR STAND LEG 2 DWG SPM6500 | 188 |
| F.14. MOTOR STAND PLATE 2 DWG SPM6600 | 189 |
| F.15. Motor to Link 1 and 5 connection -N/A | 190 |
| F.16.F.16 MOTOR STAND PLATE 1 DWG SPM6800 | 191 |
| F.17.3 TOP PLATE ASSEMBLY 3 DWG SPM3000 | 192 |
| F.18.F.18 3 TOP PLATE 3 DWG SPM3100 | 193 |
| Bibliography | 194 |
| Bibliography | 195 |

PREFACE

Landing and take-off deck for the helicopter UAV for the PVL101 Kindral Kurvits. A new flexible landing platform of about 4 by 4 meter will be designed that can be installed on (almost) any small vessel that currently does not have a landing pad. Flat and circular platform with sufficient size for the landing and take-off of UAV, supported on a system of hydraulic or electric arms with quick response actuators that will allow the platform to be horizontally continuous. By installing a small landing deck with the capability to land/launch a small UAV, small and mid-sized Coast Guards will have the capacity to perform and maintain efficient surveillance and protect security of their maritime borders. Hydrodynamic behaviour of ships and their responses to environmental influences. The result will allow for a structural design of the landing platform. Hydrodynamic behaviour of ships and their responses to the platform. The result will allow for a structural design of the landing platform.

Mechanical System to actuate and maintain it horizontally.

Chapters:

1. Introduction
2. Ship Motion
3. Two degrees of freedom Spherical parallel mechanism
4. Per-project of the 2 DOF SPM design and construction calculations

List of abbreviations and symbols

SPM - Spherical parallel Manipulator

PPA - Politsei- ja Piirivalveamet

DOF - Degrees of Freedom

LCG - Longitudinal Center of Gravity

LCB - Longitudinal Center of Bojancy

UAV - Unmanned aircraft vehicle

L_{OA} - Ships Length Overall

L_{wl} - Length on Waterline

L_{pp} - Length between perpendiculars is the longitudinal distance between the forward and aft perpendiculars where ship meets the waterline it floats at design draft from rudder stock to front of the ship;

$BL(K)$ - The keel is the lowermost point of the ship at any point of its length. The baseline of a ship is the longitudinal line that runs along the keel;

B_{max} - The beam or breadth (max) is the transverse maximum distance across maximum section;

B_{wl} - Breadth, moulded at $T=4.20$;

B - The beam or breadth is the transverse distance across section;

T - Mean Draught;

T_{dwl} - draught at designed water line, moulded;

D - Depth to free board deck (main deck);

CL - Center line of the ship as the x -axis;

A_{wp} - water plane area;

S - waterplane area;

LCB - longitudinal Center of buoyancy;

VCB - vertical center of buoyancy ;

$KM(KMT)$ - Vertical distance from BL to Transverse Metacentre (above keel) (Longitudinal metacentric height (above keel))

$GM_0 = KMT - KG$ - Transverse metacentric height;

$LCG(CGX)$ - longitudinal Center of gravity;

$TCG(CG Y)$ - Transverse center of gravity from CL;

VCG (CGZ or KG) – vertical center of gravity;

∇ - Displacement;

$\Delta = \rho g \lambda \nabla$ - weight displacement;

$C_B = \frac{\nabla}{LBT}$ = Block coefficient;

$C_M = \frac{A_M}{BT}$ – mid-ship section coefficient ;

$C_{WP} = \frac{A_{WP}}{LB}$ –water-plane coefficient;

C_P – prismatic coefficient ;

$\bar{GM} = GM_0 - GM_{corr}$ - Corrected GM_0 Transverse metacentric height with free surface correction GM_{corr} ;

$\bar{GZ} = KN - KG \sin(\theta) - DGZ$ - DGZ -free surface correction, GZ - Righting lever;

KN - 'K' represents the keel and 'N' a point that intersects the vertical line of buoyancy, which result a distance;

$BM = KM - VCB$;

NX - Siemens Computer aided design software

Solidworks - Computer aided design software

KOKKUVÕTE

Magistritöö eesmärgiks oli disainida Politsei ja Piirivalveameti laevale liikuv maandumisplatvorm, mis hoiab end horisontaalselt laeva kõikumiste korral. Toote eesmärk on lihtsustada mehitamata helikopterite maandumist väiksematele alustele ja laevadele karmides merelistes tingimustes. Toode kavandati konkreetsele PPA laevale “Kindral Kurvits”.

Politsei ja Piirivalveametil on otsene vajadus muuta laevade operatsioonid merel efektiivsemaks. Mehitamata helikopterid, mis tõenäoliselt maanduksid laevale kaaluksid 100 kuni 110 kg ning konstruktsiooni arvutused on tehtud varuga, mis peaks vastu 275 kg. Esmalt oli vaja uurida laeva liikumisi, millest laeva pöördliikumine ümber pikitelje on kõige keerulisem ja selle kõige täpsem arvutus on mittelineaarne. Antud tingimustes osutus piisavaks lineaarne arvutus. Differentiaalvõrrandid lahendati MATLAB Simulinki abil ja analüütiliselt. Võrrandite koefitsientide leidmisel kasutati “strip” teooriat ja Simsoni valemit laeva ristlõigete kaudu ruumalade arvutamiseks. Töötati välja erinevaid mudeleid võimalikust kinemaatika lahendustest ja simuleeriti nende liikumisi. Arvutati välja lahenduste keerukuse aste, mille alusel valik teha. Sfääriline paralleel manipulaator osutus kõige efektiivsemaks.

Kinemaatika ja liikumiste simuleerimisteks ja arvutusteks kasutati Solidworksi, NX 12 Siemens ja MATLAB. Töötava kinemaatika alusel disainiti konstruktsioon ja teostati tugevusarvutused vastavalt valitud koormusolukorrale, mille tugevusvaru sai valitud vastavalt ISO standard 19903 järgi. Kõige suuremat mõju avaldab 275 kg raskuse helikopteri hädamaandumine mehhanismi kolm-jalast vastassuunas. Sel juhul on vaja valida õige kaalu ja tugevuse suhe ülemisele plaadile. Ülemine plaat on disainitud keeruka profiil-struktuurina, et vähendada kaalu ja säilitada tugevust. Liikumiste võimaldamiseks ja koormustega toimetulemiseks on koost keerukas ja enamasti töötab väände. Mootorile tekkis maksimaalne väändemoment 1200 Nm ning algselt valitud mootor tuleb asendada.

Lõputöö eesmärgid ja nende saavutamine:

1. Differentiaalvõrrandid said lahendatud lineaarselt ning vastavalt laeva andmetele on võimalik öelda, et kuni 20° laeva kreeni nurga juures ei ole tulemused oluliselt erinevad mittelineaarsest. Laeva arvutuste juures Simsoni valemit kasutades lisas täpsust CAD mudel laevast, mille sektsioonid põhinesid laeva andmetele ning vastavalt ligilähedaselt reaalsele olukorrale. Laeva sumbuvus on mittelineaarne ja sellest on ka erinevused, kuid need ei mõjuta oluliselt arvutuste tulemust.

2. Konseptuaalse lahenduse leidmiseks sai teostatud erinevate lahenduste kaalumise, mille järgi osutus sfääriline paralleel manipulaator ja lineaarsete aktuaatoritega manipulaatorid keerukuselt sarnaseks. Lõplik lahendus kaldus sfäärilise lahenduse poole, sest laeva kaks perioodilist liikumist põhinevad rotatsioonil ning manipulaator on suuteline seda kiirelt teostama. Lahendatud sai kinemaatika ning üles alla liikumist (Heave) oli vaja ainult tugevuse hindamiseks. Reaalsete testimiste käigus oleks võimalik hinnata täpsemalt, kas lisada veel üht vabadusastet platvormile.
3. Disainitud on mehaaniline konstruktsioon, mis NX simulatsiooni põhjal annab töötava lahenduse. Edaspidi on vajalik disainida automaatika ja täpsustada mootor.

Plaadi platvormi materjaliks on valitud alumiinum AA6082-T651, mis sobis konstruktsioonile tugevusarvutuste kohaselt ja tootespetsifikatsiooni järgi on hea keevitavusega. Pealmise plaadi platvormi ülemine kiht tuleks täpsustada, et saavutada vajalik hõõrdepidavus kopteri liikumisele.

SUMMARY

The aim of the master's thesis was to design a mobile landing platform for the Police and the Border Guard Board, which keeps itself horizontal in case of ship fluctuations. Purpose of the product is to facilitate the landing of unmanned helicopters on smaller vessels and ships in harsh sea conditions. The product was designed for a specific PBGB ship "General Kurvits". Police and The Border Guard Agency has a direct need to make ship operations at sea more efficient. The unmanned helicopters that are likely to land on a ship would weigh between 100 and 110 kg, and design calculations have been made with a margin of 275 kg. First, it was necessary to study the movements of the ship, of which the rotational movement of the ship around the longitudinal axis is the most complex and its most accurate calculation is nonlinear. Under determined conditions, a linear calculation proved to be sufficient. Differential equations were solved using MATLAB Simulink and analytically. Ship motion equation coefficients were found using strip theory and the Simson rule for ship cross-sections to calculate volumes. Various models of possible kinematic solutions were developed and simulated their movements. The degree of complexity of the solutions was the basis of which the choice was made for optimal solution. The spherical parallel manipulator proved to be the most effective. Kinematics was developed using MATLAB, Solidworks and NX 12 Siemens were used to simulate and calculate the movements. Based on the working kinematics, the structure was designed, and strength calculations were performed according to the selected load situation for which the strength margin was selected according to ISO standard 19903. The biggest impact is the 275 kg helicopter emergency landing to opposite side of the mechanism links In this case, it is necessary to choose the right weight to strength ratio of the top plate. The top plate is designed as a complex profile structure to reduce weight and maintain strength. To allow movement and to cope with loads the assemble is complex and spatial and mostly works on torsion. The maximum reaction torque of 1200 Nm to the electric motor joint is outside of the selected motor specification. The originally selected engine must be replaced.

Objectives of the thiesis and their achievement:

1. The differential equations were solved linearly and according to the ship's data it can be said that there are no remarcable diffrences from nonlinear as the stability curve is almost linear up to 20 °. The accuracy of ship's calculations according to Simson rule were sufficient. As the CAD model of a ship added the precision whose sections were based on the ship data and according to a roughly realistic situation. Ship decay is non-linear and there are differences, but they are not significantly

affected the result of the calculations.

2. In order to find a conceptual solution, consideration was given to different solutions, according to which turned out to be the spherical parallel manipulator and linear actuators manipulators of similar complexity. The final solution was skewed to spherical solution, because the two periodic movements of the ship are based on rotation and the manipulator is able to do so efficiently. The kinematics were resolved for the platform as two degrees of freedom and up-down movement (Heave) was only needed to assess strength. In the course of actual testing, it would be possible to assess in more detail whether to add another degree of freedom to the platform.

3. A mechanical structure has been designed, which, based on the NX simulation, and provides a working solution. In the future, it is necessary to design automation and specify the engine.

The material of the plate platform is aluminum AA6082-T651, which was suitable for the construction according to the strength calculations and has good weld-ability according to the product specification. The material of the top plate platform should be specified to achieve friction resistance to hold the helicopter on the top plate.

1. INTRODUCTION

1.1. Overview

On the European Borders there have been always some kind of vessel who is looking for illegal or criminal activities. As the latest years the unmanned aircraft activities have increased and the need to use them on vessel becomes from practical part to look further and operate them on sea even when the ship is rolling or someone are in distress. The landing deck will be on small link to overcome the challenges of operating the helicopter drone in offshore. The general concept is to perform beyond line of site missions with smaller vessel. The larger ships are expensive and less available, these often-critical missions are constrained and not implemented enough. With a large number of smaller vessels to any European coastal guard or maritime police the number of critical missions could be significantly increased. Concerning the needs of the Estonian Police and Border Guard (PPA) ships and their operations, we can see a potential to increase the operation efficiency. As PPA have small vessels and are responsible of a large sea area, it is likely to occur different activities on sea, in different conditions.

The interview with Police and Border Guard officials, who's responsibility are the planning and improving the border control and Estonian sea area with vessels and ships on Baltic sea and Finnish gulf evolved interest on using the platforms and larger unmanned helicopters on vessel's. The HORIZON project proposal "Enhanced Maritime Situational Awareness Through Collection and Integration of Multiple Data Sources - EMERALD" [1] stated some goal's and constraints to use helicopter drones on vessels . The main benefit come's from the usage on very large sea areas like Mediterranean and also in rough sea, but here arises a problem. It is very difficult to land safely a helicopter on a moving ship deck. The drone will need to process continuation calculation of the ships deck, position and etc. If the deck will be steady, it will be easier to land.

The product potential market could be: Estonian Police and Border Guard; Finish Border Guard; Swedish Border Guard; European Maritime Safety Agency, FRONT EX - European Border and Coast Guard Agency; oil and gas industry; wind-energy industry. Simple calculation of the potential ships in nearby organization will give 100 to 200 vessels [2], that could be potential customers.

1.2. The landing and take-off deck

The goal is to design a flexible landing platforms of about 4 meters circular diameter for the landing and take off of the helicopter with quick response actuators or motors that will allow the platform to be horizontal. The platform should be capable to whit stand weight of unmanned aerial vehicle's, that are in a larger class, but not as heavy as manned helicopters. The Alpha Unmanned Systems Alpha 900 weight is 100 *kg* [3] and SCHIBEL CORPORATION CAMCOPTER[®] S-100 empty weight is 110 *kg* and maximum take-off weight is 200 *kg* [4, 5], which are potential vehicles, that could be used on a vessel landing platform. From these vehicles we and approximate the general layout of the platform also, as the safety area should be double the rotor diameter for example.

The requirement to hold steady the landing pad will need a deeper understanding of the ships movements, and modeling of the rolling, pitching and heaving movements in a sea condition's where the air vehicle also can operate. Generally the unmanned helicopter's can operate in a steady flight up to 20 $\frac{m}{s}$ or more, but the landing conditions should be better. For know I will assume that the operating conditions for the flexible landing platform will be up to 20 $\frac{m}{s}$ wind, which is the basis to evaluate the sea conditions and ship movement in waves. The initial challenge is to design a system that can hold steady with actuators and the thesis will try to look different kind of kinematic solutions to solve the problem optimally. The SCHIBEL CORPORATION has already designed a horizontal platform with linear actuators [?], but as the video will describe the system is on ground and probably are not designed for specific ship.

The goal is to design a solution to a specific Police Boarder Guard ship like Estonian Police and Border Guard "Kindral Kurvits PVL-101".

1.3. The mechanical design

The thesis will cover the preliminary project for the manufacture of the platform, but the author has no intention to cover all detailed design aspects. The final result should be technical drawing's of the prototype's mechanical solution, with detailed Final Element Analysis to critical parts. The automation and electrical design will get the input from the mechanical kinematic and dynamic solution and the basis for the dynamic behavior of the platform are the ship's movements. The helicopter movement and aerodynamic behavior are for future investigation with cooperation of the manufacturer of the UAV.

The kinematic solution is based on the article [9], but is adopted to the "Kindral Kurvits" probable operation in Baltic sea at the maximum wind conditions of 20 $\frac{m}{s}$. The restriction of the platform elevation to 20° comes from the fact that the ship's roll movement this high is also dangerous and probably the captain will not operate the platform in these conditions, but in beam seas it can occur very quickly.

1.4. The thesis structure

The paper has 4 chapter's and 6 Appendixes which all have their own sections. All the work has integrated references to make the reading easier and as required the bibliography is in the end of the work. When the introduction will give a brief description of the problem, it's concept and proposed method to solve the situation on a specific Estonian Police and Border Guard ship "Kindral Kurvits". As the cause of the problem is the sea and ship movement in the chapter 2 will begin the body part of the thesis, and will give a theoretical and practical aspects of the ships movement. The third chapter will search the general kinematic solution to the platform movement. The fourth chapter will propose a practical solution to the mechanics and will analyses this. All the appendixes are important part of the chapters as they will cover the required calculations, drawings and figures.

2. Ship motions

2.1. Overview

A ship moving on the surface of sea is almost always in oscillatory motion. Three linear and three rotational about three principal axes.

A = surging – motion backwards and forwards in the direction of ship travel.

B= swaying – athwart-ship motion of the ship

C=heaving – motion vertically up and down

D=rolling - angular motion about the longitudinal axis. When the ship rolls it lists alternately from starboard to port and then back to starboard (

E= pitching – angular motion about the transverse axis. When a ship pitches, it trims alternately by the bow and by the stern

F= yawing – angular motion about the vertical axis.

Only three kinds of motion, namely, heaving, rolling and pitching are purely oscillatory motions, since these motions act under a restoring force or moment when the ship is disturbed from its equilibrium position. In the case of surging, swaying, or yawing, the ship does return to its original equilibrium position, if disturbed from it unless the exciting forces or moments that cause such a disturbance act alternately from the opposite directions. All these motions are essentially critical to understand when designing a mobile platform and the rolling will effect most in the beam sea. [8, 4.1]

2.1.1. PVL-101 main dimensions

Ship geometry is an important part of the motions due to its complex shape and it has an impact on the main forces, and my calculations are based on strip theory which gives quite accurate results over a wide range of parameters. The strip theory is based on the potential flow theory. For that reason I have made a 3D model of the ship (using the ships manufacturer made body plan), that shows the shapes of sections determined by the intersection of the hull form with planes perpendicular to the buttock and waterline planes. For calculations I will use the modeled sections and their areas. The second integrals over the ship to calculate volumes for added mass, damping, restoring, exciting coefficients and etc, are done by using Simpson

first rule [21, 29, 8]. The ship movements have an impact to the platform as the motions and moments moves around the center of gravity, which I have determined when the ship is fully loaded to departure with 30 *tons* deck cargo, full fresh water and fuel oil tanks, and 94 *tons* of ballast water is loaded in order to achieve maximum draught, 4.2 m. The total weight of ship are as follows on table A.1 and look for figures: A.1 & A.2 on A (A).

2.2. Heaving

As in the case of heaving, the following four elements are in importance:

- Inertial moment;
- Damping moment;
- Restoring moment;
- Exciting moment.

The equation of motion for heaving is:

$$a\ddot{z} + b\dot{z} + cz = F_0 \cos(\omega_e t) \quad (2.1)$$

[8, 4.2 equation (4.1)]

Where:

1. the inertial force $F_a = -a\ddot{z}$ is present when the ship is in oscillatory motion and a is the virtual mass (ship mass plus added mass), and $\ddot{z} = \frac{d^2z}{dt^2}$ is the vertical acceleration;
2. the damping force, which always resists, the motion, is $F_b = b\dot{z}$, where b is the damping constant, and, $\dot{z} = \frac{dz}{dt}$ is the velocity;
3. the restoring force, which always tends to bring the ship back to its equilibrium position, is $F_c = cz$, where c is the restoring or spring constant, and z is the displacement of the center of gravity (CG) of the ship;
4. the exciting (or encountering) force, which acts on the mass of the ship, is $F = F_0 \cos(\omega_e t)$, where F_0 is the amplitude of the encountering force, ω_e is the circular frequency of the encountering force and t is time.

The required calculations for the virtual mass a , damping constant b , restoring force constant and the exciting force amplitude F_0 are covered in the Appendix 1, which are according to the [8, 4.2 examples] using strip theory to find coefficients. Strip theory physical assumptions are as follows:

1. it must be assumed that the vessel is a slender body, (i.e., its beam and draft are much less than the length and changes in cross-section vary gradually along the length);

2. fluid flow velocities in the transverse direction are much greater than in the longitudinal direction;
3. the flow field at any cross section of the ship may be approximated by the assumed two-dimensional flow in that strip.

[22]

To obtain the total effect on the ship, the effects of all individual strips are integrated along the length. The main goal of the strip theory is to reduce a three-dimensional hydrodynamic problem to a series of two-dimensional problems which are easier to solve.

The natural frequency of the heaving motion, that is

$$\omega_z = \frac{2\pi}{T} = \sqrt{\frac{c}{a}} \quad (2.2)$$

T , is the heaving period. The ship sea-keeping is dependent mainly on the forced oscillations, but the free oscillations are important for two reasons:

1. The natural frequency of a ship determines the value of a tuning factor $\Lambda = \frac{\omega_e}{\omega_z}$, and this is important in finding the region of resonance.
2. The second reason is that, at regular seas the transient motion that may cause a large amplitude is dependent on the free (through damped) oscillations. In an irregular seaway, the transient motions may take place at random.

[8, 4.2 equation (4.3)]

So as follows the four components of the ship movements which are important to my study are directly connected to the two Degrees of Freedom (DOF) Spherical Parallel Platform movements or its strength considerations. In the future studies, there could be considered the platform vertical movement also if it deems necessary for UAV operations or strength considerations. The initial condition I have chosen considering the ship operations in the Baltic Sea are as follows:

1. the ship speed or model speed $u = 1.45$ m/s;
2. the maximum wind speed 20 m/s, which gives the exciting wave height $\xi = 8$ m. [16, page 29]

2.2.1. Inertial force

The inertial force $F_a = -a\ddot{z}$ is present when the ship is in oscillatory motion and a is the virtual mass (ship mass plus added mass), and $\ddot{z} = \frac{d^2z}{dt^2}$ is the vertical acceleration, thus

$$a \frac{d^2z}{dt^2} = M \frac{d^2z}{dt^2} + \delta l = (M + a_z) \frac{d^2z}{dt^2}. \quad (2.3)$$

[8, 4.2] where M is the ship mass and a_z is the added mass.

The added mass of a total ship can be calculated as

$$a_z = \int_{-L/2}^{L/2} a_n dx = \rho \frac{\pi}{2} \int_{-L/2}^{L/2} C y^2(x) dx \quad (2.4)$$

[8, 4.2] The inertial mass coefficients for two-dimensional floating bodies in heaving motion, were you compare the ship sections with a reference section [23, 22, Figure 42] and assign a coefficient C to every section refer to A.5 in Appendix 1.

Ships at sea both encounter waves and create them by disturbance of the motion. Longer waves are influenced primarily by gravity and relatively simple equation, relating wave phase speed (or celerity) to wave length or wave period can be derived providing that the following assumptions are made:

1. The water particles rotate at a constant circular speed;
2. Once set in motion, all the energy is retained within the wave motion;
3. The particle velocity is less than the wave celerity c' .
4. The wavelength $L_w =$ length of a ship model $= L_{oa}$

The wave frequency is $\omega_w = \sqrt{\frac{2\pi g}{L_w}}$ and the encountering frequency is

$$\omega_e = \omega_w - \frac{\omega_w^2}{g} u \cos \mu \quad (2.5)$$

[22, eq: 69] where: the forward speed of a model u is a constant. For now I will consider only the case of head seas or waves directly ahead μ . The Lewis-form sections for varying $B/T, \beta_n$ I choose d the inertial coefficients by visual comparison of the body plan with the section. Calculating according to the example [8, Example 4.1 Calculation of Added Mass] the PVL101 added mass in heaving is approximately as the mass of the ship itself usually refer to the [22, 8, 19] . According to my calculation the added mass is $\approx 95.45\%$ from ships mass Δ refer to A & (A.1).

So the total virtual mass are as follows (A.2).

2.2.2. Damping force

The damping force always acts in the opposite direction to the motion of the ship and produces a gradual reduction in the amplitude of motion. Which is

$$F_b = -b \frac{dz}{dt} \quad (2.6)$$

where b is the coefficient for the damping force in heaving. this damping coefficient normally depends on the following factors:

1. type of oscillatory motion;
2. encountering frequency of oscillation, and
3. form of vessel. the damping force is considered in our case as linearly proportional to the velocity of oscillation $\frac{dz}{dt}$.

The damping in heaving is caused mainly by waves generated by the heaving motion of the ship, the damping coefficient per unit length is directly related to the amplitude of the waves. The damping for each section: [8, ref 89]

$$b_n = \frac{\rho g^2 \bar{A}^2}{\omega_e^3} \quad (2.7)$$

where ω_e is the frequency of the radiated waves (as encountering frequency (2.5)), and

$$\bar{A} = \frac{\text{Amplitude of the radiated waves}}{\text{Amplitude of the heaving motion}} = \frac{\xi_a}{z_a} \quad (2.8)$$

,this amplitude ratio \bar{A} can be obtained from [8, Fig- 4.6]; therefore the total damping coefficient can be calculated by integrating b_n over entire length of the ship, that is

$$b = \int_{-L/2}^{L/2} b_n dx \quad (2.9)$$

Calculating according to the example [8, Example 4.2 Calculation of damping coefficient] the PVL101 damping coefficient in heaving refer to A.2. In reality this coefficient will be determined experimentally in calm water with forced oscillations and both theoretical and experimental investigations enable us to say that: the damping coefficient increases as B/L increases, but decreases with increase in the block coefficient C_B of the vessel.

According to my calculation the heaving damping coefficient b_z refer to (A.3).

2.2.3. Restoring force

The restoring for heaving is given as the additional buoyancy force that acts on a body when submerged to a deeper draft. It is assumed that there is no significant change in the water-plane area during heaving, the restoring force is given as the amount of water displaced, which is equal to specific weight times additional submerged volume. Thus

$$cz = \rho g A_{WP} z \quad (2.10)$$

where the product of A_{WP} (the area of load water-plane) and z (the additional immersion of the ship) is equal to the excess of displacement volume. Therefore c , the restoring force coefficient = $\rho g A_{WP}$

$$= \rho g L B C_{WP} \quad (2.11)$$

[8, eq: 4.9]

where C_{WP} is the water-plane area coefficient. The restoring force is obtained directly from offsets as

$$c = \rho g \int_{-L/2}^{L/2} 2y(x) dx \quad (2.12)$$

[8, 4.2 (4.9) & (4.9a)] where $y(x)$ is the half-breadth at section x .

Calculating according to the example [8, Example 4.3 Calculation of restoring coefficient] the PVL101 restoring coefficient in heaving is (A.4).

According to equation above (2.10) the calculation for heaving restoring coefficient is

$$c = 6.292 \cdot 10^6 \frac{kg}{s^2}$$

which is bigger than according to the strip theory Heaving - Calculation of restoring coefficient. So as the ship is moving there are a different restoring coefficient and in my calculations I will use one that was calculated by the strip theory (A.4) as all other calculations also. The difference may come from the accuracy of my geometrical 3D model to the ships actual model. The calculation according to the (2.10) where I can use the actual ship data [7], but it is not comparable to the strip theory calculations, as each sectional area for particular bonjan curve has differences in my model.

2.2.4. Free, damped Heaving Motion ($F_0 = 0$)

In the case of equilibrium

$$a\ddot{z} + b\dot{z} + cz = 0 \quad (2.13)$$

The solution for this equation is given (provided that $b < \sqrt{2aca}$ complex conjugate pair) by

$$z = \exp^{-\nu t} (C_1 \cos(\omega_d t) + C_2 \sin(\omega_d t)) \quad (2.14)$$

or

$$z = \exp^{-\nu t} A \sin(\omega_d t - \delta) \quad (2.15)$$

[8, 4.2 equations (4.4), (4.5)]

where

$$\nu = b/2a \quad (2.16)$$

is the decaying constant, ω_d is the circular frequency of the damped oscillation, that is,

$$\omega_d = \sqrt{\omega_z^2 - \nu^2} \quad (2.17)$$

ω_z is the natural circular frequency of the undamped oscillation, and C_1 and C_2 , or A and δ , are constants to be determined from the initial conditions.

[8, 4.2 equation (4.6a)]

The damped period is given by

$$T_d = \frac{2\pi}{\omega_d} \quad (2.18)$$

[8, 4.2 equation (4.6b)]

Calculating the equation with initial conditions as: $z(0) = 0$ and the model speed (ship speed) $\dot{z} = 1.45 \text{ m/s}$ refer to (A.5). For calculation look A.4.

2.2.5. Exciting force

To determine the exciting force for ship motions, water waves must be studied, since they are the only source of ship excitation in a seaway. Let $\xi = \xi_a \cos(\omega_e t)$ the exciting force for the heaving motion is obtained by integrating the additional buoyancy due to waves along the ship. Therefore the exciting force on a section of a ship of unit length is given by

$$\rho g 2y \xi dx \quad (2.19)$$

, where ξ is the ordinate of the effective wave profile: that is, the effective wave considered to be a subsurface wave profile, or

$$\xi = \xi_a \exp^{-kT_m} \cos(k'x - \omega_e t)$$

where k' is the effective wave number, $2\pi/L'_w$, that is $k \cos \mu$, k being the normal wave number, $2\pi/L_w$; μ is the direction of the ship's heading in relation to the

waves: and T_m is the mean depth of the effective wave from the free surface. For beam seas

($\mu = 90^\circ$ or $\mu = 270^\circ$) $L_w \rightarrow \infty$, and the exciting force amplitude F_0 becomes maximum and is given as

$$F_0 = 2\rho g \xi_a BLC_{wp} = 2\rho g \xi_a A_{wp}. \quad (2.20)$$

[8, 4.2]

Hence the exciting force is the excess buoyancy force at any instant of time:

$$F = F_0 \cos(\omega_e t) \quad (2.21)$$

and F_0 the amplitude of the total exciting force, is obtained by integrating the buoyancy force of individual sections. [8, 4.2,eq:4.11a]

The exciting force for heaving is then the additional buoyancy force at any instant, and when substituting the expression for wave profile and expanding the cosine term, as well as assuming the ship to be symmetrical about the mid-ship section, we obtain the exciting force for heaving [8, 4.2,eq:4.11c and 12a] as

$$F = \left(2\rho g \xi_a \int_{-L/2}^{L/2} y \cdot \cos k'x dx \right) \cos \omega_e t = F_0 \cos(\omega_e t) \quad (2.22)$$

[8, 4.2,eq:4.12b]

The exciting force F is positive if it acts in the positive direction, that is, downward. Comparing wave profile and (2.22), we find the phase angle between the wave profile and heaving force due to waves to be $\varepsilon = 0^\circ$. The amplitude of the exciting force can be expressed nondimensionally as

$$f_0 = \frac{F_0}{\rho g \xi_a LB} \int_{-L/2}^{L/2} y(x) \cos(kx \cos(\mu)) dx \quad (2.23)$$

[8, 4.2,eq:4.13]

For beam sea condition (i.e $\beta = 90^\circ$ or 270°) the exciting force for heaving reaches the maximum value. The wave amplitude ξ_a I will choose from [16, page 28, 29] "Significant wave height prediction curves based upon the Joint North sea wave project (Jonswap 1969)" as the wind speed are $20 m/s$ and wave height $8 m$ in the North sea. Also the PhD Thesis [34, table 1] will show that the largest maximum are $8 m$ and mean wave height $7.6 m$ in the Baltic sea Vilsandi observations from 1954-2008.

Calculating according to the example [8, Example 4.6 Calculation of Amplitude if the exciting force] the PVL101 amplitude of the exciting force for heaving refer to A.5 & A.8.

2.2.6. Forced heaving Motion

In the case, for the equilibrium condition the equation of motion is

$$a\ddot{z} + b\dot{z} + cz = F_0 \cos(\omega_e t) \quad (2.1) \text{ [8, 4.2 equation (4.7a)].}$$

The solution of the equation are

$$z = \exp^{-\nu t} (C_1 \cos(\omega_d t) + C_2 \sin(\omega_d t)) + z_a \cos(\omega_e t - \varepsilon_2) \quad (2.24)$$

or

$$z = A \exp^{\nu t} \sin(\omega_d t - \beta) + z_a \cos(\omega_e t - \varepsilon_2) \quad (2.25)$$

[8, 4.2 equation 4.7b]

where z_a is the amplitude of the forced motion, and ε_2 is the phase angle of the forced motion in relation to the exciting force. According to [31, Page 209 - 210, Figure 3.8.1] ((2.24) or (2.25)) the motion is the sum of two oscillations; the first term describes a free, damped oscillation (Transient - Part 1) and the second (Steady state -Part 2) term an oscillation with the same circular frequency as that of the exciting force for heaving. The result for both oscillations if they are effective are called a transient motion in the beginning of the motion as in our case it is effective. For steady conditions the amplitude of the heaving motion z_a is given by

$$z_a = z_{st} \cdot \mu_z \quad (2.26)$$

, where

$$z_{st} = \text{static heaving amplitude} = \frac{F_0}{c} \quad (2.27)$$

$$\mu_z = \text{magnification factor} = \frac{z_a}{z_{st}} = \frac{1}{\sqrt{(1 - \Lambda^2)^2 + 4\kappa^2 \Lambda^2}} \quad (2.28)$$

[8, 4.2 equation 4.8a]

$$\Lambda = \text{tuning factor} = \frac{\text{Frequency encounter}}{\text{Natural frequency}} = \frac{\omega_e}{\omega_z} \quad (2.29)$$

$$\kappa = \text{nondimensional damping factor} = \frac{\nu}{\omega_z} \quad (2.30)$$

, as ν (2.16); ω_z (2.2);

$$\varepsilon_2 = \frac{\text{phase angle between the exciting force and the motion}}{\text{force and the motion}} = \arctan \frac{2\kappa\Lambda}{1 - \Lambda^2} \quad (2.31)$$

[8, 4.2 page 38] or [13]

2.2.7. Forced damped PVL-101 heaving differential equation and its solution

The general equation as mentioned is as follows: [8, 22] or (2.1)

$$a\ddot{z} + b\dot{z} + cz = F_0 \cos(\omega_e t)$$

Then the solution can be expressed as

$$z = A \exp^{\nu t} \sin(\omega_d t - \beta) + z_a \cos(\omega_e t - \varepsilon_2) \quad (2.32)$$

(2.25) or [20, eq:10.15]

According from [20, eq:10.7A and 10.7B] and [31, page 208-210 and Figure 3.8.1] the first part of the solution $z_1 = \exp^{-\nu t} (C_1 \cos(\omega_d t) + C_2 \sin(\omega_d t))$ are equal to the form $z_1 = A \exp^{-\nu t} \sin(\omega_d t - \beta)$ which is the ships natural movement (Transient movement Part 1). The second part $z_2 = z_a \cos(\omega_e t - \varepsilon_2)$ is the encountering movement (Steady state Part 2 - excited by waves) and hole solution: $z = z_1 + z_2$ as the total movement. The phase angle between the wave motion and the heaving motion is expressed as $\varepsilon = \varepsilon_1 + \varepsilon_2$ where ε_1 is the phase angle between the wave motion and the exciting force caused by waves, and ε_2 is the phase angle between the exciting force and the heaving motion. Now $\varepsilon_1 = 0$ [8, eq:4.12b] and from [8, page 38]

$$\varepsilon_2 = \arctan \frac{2\kappa\Lambda}{1 - \Lambda^2} \quad (2.33)$$

As for (2.25) the solution to the heaving equation are:

$$z = A \exp^{\nu t} \sin(\omega_d t - \beta) + z_a \cos(\omega_e t - \varepsilon_2)$$

and refer to calculations Heaving - PVL-101 differential equation calculation and its solution" & A.12.

Refer to graphical solution fig:A.3 - Heaving movement z and acceleration fig A.4 -Heaving-acceleration-a.

2.2.8. State-space ODE model

Considering the classical mass-spring-damper system, we can represent the ship movement also by this model, which is similar to the State-space model State space model.

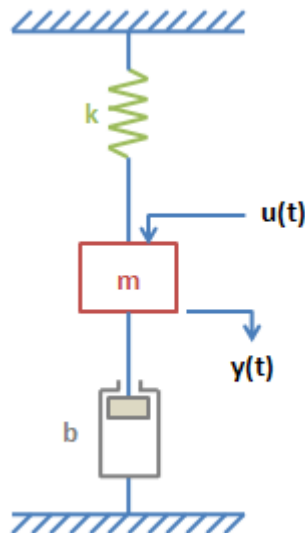


Figure 2.1.: State space model

The representation of the ship movements in state space model is necessary for the automation of the platform. Models that consist of coupled first-order differential equations are said to be in state variable form. This form, which is also called the Cauchy form, has an advantage over the reduced form, which consists of a single, higher-order equation, because it allows a linear model to be expressed in a standard and compact way that is useful for analysis and for software applications. State variable models, unlike transfer function models, can have more than one input and more than one output. Simulink has the State-Space block that represents the linear state variable model $\dot{x} = Ax + Bu, y = Cx + Du$. Unlike linear models, closed-form solutions are not available for most nonlinear differential equations, and we must therefore solve such equations numerically, but Piecewiselinear models are actually nonlinear, which are part of the Simulink. Such a model for example is a mass attached to a spring and sliding on a horizontal surface with Coulomb friction. the model is refer fig:2.1: State-space-model:

$$\begin{aligned} m\ddot{x} + kx &= f(t) - \mu mg \quad \text{if } \dot{x} \geq 0 \\ m\ddot{x} + kx &= f(t) + \mu mg \quad \text{if } \dot{x} < 0 \end{aligned}$$

these two linear equations can be expressed as the single, nonlinear equation. Where μ states for friction, k is the stiffness of the system, m mass and g - gravity.

$$m\ddot{x} + kx = f(t) - \mu mg \quad \text{where} \quad \text{sign}(\dot{x}) = \begin{cases} +1 & \text{if } \dot{x} \geq 0 \\ -1 & \text{if } \dot{x} < 0 \end{cases}$$

Therefore Simulink is especially useful for such applications. The vector u represents the inputs, and the vector y represents the outputs. For this section I will only show

the state space model of the heave movement, but for future developments it will be necessary to model it on Simulink. It will be part of the Simulink model.

This representation makes use of vector and matrix notation. The dynamical equation for this system is given by the following equation:

$$my''(t) + by'(t) + ky(t) = u(t) \quad (2.34)$$

You can represent this system with a state-space model expressed in the following form:

$$\frac{d}{dt}x(t) = A(t) \cdot x(t) + B(t) \cdot u(t)$$

$$y(t) = C(t) \cdot x(t) + D(t) \cdot u(t)$$

Where:

- A-state matrix
- B-Input matrix
- C-Output matrix
- D-Direct transmission matrix
- x-state vector
- u-Input
- y-Measured or controlled output

Use two state variables for this second order system. $x_1(t) = y(t)$; $x_2(t) = y'(t)$.

Given that: $m = a$; b ; $k = c$; $u(t) = F_0 \cos(\omega_e t)$; $\omega_z = \omega_0 = k$;

$$A(t) = \begin{bmatrix} 0 & 1 \\ -(\omega_0)^2 & \frac{-b}{m} \end{bmatrix}; \quad B(t) = \begin{bmatrix} 0 \\ 1/m \end{bmatrix}; \quad C(t) = [1 \quad 0];$$

$$D(t) = [0].$$

[32]

2.3. Accelerated rotational motion

If a purely rigid body has an accelerated rotational motion, the acceleration of any particle of the body at a perpendicular distance r from axis of rotation has two components:

1. the first is $r\alpha$, along the direction of instantaneous velocity.
2. the second is $r\omega^2$, directed toward the axis.

Here the instantaneous angular velocity is $\alpha = \frac{d\omega}{dt} = \frac{d^2\phi}{dt^2}$, with two directions, that act on a particle. Instead we add the moments of forces about the axis of rotation, therefore the sum of moments of forces $F = mr\alpha$ and $F' = mr\omega^2$ about the axis of rotation is given by $Fr = mr\alpha r = mr^2\alpha$. The total moment of all the forces about the axis of rotation is

$$\sum F_i r_i = \sum (m_i r_i^2) \alpha = \sum (m_i r_i^2) \frac{d^2\phi}{dt^2} = I \frac{d^2\phi}{dt^2} \quad (2.35)$$

where I is the moment of inertia of the body about the axis of rotation, that is $\sum (m_i r_i^2)$. Now, if I is the moment of inertia about a particular axis of a body of total mass M , a related length k is defined by the dimension ally homogeneous equation

$$I = Mk^2 \quad (2.36)$$

where k is called the radius of gyration of the ship about a particular axis. therefore we may have radius of gyration for three different rotational motions: rolling, pitching, and yawing. In practice, the radius of gyration of a vessel about any axis is obtained by considering the total weight of the vessel as the sum of many small weights and then adding the products of each small weight and the square of its distance from the particular axis concerned, that is $k^2 = \frac{\sum (w_i r_i^2)}{\Delta}$, where w_i is the weight of the i th element, r is the direct distance of the i th element from the axis of rotation, and Δ is the total weight of the vessel.

Since moment of inertia for rolling is

$$I_{xx} = Mk_{xx}^2 = \int dM(y_i^2 + z_i^2) = \sum [w_i(y_i^2 + z_i^2)] + \sum I_i \quad (2.37)$$

and moment of inertia for pitching is

$$I_{yy} = Mk_{yy}^2 = \int dM(x_i^2 + z_i^2) = \sum [w_i(x_i^2 + z_i^2)] + \sum I_i \quad (2.38)$$

The radius of gyration for rolling and pitching are as follows:

$$k_{xx} = \sqrt{\frac{\sum [w_i(y_i^2 + z_i^2)]}{\Delta}} \quad (2.39)$$

$$k_{yy} = \sqrt{\frac{\sum[w_i(x_i^2 + z_i^2)]}{\Delta}} \quad (2.40)$$

[8, 4.3]

This method for calculating the radius of gyration for rolling and pitching are acceptable if the rolling period is linear. Method for ship's rolling prediction with regard to non-linearity of GZ curve it is more complicated and are as follows:

1. I will assume that the above equation (2.39) k_{xx} and (2.40) k_{yy} will apply to homogeneously loaded ship, without taking account the added mass and the virtual radius of gyration and the ships tanks liquid free body movement as the tanks are fully loaded (B.2);
2. Assuming that for linear conditions the quantity of ships virtual radius for rolling k''_{xx} is expressed as a fraction of the beam of the ship and is normally in the range of $0.33B \leq k''_{xx} \leq 0.45B$; Assuming for pitching the quantity of ships virtual radius for pitching k''_{yy} is expressed as a fraction of the beam of the ship and is normally in the range of $0.24L_{wl} \leq k''_{yy} \leq 0.26L_{wl}$
3. Assuming that the total virtual radius of a ship in nonlinear conditions $r''_{xx} = k_{xx} + k''_{xx}$ and for simplicity I will assume that are a constant in further calculations.

[8, Page 64 & 75]

Calculating according to the example [8, Example 4.9 "Radius of gyration and inertial moments for rolling and pitching"] the PVL101 radius of gyration for rolling and pitching refer to tab B.2: "Calculation of the radius of gyration and moment of inertia for rolling and pitching" & B.2.

2.4. Pitching

A ship may undergo a simple harmonic motion about either a transverse axis ($y - axis$) or a longitudinal axis ($x - axis$) if it is displaced from its equilibrium position and then released, or if it is given a initial velocity away from its equilibrium position. we should always refer to the moments of forces, rather than the forces, when we describe angular motions like pitching and rolling.

As in the case of heaving, the following four moments act in pitching and rolling motions:

- Inertial moment;
- Damping moment;
- Restoring moment;

- Exciting moment.

The equation of motion for pitching is analogous to that for heaving and is expressed as:

$$a_{\theta}\ddot{\theta} + b_{\theta}\dot{\theta} + c_{\theta}\theta = M_0 \cos(\omega_e t) \quad (2.41)$$

where:

1. Inertial moment = $a_{\theta} \frac{d^2\theta}{dt^2}$. Here a_{θ} is the virtual mass moment of inertia, and $\frac{d^2\theta}{dt^2}$ is the angular acceleration of pitching.
2. Damping moment = $b_{\theta} \frac{d\theta}{dt}$. Here b_{θ} is the damping moment coefficient, and $\frac{d\theta}{dt}$ is the angular velocity. The damping moment is considered to be linearly proportional to the angular velocity for the simplicity, as in the case of heaving.
3. Restoring moment = $c_{\theta}\theta$. Here c_{θ} is the restoring moment coefficient, and θ is the angular displacement in pitching. Again the restoring moment is considered to be linearly proportional to the pitching displacement. this is true only for small angles of pitching.
4. The exciting moment, $M_{0\theta} \cos \omega_e t$, is considered to be fluctuating with an encountering frequency of ω_e .

If we can determine the various values of a_{θ} , b_{θ} , c_{θ} and $M_{0\theta}$ we shall be able to determine the motion characteristics for pitching. It should be noted that the coefficients a_{θ} , b_{θ} , c_{θ} and $M_{0\theta}$ of pitching are not the same as those of heaving or rolling.

[8, 4.4]&B

2.4.1. Inertial moment

Inertial moment are:

$$M_{a_{\theta}} = a_{\theta} \frac{d^2\theta}{dt^2}. \quad (2.42)$$

The virtual mass moment of inertia for pitching a_{θ} , is the vessel moment of inertia for pitching plus the added mass moment of inertia for pitching, that is

$$a_{\theta} = I_{yy} + \delta I_{yy} = \Delta r_{yy}^2 + \delta I_{yy} \quad (2.43)$$

[8, eq:4.16a]

where δI_{yy} is the added mass moment of inertia for pitching, and r_{yy} is the ship's radius of gyration for pitching. The mass moment of inertia of a ship for the pitching motion I_{yy} can be roughly estimated from the moment of inertia of the area under the ship's sectional area curve (2.44). As for PVL101 we can get the information

about the ships loading and mass displacement from [7], that is simplified in the Calculation of the radius of gyration and moment of inertia for rolling and pitching compartments for PVL-101 [8, Example 4.9][7, APPENDIX 1]. So the ships mass moment of inertia consist of the ships loading of mass over the y axis and the lightship structure mass over the y axis which is assumed by empirical formula described in the (B.1), where $I_{yy} = \Delta r_{yy}^2$ (refer to r in (B.1)).

$$I_{yy} \simeq \rho \int_{-L/2}^{L/2} A(x)x^2 dx \quad (2.44)$$

[8, eq:4.17b]

where $A(x)$ is the sectional area. It is assumed that the longitudinal distribution of mass is the same as of the longitudinal distribution of displacement: thus the vertical distribution is neglected, and it is also assumed that CG of the ship is at the mid-ship section. For my calculations the center of gravity and loading are known and the (B) will cover the calculations according to strip theory.

According to the strip theory, the ship is considered to have different sections, for each of which the added mass is obtained. then the added mass, as is the ship's moment of inertia from the ship mass. Thus

$$\delta I_{yy} = \int_{-L/2}^{L/2} a_n x^2 dx \quad (2.45)$$

[8, eq:4.17{c}]

where a_n is the added mass for each section as determined in Heaving - Calculation of added Mass a_z .

According to my calculation [8, Example 4.12] & Added mass moment of inertia of each section [8, Example 4.12], the added mass moment of inertia for pitching

$$\delta I_{yy} = \int a_n \zeta^2 d\zeta \quad (2.46)$$

where ζ is the distance of the individual strip from the LCG position and virtual mass moment of inertia for pitching according to 2.43, which are calculated by Simpson rule (B.1). The total virtual mass moment of inertia for pitching are calculated here (B.2).

B.1&(B.1) .

Ship may go a simple harmonic motion about transverse axis if it is displaced from its equilibrium position and then released.

2.4.2. Damping moment

The damping moment are:

$$M_{b_\theta} = b_\theta \frac{d\theta}{dt} \quad (2.47)$$

The damping coefficient for pitching can also be obtained by the method of strip theory, that is determined for each section and then integrated over the entire length as follows:

$$b_\theta = \int_{-L/2}^{L/2} b_n \times \zeta^2 d\zeta \quad (2.48)$$

where b_n is the damping force coefficient for each strip along the ship's length (same as for Heaving), and ζ is the distance of the individual strip from the LCG (same as the LCB) position. According to Simpson rule my calculation for pitching are (B.3). [8, Example 4.12] & (B.2)

2.4.3. Restoring moment coefficient

The restoring moment for pitching can be expressed in the simple form

$$c\theta = \rho g \theta \int_{-L/2}^{L/2} x^2 y(x) dx = \rho g \theta I_y \quad (2.49)$$

where c is the restoring moment coefficient, and I_y is the moment of inertia of the load water-plane area. For small angles of inclination

$$c\theta = \rho g \nabla \overline{GM}_L \theta = \Delta \overline{GM}_L \theta \quad (2.50)$$

That restoring moment coefficient in this manner is valid only so long as the restoring moment for pitching can be considered to be linearly proportional to the angle of inclination θ . For calculations refer to (B.4), (B.3) & (B.4) for numerical value.

[8]

2.4.4. Free, damped Pitching Motion ($M_0 = 0$)

The equation of motion for pitching in calm water is according to the (2.41)

$$a_\theta \ddot{\theta} + b_\theta \dot{\theta} + c_\theta \theta = 0 \quad (2.51)$$

The solution for this equation is given (provided that $b < \sqrt{2aca}$ complex conjugate pair) by (2.14) or (2.15). Calculating the equation with initial conditions as: $\theta(0) = 0$ and the model speed (ship speed) $\dot{\theta} = 1.45 \text{ m/s}$ refer to the particular solution (A.5). For calculation look (B.4) and graphical solution. The acceleration movement is also plotted in the (B.1).

2.4.5. Exciting moment

The exciting moment for pitching is due to unbalanced moment caused by the waves about the transverse axis of the ship similarly explained in the Exciting force as for heaving. The free surface expression $\xi = \xi_a \cos(kx \cos \mu - \omega_e t)$ as in Heaving will be the driving periodic motion that influences the ship in Pitching also. Therefore the exciting moment on a section of a ship of unit length. The pitching moment can easily be developed by means of the hydro-static pressure distribution and adding the free surface expression and assuming the ship is symmetrical about the mid ship section and $M_\theta = M_0 \sin \omega_e t$ or $M_\theta = M_0 \cos(\omega_e t - \varepsilon_1)$ we get

$$M_0 = 2\rho g \xi_a \int_{-L/2}^{L/2} y(x) \times \sin(kx \cos \mu) dx \quad (2.52)$$

[8, eq:4.19c] where phase angle relative to waves $\varepsilon_1 = +90^\circ$, k being the normal wave number, μ is the direction of the ship's heading in relation to the waves. The non dimensional amplitude of the exciting moment for pitching can be expressed as

$$f_0 = \frac{M_0}{\frac{1}{2}\rho g \xi_a B L^2} = \frac{4}{B L^2} \int_{-L/2}^{L/2} y(x) \cos(kx \cos(\mu)) dx \quad (2.53)$$

[8, eq:4.19f]

Calculating according to the example [8, Example 4.17] the PVL101 amplitude of the exciting moment for pitching refer to B.5 & B.8.

2.4.6. Forced damped PVL-101 pitching differential equation and its solution

The general equation as mentioned is as follows: [8, 22] or (2.41)

$$a_\theta \ddot{\theta} + b_\theta \dot{\theta} + c_\theta \theta = M_{0_\theta} \cos(\omega_e t)$$

Which is similar to the one in Heaving and we can use the same general solution.

Then the solution can be expressed as

$$\theta = A_1 \exp^{\nu_{\theta} t} \sin(\omega_{d_{\theta}} t - \beta) + z_{a_{\theta}} \cos(\omega_e t - \varepsilon_{2_{\theta}}) \quad (2.54)$$

(2.25) or [20, eq:10.15]

As for pitching the first part dies out for steady state and the solution has only the second part in the end. We can use the same equations in the 2.2.6 for calculation of the amplitude of the forced momentum. As for numerical solution to the pitching equation refer to calculations B.6 & B.11, with initial conditions as $\theta(0) = 0$ and $\dot{\theta}(0) = 1.45$.

Refer to graphical solution Pitching movement θ and acceleration (B.3).

2.5. Rolling

As in the case of rolling, the following four moments act in rolling as for pitching motions:

- Inertial moment;
- Damping moment;
- Restoring moment;
- Exciting moment.

The equation of motion for linear rolling is analogous to that for pitching and is expressed as:

$$a_{\phi} \ddot{\phi} + b_{\phi} \dot{\phi} + c_{\phi} \phi = M_{0_{\phi}} \cos(\omega_e t) \quad (2.55)$$

For nonlinear the equation refer to (2.60).

where:

1. Inertial moment = $a_{\phi} \frac{d^2 \phi}{dt^2}$. Here a_{θ} is the virtual mass moment of inertia, and $\frac{d^2 \phi}{dt^2}$ is the angular acceleration of rolling.
2. Damping moment = $b_{\phi} \frac{d\phi}{dt}$. Here b_{ϕ} is the damping moment coefficient, and $\frac{d\phi}{dt}$ is the angular velocity. The damping moment is considered to be linearly proportional to the angular velocity for the simplicity, as in the case of heaving.
3. Restoring moment = $c_{\phi} \phi$. Here c_{ϕ} is the restoring moment coefficient, and ϕ is the angular displacement in rolling. Again the restoring moment is considered to be linearly proportional to the pitching displacement. this is true only for small angles of pitching.

4. The exciting moment, $M_{0_\phi} \cos \omega_e t$, is considered to be fluctuating with an encountering frequency of ω_e .

If we can determine the various values of a_ϕ , b_ϕ , c_ϕ and M_{0_ϕ} we shall be able to determine the motion characteristics for rolling. It should be noted that the coefficients a_ϕ , b_ϕ , c_ϕ and M_{0_ϕ} of rolling are not the same as those of heaving or pitching.

[8, 4.5]&C

2.5.1. Inertial moment

Inertial moment are:

$$M_{a_\phi} = a_\theta \frac{d^2\phi}{dt^2}. \quad (2.56)$$

The virtual mass moment of inertia for rolling a_ϕ , is the vessel moment of inertia for rolling plus the added mass moment of inertia for rolling, that is

$$a_\phi = I_{xx} + \delta I_{xx} = \Delta r_{xx}^2 + \delta I_{xx} \quad (2.57)$$

[8, eq:4.19r]

Were r_{xx} is the ships radius of gyration for rolling (refer to Accelerated rotational motion), and δI_{xx} is the added mass moment of inertia for rolling. By analytical and experimental investigations it has been found that the added mass moment of inertia for rolling is about 20% of the mass moment of inertia of the actual ship. The coefficient a_ϕ can be expressed as

$$I_{xx}'' = I_{xx} + \delta I_{xx} = \Delta r_{xx}''^2$$

[8, eq:4.19s&4.19t]

where δI_{yy} is the added mass moment of inertia for rolling, and r_{xx}'' is the virtual radius of gyration for rolling C.1. The mass moment of inertia of a ship for the rolling motion I_{xx} can be roughly estimated from the moment of inertia of the area under the ship's sectional area curve similarly as in here (2.44). As for PVL-101 we can get the information about the ships loading and mass displacement from [7], that is simplified in the Calculation of the radius of gyration and moment of inertia for rolling and pitching compartments for PVL-101 [8, Example 4.9][7, APPENDIX 1], which were the basis for the ship's mass moment of inertia calculations. So the ships mass moment of inertia consist of the ships loading of mass over the x axis and the lightship structure mass over the x axis which is assumed by empirical formula described in the (C.1), where $I_{xx} = \Delta r_{xx}^2$ (refer to r_{xx} in (C.1)).

Total virtual mass moment of inertia a_ϕ refer to Rolling - Calculation of the virtual mass moment of inertia a_ϕ also consist the added mass moment of inertia as in the

(2.57). The virtual mass moment of inertia of a ship for the rolling motion δI_{xx} can be roughly estimated from the moment of inertia of the area under the ship's sectional area curve also, but for simplicity and limited time considerations the calculation will be skipped and the empirical formula will be used $\delta I_{xx} = 0.2I_{xx}$ [8, page 75]. As the added mass moment of inertia is much smaller than the mass moment of inertia of the ship itself for rolling motion [8, 4.5].

The virtual moment of inertia for ship's rolling (I''_{xx} or a_ϕ), the added radius of gyration for rolling r''_{xx} and the ship's metacentric height GM over which the rotation takes place. Ship may go a simple harmonic motion about longitudinal axis if it is displaced from its equilibrium position and then released.

2.5.2. Damping moment

The damping moment are:

$$M_{b_\phi} = b_\phi \frac{d\phi}{dt} \quad (2.58)$$

The damping forces acting on a ship during rolling motion can be due to any combination of the following:

1. Waves generated - b_w ;
2. Water friction on the ship surface or eddy making - b_f ;
3. Bilge keels, skeg and other appendages - b_{bk}
4. Resistance between the ship and the air.
5. Energy loss of heat generated during the rolling motion.
6. Surface tension.

The effects due to causes 1, 2, and 3 are significant, whereas those due to causes 4, 5 and 6 are considered to be very small. As in the case of heaving and pitching motions, the damping coefficient is very important in rolling motion especially because the roll damping coefficient is relatively small, and the magnification factor may reach a value between 5 and 10. The damping coefficient b , due to wave making during the rolling motion, can also be calculated by the strip method. Since frictional effect plays a significant role in roll-damping the damping due to wave making alone may not be sufficiently accurate. In the first place the bilge keels or other appendages fitted to a ship may contribute significantly to the total roll damping effect caused by the generation of eddies. Second the ship's speed is also a contributing factor in roll damping, which has been found to be as much as three times larger when the ship is in motion than when it is not under way. Lastly, if the angle of roll is large, the linear damping law roll damping moment = $b(d\phi/dt)$ is not valid.

[8, 4.5]

There are various components of roll damping and in general practice to present the non-linear damping $b_\phi \frac{d\phi}{dt}$ are shown as follows:

$$b_\phi \dot{\phi} = b_{\phi_1} \dot{\phi} + b_{\phi_2} \dot{\phi} |\dot{\phi}| + b_{\phi_3} \dot{\phi}^3 \quad (2.59)$$

[15, eq:2-15]

where b_{ϕ_1} - linear damping coefficients; b_{ϕ_2} - quadratic drag coefficients; b_{ϕ_3} - cubic damping coefficients. As for simplicity I will not calculate the various damping coefficients due to I have information about the ship's rolling period in calm water and will make a assumption, that the rolling period of ships turn will be approximately the same as ships free rolling period in beam sea. For simplification the ship operator conducted a test as mentioned and I received information about the ships period on a turn and made some approximation calculation with damping to approximate it when the period of the ship were $T = 8 s$ in a 20° roll angle. For large amplitudes the rolling motion is complicated due to non-linear damping and non-linear restoring moment and is out of the current thesis and will not be covered.

Calculation of the numeric damping coefficient based on a ships operator test in turn refer to (C.2). The general consent of the calculation are as follows:

The roll movement angular frequency measured in test look the (C.1):

$$\omega_{d_\phi} = \frac{2\pi}{T} \quad (2.2)$$

Calculated from rolling restoring coefficient and inertial moment the ship, we can calculate the natural frequency, refer to (2.5.3) :

$$\omega_\phi = \sqrt{\frac{c_\phi}{a_\phi}} \quad (C.7)$$

Referring to the previous equations for the Heaving and Pitching differential equations, we can calculate the following for rolling. As I know the circular frequency of the damped rolling motion ω_{d_ϕ} , that was measured by the ship operator and from equation (2.17) I can calculate the decaying constant ν_ϕ for rolling

$$\nu_\phi = \sqrt{\omega_\phi^2 + \omega_{d_\phi}^2}$$

and from decaying constant equation (2.16) I can calculate the non-linear damping b_ϕ

$$b_\phi = 2a_\phi \cdot \nu_\phi$$

2.5.3. Restoring moment coefficient

The swing analogy leads to the differential equation of a variable length pendulum. the general equation for non-linear roll angle is:

$$a_\phi \ddot{\phi} + b_\phi \dot{\phi} + C(t)_\phi \sin \phi = 0 \quad (2.60)$$

[12] or

$$a_\phi \ddot{\phi} + b_\phi \dot{\phi} + c_\phi (\phi) = 0$$

With assumption that $C(t)$ and [12] showed that in calm water GM oscillates around its mean value GM_m and also that the amplitude GM_a of the oscillation is proportional to the wave elevation. The [12] describes dynamical models of extreme rolling of vessels, which are in resonant conditions as the ship length is about the length of the encountering wave. This could be in the Baltic sea with wave period of $7.7 s$, average length of $61.8 m$ and height of $3.2 m$ [14]. In the case of a single frequency wave with angular velocity ω , [?, Dunwood [5]ClaudeArcher results give:

$$C(t)_\phi = \Delta(GM_m + GM_a \cos(\omega t)) \quad (2.61)$$

[12, eq:1.2]. For simplicity I will not calculate the resonant case as the encountering wave length in my assumption are not in the resonant conditions.

For small angles of inclination $c_\phi \phi \simeq \Delta GM$, ϕ , which is a linear representation it will be used the (2.55) and the solution is similar to Pitching and the restoring coefficient can be expressed as follows with numerical value (C.4):

$$c_\phi = \rho g \nabla \bar{GM} \quad (2.62)$$

[8, 4.21c]

For nonlinear the restoring moment of a ship for rolling motion is the righting moment at any particular angle, that are bigger than 10° and for any particular angle of inclemation is expressed as

$$c_{\phi_{nonlin}} = g \Delta \bar{GZ}(\phi) \quad (2.63)$$

[8, eq:4.21b]

where Δ is the displacement of the ship and $GZ = KN - \bar{K}G \sin(\theta) - DGZ$ (A) are the rightening arm which both are known conditions in current case C.2 & [7]. So I can calculate the c_ϕ as for non-linear case, assuming that we have the wall-sided ship. I know heeling angle is $\phi = 0.349 rad$ or (20°) and the rightening arm in that

condition [7]. As large angles of inclination, it can be shown that for a wall-sided ship, up to the angle at which the deck edge enters the water (Rawson and Tupper, 1965):

$$\bar{GZ}(\phi) = \bar{GM} \sin \phi + \frac{\bar{BM}}{2} \cdot \tan^2 \phi \cdot \sin \phi \quad (2.64)$$

[21, Section 4.12 eq: (12)], where \bar{GM} and \bar{BM} refer to C.2.

So I will calculate firstly the linear restoring coefficient (C.4) and then I will approximate the nonlinear restoring coefficient which is here (C.5). For small angles of inclination is valid only for small amplitudes of rolling displacement (say 10°), were I can get the natural frequency, but in our case I will solve the equation numerically by MATLAB, as I know the initial conditions (say 20°) for the function. So I can also calculate the natural frequency refer to (C.7).

$$\omega_\phi = \sqrt{\frac{c_\phi}{a_\phi}} \quad (2.65)$$

Based on the [7, APPENDIX 1] data in the figure 2.2 it is necessary to linerize the \bar{GZ} and according to the [33, eq: 2.7] it seems that most popular approach is the application of a polynomial power series. For simplification I will use the 3th order polynomial power series to fit the \bar{GZ} curve. Which I find to be by MATLAB function poly-fit:

$$p(\phi) = \bar{GZ}(\phi) = C_1\phi^3 + C_2\phi^2 + C_3\phi^1 + C_4\phi^0 \quad (2.66)$$

For exact solution refer to (C.9) and the nonlinear restoring coefficients $c_{\phi_{nonlin}}$ can be calculated according to the (2.63), which are here (C.10).

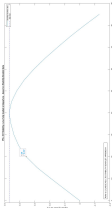


Figure 2.2.: PVL-101 Stability curve \bar{GZ} fully loaded at departure - based on Stability Booklet data[7, APPENDIX 1]

2.5.4. Free, damped Rolling Motion ($M_0 = 0$)

The equation of motion for pitching in calm water is according to the (2.41)

$$a_\theta \ddot{\phi} + b_\theta \dot{\phi} + c_\theta \phi = 0 \quad (2.67)$$

and in ship theory the equation is expressed in normalized form for simplification as

$$\ddot{\phi} + 2\nu_\phi \dot{\phi} + \omega_\phi^2 \phi = 0 \quad (2.68)$$

I will assume that we are looking a function in a form as firstly is needed to calculate the free rolling movement without damping in small inclining angles and the linear representation.

$$\phi = A \cos \omega_\phi t \quad (2.69)$$

The solution for this equation is given (provided that $b < \sqrt{2aca}$ complex conjugate pair) by (2.14) or (2.15). If to take into account the damping then I will assume that we are looking for a solution that is distinct with real roots as the rolling motion is over-damped and the solution will be:

$$\phi = B1 \exp^{\lambda_1 t} + B2 \exp^{\lambda_2 t} \quad (2.70)$$

[13] for exact solution refer to (C.4), where λ_1 and λ_2 are the characteristic equation solution's and $B1$ and $B2$ are constants. Calculating the equation with initial conditions as: $\phi(0) = 10^\circ$ and the model speed (ship angular speed) $\dot{\phi} = 0$. For calculation look added MATLAB printout and graphical solution in here C.4 . The acceleration movement is also plotted (C.4).

As in the case the equation are non-linear (if heeling angle over 10°) the restoring coefficient c_ϕ and the rightening arm \bar{GZ} are not linearly dependent refer to the (2.63) and (2.66). For simplicity I will assume the damping coefficient is linear. Then the normalized roll equation becomes:

$$\ddot{\phi} + 2\nu_\phi \dot{\phi} + \frac{g}{r''_{xx}} \bar{GZ}(\phi) = 0 \quad (2.71)$$

[26, eq:2.6] where g is the gravity acceleration and r''_{xx} is the virtual gyration radius of the ship (which is assumed to be constant). The assumption is made for the linear case that the damping motion and the inertia moment are functions of ϕ alone and the non linearity will be avoided. Also it should be noted that the vessel is rolling in waves and the angle of roll must include the wave slope. The nonlinear equation and the exciting moment will be presented in the next section as the rolling in large angles (over 10°) takes place only with some moments that will effect on the vessel. Evaluation the PVL-101 Stability curve \bar{GZ} , it can be said that up to 20° it is almost linearly dependent and for time limitations I will not calculate the non-linear equation solution for rolling.

2.5.5. Exciting moment and linear forced rolling motion with damping

The exciting moment for rolling is due to unbalanced moment caused by the changes of buoyant force while the ship is in waves. The moment is calculated by integrating for each ship section the difference in buoyancy of the triangles in the figure C.5. The free surface expression $\xi = \xi_a \cos(kx \cos \mu - \omega_e t)$ as in Heaving and Pitching will be the driving periodic motion that influences the ship in rolling also. Therefore the exciting moment on a section of a ship of unit length. The rolling moment can easily be developed by means of the hydro static pressure distribution and adding the free surface expression and assuming the ship is symmetrical. [8] The slope of the free surface is as the

$$\tan \phi = \frac{z}{y}$$

and

$$z = y \times \tan \phi$$

where y is the half breadth of the ship and ϕ is the rolling angle. The area PQR from figure C.5 is $\frac{1}{2}y \times \tan \phi$, and the moment of buoyancy for the triangle is $\rho g (\text{volume}) \times \frac{2}{3}y$. [8, page 85]

The moment is then

$$M_\phi = \left[\frac{2}{3} \rho g k \xi_a \sin(\mu) \int_{-L/2}^{L/2} \cos(kx \cos(\mu)) y^3 \cdot dx \right] \sin \omega_e t \quad (2.72)$$

[8, eq: 4.26a] since the free surface expression $\xi = \xi_a \cos(kx \cos \mu - \omega_e t)$ the wave slope

$$\frac{\partial \xi}{\partial y} = \alpha'_m \cos(kx \cos(\mu)) = k \xi_a \sin \mu \cos(kx \cos(\mu)) \quad (2.73)$$

where μ is the encountering angle of the wave and ship. As wave height H are known from [16, page 28] the wave amplitude are $\xi_a = \frac{H}{2}$. And the exciting moment is assumed to be $M_\phi = M_0 \sin(\omega_e t + \varepsilon_1) t$ or $M_\theta = M_0 \cos(\omega_e t - \varepsilon_1)$ with the amplitude

$$M_0 = \frac{2}{3} \rho g k \xi_a \sin \mu \int_{-L/2}^{L/2} \cos(kx \cos(\mu)) y^3 dx \quad (2.74)$$

[8, eq:4.26b] where phase angle between exciting moment and wave elevation is $\varepsilon_1 = -90^\circ$, k being the normal wave number, μ is the direction of the ship's heading in relation to the waves. The non dimensional amplitude of the exciting moment for rolling can be expressed as

$$f_0 = \frac{M_0}{\rho g k \xi_a L B^2 T} = \frac{2 \sin \mu}{3 L B^2 T} \int_{-L/2}^{L/2} \cos(kx \cos(\mu)) y^3 \cdot dx \quad (2.75)$$

[8, eq:4.26d]

And the exiting moment amplitude in beam seas ($\mu = 90^\circ$):

$$M_0 = \rho g \nabla k \xi_a G M \quad (2.76)$$

[8, eq:4.26e]. Since $\frac{2}{3} \int y^3 dx$ is the transverse moment of inertia of the water plane area and the wave slope are $k \xi_a$, as we have the $\alpha_m = k \xi_a \sin \mu$. For any other angle of wave

$$M_0 = \rho g \nabla \alpha_m G M$$

$$M_\phi = c_\phi \alpha_m \sin \omega_e t \quad (2.77)$$

where c_ϕ is the restoring moment coefficient.

Calculating according to the example [8, Example 4.23] the PVL101 amplitude of the exciting moment for rolling refer to C.5 and C.1 with numerical value in C.14.

2.5.5.1. Forced damped PVL-101 rolling differential equation and its linear solution

The general equation as mentioned is as follows for linear rolling: [8, 22] or (2.41)

$$a_\phi \ddot{\phi} + b_\phi \dot{\phi} + c_\phi \phi = M_{0_\phi} \cos(\omega_e t)$$

Which is similar to the one in Heaving and Pitching and we can use the same general solution.

Then the solution can be expressed as

$$\phi = A1 \exp^{\nu_\phi t} \sin(\omega_{d_\phi} t - \beta) + z_{a_\phi} \cos(\omega_e t - \varepsilon_{2_\phi}) \quad (2.78)$$

(2.25) or [20, eq:10.15]. The first part is the (2.70) and graphical solution in MATLAB printout at (C.4).

As for rolling the first part dies out for steady state and the solution has only the second part in the end. We can use the same equations in the 2.2.6 for calculation of the amplitude of the forced momentum. As for numerical solution to the rolling equation refer to calculations C.6, with initial conditions as $\phi(0) = 20^\circ$ and $\dot{\phi}(0) = 0$.

Refer to graphical solution Rolling in beam seas of the PVL-101 θ and acceleration (C.7). Also the bow seas (C.8) and acceleration (C.9).

Due to limited time, calculations of the non-linear equation are non, and it will be assumed that for current conditions the linear equation are satisfactory, as the restoring of the ship in 20° are almost linear (refer to 2.2).

3. Two Degrees of Freedom

Spherical parallel mechanism

3.1. Overview and problem statement

The purpose is to design a UAV helicopter landing platform that are projected on a Estonian Police and Border Guard ship “Kindral Kurvits” PVL-101, that will try to hold the top plate steady as ship will Roll or Pitch. For simplification the Heave motion or vertical motion for the platform function will be neglected as for helideck’s on ships it will be measured as Significant Heave Rate (SHR). The value of the SHR is the average of the one-third highest values of instantaneous heave rate recorded during the previous 20-minute monitoring period. This can more conveniently be calculated by:

$$RMS_{hr} = \sqrt{\frac{1}{20\text{min}} \left(\int_{t-20\text{min}}^t hr(t)^2 dt \right)} \quad (3.1)$$

where hr is the heave rate in meters per second and for category A and category B helicopters the maximum value are 1.0 m/s [17, 10].

As for UAV helicopter there are no requirements and this value should be calculated by the UAV manufacturer or operator how this will influence the drone. So the Heave motion compensation of the platform will be the future development issue. The PVL-101 Heave motion in my calculated condition’s are quite large, refer to figure (A.3), and it will be wise to add a degree of freedom to the platform, but this will complicate the technical solution and my study will focus on the two degrees of freedom mechanism.

3.1.1. Two degrees of freedom mechanisms design and comparison

In this section it will be compared of 4 different kind of technical solutions, that could be possible and justify preferred choice for the spherical parallel manipulator. The customer needs are described in the first chapter and answers to the question “What is the problem?”, which are related to the functional requirements as “How?” the

problem will be solved. The detailed description of the complicated ship movement is part of the customer problem and are necessary to address the functional domain. I will use the axiomatic design principles, which are developed by the professor Nam P. Suh:

- Axiom one: Maintain the independence of the functional elements. An optimal design always maintains the independence of functions;
- Axiom two: Minimize the information content. The best design is a functionally uncoupled design that has minimum information content.

[6, Chapter 13]

To ask the question “How the design looks?”: refer to:

- the kinematic sketch for general concept refer to figure (D.1);
- design parameters for mechanical parts refer to chapter (4);
- design parameters for platform automation concept process for rolling and pitching refer to chapter (??).

As for limited time, this thesis do not try to give fully detailed design of the product and can not answer to the question “How to produce the platform?”, but will keep in mind the Design For Manufacturing concept. The constraints list will be described in the chapter (4). As for the design process of the 2DOF SPM, there are implemented the zigzagging decomposition between domains to get the best solution for the customer. The zigzagging are done intuitively.

[6, Chapter 13]

The ship motions where described earlier and for know I will not take into account the coupling of the 3 motions to simplify the problem. The modeling of hydrodynamic behavior of ships and their responses to environmental influences are the distrurbances to the platform. Firstly I developed a table of the different 2 DOF mechanisms and the principal functions to solve the platform roll and pitch motion kinematics which refer to (D.1). The joint type complexity of the solution is a value from [0 to 1] and are calculated according to the following equation:

$$K_j = \frac{1}{n} (nR \cdot K_{G|R} + nP \cdot K_{G|P} + nC \cdot K_{G|C} + nS \cdot K_{G|S} + nH \cdot K_{G|H} + nF \cdot K_{G|F}) \quad (3.2)$$

where n is the total joints used; nR , nP , nC , nS , nH , nF are the number of revolute (nR), prismatic or transnational (nP or nT), cylindrical (nC), spherical (nS), helical (nH), and planar (nF) joints [24, eq: IV.4].

The joints geometric complexity values are taken from the [24, table IV.1]. Besides the Two degrees of freedom mechanisms design and comparison I will account also the axiomatic design principles for the simplified geometric complexity value (every aspect that conflict the design rules gives 0.1). According to the complexity based rules [30] a robot architecture should be minimally complex if we take into account

six aspects, where calculated the complexity for all four solutions accordant to the (3.3) and refer to tab (D.1). Due to simplicity will not be calculated the link diversity and actuator-diversity as will be use only elector-mehcanical actuators and the links are parallel, which i will take into account by analyzing geometrically and analytically the solution. A set of design rules that I will take into account are following:

1. The number of joints in a robot should be minimized to increase stiffness, which lead to a trade off between the stiffness and the mass of the joint;
2. Increasing the number of loops has a minor impact on the stiffness of the robot and needs to be justified;
3. Elector-mehcanical actuators are more compliant than hydraulic actuators - as the torque applied is proportional to the current passing through;
4. Increasing the number of joints and loops increases the manufacturing cost;
5. The six lower kinematic pairs are analyzed as “loss of regularity” (How far a given surface lies from singularities). At singular configuration, the end-effect or or kinematic pair has an uncontrollable DOF-s and loses its inherent stiffness;
6. The revolute joints are easiest to maintain and are preferred;
7. Increasing the diversity in geometric constraints between joints increases the manufacturing cost;
8. Electromagnetic actuators have a lower life-cycle cost than their hydraulic counterparts;
9. Increasing the actuator diversity increases the cost of the robot;
10. Increasing the number of loops can only decrease the workspace volume,
11. A Revolute joint at the base of a serial robot is desirable for an axially symmetric work- space;
12. A Prismatic joint at the base of a serial robot is desirable for work spaces with extruded symmetry;
13. Increasing the number of joints decreases agility;
14. Addition of loops to allow actuator(s) placed closer to the base increases agility;
15. In robotics, the use of hydraulic actuators increase agility.

[30]

The simplified geometric complexity of the solution:

$$K = w_A K_A + w_{CO} K_{CO} + w_{Acc} K_{ACC} + w_N K_N + w_j K_j + w_L K_L \quad (3.3)$$

[30] where weight's $w_A = 0.2$; $w_{CO} = 0.3$; $w_{Acc} = 0.2$; and $w_N = w_j = w_L = 0.1$ as all the weights must equal 1. Refer to the (D.1) for the complexity coefficient's K_A , K_{CO} , and etc.

As the simplest solution are Spherical Parallel Manipulator refer to tab (D.1) and taking into account the design rules the solution one is the optimum. The further axiomatic design concept will be implemented only to solution number one (SPM). As the SPM has two loops or branches it is independent only on pitching, as we can adjust the pitching separately and the rolling are dependent on both motor actuation [9]. Similar to the solution two in the (D.1), the Airbus has developed a moving platform with linear actuators ("Deck Finder" [?]), but as the principal solution is quite complicated in that case and the manufacturer will define the product as a high-end positioning sensor that supports naval operations. The Airbus solution has 3 Degrees of Freedom, so it is out of this study. Concerning the concept for the automation and working as a sensor for remotely piloted aerial vehicles (RPAS) will be analyzed in the 5th chapter, as the 2 degrees of freedom solution probably will have similar solution.

Brief description of the solution one:

The kinematics of a two rotational degrees-of-freedom (DOF) spherical parallel manipulator (SPM) is developed based on the coordinate transformation approach and the cosine rule of a trihedral angle. The angular displacement, angular velocity, and angular acceleration between the actuators and end-effect or are thus determined. Moreover, the dynamic model of the 2-DOF SPM is established by using the virtual work principle and the first-order influence coefficient matrix of the manipulator. Eventually, a typical motion plan and simulations are carried out, and the actuating torque needed for these motions are worked out by employing the derived inverse dynamic equations.

[9]

3.2. Description of the Spherical Parallel Manipulator

As shown in figure (D.1), the lower triangular platform of the 2-DOF SPM is the base, and the upper platform is the end-effect or (more generally called the mobile platform), which has only two rotational degrees of freedom. The mobile platform and the base are connected by two active branches and one vertical supporting column. All the joints between links in the two branches of the manipulator are revolute. The lower end of the supporting column is fixedly mounted to the base, and its upper end is hinged with the mobile platform with a universal joint. According to the conventions of the spherical mechanism, when putting into operation, all points on the branch linkages move on a spherical surface whose center is a specified point. Additionally, all the axes of the revolute joints intersect at a center point called the

kinematic center. Grubler formula

$$M = d(n - g - 1) + \sum_{i=1}^g f_i + v - \zeta \quad (3.4)$$

[9] where $d = 3$ is the number of common constraints for the spherical mechanism, n is the number of parts, g is the number of joints, f_i is the degrees of freedom of the i th joint, v is the number of redundant constraints, and ζ is the isolated degree of freedom. In this case, $n = 6$, and the number of joints is $g = 7$. For the universal joint, $f_1 = 2$, for the other six revolute joints, $f_i = 1$. There is no redundant constraint and isolated degree of freedom, so $v = 0$, $\zeta = 0$. Thus, the degrees of freedom of this mechanism are $M = 2$. In order to describe this 2-DOF SPM, a global coordinate system $O - XYZ$ and the local coordinate systems $O - X_{ij}Y_{ij}Z_{ij}$ were established. as shown in figure (D.1).

The position vectors of the six revolute joints in their local coordinate systems are presented in figure (D.1):

$$\begin{aligned} p_1 &= [R, 0, 0]^T, & p_2 &= [0, R, 0]^T, & b_1 &= [R, 0, 0]^T \\ t_1 &= [R, 0, 0]^T, & t_2 &= [0, R, 0]^T, & b_2 &= [0, R, 0]^T \end{aligned} \quad (3.5)$$

where P_1, T_1, B_1, P_2, T_2 and B_2 represents the position vectors of center point of each revolute joint in the global coordinate system ($O - XYZ$), and R is the top plate radius. As the local coordinate systems $O - X_{1j}Y_{1j}Z_{1j}$, in branch 1 and 2 (as $j = 1, 2, 3$) constantly points to the center of the revolute joint from origin O . [9]

3.2.1. Kinematics

Due to the mechanical constraint of the universal joint, the mobile platform practically has only two degrees of freedom, including roll angle ϕ_x and pitch angle θ_y . Based on the knowledge of robotics, the coordinate transformation matrices of the mobile platform in Euler angle form are:

$$R_y(\theta_y) = \begin{bmatrix} \cos(\theta_y) & 0 & \sin(\theta_y) \\ 0 & 1 & 0 \\ -\sin(\theta_y) & 0 & \cos(\theta_y) \end{bmatrix} \quad (3.6)$$

$$R_x(\phi_x) = \begin{bmatrix} 1 & 0 & 0 \\ 0 & \cos(\phi_x) & -\sin(\phi_x) \\ 0 & \sin(\phi_x) & \cos(\phi_x) \end{bmatrix} \quad (3.7)$$

where ϕ_x and $\theta_y = \phi_y$ are roll and pitch angles of the mobile platform. [9]

Assume that the original state of the 2-DOF SPM is that the local coordinate system $O - X_{11}Y_{11}Z_{11}$ coincides with the global coordinate system $O - XYZ$.

The detailed description is in the article [9] about kinematics and the two equations for the roll and pitch are as follows:

$$\phi_y = \theta_y = \arcsin \frac{c1}{\sqrt{a_1^2 + b_1^2}} - \arctan \frac{b_1}{a_1} \quad (3.8)$$

$$\phi_x = \arccos \frac{c2}{\sqrt{a_2^2 + b_2^2}} - \arctan \frac{b_2}{a_2} \quad (3.9)$$

where $a_1 = \sin \beta \cdot \cos \alpha_1 - \cos \beta \cos \theta_1 \sin \alpha_1$, $b_1 = \cos \beta \cos \alpha_1 + \sin \beta \cos \theta_1 \sin \alpha_1$, $c_1 = \cos \alpha_2$, $a_2 = -\sin \phi_2 \sin \alpha_1 \sin \theta_y + (\cos \beta \cos \theta_2 \sin \alpha_1 - \sin \beta \cos \alpha_1) \cos \theta_y$, $c_2 = \cos \alpha_2$. With initial conditions ($\beta = 36.87^\circ$; $\alpha_1 = 25^\circ$; $\alpha_2 = 35^\circ$; $\theta_1 = 0^\circ$; $\theta_2 = 0^\circ$) look the MAT LAB script for calculations in the Appendix (E.2). From the solutions to the forward kinematics mentioned above, one can infer that the rotation of the mobile platform around the Y axis is only dependent on the motion of actuator 1. Compared with this conclusion, the rotation of the mobile platform around X axis is dependent on the motion of both actuators. [9]

3.2.2. Analysis of Velocity and Acceleration

The velocity and acceleration analysis plays a key role in the mechanical design, controller design, and hardware configuration. Let

$$\phi = (\phi_y, \phi_x)^T, \dot{\phi} = (\dot{\phi}_y, \dot{\phi}_x)^T, \text{ and } \ddot{\phi} = (\ddot{\phi}_y, \ddot{\phi}_x)^T$$

be the orientation, rotation velocity, and rotation acceleration vectors of the mobile platform, respectively. Let

$$\phi = (\phi_1, \phi_2)^T, \dot{\phi} = (\dot{\phi}_1, \dot{\phi}_2)^T, \text{ and } \ddot{\phi} = (\ddot{\phi}_1, \ddot{\phi}_2)^T.$$

be the angular displacement, angular velocity, and angular acceleration vectors of the actuators, respectively. This section will deal with the input–output relation of the velocity and acceleration of the 2-DOF SPM. By differentiating Equations(3.8) and (3.9) with respect to time, Equation can be obtained in the following form

$$\mathbf{A}\dot{\phi} + \mathbf{B}\ddot{\phi} = \mathbf{0} \quad (3.10)$$

where

$$A = \begin{bmatrix} f_{11} & 0 \\ f_{21} & f_{22} \end{bmatrix}$$

$$B = \begin{bmatrix} l_{11} & 0 \\ 0 & l_{22} \end{bmatrix}$$

and

$$f_{11} = (\cos \alpha_1 \sin \beta - \cos \beta \cos \theta_1 \sin \alpha_1) \cos \theta_y - (\cos \alpha_1 \cos \beta + \cos \theta_1 \sin \alpha_1 \sin \beta) \sin \theta_y;$$

$$f_{21} = (\cos \alpha_1 \sin \beta - \cos \beta \cos \theta_1 \sin \alpha_1) \sin \theta_y \sin \theta_x - \sin \alpha_1 \sin \phi_2 \cos \theta_y \sin \theta_x;$$

$$f_{22} = \cos \theta_x [\cos \theta_y (\cos \beta \cos \phi_2 \sin \alpha_1 - \cos \alpha_1 \sin \beta) - \sin \alpha_1 \sin \phi_2 \sin \theta_y] - (\cos \beta \cos \alpha_1 + \cos \phi_2 \sin \alpha_1 \sin \beta) \sin \theta_x;$$

$$l_{11} = -\cos \theta_y \sin \alpha_1 \sin \beta \sin \phi_1 + \cos \beta \cos \alpha_1 \sin \phi_1 \sin \theta_y;$$

$$l_{22} = -\cos \theta_x \sin \alpha_1 \sin \beta \sin \phi_2 - \cos \beta \cos \phi_y \sin \phi_1 \sin \theta_2 \sin \theta_x - \cos \phi_2 \sin \alpha_1 \sin \theta_x \sin \theta_y$$

[9]

For kinematic calculation's refer to the appendix E.2 and the representation of the joints for initial conditions look D.5.

4. Per-project of the 2 DOF SPM design and construction calculations

4.1. Overview

In this chapter the construction will be physically modeled. For reference is the kinematic analysis of the joints, some requirements from standards for offshore Helicopter landing areas and customer requirement. The failure criteria is the failure by yielding or plastic deformation. The purpose is also to calculate the stresses in the links and joints and for that it will be modeled a simplified loading condition scenario. The basis for this chapter are the ships motions and the kinematic analysis of the construction.

4.2. The mechanical concept, constraints and design steps

The start point of the project will be the kinematic diagram figure and schematic (D.3), 2DOF SPM calculations and the joints initial conditions (in figure (D.5)). The initial statement were that the maximum heeling angle will be 20° were we will try to operate the platform. So all other constraint and requirements will come from that and are as follows:

1. Platform maximum rolling and pitching angle, where the top plate will be horizontal: $\pm 20^\circ \pm 1^\circ$;
2. Calculated minimum height from deck and base plate are 1.2 m , if the motors are in the base plate;
3. The ships maximum acceleration in roll, pitch and heave are the external forces for the platform loading (refer to (2));
4. Circular Platform top plate diameter are 4 m ;
5. Platform must tolerate up to 275 kg static external load;
6. the max MTOW of the UAV 110 kg ;

7. Initial material to be considered is aluminum alloy (as it is lighter than steel);
8. Air temperature $-25^{\circ}C$ up to $+50^{\circ}C$;
9. Offshore environment with water temperature $-0.8^{\circ}C$ up to $20^{\circ}C$;
10. The initial concept of the platform is the solution number one in the fig (D.1);
11. Requirements for structural design I will take from: ISO 19901-3 [18]; [25]; and [17];
12. Initially I will choose the Yaskawa rotary Servo motor SGMGV-09A with power $P = 0.85 kW$ and rated torque $T = 5.39 Nm$, which has the encoder, speed reducer and brake;
13. Cost is approximately 10000 €.

4.2.1. Mechanical Design steps

1. Layout configuration and specifying the functions of elements. Constructing the preliminary model of the platform with all links and joints and calculate the reaction forces after solving the kinematics and dynamics with the worst scenario as the UAV helicopter will try to land on the edge of the platform and opposite to the Branch X and Branch Y. Firstly will be choose d the the link 1, 2 and 4, 5 positions according to the kinematic diagram (D.1). After that it will be inserted the motor positions and re-evaluate the kinematic structure, but the main coordinate system will be the same for all joints. The difference will be only about the link 1, 2 and 4,5 length. the rotation must be positioned in the described axes (X11, X12, X13 etc). Then it will be modeled the platform kinematics and dynamics and compare the motor maximum torque to the required torque as the initial material was aluminum and the top plate mass are 362 kg. The torque calculation will take into account only the number 3 Top plate moment of inertia over x-axis and y axis as the ships angular accelerations for roll and pitch have already calculated. Also I will take into account the heave motion (up and down), and the UAV helicopter weight as the external force.
2. Selecting the parts and material for assembly all functions. Looking for standards parts.
3. Selecting the initial manufacturing processes for parts.
4. Selecting the potential critical sections and critical points for detailed analysis (points that have high probability to fail).
5. Design of components: I will determine the stresses acting on the platform, choose proper material, determine the likely failure mode in the worst scenario, and determine the geometric dimensions. This will be done mainly by the FEM analysis to the critical parts, but if the simple analytical calculation is faster

it will be used for other necessary parts. The over check calculations will be done in the end if necessary and standard part will not be calculated.

6. Design of other considerations: corrosion, maintainability, assemble of the platform and work drawings. General arrangement of the platform in the ship.

4.3. Preliminary model

The preliminary model of the platform is based on the kinematic's in the figure D.1 and the section E.2 joints calculations. The figure 4.1 is the initial assembly, which maximum elevation angle on both of the Branches are 20° , which motion envelope can be seen in figure 4.2. Compared to the initial kinematics (refer to figure D.1) the actual assembly joint location's are bit different, but all of them are located in the local axes as in the sketch. The cause of this is the location of the motor gearbox and associated bearings and connections, which all will need to be in the same axis es on both branches. The links are connected with revolute joints, as the joint has two sleeve bearings and upper links (number 1 and 4) are connected with the lower ones with ears, bushings and the shaft is centered and fixed with a clevis pin or bolt. The center of the plate a connected to the fixed post with universal joint, that are used in the car industry. The universal joint yoke's and center cross (spider) are connected through pivot needle bearings to bearing cap, lock plate and cap screws. As to time limitations, these components are not going to be modeled and the Assembly only has the virtual parts. Refer to the table for the parts and their function.

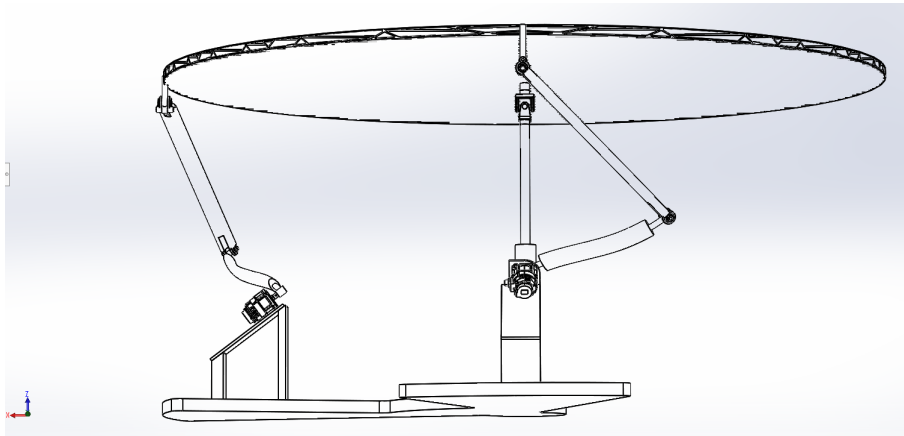


Figure 4.1.: Initial Assembly

The following table will give an overview of the assembly parts and their functions. if the part is commercially available, it will be added the manufacturer part number and approximate price. The table will give a top-down assembly model. As

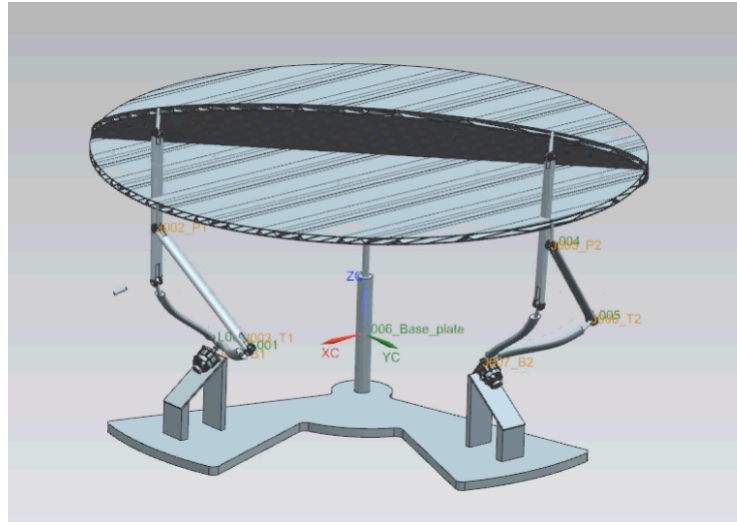


Figure 4.2.: Assembly motion envelope

Top-down assembly modeling is an assembly-centric modeling method where the assembly design is started at the highest level possible, and individual parts and sub assemblies are defined within the context of the overall assembly. With this approach, an assembly layout is created first as the chapter 3 kinematic approach was. This assembly layout is used to define individual part geometry and position and if needed in future the assembly can be continually improved over the product life cycle.

| |
|--------------------------------------|
| Principal Mechanical Solution |
|--------------------------------------|

Table 4.1.: 2 DOF platform's principal solutions and functional requirements comparison

| Part or sub assembly name | Functional requirement | Initial Manufacture and material | Part number and manufacturer | Critical part | Price |
|--|--|--|---|---------------|--|
| 03 Top Plate Assembly (Top Plate- link 3, Center Yoke, X branch, and Y branch revolute joint links connection, 2 x shaft) | To hold the UAV helicopter weight and give a reference landing point and connect the plate to links (X and Y branch, center to universal link spider). Shaft will provide the rotational movement on X and Y branch and takes the torsional loads. | Extruded customized aluminum profile blocks welded together. Revolute joint links are machined CNC part and welded to the Top plate structure. | 6082 T6T651, Aalco,; Shaft material AW6060/6061 p/n AWMP-30; MOOG yoke that fits the U_JOINT 231. | Yes | $3 \text{ €/kg} \times 362 \text{ kg} = 1086 \text{ €}$. Also depends on the welding |
| 01 Link 1 Assembly (Link 1, 2 × Bushing link 1 Middle, 4 × Sleeve bearing) | Connect the top plate with Link 2 (2 Link 2 bend) to give the rotational movement over the X11 & X12 axis. Transfer the driving link loads to the Top plate. | Bend link is CNC machined part with Aluminum 6082 T6T651. Bushings CNC made. | Sleeve bearing P/N XSM-3034-16 | Yes | Depends on the machining. |
| 04 Link 4 Assembly (Link 4, 2 × Bushing link 1 Middle, 4 × Sleeve bearing) | Connect the top plate with Link 5 (5 Link 5 bend) to give the rotational movement over the Y21 & Y22 axis. Transfer the driving link loads to the Top plate. | Bend link is CNC machined part with Aluminium 6082 T6T651. Bushings CNC made. | Sleeve bearing P/N XSM-3034-16 | Yes | Depends on the machining. |

Principal Mechanical Solution

Table 4.1.: 2 DOF platform's principal solutions and functional requirements comparison

| | | | | | |
|---|--|---|--------------------------------|-----|--|
| UJ – bearing cross (Spider) | Connects the Top plate to the fixed Yoke and gives the 2 DOF rotational movement over the x and y axis. Supports the loads and transfers them to the needle bearings. | MOOG Aluminium 6061 | P/N 231 | Yes | 30 € |
| 02 Link 1 Assembly (Link 1, 2 × Bushing link 1 Middle, 4 × Sleeve bearing) | Driving Link. Connect the top plate with Link 1 (1 Link 1 bend) and Drive to give the rotational movement over the X12 & X13 axis. Transfer the driving link loads to the Top plate. | Bend link is CNC machined part with Aluminium 6082 T6T651. Bushings CNC made. Shaft 6061. | Sleeve bearing P/N XSM-3034-16 | Yes | Depends on the machining. |
| 05 Link 1 Assembly (5 Link 5 bend, SHAFT) | Driving link. Connect the top plate with Link 4 (4 Link 4 bend) and Drive to give the rotational movement over the Y22 & Y23 axis. Transfer the driving link loads to the Top plate. | Bend link is CNC machined part with Aluminium 6082 T6T651. Bushings CNC made. Shaft 6061. | Sleeve bearing P/N XSM-3034-16 | Yes | Depends on the machining. Shaft $45.48 \frac{\text{€}}{\text{m}}$ $\sim 1 \dots 1.5 \text{ m}$. |
| Support structure Assembly : center mast, base plate, drive support stand, Link 2 and Link 5 connection bearings and gearbox connections to the Base plate, fixed Yoke, etc. | Support the critical Assemblies to function the kinematics. | Aluminium 6061 or 6082. | - | Yes | N/A |

| |
|--------------------------------------|
| Principal Mechanical Solution |
|--------------------------------------|

Table 4.1.: 2 DOF platform's principal solutions and functional requirements comparison

| | | | | | |
|---|--|------------------------------|---|-----|--------------|
| Drive, gearbox | Energy (Torque = $1105573 N \cdot mm \sim 1200 N \cdot m$) and transmission rate from $3000 rpm$ to $3.28 rpm$ with max acceleration $0.28 \frac{rad}{s^2}$ | Siemens, Yaskawa or Beckhoff | - | Yes | 800...2500 € |
| Electrical system, sensors and automation | To distribute the electrical energy to the Drive, send GPS signal to the Helicopter drone, manage and control the platform. | Siemens, Yaskawa | - | yes | N/A |

4.4. Preliminary model for motion simulation

The model motion calculation and reaction forces were solved by NX 12. The steps for the analysis were as follows:

1. Model all the Parts and sub-assemblies;
2. Constrain them properly;
3. Check all the way the platform movement by manually moving the parts;
4. Check the model by moving the part by constrains;
5. Define links, joints (six revolute joints and one spherical);
6. Fix the base plate;
7. For final solution define also the drivers, but for preliminary project for mechanical part the precise movement solution is not necessary as the NX will solve the general solution were the reaction forces will be the same;
8. Apply the external loads (Heave, gravity and UAV helicopter load with safety factor) , moments (rolling, pitching);
9. define the solving criteria (time and steps);
10. Solve.

The solved solution is in the figure 4.2. The external loads from ship movement and helicopter landing are illustrated in the figure 4.5 and reaction forces are in the figure 4.6. the numerical values are covered in the Appendix 5 for each link FEM analysis report. As the top plate is the most critical part of the structure, I started the calculation with Top plate 3, which was over complicated at firstly and the FEM analysis was made in Solid-works. Which shows stress and displacement problems (look for figure 4.4). The structure was designed (look for figure 4.3) which general concept was on the NCMP brochure [?], but with much less width.

The second iteration for the top plate I redesigned the stiffening profile (look the figure 4.7) and also added a rectangular profile in the x-axis and y axis, which made the stresses acceptable. Look for detailed drawings.

4.5. Analysis of the preliminary model

As the top plate is most stressed and the weight of the plate has an impact to other assemblies the goal is to design a top plate with minimum weight that holds Helicopter in emergency landing scenario. The authors effort to design the light weight landing plate has many challenges:

1. The model will go easily over complicated and can not be calculated;

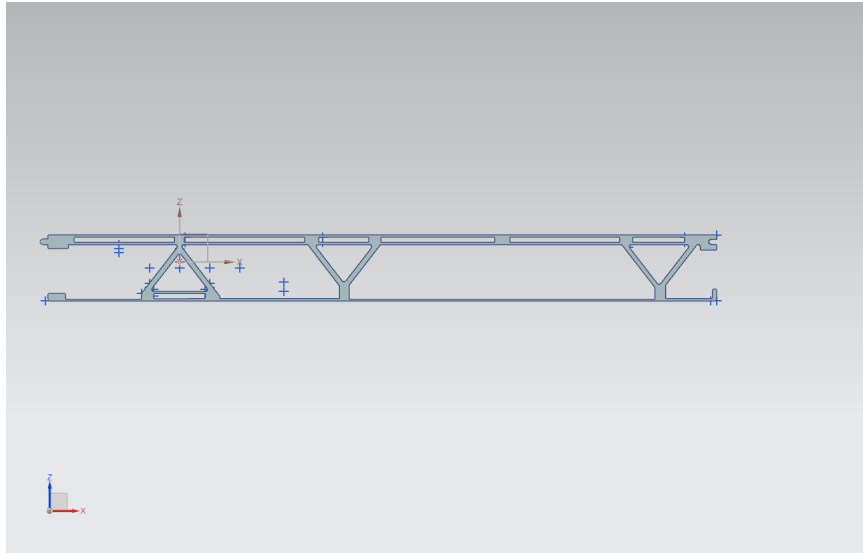


Figure 4.3.: Initially designed stiffening profile

2. To simplify the model the geometry will need to be as precise as needed where the stresses are expected, but also the joints need to be simplified;
3. the loading scenario for top plate will be choose d only the Helicopter weight and the joint connections will be calculated separately due to computer limitations;
4. Considering the manufacture of the top plate, it will be extruded, but the knowledge of dies and theology must be consulted with known manufactures.

4.6. Drive and gearbox

The initially selected electric drive Initially (Yaskawa rotary Servo motor SGMGV-09A with power $P = 0.85 \text{ kW}$ and rated torque $T = 5.39 \text{ Nm}$,) is not suitable as the reaction torque to the driving joints ($B1$ and $B2$) are 1200 Nm . The load motion profile if the platform will try to move on maximum elevation are as follows:

1. Maximum acceleration 0.28 rad/s^2 ;
2. Maximum speed 3.28 rpm ;
3. Load torque 1200 Nm ;
4. Load inertia $362,226 \text{ kgm}^2$.

The further work will require the selection of proper Drive and gearbox. The selection should consider the maximum load, that the second iteration design solution did provide.

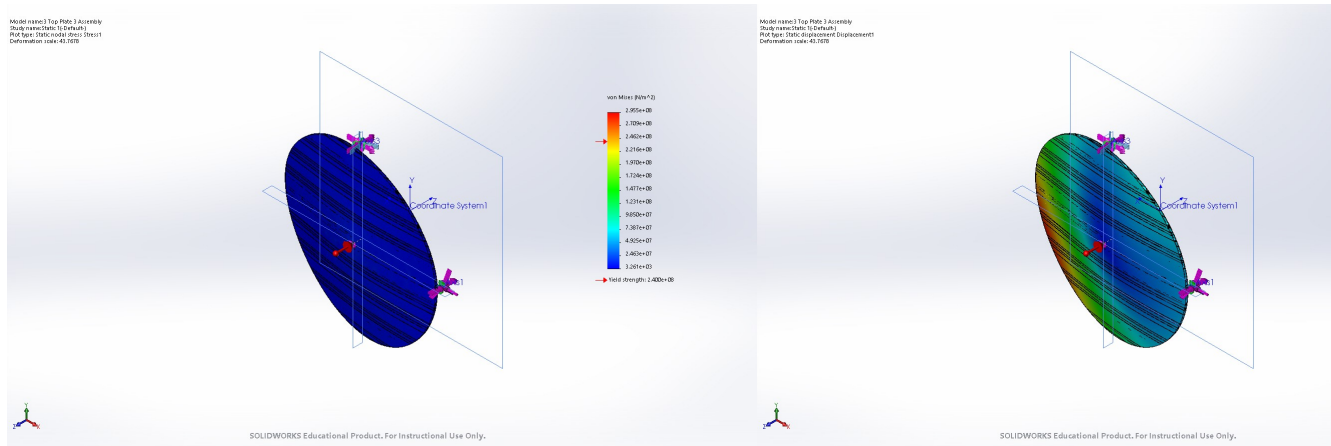


Figure 4.4.: Initial top plate stress and displacement analysis

4.7. Conclusion

The preliminary mechanical solution to the problem are designed and is formalized in the APPENDIX 6 F, with the general layout of the mechanism on the ship. The solution to the assembly are here F.1. All the final element analysis can be reviewed here E. For future development the top plate optimization may be necessary to provide friction for the vehicle landing the coating and material should be over looked. Also the hook system may be developed to hold the UAV steady on rough sea. The general concept for the automation of the platform control depends on the mathematical model, and the dynamic behavior should be further investigated.

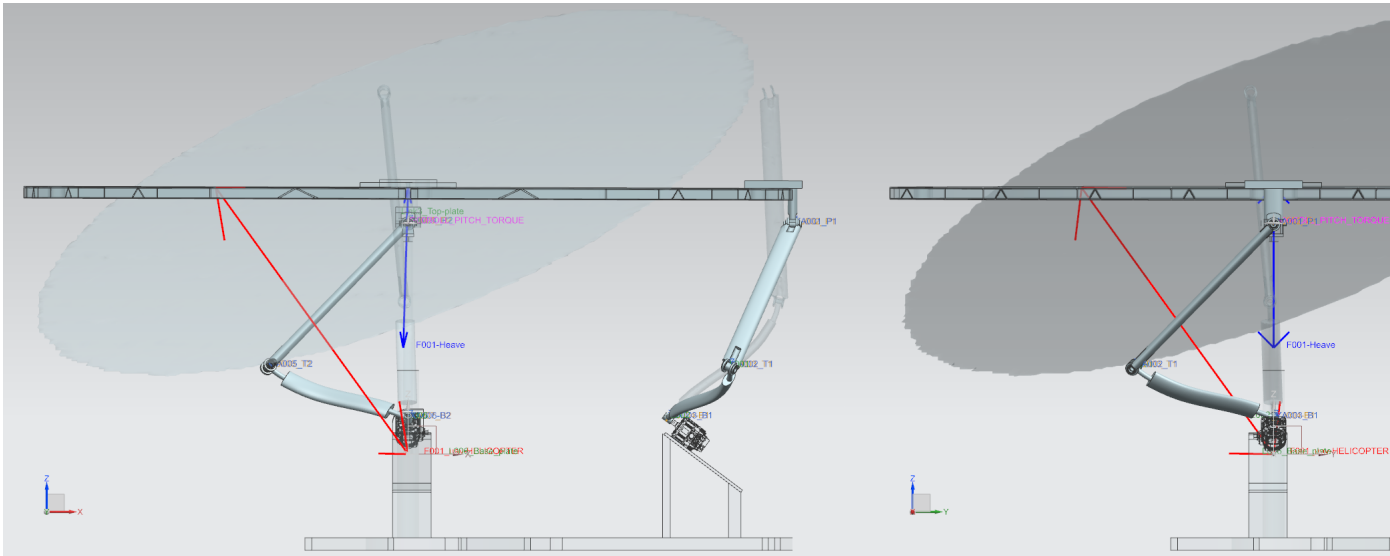


Figure 4.5.: Preliminary model loads

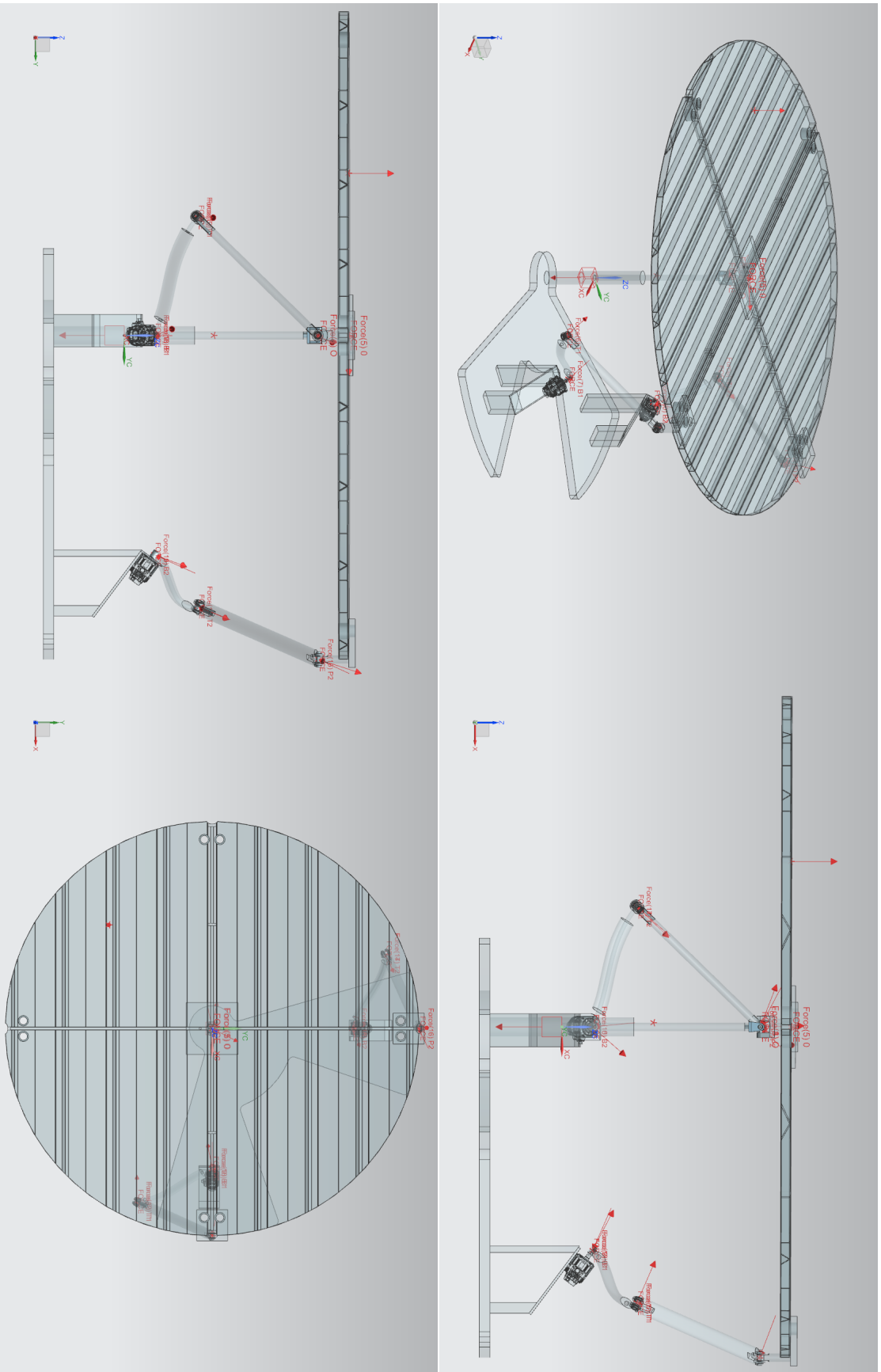


Figure 4.6.: Preliminary model reaction forces

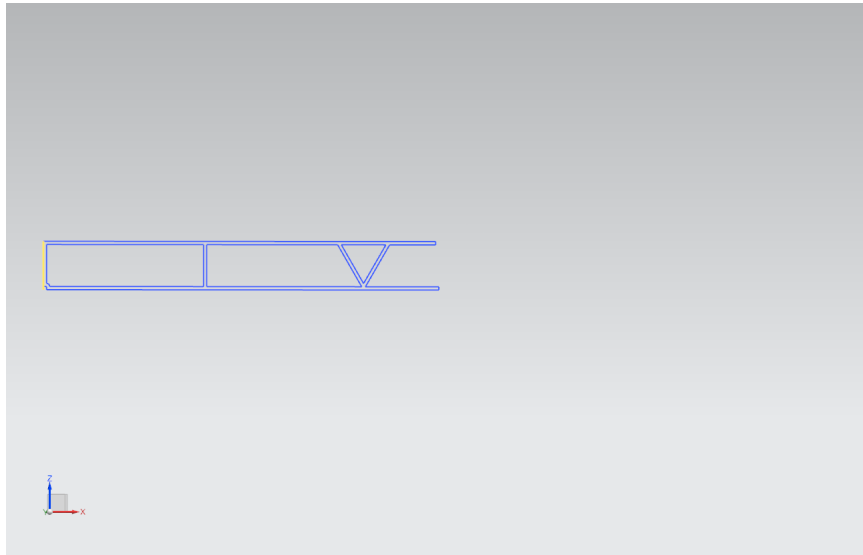


Figure 4.7.: Second iteration designed stiffening profile

Figure 4.8.: Automation concept

Acknowledgments

The sincere graduation of all the support goes to my wife, without her I could not been able to finish the work.

Special thanks to my supervisor for helping my on a right path.

A. : Appendix 1: Heaving Calculations

Main Dimensions

The total weight of ship are as follows A.1 and look for figures A.1 & A.2 with main dimensions and parameters:

| Weight | Mass - t | XM - m | YM - m | ZM - m |
|---------------|------------|----------|----------|----------|
| - Lightweight | 1029.3 | 24.71 | 0.01 | 5.11 |
| Deadweight | 340.3 | 19.72 | -0.05 | 2.70 |
| Total weight | 1369.6 | 23.47 | 0.00 | 4.51 |

Table A.1.: Total weight of the ship[7, 8]

1. L_{OA} – 63.62 m (The maximum length from the forward most point of the ship's hull to the aft-most point, is called Length Overall.);
2. L_{wl} – 61.06 m (The length of the ship's hull intersecting the surface of the water is called Length on Waterline);
3. L_{pp} – 55.14 m (Length between perpendiculars is the longitudinal distance between the forward and aft perpendiculars where ship meets the waterline it floats at design draft from rudder stock to front of the ship);
4. $BL(K)$: The keel is the lowermost point of the ship at any point of its length. The baseline of a ship is the longitudinal line that runs along the keel;
5. B_{max} – 10.2 m (The beam or breadth (max) is the transverse maximum distance across maximum section);
6. B_{wl} – 10.02 m (Breadth, moulded at T=4.20);
7. B – 10.2 m (The beam or breadth is the transverse distance across section);
8. T - 4.19 m (Mean Draught);
9. T_{dwl} – 4.2 m (draught at designed water line, moulded);

10. D – 5.30 m (Depth to free board deck (main deck));
11. CL - Center line of the ship as the x -axis;
12. A_{wp} – 638.8 m^2 (water plane area);
13. S – 797 m^2 ;
14. LCB -23.56 m (longitudinal Center of buoyancy);
15. VCB – 2.69 m (vertical center of buoyancy) ;
16. KM (KMT) - 5.77m (Vertical distance from BL to Transverse Metacentre (above keel))
17. (Longitudinal metacentric height (above keel))
18. $GM_0 = KMT - KG$ - 1.26 m (Transverse metacentric height if T.4.2);
19. LCG (CGX) - 23.47 m ((longitudinal Center of gravity);
20. TCG (CGY) -0.0 m (Transverse center of gravity from CL);
21. VCG (CGZ or KG) – 4.51 m (vertical center of gravity);
22. ∇ - 1360 m^3 (Displacement);
23. $\Delta - \rho g \lambda \nabla$ - 1367 t (weight displacement);
24. $C_B = \frac{\nabla}{LBT} = 0.5863$ (Block coefficient);
25. $C_M = \frac{A_M}{BT} = 0.7344$ (mid-ship section coefficient) ;
26. $C_{WP} = \frac{A_{WP}}{LB} = 0.9844$ (water-plane coefficient);
27. $C_P = 0.7983$ prismatic coefficient);
28. $\bar{GM} = GM_0 - GM_{corr} = 1.08$ m (Corrected GM_0 Transverse metacentric height with free surface correction $GM_{corr} = -0.18$ m);
29. $\bar{GZ} = KN - KG \sin(\theta) - DGZ = 0.357$ m - (DGZ -free surface correction - 0.059 m (GZ - Righting lever at 20°);
30. KN - 1.955 m ('K' represents the keel and 'N' a point that intersects the vertical line of buoyancy, which result a distance;
31. $BM = KM - VCB = 5.77 m - 2.69 m = 3.08 m$.

[7]

| Station | 2 - | 3 - | 4 - | 5 - | 6 - | 7 - | 8 - | 9 - | 10 - | 11 - | 12 - | 13 - | 14 - |
|---------|-------|-------|-------------------|-----------------------------------|-------------------|-------------------|-----------------------------|------|-------------------|---------------------------------|---|-------------------------|--|
| Unit | B_n | T_n | S_n | $\frac{\omega_e^2}{2g} \cdot B_n$ | $\frac{B_n}{T_n}$ | $B_n \cdot T_n$ | $\frac{S_n}{B_n \cdot T_n}$ | C | B_n^2 | $\frac{\rho\pi}{8} \cdot B_n^2$ | $C \cdot \frac{\rho\pi}{8} \cdot B_n^2$ | multiplier | Product |
| | [m] | [m] | [m ²] | [-] | [-] | [m ²] | [-] | [-] | [m ²] | $\frac{kg}{m}$ | $\frac{kg}{m}$ | [-] | $\frac{kg}{m}$ |
| -2 | 0.00 | 0.00 | 0 | 0 | 1 | 0.00 | 0.82 | 0 | 0 | 0 | 0 | 1 | 0 |
| -1 | 9.54 | 1.40 | 10.98 | 0.37 | 6.816 | 13.36 | 0.82 | 0.75 | 91.05 | 35930 | 26950 | 4 | 1.078·10 ⁵ |
| 0 | 9.54 | 1.40 | 10.98 | 0.37 | 6.816 | 13.36 | 0.74 | 0.75 | 91.05 | 35930 | 26950 | 2 | 5.390·10 ⁴ |
| 1 | 9.54 | 2.10 | 14.74 | 0.37 | 4.544 | 20.04 | 0.71 | 0.75 | 91.05 | 35930 | 26950 | 4 | 1.078·10 ⁵ |
| 2 | 9.54 | 2.90 | 19.53 | 0.37 | 3.29 | 27.67 | 0.61 | 0.75 | 91.05 | 35930 | 26950 | 2 | 5.390·10 ⁴ |
| 3 | 9.54 | 3.38 | 19.53 | 0.37 | 2.83 | 32.20 | 0.68 | 0.75 | 91.05 | 35930 | 26950 | 4 | 1.078·10 ⁵ |
| 4 | 9.54 | 3.72 | 24.25 | 0.37 | 2.56 | 35.51 | 0.67 | 0.8 | 91.05 | 35930 | 28750 | 2 | 5.749·10 ⁴ |
| 5 | 9.54 | 3.95 | 25.30 | 0.37 | 2.42 | 37.68 | 0.69 | 0.8 | 91.05 | 35930 | 28750 | 4 | 1.150·10 ⁵ |
| 6 | 9.41 | 3.99 | 25.77 | 0.37 | 2.36 | 37.53 | 0.65 | 0.8 | 88.59 | 34960 | 27970 | 2 | 5.594·10 ⁴ |
| 7 | 9.70 | 4.07 | 25.69 | 0.38 | 2.38 | 39.50 | 0.67 | 0.8 | 94.05 | 37120 | 29690 | 4 | 1.188·10 ⁵ |
| 8 | 9.70 | 4.07 | 26.37 | 0.38 | 2.38 | 39.50 | 0.67 | 0.78 | 94.05 | 37120 | 28950 | 2 | 5.790·10 ⁴ |
| 9 | 9.70 | 4.07 | 26.39 | 0.38 | 2.38 | 39.50 | 0.65 | 0.78 | 91.05 | 37120 | 28950 | 4 | 1.158·10 ⁵ |
| 10 | 9.70 | 4.20 | 26.39 | 0.38 | 2.31 | 40.68 | 0.66 | 0.78 | 94.05 | 37120 | 28950 | 2 | 5.790·10 ⁴ |
| 11 | 9.70 | 4.20 | 26.70 | 0.38 | 2.31 | 40.73 | 0.66 | 0.78 | 91.59 | 37120 | 28950 | 4 | 1.158·10 ⁵ |
| 12 | 9.57 | 4.20 | 26.59 | 0.38 | 2.28 | 40.19 | 0.67 | 0.78 | 79.39 | 36150 | 28190 | 2 | 5.639·10 ⁴ |
| 13 | 8.91 | 3.76 | 22.59 | 0.35 | 2.37 | 33.511 | 0.59 | 0.75 | 67.27 | 31330 | 23500 | 4 | 9.399·10 ⁴ |
| 14 | 8.20 | 3.59 | 17.39 | 0.32 | 2.28 | 29.47 | 0.43 | 0.75 | 60.50 | 26550 | 19910 | 2 | 3.983·10 ⁴ |
| 15 | 7.78 | 3.36 | 11.25 | 0.30 | 2.32 | 26.13 | 0.35 | 0.75 | 38.51 | 23880 | 17910 | 4 | 7.163·10 ⁴ |
| 16 | 6.21 | 3.28 | 7.16 | 0.24 | 1.89 | 20.34 | 0.31 | 0.8 | 24.01 | 15200 | 12160 | 2 | 2.432·10 ⁴ |
| 17 | 4.90 | 2.67 | 4.08 | 0.19 | 1.84 | 13.09 | 0.03 | 0.8 | 10.59 | 9476 | 7581 | 4 | 3.032·10 ⁴ |
| 18 | 3.25 | 2.71 | 0.22 | 0.13 | 1.20 | 8.81 | 3.43·10 ⁻⁴ | 0.8 | 0.56 | 4179 | 3343 | 2 | 6.686·10 ³ |
| 19 | 0.75 | 0.78 | 0.00 | 0.03 | 0.96 | 0.58 | 0 | 0.8 | 0.56 | 222 | 178 | 4 | 710 |
| 20 | 0.75 | 0.78 | 0 | 0.03 | 0.96 | 0.58 | 0 | 0 | 0 | 0 | 0 | 2 | 0 |
| 21 | 0 | 0 | 0 | 0 | 0 | 0 | 0 | 0 | 0 | 0 | 0 | 1 | 0 |
| 22 | 0 | 0 | 0 | 0 | 0 | 0 | 0 | 0 | 0 | 0 | 0 | 1 | 0 |
| | | | | | | | | | | | | SUM_{az} | 1.45·10⁶ · $\frac{kg}{m}$ |

Table A.2.: Calculation of added mass for Heaving [8, Example 4.1]

A.1. Heaving - Calculation of added Mass a_z

A body having an accelerated motion in a continuous medium of fluid experiences a force that is greater than the mass of the body times acceleration. This can be defined as the product of body acceleration and a quantity having the same dimension as the mass, it is termed added mass. This concept is needed to discuss the inertial force of a ship: the inertial force of a ship is:

$$a \frac{d^2z}{dt^2} = M \frac{d^2z}{dt^2} + \delta l \quad (2.3)$$

where $M = \text{mass}$ of the vessel and $\delta l = \text{force}$ increment or liquid accelerating force. Thus

$$a \frac{d^2z}{dt^2} = M \frac{d^2z}{dt^2} + \delta l = (M + a_z) \frac{d^2z}{dt^2}. \quad (2.3)$$

The added mass of a total ship can be calculated as

$$a_z = \int_{-L/2}^{L/2} a_n dx = \rho \frac{\pi}{2} \int_{-L/2}^{L/2} C y^2(x) dx, \quad (2.4)$$

which is done by Simpson rule refer to Table A.1: "Calculation-of-added mass for Heaving" and Heaving - Calculation of added Mass a_z . As I am integrating in two dimensions over the ship sectional beam-to-draft ratio ($\frac{B(x)}{T(x)}$), and the sectional area coefficient $\beta_n = \frac{S(x)}{T(x)B(x)}$ (look the figure fig A.5: "Lewis-form-sections-for varying B/T").

According to [23] and [8, (4.2)], an inertial coefficient C is defined as:

$$C = \frac{\text{Added mass of the section of unit length beam } B_n \text{ and section draft } T_n \text{ to bottom of section}}{\text{Half of the added mass for a circular section segment of unit length and diameter } B_n}$$

Now, half of the added mass for a circular section segment of unit length and diameter B_n is

$$\frac{1}{2} \rho \pi r^2 = \frac{\rho \pi B_n^2}{8}$$

where breadth $B_n = 2r$. For shapes other than semicircular ones, the added mass of a ship section, a_n is found to be [23] and [8, (4.2)]:

$$a_n = C \frac{\rho \pi B_n^2}{8}$$

The inertial coefficient C for Lewis-form sections is obtained from fig A.5: "Lewis-form-sections-for varying B/T" [23, 22, Fig. 42]. This is done by visual comparison of the body plan with the section.

Added mass for Heaving as the ships section spacing is $L_{spacing} = 2.7 m$:

$$a_z = \frac{1}{3} \cdot L_{spacing} \cdot \mathbf{SUM}_{\mathbf{az}} = 1.305 \cdot 10^6 \cdot kg. \quad (\text{A.1})$$

As per section 2.2 a is the virtual mass (ship mass $M = \Delta$ plus added mass a_z) and I can calculate:

$$a = \Delta + a_z = 2.672 \cdot 10^6 \cdot kg \quad (\text{A.2})$$

[8].

A.2. Heaving - Calculation of damping coefficient

Calculating according to the example [8, Example 4.2 Calculation of damping coefficient] the PVL101 damping coefficient in heaving as part of sectional integration refer to Table A.2: "Calculation-of-damping coefficient for Heaving". Damping coefficient for Heaving as the ships section spacing is $L_{spacing} = 2.7 m$:

$$b_z = \frac{1}{3} \cdot L_{spacing} \cdot \mathbf{SUM}_{\mathbf{bz}} = 1.705 \cdot 10^6 \cdot \frac{kg}{s}. \quad (\text{A.3})$$

A.3. Heaving - Calculation of restoring coefficient

The restoring force for heaving is given as the additional buoyancy force that acts on a body when it is submerged to a deeper draft. There is assumed that there is no significant change in the water-plane area during heaving and the restoring force is given as the amount of water displaces, which is equal to specific weight times additional submerged volume. Restoring force is obtained directly from offsets as mentioned (2.12) and Table A.3: "Calculation-of-restoring coefficient for Heaving". Restoring coefficient for Heaving as the ships section spacing is $L_{spacing} = 2.7 m$:

$$c_z = \frac{1}{3} \cdot L_{spacing} \cdot \mathbf{SUM}_{\mathbf{cz}} = 4.691 \cdot 10^6 \cdot kg. \quad (\text{A.4})$$

| Station | 1 - | 2 - | 3 - | 4 - | 5 - | 6 - | 7 - | 8 - | 9 - |
|---------|-----------------------------------|-------------------|-----------|-----------|-------------|-------------------------------------|-------------------------|---|-----|
| Unit | $\frac{\omega_c^2}{2g} \cdot B_n$ | $\frac{B_n}{T_n}$ | β_n | \bar{A} | \bar{A}^2 | $\rho_{\omega_c}^2 \cdot \bar{A}^2$ | multiplier | Product | |
| Unit | [-] | [-] | [-] | [-] | [-] | [-] | [-] | $\frac{kg}{m \cdot s}$ | |
| -2 | 0 | 1 | 0.00 | 0 | 0 | 0 | 1 | 0 | |
| -1 | 0.618 | 6.82 | 0.822 | 0.5 | 0.25 | $1.66 \cdot 10^4$ | 4 | $6.74 \cdot 10^4$ | |
| 0 | 0.618 | 6.82 | 0.822 | 0.5 | 0.25 | $1.69 \cdot 10^4$ | 2 | $3.37 \cdot 10^4$ | |
| 1 | 0.618 | 4.54 | 0.735 | 0.5 | 0.25 | $1.66 \cdot 10^4$ | 4 | $6.74 \cdot 10^4$ | |
| 2 | 0.618 | 3.29 | 0.706 | 0.6 | 0.30 | $2.04 \cdot 10^4$ | 2 | $4.08 \cdot 10^4$ | |
| 3 | 0.618 | 2.83 | 0.606 | 0.7 | 0.49 | $3.3 \cdot 10^4$ | 4 | $1.32 \cdot 10^5$ | |
| 4 | 0.618 | 2.56 | 0.683 | 0.7 | 0.49 | $3.31 \cdot 10^4$ | 2 | $6.61 \cdot 10^4$ | |
| 5 | 0.618 | 2.42 | 0.671 | 0.7 | 0.49 | $3.31 \cdot 10^4$ | 4 | $1.322 \cdot 10^5$ | |
| 6 | 0.610 | 2.36 | 0.687 | 0.7 | 0.49 | $3.31 \cdot 10^4$ | 2 | $6.61 \cdot 10^4$ | |
| 7 | 0.628 | 2.38 | 0.650 | 0.8 | 0.61 | $4.1 \cdot 10^4$ | 4 | $1.64 \cdot 10^5$ | |
| 8 | 0.628 | 2.38 | 0.668 | 0.8 | 0.61 | $4.11 \cdot 10^4$ | 2 | $8.21 \cdot 10^4$ | |
| 9 | 0.628 | 2.38 | 0.668 | 0.8 | 0.61 | $4.1 \cdot 10^4$ | 4 | $1.64 \cdot 10^5$ | |
| 10 | 0.628 | 2.31 | 0.649 | 0.8 | 0.61 | $4.11 \cdot 10^4$ | 2 | $8.21 \cdot 10^4$ | |
| 11 | 0.628 | 2.31 | 0.656 | 0.8 | 0.61 | $4.1 \cdot 10^4$ | 4 | $1.64 \cdot 10^5$ | |
| 12 | 0.620 | 2.28 | 0.662 | 0.8 | 0.61 | $4.1 \cdot 10^4$ | 2 | $8.21 \cdot 10^4$ | |
| 13 | 0.577 | 2.37 | 0.674 | 0.8 | 0.61 | $4.1 \cdot 10^4$ | 4 | $1.64 \cdot 10^5$ | |
| 14 | 0.532 | 2.28 | 0.590 | 0.8 | 0.61 | $84.1 \cdot 10^4$ | 2 | $8.21 \cdot 10^4$ | |
| 15 | 0.504 | 2.32 | 0.431 | 0.7 | 0.49 | $1.65 \cdot 10^4$ | 4 | $6.61 \cdot 10^4$ | |
| 16 | 0.402 | 1.89 | 0.352 | 0.7 | 0.49 | $2.73 \cdot 10^4$ | 2 | $5.46 \cdot 10^4$ | |
| 17 | 0.318 | 1.84 | 0.312 | 0.5 | 0.20 | 0.68 | 4 | $2.73 \cdot 10^4$ | |
| 18 | 0.211 | 1.20 | 0.025 | 0.5 | 0.20 | 1.22 | 2 | $2.43 \cdot 10^4$ | |
| 19 | 0.049 | 0.96 | 0.0..3 | 0.3 | 0.09 | 0.34 | 4 | 1.35 | |
| 20 | 0.049 | 0.96 | 0 | 0 | 0 | 0 | 2 | 0 | |
| 21 | 0 | 0 | 0 | 0 | 0 | 0 | 1 | 0 | |
| 22 | 0 | 0 | 0 | 0 | 0 | 0 | 1 | 0 | |
| | | | | | | | SUM_{bz} | $1.895 \cdot 10^6 \cdot \frac{kg}{m \cdot s}$ | |

Table A.3.: Calculation of the damping coefficient for Heaving [8, Example 4.2]

A.4. Heaving - Calculation of Free damped Heaving equation solution

The simplified expression are:

$$z = \frac{2900 \cdot \sqrt{6615679} \cdot \exp\left(\frac{639 \cdot t}{2000}\right) \cdot \sin\left(\frac{\sqrt{6615679} \cdot t}{2000}\right)}{6615679} \quad (\text{A.5})$$

where t is time. The expression which has 2 solution as the characteristic equation where $z^2 + 0.639z + 1.756 = 0$ with roots

$$r = \begin{bmatrix} -0.319 + 1.286i \\ -0.319 - 1.286i \end{bmatrix}.$$

Acceleration in free, damped motion of the PVL-101 ship Differentiating the solution of the (2.13) and revealing the equation for acceleration:

$$\frac{d^2 z}{dt^2} = -A_1 \exp^{-\nu t} (B_1 \cos(\omega_d t) + C_2 \sin(\omega_d t)) = -A \omega_d^2 \exp^{-\nu t} \sin(\omega_d t)$$

The graphical representation of the expression :

MAT LAB solution:

Free, damped Heaving Motion

14.10.2020 @ j.urb

```
% a*(d^2)z/dt + b*dz/dt + cz =0 or d^2z/dt + 0.639*dz/dt + 1.756*z=0  
  
% a*(d^2)z/dt + b*dz/dt + cz =0  
  
m = 2.672*10^6; % m=a ship mass(M) + added mass(az) -inertial coef  
b1 = 1.705*10^6; % b - damping coef  
k = 4.691*10^6; % k=c - stiffness or restoring coef
```

Initial conditions

```
l = 0; % initial heaving movement  
v = 1.45; % initial z'(0) model speed
```

Second order differential equation solution

```
syms z(t)  
Dz = diff(z);  
eqn = diff(z,t,2)+0.639*diff(z,t)+1.756*z == 0;  
cond = [z(0)==1, Dz(0)==v];  
zSol(t) = dsolve(eqn,cond); simple = simplify(zSol(t))
```

simple =

$$\frac{2900 \sqrt{6615679} e^{-\frac{639t}{2000}} \sin\left(\frac{\sqrt{6615679} t}{2000}\right)}{6615679}$$

Solution

Heave_free $d^2z/dt + 0.639*dz/dt + 1.756*z=0$ - inital equation

```
% Define as a symbol and function  
fordiff= @(t) (2900*6615679^(1/2)*exp(-(639*t)/2000).*...  
    sin((6615679^(1/2)*t)/2000))/6615679;  
syms t  
simple2 = simplify(fordiff(t))
```

simple2 =

$$\frac{286040184030201 e^{-\frac{639t}{2000}} \sin\left(\frac{707012427285683 t}{549755813888000}\right)}{253697544159232}$$

```
dz=diff(fordiff(t),t);  
dz1= @(t) (202233964812435868202126912283*cos((707012427285683*t)/...  
    549755813888000)*exp(-(639*t)/2000))/139471699870645408829014016000 ...  
    - (182779677595298439*exp(-(639*t)/2000)*sin((707012427285683*t)/...  
    549755813888000))/507395088318464000;
```

Free damping equation acceleration $d^2z/dt^2 = -0.639*dz/dt - 1.756*z$

```
dz2 = @(t) (-0.639)*((202233964812435868202126912283*...
    cos((707012427285683*t)/...
    549755813888000)*exp(-(639*t)/2000))/139471699870645408829014016000 ...
    - (182779677595298439*exp(-(639*t)/2000)*sin((707012427285683*t)/...
    549755813888000))/507395088318464000) - 1.756*((2900*6615679^(1/2)*...
    exp(-(639*t)/2000).*sin((6615679^(1/2)*t)/2000))/6615679);
```

```
simplifiedz2 = simplify(dz2(t))
```

```
simplifiedz2 =
```

$$- \frac{3 e^{-\frac{639t}{2000}} \left(2448577703549338026 \cos\left(\frac{707012427285683t}{549755813888000}\right) + 4623838085055574031 \sin\left(\frac{707012427285683t}{549755813888000}\right) \right)}{7928048254976000000}$$

END

A.5. Heaving - Calculation of exciting coefficient

Let us suppose that ship is wall sided in the region of the load waterline, and that while the wave approaches the ship, the time t is recorded when the wave crest is amidships. Then the wave at any position x from the mid-ship section is given by (2.22). The exciting force for heaving is the additional buoyancy force at any instant and we assume that the ship is symmetrical about the mid-ship section and the wave profile hits every section. We obtain the exciting force for heaving: as mentioned by two dimensional integrating over the ship sections and wave profile over the ship length (2.22) Table A.4: "Calculation-of-exciting coefficient". Exciting coefficient for Heaving as the ships section spacing is $L_{spacing} = 2.7 m$:

$$integral_{Fz} = \frac{1}{3} \cdot L_{spacing} \cdot \mathbf{SUM}_{Fz} = 237.817 m^2. \quad (A.6)$$

Refer (2.23) and

$$f_{0_{Fz}} = \frac{2}{L_{wl} \cdot B_{max}} \cdot integral_{Fz} = 0.764. \quad (A.7)$$

and

$$F_{0_z} = \rho g \xi_a L_{wl} B_{max} \cdot f_{0_{Fz}} = 3.748 \cdot 10^7 N \quad (A.8)$$

A.6. Heaving - PVL-101 differential equation calculation and its solution"

The equation is as follows: (2.1)

$$a\ddot{z} + b\dot{z} + cz = F_0 \cos(\omega_e t)$$

Virtual mass:

$$a = 2.672 \cdot 10^6 kg$$

Damping coefficient:

$$b = 1.705 \cdot 10^6 \frac{kg}{s}$$

Restoring coefficient:

$$c = 6.106 \cdot 10^6 \frac{kg}{s^2}$$

Amplitude of the exciting force:

$$F_0 = 3.748 \cdot 10^7 N.$$

Encountering wave frequency: $\omega_e = \frac{2\pi}{T_e}, T_e = 10 s$ [16, page 29], $\omega_e = 0.628 \frac{1}{s}$. Natural frequency:

$$\omega_z = \sqrt{\frac{c}{a}} = 1.325 \frac{1}{s} \quad (2.2). \text{ The tuning factor:}$$

$$\Lambda = \frac{\omega_e}{\omega_z} = 0.474$$

(2.29). The non-dimensional damping factor

$$\kappa = \frac{\nu}{\omega_z} = 0.241 \frac{1}{s}$$

or $\zeta = \frac{b}{2\sqrt{a \cdot c}}$ [13, page 100] where $\nu = \frac{b}{2a} = 0.319 \frac{1}{s^2}$ (2.16).

The circular frequency of the damped oscillation, that is [8, eq:4.6a] $\omega_d = \sqrt{\omega_z^2 - \nu^2} = 1.286 \frac{1}{s}$. The heaving amplitude

$$z_a = z_{st} \cdot \mu_z = 9.886 m$$

where $z_{st} = \frac{F_0}{c} = 7.989 m$ (2.26)&(2.27).

Then the equation can be expressed as: [20, ch:10] or [13, eq:4.14]

$$\ddot{z} + 2\kappa\omega_z\dot{z} + \omega_z^2 z = z_a \cos(\omega_e t) \quad (A.9)$$

or

$$\ddot{z} + 2\zeta\omega_z\dot{z} + \omega_z^2 z = \frac{F_0}{a} \cos(\omega_e t) \quad (A.10)$$

$$\ddot{z} + 0.639\dot{z} + 1.756z = 9.886 \cdot \cos(0.628t - 0.287) \quad (A.11)$$

The roots for the characteristic equation are: $z^2 + 2\zeta\omega_z z + \omega_z^2 = 0$

$$r = \begin{bmatrix} -0.319 + 1.286i \\ -0.319 - 1.286i \end{bmatrix}$$

Then the solution can be expressed as

$$z = A \exp^{\nu t} \sin(\omega_d t - \beta) + z_a \cos(\omega_e t - \varepsilon_2)$$

(2.32) or [20, eq:10.7B & eq:10.15]

According from [20, eq:10.7A and 10.7B] the first part of the solution

$$z_1 = \exp^{-\nu t} (C_1 \cos(\omega_d t) + C_2 \sin(\omega_d t)) a$$

are equal to the form $z_1 = A \exp^{-\nu t} \sin(\omega_d t - \beta)$ which is the ships natural movement. The second part

$$z_2 = z_a \cos(\omega_e t - \varepsilon_2) i$$

s the encountering movement. Hole solution: $z = z_1 + z_2$. The phase angle between the wave motion and the heaving motion is expressed as

$$\varepsilon = \varepsilon_1 + \varepsilon_2$$

where ε_1 is the phase angle between the wave motion and the exciting force caused by waves, and ε_2 is the phase angle between the exciting force and the heaving motion.

Now $\varepsilon_1 = 0$ [8, eq:4.12b] and from [8, page 38]

$$\varepsilon_2 = \arctan \frac{2\kappa\Lambda}{1 - \Lambda^2} = 0.287 \text{ rad}$$

As for free, undamped the $A = 9.886 m$. As for 2.32 the solution to the heaving equation are:

$$z = A \exp^{\nu t} \sin(\omega_d t - \beta) + z_a \cos(\omega_e t - \varepsilon_2)$$

and

$$z = \frac{2900 \cdot \sqrt{6615679}}{6615679} \exp^{-0.0319t} \sin(1.286t) + 9.886 \cos(0.628t - 0.287) \quad (\text{A.12})$$

MAT LAB solution:

Forced, damped Heaving Motion

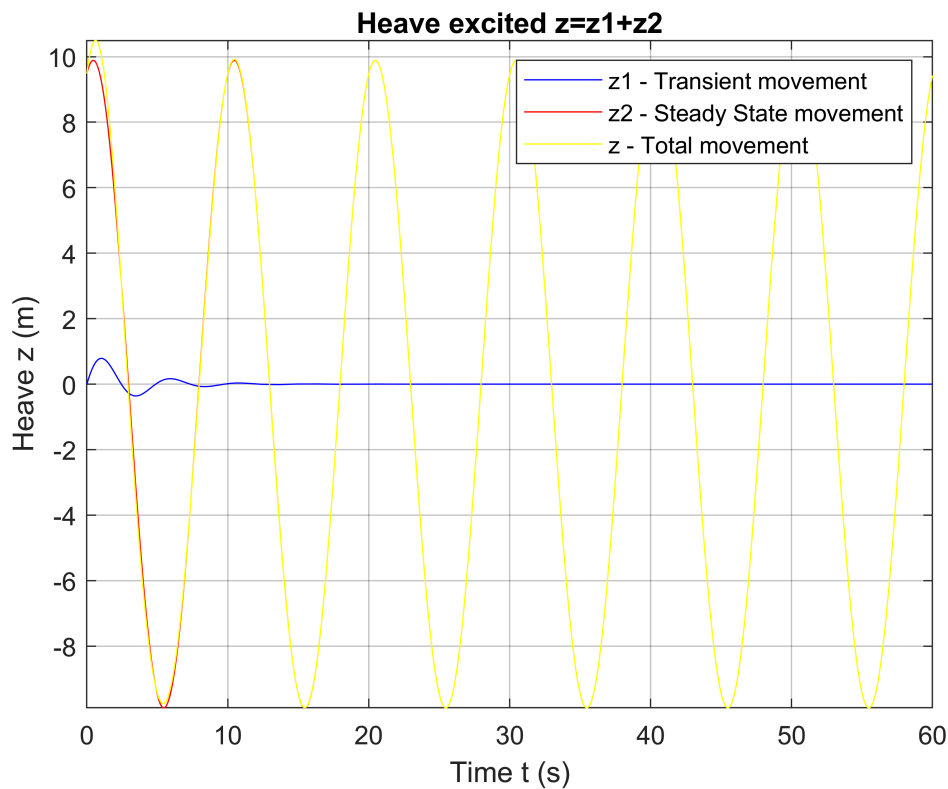
14.10.2020 @ j.urb

Initial conditions

$$l = 0$$

$$v = 1.4500$$

Second order differential equation solution



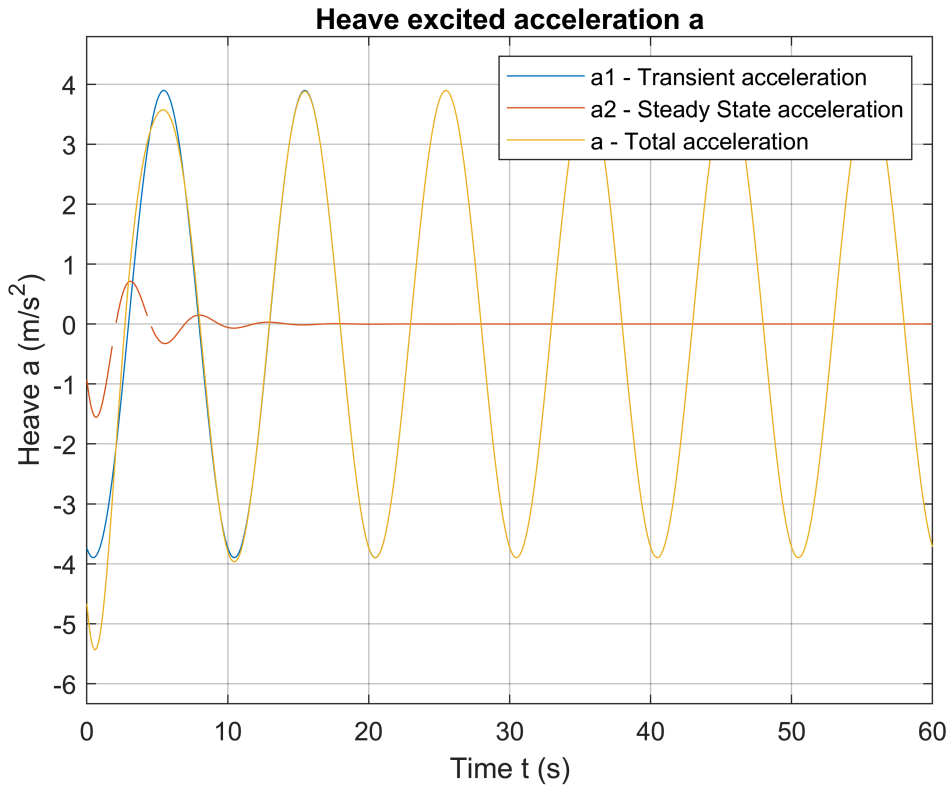
simple1 =

$$\frac{4943 \cos\left(\frac{157t}{250} - \frac{287}{1000}\right)}{500} + \frac{286040184030201 e^{-\frac{639t}{2000}} \sin\left(\frac{707012427285683t}{549755813888000}\right)}{253697544159232}$$

simple2 =

$$-\frac{121840007 \cos\left(\frac{157t}{250} - \frac{287}{1000}\right)}{31250000} - \frac{134157053921787547311405195747022514067902433 e^{-\frac{639t}{2000}} \sin\left(\frac{707012427285683t}{549755813888000}\right)}{7667537787672953105064510139463945420800000}$$

Acceleration plot



Solve a nonhomogenous Second-order Differential Equaton Numerically

14.10.2020 @j.urb

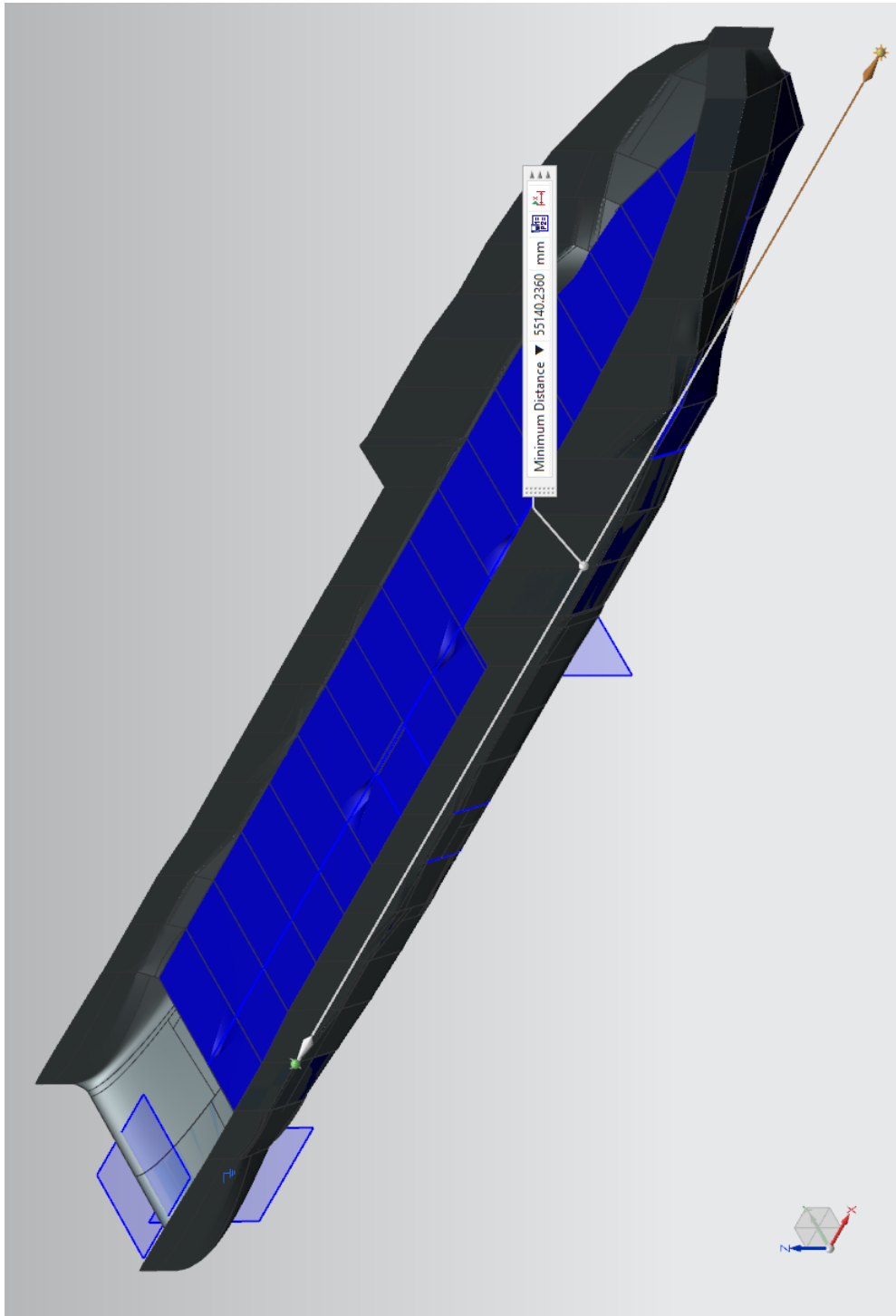


Figure A.1.: Ship Displacement (blue) and sections

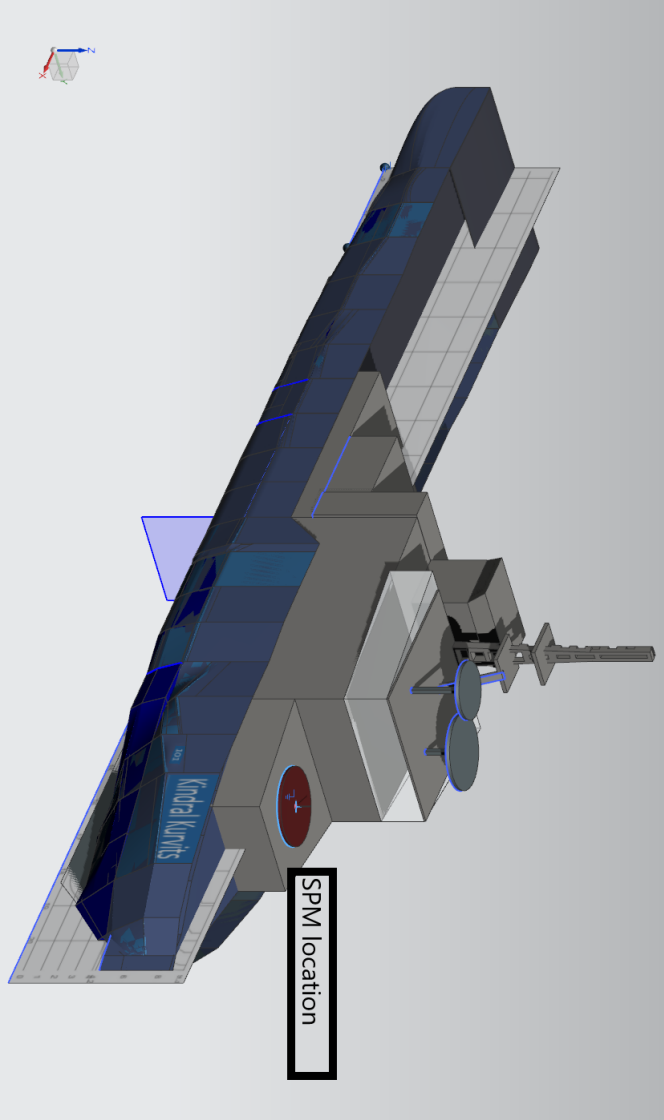


Figure A.2.: The platform location on PVL-101

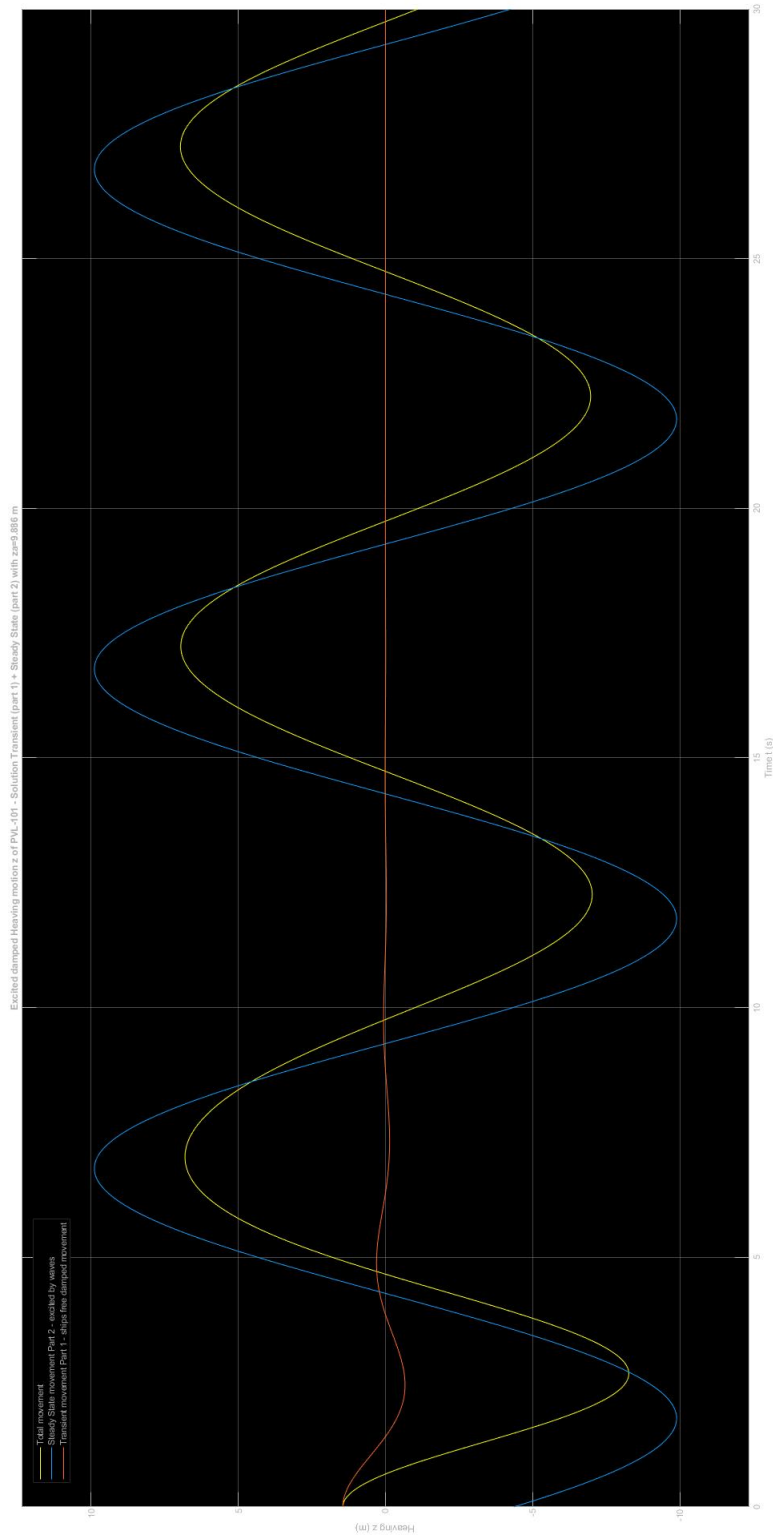


Figure A.3.: Heaving movement z

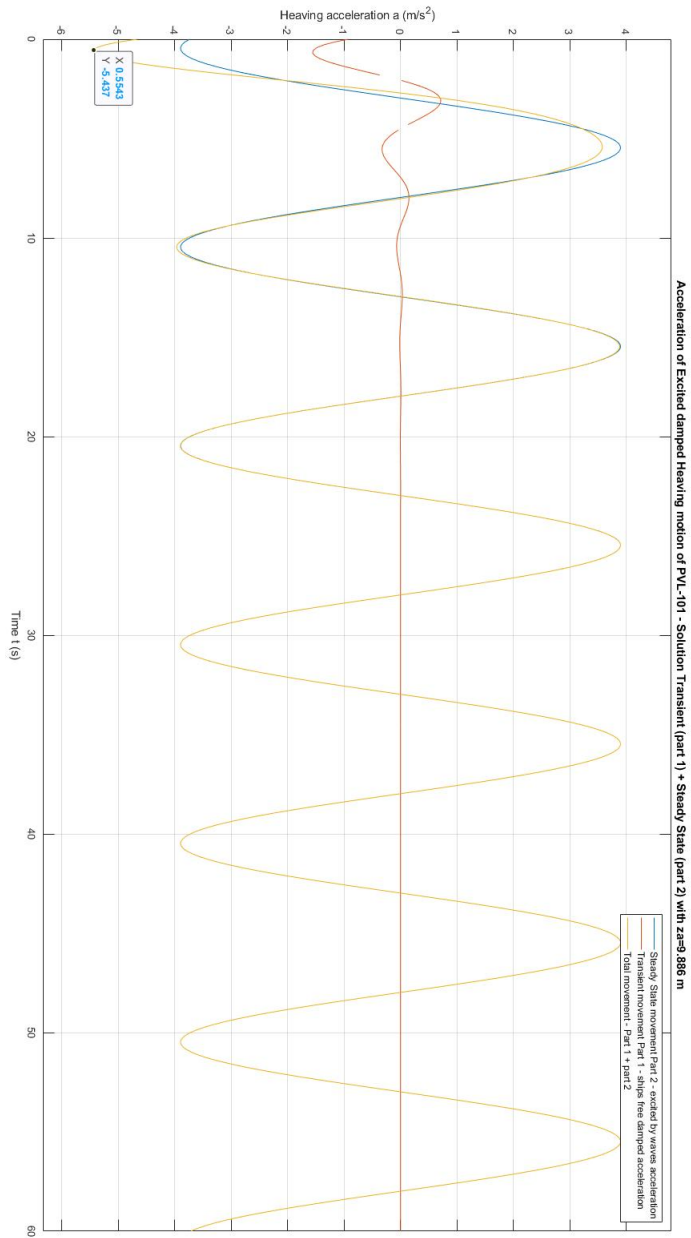


Figure A.4.: Heaving acceleration a

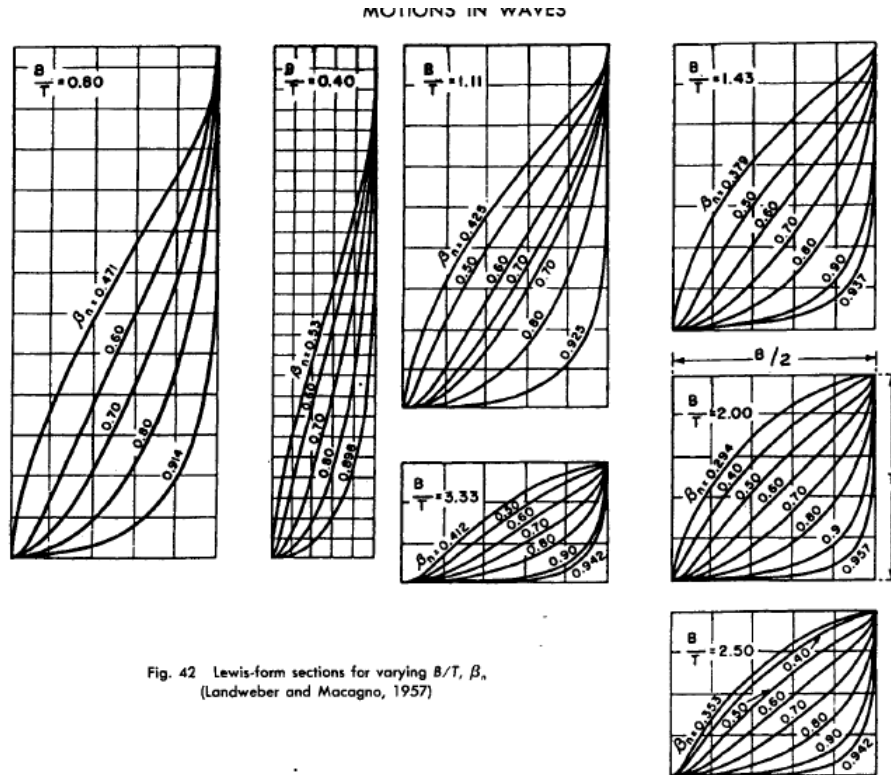
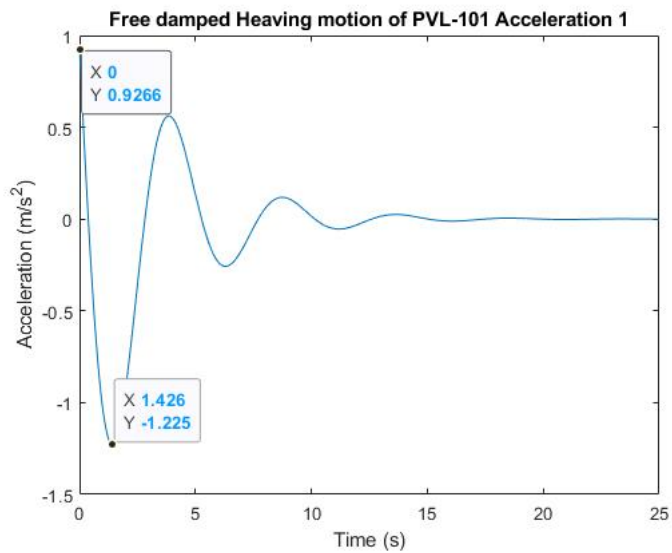


Figure A.5.: Lewis form sections for varying B/T [22, Fig 42]



| 1 - | 2 - | 3 - | 4 - | 5 - |
|------------|------------|--------------------|-------------------------|---|
| Station | B_n | $c_n = \rho g B_n$ | multiplier | Product |
| Unit | [m] | $\frac{kg}{m^2}$ | [-] | |
| -2 | 0.00 | 0 | 1 | 0 |
| -1 | 9.54 | $9.398 \cdot 10^4$ | 4 | $3.759 \cdot 10^5$ |
| 0 | 9.54 | $9.398 \cdot 10^4$ | 2 | $1.880 \cdot 10^5$ |
| 1 | 9.54 | $9.398 \cdot 10^4$ | 4 | $3.759 \cdot 10^5$ |
| 2 | 9.54 | $9.398 \cdot 10^4$ | 2 | $1.880 \cdot 10^5$ |
| 3 | 9.54 | $9.398 \cdot 10^4$ | 4 | $3.759 \cdot 10^5$ |
| 4 | 9.54 | $9.398 \cdot 10^4$ | 2 | $1.880 \cdot 10^5$ |
| 5 | 9.54 | $9.398 \cdot 10^4$ | 4 | $3.759 \cdot 10^5$ |
| 6 | 9.41 | $9.27 \cdot 10^4$ | 2 | $1.854 \cdot 10^5$ |
| 7 | 9.70 | $9.552 \cdot 10^4$ | 4 | $3.821 \cdot 10^5$ |
| 8 | 9.70 | $9.552 \cdot 10^4$ | 2 | $1.910 \cdot 10^5$ |
| 9 | 9.70 | $9.552 \cdot 10^4$ | 4 | $3.821 \cdot 10^5$ |
| 10 | 9.70 | $9.552 \cdot 10^4$ | 2 | $1.910 \cdot 10^5$ |
| 11 | 9.70 | $9.552 \cdot 10^4$ | 4 | $3.821 \cdot 10^5$ |
| 12 | 9.57 | $9.425 \cdot 10^4$ | 2 | $1.885 \cdot 10^5$ |
| 13 | 8.91 | $8.775 \cdot 10^4$ | 4 | $1.885 \cdot 10^5$ |
| 14 | 8.20 | $8.078 \cdot 10^4$ | 2 | $3.510 \cdot 10^5$ |
| 15 | 7.78 | $7.661 \cdot 10^4$ | 4 | $1.616 \cdot 10^5$ |
| 16 | 6.21 | $6.112 \cdot 10^4$ | 2 | $3.064 \cdot 10^5$ |
| 17 | 4.90 | $4.826 \cdot 10^4$ | 4 | $1.222 \cdot 10^5$ |
| 18 | 3.25 | $3.205 \cdot 10^4$ | 2 | $1.930 \cdot 10^5$ |
| 19 | 0.75 | $7.387 \cdot 10^3$ | 4 | $6.410 \cdot 10^4$ |
| 20 | 0.75 | $7.387 \cdot 10^3$ | 1 | $2.955 \cdot 10^4$ |
| 21 | 0.75 | $7.387 \cdot 10^3$ | 0 | $1.447 \cdot 10^4$ |
| 22 | 0 | 0 | 0 | 0 |
| | | | SUM_{cz} | $5.212 \cdot 10^6 \cdot \frac{kg}{m^2}$ |

Table A.4.: Calculation of restoring coefficient for Heaving[8, Examlle 4.3]

| 1 - | 2 - | 3 - | 4 - | 5 - | 6 - | 7 - | 13 - | 14 - |
|---------|-----------------|------------|------|-------------------|---------------------|------------------------|-------------------------|------------------|
| Station | $\frac{B_n}{2}$ | $\cos \mu$ | x | $k' = k \cos \mu$ | $\cos(kx \cos \mu)$ | $y \cos(k'x \cos \mu)$ | multiplier | Product |
| Unit | [m] | [rad] | [m] | [-] | [-] | [m] | [-] | [m] |
| -2 | 0.00 | 0.00 | 35.1 | 0.00 | 1 | 0.00 | 1 | 0.00 |
| -1 | 4.77 | 0.00 | 32.4 | 0.00 | 1 | 4.77 | 4 | 19.084 |
| 0 | 4.77 | 0.00 | 29.7 | 0.00 | 1 | 4.77 | 2 | 9.542 |
| 1 | 4.77 | 0.00 | 27.0 | 0.00 | 1 | 4.77 | 4 | 19.084 |
| 2 | 4.77 | 0.00 | 24.3 | 0.00 | 1 | 4.77 | 2 | 9.542 |
| 3 | 4.77 | 0.00 | 21.6 | 0.00 | 1 | 4.77 | 4 | 19.084 |
| 4 | 4.77 | 0.00 | 18.9 | 0.00 | 1 | 4.77 | 2 | 9.542 |
| 5 | 4.77 | 0.00 | 16.2 | 0.00 | 1 | 4.77 | 4 | 19.084 |
| 6 | 4.71 | 0.00 | 13.5 | 0.00 | 1 | 4.71 | 2 | 9.412 |
| 7 | 4.85 | 0.00 | 10.8 | 0.00 | 1 | 4.85 | 4 | 19.396 |
| 8 | 4.85 | 0.00 | 8.1 | 0.00 | 1 | 4.85 | 2 | 9.689 |
| 9 | 4.85 | 0.00 | 5.4 | 0.00 | 1 | 4.85 | 4 | 19.396 |
| 10 | 4.85 | 0.00 | 2.7 | 0.00 | 1 | 4.85 | 2 | 9.689 |
| 11 | 4.85 | 0.00 | 0 | 0.00 | 1 | 4.85 | 4 | 19.396 |
| 12 | 4.79 | 0.00 | 2.7 | 0.00 | 1 | 4.79 | 2 | 9.570 |
| 13 | 4.46 | 0.00 | 5.4 | 0.00 | 1 | 4.46 | 4 | 17.820 |
| 14 | 4.10 | 0.00 | 8.1 | 0.00 | 1 | 4.10 | 2 | 8.202 |
| 15 | 3.89 | 0.00 | 10.8 | 0.00 | 1 | 3.89 | 4 | 15.556 |
| 16 | 3.10 | 0.00 | 13.5 | 0.00 | 1 | 3.10 | 2 | 6.206 |
| 17 | 2.45 | 0.00 | 16.2 | 0.00 | 1 | 2.45 | 4 | 9.800 |
| 18 | 1.62 | 0.00 | 18.9 | 0.00 | 1 | 1.63 | 2 | 3.254 |
| 19 | 0.38 | 0.00 | 21.6 | 0.00 | 1 | 0.38 | 4 | 1.500 |
| 20 | 0.38 | 0.00 | 24.3 | 0.00 | 1 | 0.38 | 2 | 0.375 |
| 21 | 0.00 | 0 | 27 | 0 | 1 | 0.00 | 1 | 0.000 |
| 22 | 0 | 0 | 0 | 0 | 0 | 0 | 1 | 0 |
| | | | | | | | SUM_{Fz} | 264.241 m |

Table A.5.: Calculation of exciting coefficient [8, Example 4.6]

B. : Appendix 2: Pitching Calculation of coefficients

B.1. Pitching - Calculation of the virtual mass moment of inertia a_θ

According to my calculation the total inertia for pitching:

1. virtual moment of inertia for pitching is

$$I''_{yy} = I'_{yy} + I_{yy} = 7.808 \cdot 10^8 \text{ kg} \cdot \text{m}^2$$

(2.43) where virtual radius for pitching (with added mass) is

$$r''_{yy} = \sqrt{\frac{I''_{yy}}{\Delta}} = 23.37 \text{ m}$$

(2.36) and the ship's radius of gyration for pitching for fully loaded conditions k_{yy} refer to (B.2)

$$r_{yy} = k''_{yy} + k_{yy} = 20.07 \cdot \text{m}.$$

I will assume according to the [8, page 64]

$$k''_{yy} = 0.24L_{wl} = 14.654 \text{ m}$$

Look for I'_{yy} (B.1). As the ships inertia

$$I_{yy} = \Delta \cdot r_{yy}^2 = 5.506 \cdot 10^8 \cdot \text{kg} \cdot \text{m}^2$$

Ship may go a simple harmonic motion about longitudinal axis if it is displaced from its equilibrium position and then released. The virtual moment of inertia for pitching a_θ , is the vessel moment of inertia for pitching plus the added mass moment of inertia for pitching refer to (2.43).

where δl_{yy} is the added mass moment of inertia which is calculated according to following equation (2.46)

$$\delta l_{yy} = \int_{-L/2}^{L/2} a_n \zeta^2 d\zeta$$

| 1 - | 2 - | 3 - | 4 - | 5 - | 6 - | 7 - |
|---------|--|-------------|---------------|-------------------------|---|--------------------------------------|
| Station | $a_n = C \cdot \frac{\rho x}{8} \cdot B_n^2$ | ς | ς^2 | $\varsigma^2 a_n$ | multiplier | Product |
| Unit | $\left[\frac{kg}{m} \right]$ | $[m]$ | $[m^2]$ | $[kg \cdot m]$ | $[-]$ | $[kg \cdot m]$ |
| -2 | 0 | 0.00 | 0 | 0 | 1 | 0 |
| -1 | 26950 | 0.00 | 0 | 0 | 4 | 0 |
| 0 | 26950 | 21.6 | 466.56 | 1.25710 ⁷ | 2 | 2.515·10 ⁷ |
| 1 | 26950 | 18.6 | 345.96 | 9.324·10 ⁶ | 4 | 3.730·10 ⁷ |
| 2 | 26950 | 16.2 | 262.44 | 7.073·10 ⁶ | 2 | 1.415·10 ⁷ |
| 3 | 26950 | 13.5 | 182.25 | 4.912·10 ⁶ | 4 | 1.965·10 ⁷ |
| 4 | 28750 | 10.8 | 116.64 | 3.353·10 ⁶ | 2 | 6.706·10 ⁶ |
| 5 | 28750 | 8.1 | 65.61 | 1.886 · 10 ⁶ | 4 | 7.544·10 ⁶ |
| 6 | 27970 | 5.4 | 29.16 | 8.156·10 ⁵ | 2 | 1.631·10 ⁴ |
| 7 | 29690 | 2.7 | 7.29 | 2.165·10 ⁵ | 4 | 8.659·10 ⁵ |
| 8 | 28950 | 1.35 | 1.82 | 5.277·10 ⁴ | 2 | 1.055·10 ⁵ |
| 9 | 28950 | -2.7 | 7.29 | 2.111·10 ⁵ | 4 | 8.443·10 ⁵ |
| 10 | 28950 | -5.4 | 29.16 | 8.443·10 ⁵ | 2 | 1.689·10 ⁶ |
| 11 | 28950 | -8.1 | 65.61 | 1.900·10 ⁶ | 4 | 7.598·10 ⁶ |
| 12 | 28190 | -10.8 | 116.64 | 3.288·10 ⁶ | 2 | 6.577·10 ⁶ |
| 13 | 23500 | -13.5 | 182.25 | 4.283·10 ⁶ | 4 | 1.713·10 ⁷ |
| 14 | 19910 | -16.2 | 262.44 | 5.226·10 ⁶ | 2 | 1.045·10 ⁷ |
| 15 | 17910 | -18.9 | 357.21 | 6.397·10 ⁶ | 4 | 2.559·10 ⁷ |
| 16 | 12160 | -21.6 | 466.56 | 5.673·10 ⁶ | 2 | 1.135·10 ⁷ |
| 17 | 7581 | -24.3 | 590.49 | 4.476·10 ⁶ | 4 | 1.791·10 ⁷ |
| 18 | 3343 | -27.0 | 729.00 | 2.437·10 ⁶ | 2 | 4.874·10 ⁶ |
| 19 | 178 | -29.7 | 882.09 | 1.567·10 ⁵ | 4 | 6.266·10 ⁵ |
| 20 | 0 | 0 | 0 | | 2 | 0 |
| 21 | 0 | 0 | 0 | 0 | 1 | 0 |
| 22 | 0 | 0 | 0 | 0 | 1 | 0 |
| | | | | | SUM_{aθ} | 2.177·10⁸ · kg · m |

Table B.1.: Added mass moment of inertia of each section [8, Example 4.12]

B.1 Pitching - Calculation of the virtual mass moment of inertia a_θ

| 1 - | 2 - | 3 - | 4 - | 5 - | 6 - | 7 - | 8 - | 9 | 10 - | 11 - | 12 - |
|------------------------------------|---------|-------|--------|------|--------|-------------------|-------|-------------------|-------------------|------------------------|-------------------------|
| Name | m_i | xM | yM_n | zM | x_i | y_i | z_i | $(y_i^2 + z_i^2)$ | $(x_i^2 + z_i^2)$ | $m_i(y_i^2 + z_i^2)$ | $m_i(x_i^2 + z_i^2)$ |
| Unit | [Tonne] | [m] | [m] | [m] | [m] | [m ²] | [m] | [m ²] | [m ²] | [kg · m ²] | [kg · m ²] |
| Lightweight ship | 1029.3 | 24.71 | 0.01 | 5.11 | 1.24 | 0.01 | 0.6 | 0.360 | 1.898 | 370700 | 1.953 · 10 ⁶ |
| DO, Diesel Oil (RHO=0.85) | 136.0 | 19.26 | 0.22 | 2.07 | -4.21 | 0.22 | -2.44 | 6.002 | 23.678 | 816300 | 3.220 · 10 ⁶ |
| W, Domestic Fresh Water (RHO=1) | 39.7 | 34.12 | -0.06 | 1.17 | 10.65 | -0.06 | -3.34 | 11.159 | 124.578 | 443000 | 4.946 · 10 ⁶ |
| GW, Grey Water (RHO=1) | 20.0 | 39.29 | 0.00 | 1.43 | 15.82 | 0.00 | -3.08 | 9.486 | 259.759 | 189700 | 5.195 · 10 ⁶ |
| LO, Lubricating Oil (RHO=0.9) | 3.0 | 23.70 | -0.23 | 6.56 | 0.23 | -0.23 | 2.05 | 4.255 | 94.255 | 12770 | 1.277 · 10 ⁶ |
| SW, Service Water (RHO=1) | 10.0 | 28.64 | -0.08 | 0.57 | 5.17 | -0.08 | -3.94 | 15.530 | 42.253 | 155300 | 4.225 · 10 ⁶ |
| WB, Ballast Water (RHO=1.025) | 94.3 | 12.74 | -0.40 | 2.80 | -10.73 | -0.40 | -1.71 | 3.084 | 118.057 | 290800 | 1.113 · 10 ⁶ |
| CARGO, (RHO=0) | 30.0 | 4.20 | 0.00 | 7.80 | -19.27 | 0.00 | 3.29 | 10.824 | 382.157 | 324700 | 1.146 · 10 ⁶ |
| FLUID, (RHO=0) | 1.0 | 6.30 | 3.30 | 4.10 | -17.17 | 3.30 | -0.41 | 11.058 | 294.977 | 11060 | 2.950 · 10 ⁶ |
| PEOPLE, (RHO=0) | 2.3 | 36.60 | 0.00 | 9.00 | -17.17 | 3.30 | -0.41 | 11.058 | 294.977 | 25430 | 6.784 · 10 ⁶ |
| STORES, (RHO=0) | 4.0 | 43.80 | -2.00 | 3.50 | 13.13 | 0 | 4.49 | 20.160 | 192.557 | 80640 | 7.702 · 10 ⁶ |
| Total | 1369.6 | | | | | | | | | 2.72 · 10 ⁶ | 4.009 · 10 ⁷ |
| | | | | | | | | | | k_{xx} | = 1.411 m |
| | | | | | | | | | | k_{yy} | = 5.415 m |

Table B.2.: Calculation of the radius of gyration and moment of inertia for rolling and pitching compartments for PVL-101 [8, Example 4.9][7, APPENDIX 1]

The equation can be written as earlier with coefficient C (2.4)

The calculation are done by Simpson rule in the table Added mass moment of inertia of each section [8, Example 4.12] and Pitching - Calculation of the virtual mass moment of inertia a_θ . The added mass moment of inertia as the ships section spacing is $L_{spacing} = 2.7 m$:

$$I'_{yy} = \delta l_{yy} = \frac{1}{3} \cdot L_{spacing} \cdot \mathbf{SUM}_{a\theta} = 1.959 \cdot 10^8 kg \cdot m^2. \quad (B.1)$$

As per Inertial momenta virtual mass moment of inertia for pitching (ship inertia l_{yy} plus the added mass moment of inertia δI_{yy} , which is calculated according to the following references: Accelerated rotational motion & Added mass moment of inertia of each section [8, Example 4.12] & Accelerated rotational motion . I can calculate the pitching virtual moment of inertia where the ships inertial moment and rotational moment radius is calculated according to the(2.3) and (B.2) :

$$a_\theta = \delta l_{yy} + I_{yy} = 1.959 \cdot 10^8 \cdot kg \cdot m^2 + 1.367 \cdot 10^6 kg \cdot (20.07 \cdot m)^2 = 7.466 \cdot 10^8 kg \cdot m^2 \quad (B.2)$$

Ship may go a simple harmonic motion about transverse axis if it is displaced from its equilibrium position and then released.

[8].

B.2. Pitching - Calculation of damping coefficient

The damping moment always acts in the opposite direction to the motion of the ship and produces a gradual reduction in the amplitude of motion. Which is (2.47)

$$M_{b_\theta} = b_\theta \frac{d\theta}{dt}$$

where b_θ is the coefficient for the damping force in pitching, this damping coefficient normally depends on the following factors: 1) type of oscillatory motion; b) encountering frequency of oscillation, and c) form of vessel. The damping force is considered in our case as linearly proportional to the angular velocity of oscillation $\frac{d\theta}{dt}$. The damping in pitching is caused mainly by waves generated by the heaving motion of the ship, the damping coefficient per unit length is directly related to the amplitude of the waves refer to (2.7) [8, ref 89] which is

$$b_n = \frac{\rho g^2 \bar{A}^2}{\omega_e^3}$$

where ω_e is the frequency of the radiated waves (as encountering frequency), and (2.8), amplitude ratio \bar{A} can be obtained from . [8, Fig- 4.6]; therefore the total

damping coefficient can be calculated by integrating b_n over entire length of the ship, refer to (2.9) that is

$$b = \int_{-L/2}^{L/2} b_n dx$$

Calculating according to the example [8, Example 4.13 Calculation of damping coefficient] the PVL101 damping coefficient in pitching is according to the (2.48) & (B.3)

$$b_\theta = \int_{-L/2}^{L/2} b_n \times \zeta^2 d\zeta = \frac{1}{3} \times s \times \mathbf{SUM}_{b\theta} = 2.884 \cdot 10^8 \cdot \frac{kg \cdot m^2}{s} \quad (\text{B.3})$$

The damping for the pitching motion is increased by the following:

- increase of beam
- Decrease of draft
- decrease of vertical prismatic coefficient.

B.3. Pitching - Calculation of restoring coefficient

Determine the restoring moment for the ship according to the strip theory and (B.4), (2.49)&(2.50) by Simpson rule:

$$c_{c\theta} = \rho g \theta \int_{-L/2}^{L/2} x^2 y(x) dx = \frac{1}{3} \times s \times \mathbf{SUM}_{c\theta} = 8.152 \cdot 10^8 \cdot N \cdot m \quad (\text{B.4})$$

B.4. Pitching - Calculation of Free damped Pitching equation solution

The simplified expression according to (2.15) with calculated initial conditions are:

$$\theta = \frac{87 e^{-\frac{823 t}{2000}} \left(3690671 \cos \left(\frac{\sqrt{3690671} t}{2000} \right) + 823 \sqrt{3690671} \sin \left(\frac{\sqrt{3690671} t}{2000} \right) \right)}{3690671000} \quad (\text{B.5})$$

| 1 - | 7 - | 3 - | 4 - | 5 - | 6 - | 7 - |
|---------|--|---------|-------------------|--------------------|---|---|
| Station | $b_n = \rho \frac{g^2}{m^3} \cdot \bar{A}^2$ | ζ | ζ^2 | $\zeta^2 b_n$ | multiplier | Product |
| Unit | [-] | [m] | [m ²] | [kg · m] | $\frac{kg \cdot m}{s}$ | $\frac{kg \cdot m}{s}$ |
| -2 | 0 | 0.00 | 0 | 0 | 1 | 0 |
| -1 | $1.66 \cdot 10^4$ | 0.00 | 0 | 0 | 4 | 0 |
| 0 | $1.69 \cdot 10^4$ | 21.6 | 466.56 | $7.865 \cdot 10^6$ | 2 | $1.573 \cdot 10^7$ |
| 1 | $1.66 \cdot 10^4$ | 18.6 | 345.96 | $5.832 \cdot 10^6$ | 4 | $2.333 \cdot 10^7$ |
| 2 | $2.04 \cdot 10^4$ | 16.2 | 262.44 | $5.353 \cdot 10^6$ | 2 | $1.071 \cdot 10^7$ |
| 3 | $3.3 \cdot 10^4$ | 13.5 | 182.25 | $6.022 \cdot 10^6$ | 4 | $2.409 \cdot 10^7$ |
| 4 | $3.31 \cdot 10^4$ | 10.8 | 116.64 | $3.854 \cdot 10^6$ | 2 | $7.708 \cdot 10^6$ |
| 5 | $3.31 \cdot 10^4$ | 8.1 | 65.61 | $2.168 \cdot 10^6$ | 4 | $8.671 \cdot 10^6$ |
| 6 | $3.31 \cdot 10^4$ | 5.4 | 29.16 | $9.634 \cdot 10^5$ | 2 | $1.927 \cdot 10^6$ |
| 7 | $4.1 \cdot 10^4$ | 2.7 | 7.29 | $2.991 \cdot 10^5$ | 4 | $1.196 \cdot 10^6$ |
| 8 | $4.11 \cdot 10^4$ | 1.35 | 1.82 | $7.477 \cdot 10^4$ | 2 | $1.495 \cdot 10^5$ |
| 9 | $4.1 \cdot 10^4$ | -2.7 | 7.29 | $2.991 \cdot 10^5$ | 4 | $1.196 \cdot 10^6$ |
| 10 | $4.11 \cdot 10^4$ | -5.4 | 29.16 | $1.196 \cdot 10^6$ | 2 | $2.392 \cdot 10^6$ |
| 11 | $4.1 \cdot 10^4$ | -8.1 | 65.61 | $2.692 \cdot 10^6$ | 4 | $1.077 \cdot 10^7$ |
| 12 | $4.1 \cdot 10^4$ | -10.8 | 116.64 | $4.785 \cdot 10^6$ | 2 | $9.570 \cdot 10^6$ |
| 13 | $4.1 \cdot 10^4$ | -13.5 | 182.25 | $7.477 \cdot 10^6$ | 4 | $2.991 \cdot 10^7$ |
| 14 | $84.1 \cdot 10^4$ | -16.2 | 262.44 | $1.077 \cdot 10^7$ | 2 | $2.153 \cdot 10^7$ |
| 15 | $1.65 \cdot 10^4$ | -18.9 | 357.21 | $1.180 \cdot 10^6$ | 4 | $4.721 \cdot 10^7$ |
| 16 | $2.73 \cdot 10^4$ | -21.6 | 466.56 | $1.542 \cdot 10^7$ | 2 | $3.083 \cdot 10^7$ |
| 17 | 0.68 | -24.3 | 590.49 | $8.063 \cdot 10^6$ | 4 | $3.225 \cdot 10^7$ |
| 18 | 1.22 | -27.0 | 729.00 | $9.954 \cdot 10^6$ | 2 | $1.991 \cdot 10^7$ |
| 19 | 0.34 | -29.7 | 882.09 | $5.353 \cdot 10^6$ | 4 | $2.141 \cdot 10^7$ |
| 20 | 0 | 0 | 0 | 0 | 2 | 0 |
| 21 | 0 | 0 | 0 | 0 | 1 | 0 |
| 22 | 0 | 0 | 0 | 0 | 1 | 0 |
| | | | | | SUM_{bθ} | $3.205 \cdot 10^8 \cdot \frac{kg \cdot m}{s}$ |

Table B.3.: Calculation of the damping coefficient for pitching [8, Example 4.13]

where t is time. The expression which has 2 solution has the characteristic equation $\theta^2 + 0.823 \cdot \theta + 1.092 = 0$ with roots

$$r = \begin{bmatrix} -0.412 + 0.96i \\ -0.412 - 0.96i \end{bmatrix}.$$

I know all the coefficients from (2.51) and I can calculate all the necessary parameters to fully solve the equation and later use them in the excited motion equation also.

Acceleration in free, damped motion of the PVL-101 ship Differentiating the solution of the (B.5) twice and revealing the equation for acceleration:

$$\frac{d^2z}{dt^2} = -A\omega_d^2 \exp^{-\nu t} \sin(\omega_d t)$$

The graphical representation of the acceleration expression refer to (B.1)

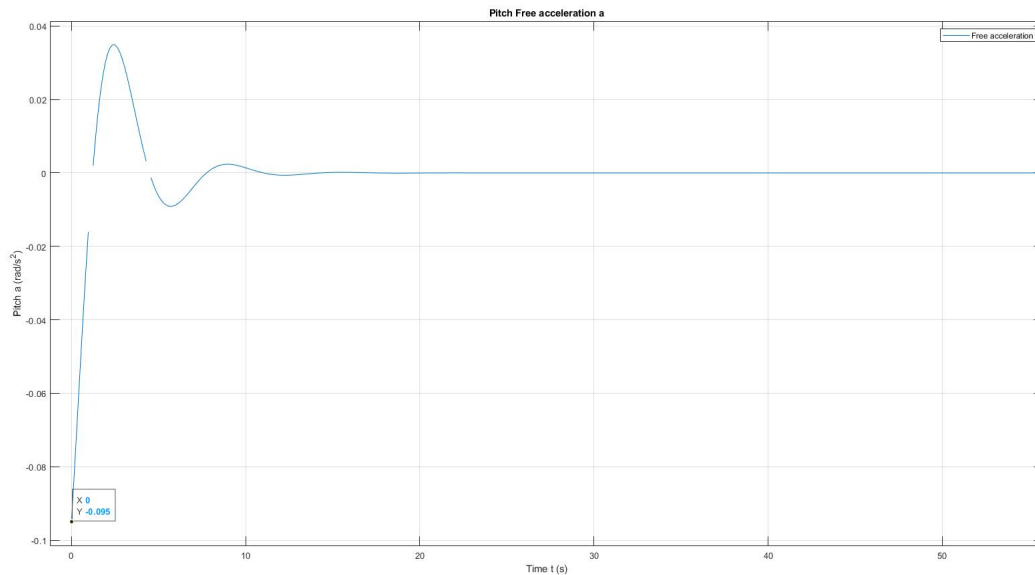


Figure B.1.: Free damped pitch movement acceleration

Free, damped Pitching Motion

14.10.2020 @ j.urb

Initial conditions

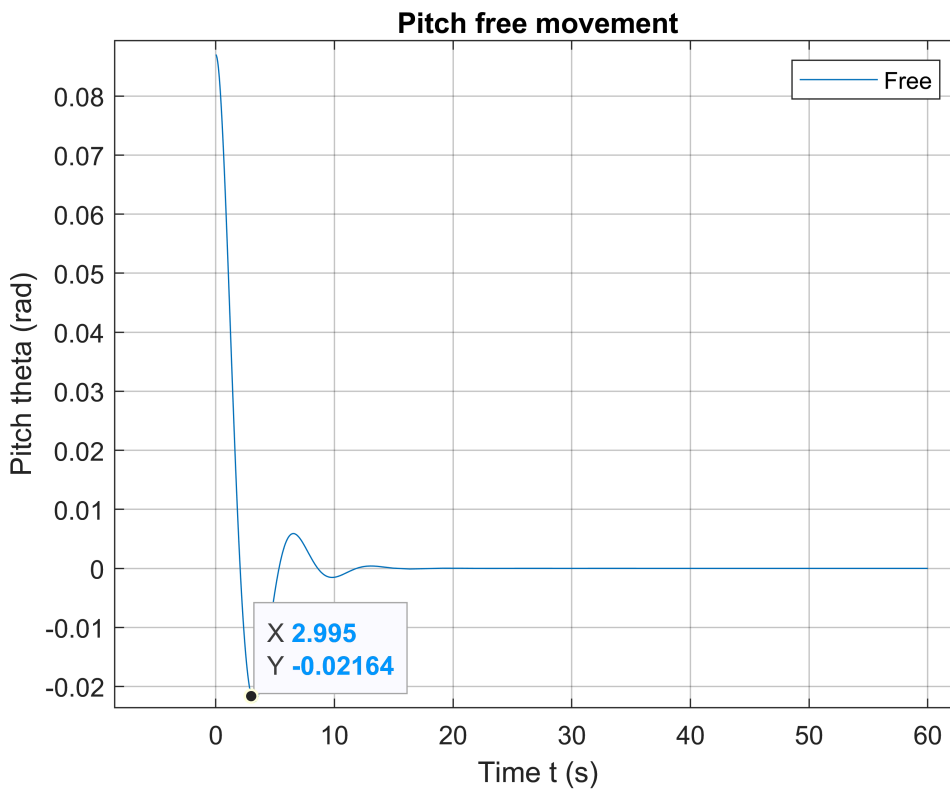
$$l = 0.0870$$

$$v = 0$$

Second order differential equation solution

simple =

$$\frac{87 e^{-\frac{823 t}{2000}} \left(3690671 \cos\left(\frac{\sqrt{3690671} t}{2000}\right) + 823 \sqrt{3690671} \sin\left(\frac{\sqrt{3690671} t}{2000}\right) \right)}{3690671000}$$



simple2 =

$$\frac{87 e^{-\frac{823 t}{2000}} \left(16740848726072534098561595781896665123975593984 \cos\left(\frac{8449139566704239 t}{8796093022208000}\right) - 717 \right)}{1533044755134847265489302033428724}$$

Acceleration plot

B.5. Pitching - Calculation of Exciting moment

By performing numerical calculations, we can conclude:

1. When, the effective wavelength is less than half the ship's length, the pitching moment is small.
2. When the effective wavelength equals the ship's length, the. the pitching moment is high. It attains its maximum value, which is dependent on the form (for example the water plane coefficient), for $1.0 < L_w/L < 1.5$.
3. the asymptotic value of the pitching moment as the effective wavelength approaches infinity is zero, as the constant wave height and infinite length the wave slope tends to disappear.

The exciting moment for pitching is due to unbalanced moment caused by the waves about the transverse axis of the ship. We obtain the exciting moment for pitching: by two dimensional integrating over the ship sections and wave profile over the ship length and multiplying each section wave force with distance to LCG (2.52) Table B.5: "Calculation-of-exciting moment". Where ζ is the distance from LCG, y is the Half-Breadth of water plane, $k = \frac{2\pi}{L_{wl}}$ is wave number and calculations are with head seas $\mu = 180^\circ$. Exciting coefficient for Pitching as the ships section spacing is $L_{spacing} = 2.7 m$:

$$integral_{M\theta} = \frac{1}{3} \cdot L_{spacing} \cdot \mathbf{SUM}_{M\theta} = -376.04 m^3. \quad (B.6)$$

Refer (2.53) and non dimensional amplitude of the exciting moment

$$f_{0_{M\theta}} = \frac{4}{L_{wl}^2 \cdot B_{max}} \cdot (integral_{M\theta}) = -0.02. \quad (B.7)$$

and

$$M_{0_\theta} = \rho g \xi_a L_{wl}^2 B_{max} \cdot f_{0_{M\theta}} = -5.926 \cdot 10^7 N \cdot s \quad (B.8)$$

B.6. 5.Pitching - PVL-101 differential equation calculation and its solution"

The equation is as follows: (2.41)

$$a_\theta \ddot{\theta} + b_\theta \dot{\theta} + c_\theta \theta = M_{0_\theta} \cos(\omega_c t)$$

Virtual mass:

$$a_\theta = 7.466 \cdot 10^8 \text{ kg} \cdot \text{m}^2.$$

Damping coefficient:

$$b_\theta = 6.146 \cdot 10^8 \cdot \frac{\text{kg} \cdot \text{m}^2}{\text{s}}$$

. Restoring coefficient:

$$c_\theta = 8.152 \cdot 10^8 \cdot \text{N} \cdot \text{m}.$$

Amplitude of the exciting force: $M_0 = 5.926 \cdot 10^7 \text{ N} \cdot \text{s}$.

Encountering wave frequency: $\omega_e = \frac{2\pi}{T_e}, T_e = 10 \text{ s}$ [16, page 29], $\omega_e = 0.628 \frac{1}{\text{s}}$. Natural frequency: $\omega_\theta = \sqrt{\frac{c_\theta}{a_\theta}} = 1.045 \frac{1}{\text{s}}$ (2.2). The tuning factor:

$$\Lambda_\theta = \frac{\omega_e}{\omega_\theta} = 0.601$$

(2.29). The non-dimensional damping factor

$$\kappa_\theta = \frac{\nu_\theta}{\omega_\theta} = 0.394 \frac{1}{\text{s}}$$

[13, page 100] where $\nu_\theta = \frac{b_\theta}{2a_\theta} = 0.412 \frac{1}{\text{s}^2}$ (2.16). The circular frequency of the damped oscillation, that is [8, eq:4.6a] $\omega_{d_\theta} = \sqrt{\omega_\theta^2 - \nu_\theta^2} = 0.96 \frac{1}{\text{s}}$. The heaving amplitude

$$z_{a_\theta} = z_{st_\theta} \cdot \mu_\theta = -0.091 \text{ rad}$$

where $z_{st_\theta} = \frac{M_0}{c_\theta} = -0.073$ (2.26)&(2.27).

Then the equation can be expressed as: [20, ch:10] or [13, eq:4.14]

$$\ddot{\theta} + 2\kappa_\theta\omega_\theta\dot{\theta} + \omega_\theta^2\theta = z_{a_\theta} \cos(\omega_e t) \quad (\text{B.9})$$

$$\ddot{\theta} + 0.823 \cdot \dot{\theta} + 1.092 \cdot \theta = -0.091 \cdot \cos(0.628 \cdot t - 2.209) \quad (\text{B.10})$$

The roots for the characteristic equation refer to (B.4).

Then the solution can be expressed as

$$\theta = A1 \exp^{\nu_\theta t} \sin(\omega_{d_\theta} t - \beta) + z_{a_\theta} \cos(\omega_e t - \varepsilon_\theta)$$

(2.54).

According from [20, eq:10.7A and 10.7B] the first part of the solution

$$\theta_1 = A1 \exp^{-\nu_{\theta}t} \sin(\omega_{d_{\theta}}t - \beta)$$

which is the ships natural movement. The second part

$$\theta_2 = z_{a_{\theta}} \cos(\omega_e t - \varepsilon_{2_{\theta}})$$

is the encountering movement. Hole solution: $\theta = \theta_1 + \theta_2$. The phase angle between the wave motion and the pitching motion is expressed as

$$\varepsilon_{\theta} = \varepsilon_{1_{\theta}} + \varepsilon_{2_{\theta}}$$

where ε_1 is the phase angle between the wave motion and the exciting force caused by waves, and ε_2 is the phase angle between the exciting force and the heaving motion. Now $\varepsilon_{1_{\theta}} = 90^\circ$ [8, eq:4.12b] and from [8, page 38]

$$\varepsilon_{2_{\theta}} = \arctan \frac{2\kappa_{\theta}\Lambda_{\theta}}{1 - \Lambda_{\theta}^2} = 0.638 \text{ rad}$$

and $\varepsilon_{\theta} = 2.209 \text{ rad}$. As for (2.54) the solution to the pitching movement is as follows and refer to the graphical solution (B.2) and acceleration look fig B.3:Pitching-acceleration-a.

$$\theta = \frac{87 e^{-\frac{823t}{2000}} \left(3690671 \cos\left(\frac{\sqrt{3690671}t}{2000}\right) + 823 \sqrt{3690671} \sin\left(\frac{\sqrt{3690671}t}{2000}\right) \right)}{3690671000} - 0.091 \cdot \cos(0.628 \cdot t - 2.209) \quad (\text{B.11})$$

| 1 - | 2 - | 3 - | | 3 - | 4 - | 5 | 6 - | 7 - |
|------------|------------|--------------------|-----------------|-------------|-------------------|-------------------------|---|--|
| Station | B_n | $c_n = \rho g B_n$ | | ς | ς^2 | $c_n \cdot \varsigma^2$ | multiplier | Product |
| Unit | [m] | | $\frac{N}{m^2}$ | [m] | [m ²] | [N] | [-] | [N] |
| -2 | 0.00 | 0 | | 0.00 | 0 | 0 | 1 | 0 |
| -1 | 9.54 | $9.398 \cdot 10^4$ | | 0.00 | 0 | 0 | 4 | 0 |
| 0 | 9.54 | $9.398 \cdot 10^4$ | | 21.6 | 466.56 | $4.385 \cdot 10^7$ | 2 | $8.769 \cdot 10^7$ |
| 1 | 9.54 | $9.398 \cdot 10^4$ | | 18.6 | 345.96 | $3.251 \cdot 10^7$ | 4 | $1.301 \cdot 10^8$ |
| 2 | 9.54 | $9.398 \cdot 10^4$ | | 16.2 | 262.44 | $2.466 \cdot 10^7$ | 2 | $4.933 \cdot 10^7$ |
| 3 | 9.54 | $9.398 \cdot 10^4$ | | 13.5 | 182.25 | $1.713 \cdot 10^7$ | 4 | $6.851 \cdot 10^7$ |
| 4 | 9.54 | $9.398 \cdot 10^4$ | | 10.8 | 116.64 | $1.096 \cdot 10^7$ | 2 | $2.192 \cdot 10^7$ |
| 5 | 9.54 | $9.398 \cdot 10^4$ | | 8.1 | 65.61 | $6.166 \cdot 10^6$ | 4 | $2.466 \cdot 10^7$ |
| 6 | 9.41 | $9.27 \cdot 10^4$ | | 5.4 | 29.16 | $2.703 \cdot 10^6$ | 2 | $5.406 \cdot 10^6$ |
| 7 | 9.70 | $9.552 \cdot 10^4$ | | 2.7 | 7.29 | $6.963 \cdot 10^5$ | 4 | $2.785 \cdot 10^6$ |
| 8 | 9.70 | $9.552 \cdot 10^4$ | | 1.35 | 1.82 | $1.741 \cdot 10^5$ | 2 | $3.482 \cdot 10^5$ |
| 9 | 9.70 | $9.552 \cdot 10^4$ | | -2.7 | 7.29 | $6.963 \cdot 10^5$ | 4 | $2.785 \cdot 10^6$ |
| 10 | 9.70 | $9.552 \cdot 10^4$ | | -5.4 | 29.16 | $2.785 \cdot 10^6$ | 2 | $5.570 \cdot 10^6$ |
| 11 | 9.70 | $9.552 \cdot 10^4$ | | -8.1 | 65.61 | $6.267 \cdot 10^6$ | 4 | $2.507 \cdot 10^7$ |
| 12 | 9.57 | $9.425 \cdot 10^4$ | | -10.8 | 116.64 | $1.099 \cdot 10^7$ | 2 | $2.199 \cdot 10^7$ |
| 13 | 8.91 | $8.775 \cdot 10^4$ | | -13.5 | 182.25 | $1.599 \cdot 10^7$ | 4 | $6.397 \cdot 10^7$ |
| 14 | 8.20 | $8.078 \cdot 10^4$ | | -16.2 | 262.44 | $2.120 \cdot 10^7$ | 2 | $4.240 \cdot 10^7$ |
| 15 | 7.78 | $7.661 \cdot 10^4$ | | -18.9 | 357.21 | $2.736 \cdot 10^7$ | 4 | $1.095 \cdot 10^8$ |
| 16 | 6.21 | $6.112 \cdot 10^4$ | | -21.6 | 466.56 | $2.852 \cdot 10^7$ | 2 | $5.703 \cdot 10^7$ |
| 17 | 4.90 | $4.826 \cdot 10^4$ | | -24.3 | 590.49 | $2.850 \cdot 10^7$ | 4 | $1.140 \cdot 10^8$ |
| 18 | 3.25 | $3.205 \cdot 10^4$ | | -27.0 | 729.00 | $2.336 \cdot 10^7$ | 2 | $4.673 \cdot 10^5$ |
| 19 | 0.75 | $7.387 \cdot 10^3$ | | -29.7 | 882.09 | $6.516 \cdot 10^6$ | 4 | $2.606 \cdot 10^4$ |
| 20 | 0.75 | $7.387 \cdot 10^3$ | | 0 | 0 | 0 | 1 | 0 |
| 21 | 0.75 | $7.387 \cdot 10^3$ | | 0 | 0 | 0 | 0 | 0 |
| 22 | 0 | 0 | | 0 | 0 | 0 | 0 | 0 |
| | | | | | | | SUM_{cθ} | $9.058 \cdot 10^8 \cdot N$ |

Table B.4.: Calculation of restoring coefficient for Pitching[8, Examlle 4.14]

| 1 - | 2 - | 3 - | 4 - | 5 - | 6 - | 7 - | 8 - | 9 - |
|---------|---------------------|---------|-------------------|--------------------------------|--------------------------------|--|-------------------------|-------------------------------|
| Station | $y = \frac{B_n}{2}$ | ζ | $y \cdot \zeta$ | $k \cdot \zeta \cdot \cos \mu$ | $\sin(k \cdot \zeta \cos \mu)$ | $y \cdot \zeta \cdot \sin(k \cdot \zeta \cos \mu)$ | multiplier | Product |
| Unit | [m] | [m] | [m ²] | [-] | [-] | [m ²] | [-] | [m ²] |
| -2 | 0.00 | 0.0 | 0.00 | 0.000 | 0.000 | 0.000 | 1 | 0.00 |
| -1 | 4.77 | 0.0 | 0.00 | 0.000 | 0.000 | 0.000 | 4 | 0.00 |
| 0 | 4.77 | 21.6 | 103.054 | 1.357 | -0.977 | 42.241 | 2 | 84.481 |
| 1 | 4.77 | 18.6 | 88.741 | -1.169 | -0.92 | 39.775 | 4 | 159.102 |
| 2 | 4.77 | 16.2 | 77.290 | -1.018 | -0.851 | 36.783 | 2 | 73.565 |
| 3 | 4.77 | 13.5 | 64.409 | -0.848 | -0.750 | 32.422 | 4 | 129.689 |
| 4 | 4.77 | 10.8 | 51.527 | -0.679 | -0.628 | 27.131 | 2 | 54.262 |
| 5 | 4.77 | 8.10 | 38.645 | -0.509 | -0.487 | 21.061 | 4 | 84.242 |
| 6 | 4.71 | 5.40 | 25.412 | -0.339 | -0.333 | 14.386 | 2 | 28.771 |
| 7 | 4.85 | 2.70 | 13.092 | -0.170 | -0.169 | 7.298 | 4 | 29.19 |
| 8 | 4.85 | 1.35 | 6.546 | -0.085 | -0.085 | 3.662 | 2 | 7.324 |
| 9 | 4.85 | -2.7 | -13.092 | 0.170 | 0.169 | -7.298 | 4 | -29.19 |
| 10 | 4.85 | -5.4 | -26.185 | 0.339 | 0.333 | -14.386 | 2 | -28.771 |
| 11 | 4.85 | -8.1 | -39.277 | 0.509 | 0.487 | -21.061 | 4 | -84.242 |
| 12 | 4.79 | -10.8 | -51.678 | 0.679 | 0.628 | -27.131 | 2 | -54.262 |
| 13 | 4.46 | -13.5 | -60.143 | 0.848 | 0.750 | -32.422 | 4 | -129.689 |
| 14 | 4.10 | -16.2 | -66.436 | 1.018 | 0.851 | -36.783 | 2 | -73.565 |
| 15 | 3.89 | -18.9 | -73.502 | 1.188 | 0.927 | -40.087 | 4 | -160.349 |
| 16 | 3.10 | -21.6 | -67.025 | 1.357 | 0.977 | -42.241 | 2 | -84.481 |
| 17 | 2.45 | -24.3 | -59.535 | 1.527 | 0.999 | -43.181 | 4 | -172.726 |
| 18 | 1.62 | -27.0 | -43.929 | 1.696 | 0.992 | -42.882 | 2 | -85.765 |
| 19 | 0.38 | -29.7 | -11.138 | 1.866 | 0.957 | -41.352 | 4 | -165.409 |
| 20 | 0.38 | 0 | 0 | 0 | 0 | 0 | 2 | 0.000 |
| 21 | 0.00 | 0 | 0 | 0 | 0 | 0 | 1 | 0.000 |
| 22 | 0 | 0 | 0 | 0 | 0 | 0 | 1 | 0 |
| | | | | | | | SUM_{M0} | -417.823 m² |

Table B.5.: Calculation of exciting moment [8, Example 4.6]

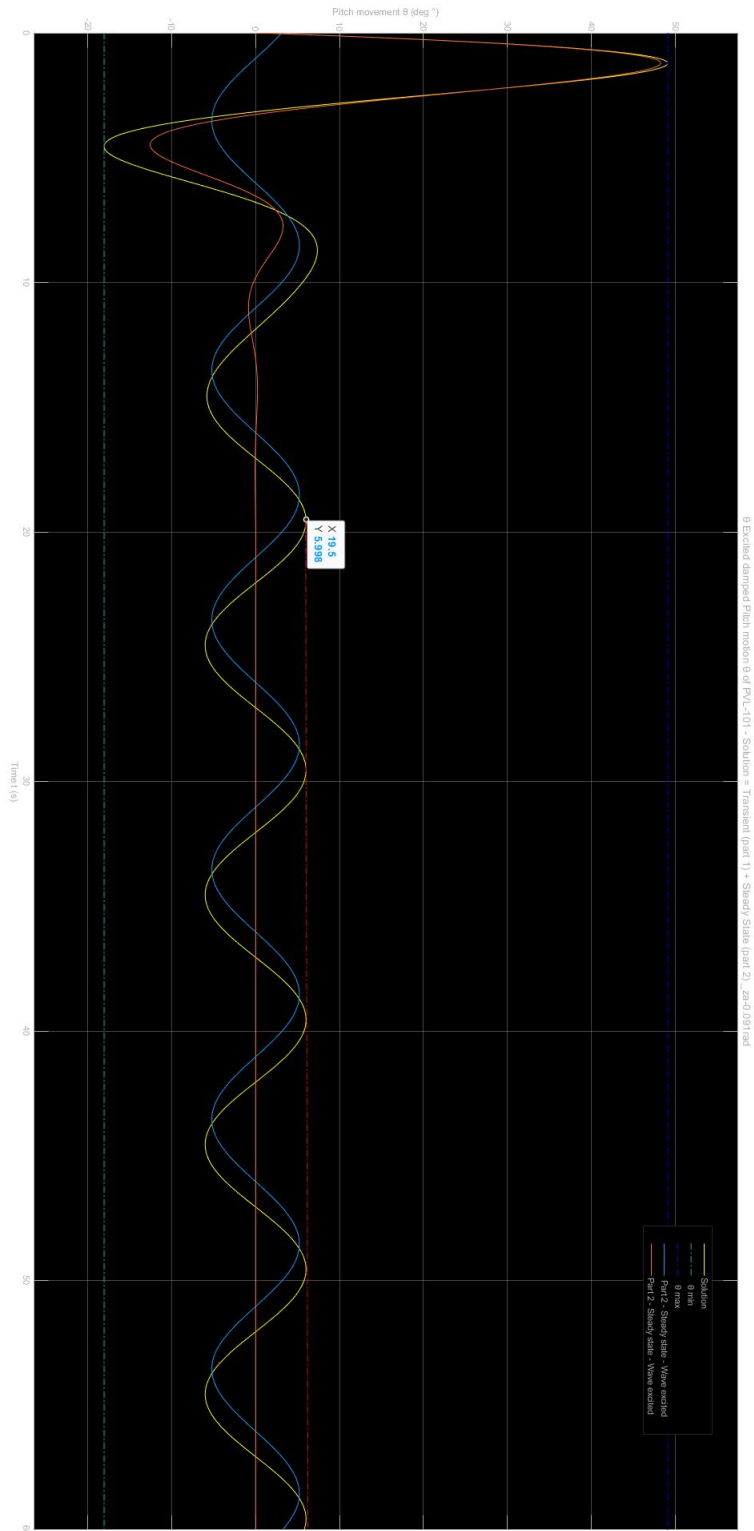


Figure B.2.: Pitching movement θ

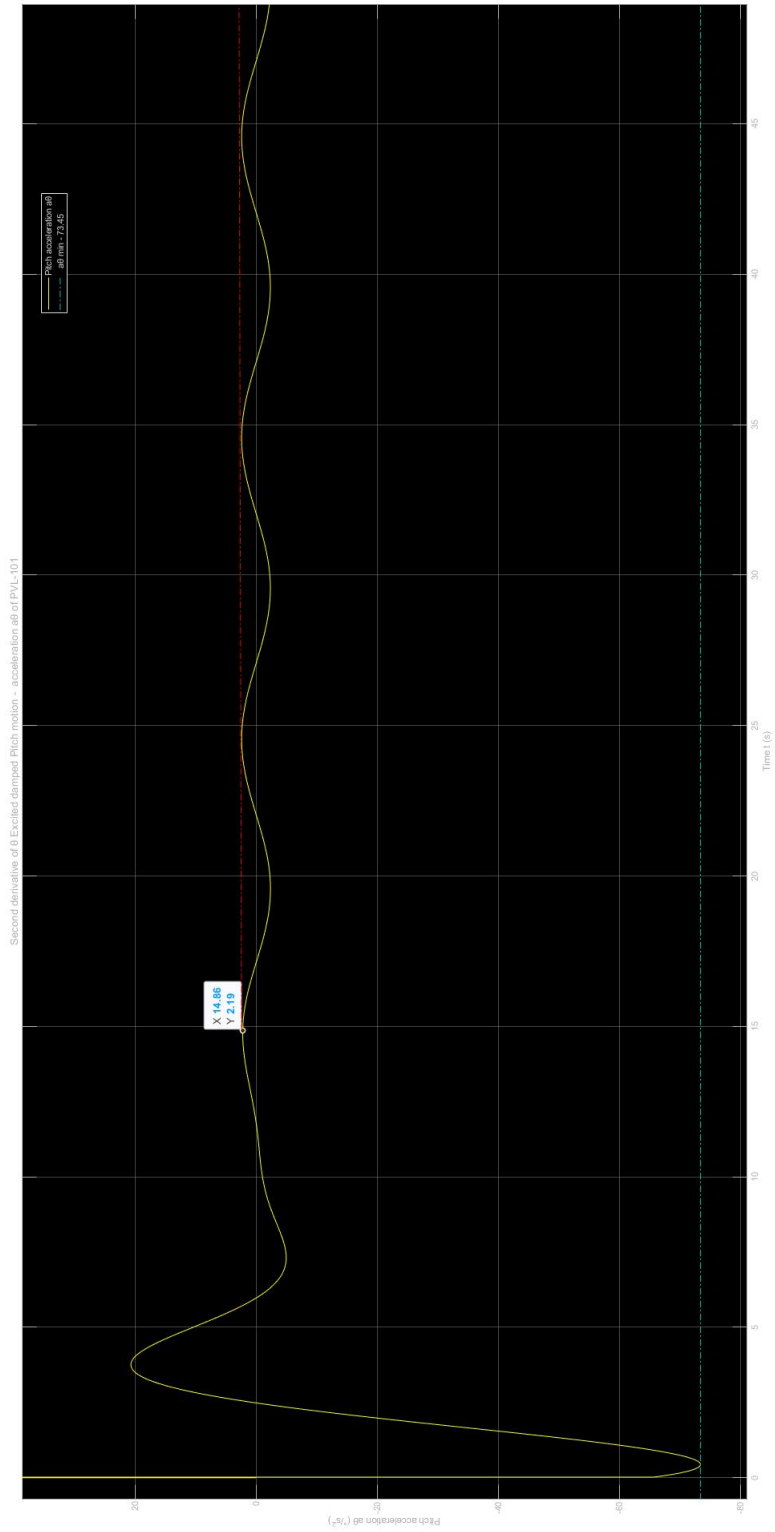


Figure B.3.: Pitching acceleration a

C. : Appendix 3: Rolling Calculation of coefficients

C.1. Rolling - Calculation of the virtual mass moment of inertia a_ϕ

According to my calculation the total moment of inertia for rolling :

1. virtual moment of inertia for rolling is

$$I''_{xx} = I'_{xx} + I_{xx} = 3.743 \cdot 10^7 \text{ kg} \cdot \text{m}^2$$

where virtual radius for rolling (with added mass) is

$$r''_{xx} = \sqrt{\frac{I''_{xx}}{\Delta}} = 5.23 \text{ m}$$

(2.36) and the ship's radius of gyration for rolling for fully loaded conditions k_{xx} refer to (B.2)

$$r_{xx} = k''_{xx} + k_{xx} = 4.78 \cdot \text{m}$$

[8, pages 75]

$$k''_{xx} = 0.33B = 3.37 \text{ m}$$

Look for I'_{yy} (C.1). As the ships inertia

$$I_{xx} = \Delta \cdot r_{xx}^2 = 3.119 \cdot 10^7 \cdot \text{kg} \cdot \text{m}^2$$

Ship may go a simple harmonic motion about longitudinal axis if it is displaced from its equilibrium position and then released. The virtual moment of inertia for rolling a_ϕ , is the vessel moment of inertia for rolling plus the added mass moment of inertia for rolling refer to (2.57). The virtual mass moment of inertia is (2.57) & (2.3):

$$I'_{yy} = 0.2 \cdot I_{xx} = 6.238 \cdot 10^6 \cdot \text{kg} \cdot \text{m}^2 \quad (\text{C.1})$$

$$a_\phi = I'_{xx} + I_{xx} = 3.743 \cdot 10^7 \text{ kg} \cdot \text{m}^2 \quad (\text{C.2})$$

[8].

C.2. Rolling - Calculation of damping coefficient b_ϕ

The damping moment always acts in the opposite direction to the motion of the ship and produces a gradual reduction in the amplitude of motion. Which is (2.48) and the calculation of the numeric damping coefficient based on a ships operator test in turn refer to (E.2). The general concept of the calculation are as follows:

The roll movement angular frequency measured in test:

$$\omega_{d\phi} = \frac{2\pi}{T} = 0.785 \cdot \frac{1}{s} \quad (2.2)$$

Calculated from rolling restoring coefficient and inertial moment the ship, we can calculate the natural frequency, refer to (2.5.3) :

$$\omega_\phi = \sqrt{\frac{c_\phi}{a_\phi}} \cdot \frac{1}{s} \quad (C.7)$$

Referring to the previous equations for the Heaving and Pitching differential equations, we can calculate the following for rolling. As I know the circular frequency of the damped rolling motion $\omega_{d\phi}$, that was measured by the ship operator and from equation (2.17) I can calculate the decaying constant ν_ϕ for rolling

$$\nu_\phi = \sqrt{\omega_\phi^2 + \omega_{d\phi}^2} = 1.002 \cdot \frac{1}{s}$$

and from decaying constant equation (2.16) I can calculate the non-linear damping b_ϕ

$$b_\phi = 2a_\phi \cdot \nu_\phi = 7.498 \cdot 10^7 \cdot kg \cdot m^2 \quad (C.3)$$

C.3. Rolling - Calculation of restoring coefficient c_ϕ

Linear restoring coefficient according to the (2.62):

$$c_\phi = \Delta \bar{GM} \cdot g = 1.447 \cdot 10^7 \cdot J \quad (C.4)$$

where Δ is the displacement of the ship and \bar{GM} are the metacentric height.

As I know the Δ displacement of the ship and \bar{GZ} the rightening arm which both are known conditions in current case. So I can calculate the $c_{\phi 1}$ in non-linear condition as

I know heeling angle. [7] The restoring coefficient I can calculate according to (2.63), where in the (C.5) I have acquired the \bar{GZ} from [7] and the second calculation (C.6) the \bar{GZ} is calculated by the (2.64). The difference should be only the measure of added mass and correction's to the \bar{GZ} which are $\sim 19\%$ as approximately the added mass is. So I will use the coefficient (C.4) in my linear differential equation. For the non-linear calculation it is possible to use the $c_{\phi 2}$, but as I further investigated the most accurate will be the power series method for a long term solution of Duffing oscillator or the use of a Bessel function [11]. As these calculations will be too complicated for this study and the $c_{\phi 1}$ or $c_{\phi 2}$, are not accurate for bigger angles I will use the recommended power series method by [33, eq: 2.7] and [8, sec: 10.2]. For comparison of the restoring coefficients of different methods are calculated below:

$$c_{\phi 1} = \Delta \bar{GZ} \cdot g = 4.783 \cdot 10^6 \cdot J \quad (C.5)$$

$$c_{\phi 2} = \Delta \cdot (G\bar{M} \sin \phi + \frac{B\bar{M}}{2} \cdot \tan^2 \phi \cdot \sin \phi) = 5.882 \cdot 10^6 \cdot J \quad (C.6)$$

(2.63)&(2.64). The simple method of multiplying the known value of \bar{GZ} refer to (C.5) when acquiring to the linear equation (2.62), gives a correct answer only to that condition and is not suitable for non-linear form.

For small angles of inclination is valid only for small amplitudes of rolling displacement (say 10°) the coefficient is in linear form, but in our case I will solve the equation numerically by MAT LAB, as I know the initial conditions.

So I can also calculate the natural frequency

$$\omega_\phi = \sqrt{\frac{c_\phi}{a_\phi}} = 0.622 \cdot \frac{1}{s} \quad (C.7)$$

For linearizing the \bar{GZ} according to the [7] acquired data and according to the 2.66 the polynomial in degrees form are:

$$\bar{GZ} = 8.2527 \cdot 10^{-7} \cdot \phi^3 - 3.9815 \cdot 10^{-4} \phi^2 + 0.0264 \cdot \phi^1 - 0.0153 \cdot \phi^0 \quad (C.8)$$

and in radians

$$\bar{GZ} = 0.1552 \cdot \phi^3 - 1.3070 \cdot 10^{-4} \phi^2 + 1.5100 \cdot \phi^1 - 0.0153 \cdot \phi^0 \quad (C.9)$$

The nonlinear restoring coefficient according to the (2.63):

$$c_{\phi_{nonlin}} = c_{1\phi_{nonli}} \phi^3 + c_{2\phi_{nonli}} \phi^2 + c_{3\phi_{nonli}} \phi^1 + c_{4\phi_{nonli}} \quad (C.10)$$

, where

$$c_{1\phi_{nonli}} = 2.079 \cdot 10^6 N \cdot m;$$

$$c_{2\phi_{nonli}} = -1.751 \cdot 10^7 N \cdot m;$$

$$c_{3\phi_{nonli}} = 2.023 \cdot 10^7 N \cdot m;$$

$$c_{4\phi_{nonli}} = -2.05 \cdot 10^5 N \cdot m.$$

C.4. Rolling - Calculation of Free damped rolling equation solution

The solution for the free rolling motion from equation (2.68), that are in numerical form:

$$\ddot{\phi} + 0.387\phi = 0$$

The simplified expression according to (2.15) with calculated initial conditions ($\phi = 10^\circ$ and $\dot{\phi} = 0$) for free rolling without damping are:

$$\phi = \frac{3144105663975531 \cos\left(\frac{3\sqrt{430}t}{100}\right)}{18014398509481984} \quad (C.11)$$

where t is time and the graphical solution are (C.3).

The expression for free damped motion has 2 solution and the characteristic equation if we assume the equation is linear (up to 10° heel) $\phi^2 + 2.003 \cdot \phi + 0.387 = 0$ with roots

$$r = \begin{bmatrix} -1.787 \\ -0.216 \end{bmatrix}$$

and this is a over damped differential equation with real roots. The free damped rolling motion is also calculated and the MAT LAB printout are in the end of this Appendix C.4 section.

I know all the coefficients from (2.51) and I can calculate all the necessary parameters to fully solve the equation and later use them in the excited motion equation also.

The graphical representation of the (C.11) acceleration expression refer to (C.4).

As in the case the equation are non-linear (if heeling angle over 10°) for the restoring coefficient refer to the (C.9) for \bar{GZ} and for simplicity I will assume the damping coefficient is linear. Then the roll equation becomes

Free, damped Rolling Motion

02.11.2020 @ j.urb

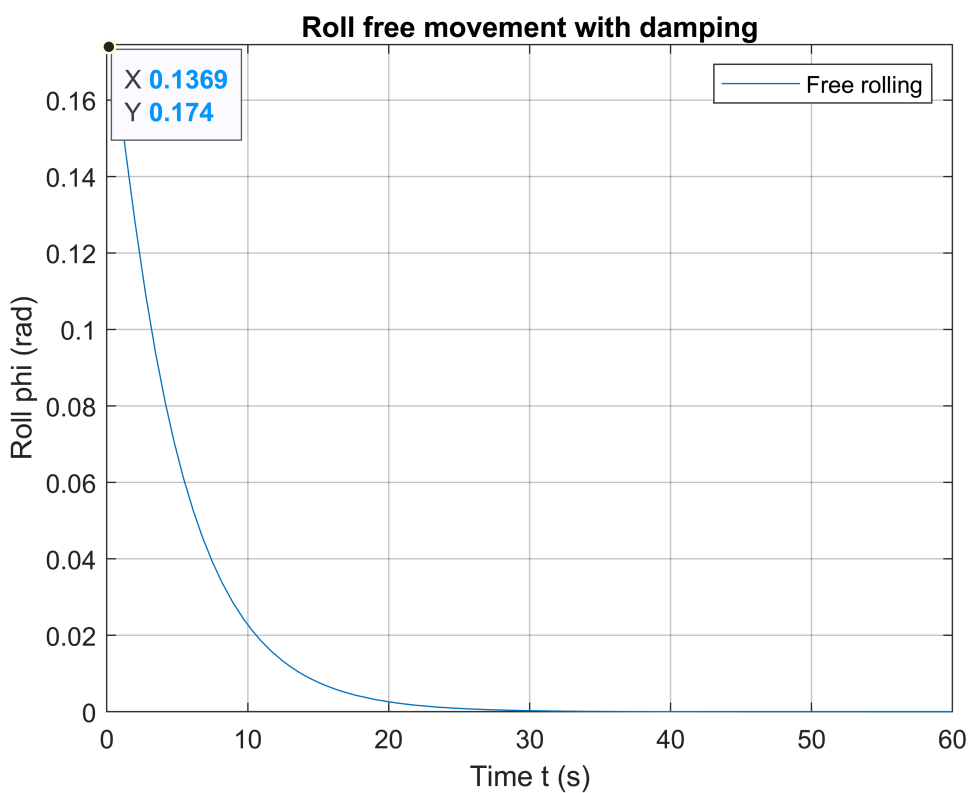
Initial conditions

$$l = 0.1745$$

$$v = 0$$

yNotSimplified =

$$\frac{3144105663975531 \sqrt{2464009}}{88775280113900387827712} e^{t \left(\frac{\sqrt{2464009} - 2003}{2000} \right)} (\sqrt{2464009} + 2003) - e^{-t \left(\frac{\sqrt{2464009} + 2003}{2000} \right)} \left(\frac{6297643644}{88775280113900387827712} \right)$$



Simple

simple =

$$\frac{3144105663975531 \sqrt{2464009}}{88775280113900387827712} e^{t \left(\frac{\sqrt{2464009} - 2003}{2000} \right)} (\sqrt{2464009} + 2003) - e^{-t \left(\frac{\sqrt{2464009} + 2003}{2000} \right)} \left(\frac{6297643644}{88775280113900387827712} \right)$$

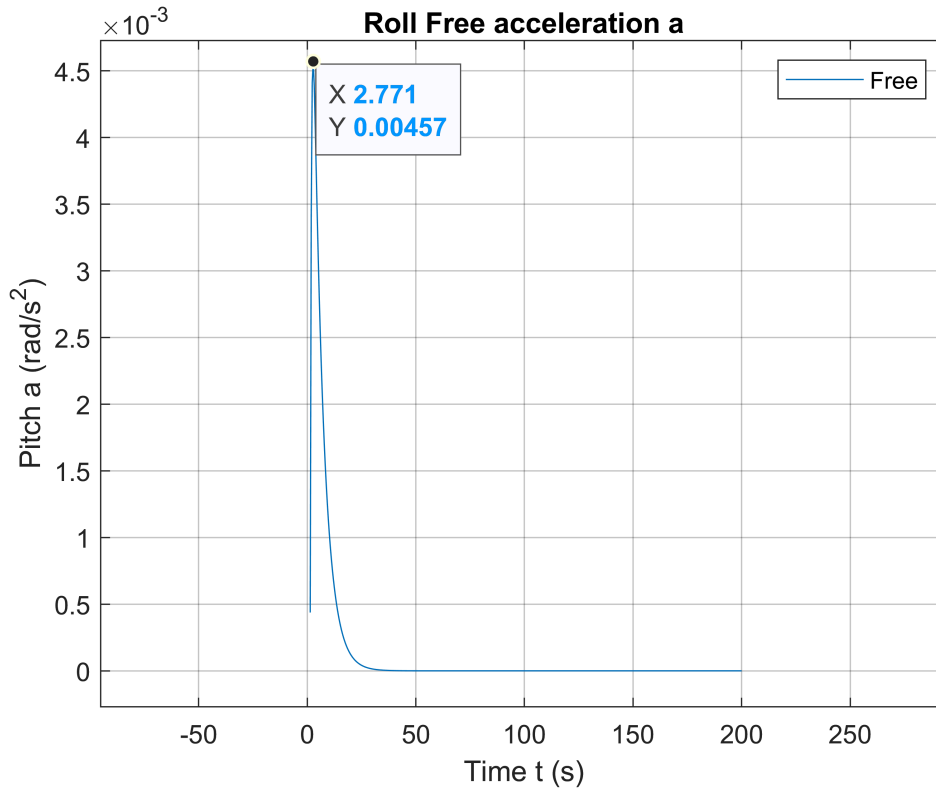
simple1 =

$$\frac{18932879421272226600420356001465 e^{-\frac{1951336686408429 t}{9007199254740992}} - 216964376097073 e^{-\frac{4022520855209445 t}{2251799813685248}}}{95321731195610330180434880626688}$$

simple2 =

$$\frac{72091006385461662715335204122418451750954588144947946889380065 e^{-\frac{1951336686408429 t}{9007199254740992}} - \frac{35106298}{4}}{7733417584954199941109129830444249459136974368179190608043180032}$$

Acceleration plot



Solve a nonhomogenous Second-order Differential Equation Numerically

02.11.2020 @j.urb

END

C.5. Rolling - Calculation of Exciting moment

By performing numerical calculations, we can conclude:

1. For the maximum encounter of the waves I choose d the beam seas conditions to take into account the maximum forces.
2. Probably the ships captain will not operate in this conditions, because as my calculations show it is nearly resonance conditions with this kind of waves.
3. the asymptotic value of the pitching moment as the effective wavelength approaches infinity is zero, as the constant wave height and infinite length the wave slope tends to disappear.

The exciting moment for rolling is due to unbalanced moment caused by the waves about the transverse axis of the ship. We obtain the exciting moment for pitching: by two dimensional integrating over the ship sections and wave profile over the ship length and multiplying each section wave force with distance to LCG (2.52) Table C.1: "Calculation-of-exciting moment for rolling". Where ζ is the distance from LCG, y is the Half-Breadth of water plane, $k = \frac{2\pi}{L_{wl}}$ is wave number and calculations are with beam seas $\mu = 90^\circ$. Exciting coefficient for Rolling as the ships section spacing is $L_{spacing} = 2.7 m$:

$$integral_{M\phi} = \frac{1}{3} \cdot L_{spacing} \cdot SUM_{\phi} = 4.946 m^4. \quad (C.12)$$

Refer (2.75) and non dimensional amplitude of the exciting moment

$$f_{0_{M\phi}} = \frac{2}{3} \frac{\sin \mu}{L_{wl} \cdot B_{max}^2 \cdot T} \cdot (integral_{M\phi}) = 0.124 \quad (C.13)$$

and (2.74) to exciting moment amplitude

$$M_{0_{\phi}} = \rho g k \xi_a L_{wl}^2 B_{max} \cdot f_{0_{M\phi}} = 2.673 \cdot 10^7 N \cdot s. \quad (C.14)$$

I did also a calculation of the exciting moment according to the beam seas ($\mu = 90^\circ$) equation (2.76)

$$M_0 = \rho g \nabla k \xi_a GM = 1.191 \cdot 10^7 N \cdot s$$

As it can be seen the integral calculation is more precise, the difference in the moments are 2.244 times as the integral value are bigger because it takes into account the ships complicated geometry.

| Station | 1 - | 2 - | 3 - | 4 - | 5 - | 6 - | 7 - | 8 - | 9 - |
|---------|------|--------------------|-------------------------|-------------------|---------------------|-------------------------|--|----------------------------------|-----|
| Unit | x | $y = \frac{Bx}{2}$ | y | $k' = k \cos \mu$ | $\cos(kx \cos \mu)$ | $y^3 \cos(kx \cos \mu)$ | multiplier | Product | |
| | [m] | [m] | [m ³] | [-] | [-] | [L] | [-] | [L] | |
| -2 | 35.1 | 0.00 | 0.0 | 0.00 | 1 | 0.0 | 1 | 0.00 | |
| -1 | 32.4 | 4.77 | 1.086 · 10 ⁵ | 0.00 | 1 | 1.086 · 10 ⁵ | 4 | 4.344 · 10 ⁵ | |
| 0 | 29.7 | 4.77 | 1.086 · 10 ⁵ | 0.00 | 1 | 1.086 · 10 ⁵ | 2 | 2.172 · 10 ⁵ | |
| 1 | 27.0 | 4.77 | 1.086 · 10 ⁵ | 0.00 | 1 | 1.086 · 10 ⁵ | 4 | 4.344 · 10 ⁵ | |
| 2 | 24.3 | 4.77 | 1.086 · 10 ⁵ | 0.00 | 1 | 1.086 · 10 ⁵ | 2 | 2.172 · 10 ⁵ | |
| 3 | 21.6 | 4.77 | 1.086 · 10 ⁵ | 0.00 | 1 | 1.086 · 10 ⁵ | 4 | 4.344 · 10 ⁵ | |
| 4 | 18.9 | 4.77 | 1.086 · 10 ⁵ | 0.00 | 1 | 1.086 · 10 ⁵ | 2 | 2.172 · 10 ⁵ | |
| 5 | 16.2 | 4.77 | 1.086 · 10 ⁵ | 0.00 | 1 | 1.086 · 10 ⁵ | 4 | 4.344 · 10 ⁵ | |
| 6 | 13.5 | 4.71 | 1.042 · 10 ⁵ | 0.00 | 1 | 1.042 · 10 ⁵ | 2 | 2.084 · 10 ⁵ | |
| 7 | 10.8 | 4.85 | 1.14 · 10 ⁵ | 0.00 | 1 | 1.14 · 10 ⁵ | 4 | 4.561 · 10 ⁵ | |
| 8 | 8.1 | 4.85 | 1.14 · 10 ⁵ | 0.00 | 1 | 1.14 · 10 ⁵ | 2 | 2.28 · 10 ⁵ | |
| 9 | 5.4 | 4.85 | 1.14 · 10 ⁵ | 0.00 | 1 | 1.14 · 10 ⁵ | 4 | 4.561 · 10 ⁵ | |
| 10 | 2.7 | 4.85 | 1.14 · 10 ⁵ | 0.00 | 1 | 1.14 · 10 ⁵ | 2 | 2.28 · 10 ⁵ | |
| 11 | 0 | 4.85 | 1.14 · 10 ⁵ | 0.00 | 1 | 1.14 · 10 ⁵ | 4 | 4.561 · 10 ⁵ | |
| 12 | 2.7 | 4.79 | 1.096 · 10 ⁵ | 0.00 | 1 | 1.096 · 10 ⁵ | 2 | 2.191 · 10 ⁵ | |
| 13 | 5.4 | 4.46 | 8.842 · 10 ⁴ | 0.00 | 1 | 8.842 · 10 ⁴ | 4 | 3.537 · 10 ⁴ | |
| 14 | 8.1 | 4.10 | 6.897 · 10 ⁴ | 0.00 | 1 | 6.897 · 10 ⁴ | 2 | 1.379 · 10 ⁴ | |
| 15 | 10.8 | 3.89 | 5.882 · 10 ⁴ | 0.00 | 1 | 5.882 · 10 ⁴ | 4 | 2.353 · 10 ⁴ | |
| 16 | 13.5 | 3.10 | 2.988 · 10 ⁴ | 0.00 | 1 | 2.988 · 10 ⁴ | 2 | 5.976 · 10 ⁴ | |
| 17 | 16.2 | 2.45 | 1.471 · 10 ⁴ | 0.00 | 1 | 1.471 · 10 ⁴ | 4 | 5.882 · 10 ⁴ | |
| 18 | 18.9 | 1.62 | 4.307 · 10 ³ | 0.00 | 1 | 4.307 · 10 ³ | 2 | 8.614 · 10 ³ | |
| 19 | 21.6 | 0.38 | 52.734 | 0.00 | 1 | 52.734 | 4 | 210.938 | |
| 20 | 24.3 | 0.38 | 52.734 | 0.00 | 1 | 52.734 | 2 | 52.734 | |
| 21 | 27 | 0.00 | 0 | 0 | 1 | 0 | 1 | 0 | |
| 22 | 0 | 0 | 0 | 0 | 0 | 0 | 1 | 0 | |
| | | | | | | | SUM_{ϕ} | 5.4995 · 10⁶ L | |

Table C.1.: Calculation of exciting moment for rolling [8, Example 4.23]

C.6. Rolling - PVL-101 differential equation calculation and its solution"

The equation is as follows: (2.55)

$$a_{\phi}\ddot{\phi} + b_{\phi}\dot{\phi} + c_{\phi}\phi = M_{0_{\phi}} \cos(\omega_e t)$$

Virtual mass: $a_{\phi} = 3.743 \cdot 10^7 \text{ kg} \cdot \text{m}^2$. Damping coefficient: $b_{\phi} = 7.498 \cdot 10^7 \cdot \frac{\text{kg} \cdot \text{m}^2}{\text{s}}$.
Linear restoring coefficient: $c_{\phi} = 1.447 \cdot 10^7 \cdot \text{N} \cdot \text{m}$.

Beam sea waves: Amplitude of the exciting force in beam seas:

$$M_{0_{\phi}} = 2.673 \cdot 10^7 \text{ N} \cdot \text{s}.$$

Encountering wave frequency with beam seas is the wave frequency:

$$\omega_e = \frac{2\pi}{T_e}, T_e = 10 \text{ s}$$

[16, page 29], $\omega_e = 0.628 \frac{1}{\text{s}}$. Natural frequency: $\omega_{\phi} = \sqrt{\frac{c_{\phi}}{a_{\phi}}} = 0.622 \frac{1}{\text{s}}$ (2.2). The tuning factor:

$$\Lambda_{\phi} = \frac{\omega_e}{\omega_{\phi}} = 1.011$$

(2.29), as this is near resonance the captain need to change the course and speed. The non-dimensional damping factor

$$\kappa_{\phi} = \frac{\nu_{\phi}}{\omega_{\phi}} = 1.611 \frac{1}{\text{s}}$$

[13, page 100] where $\nu_{\theta} = \frac{b_{\phi}}{2a_{\phi}} = 1.002 \frac{1}{\text{s}^2}$ (2.16). The circular frequency of the damped oscillation, that is [8, eq:4.6a]

$$\omega_{d_{\phi}} = \sqrt{\omega_{\phi}^2 - \nu_{\phi}^2} = 0.785i \frac{1}{\text{s}}.$$

The rolling amplitude

$$z_{a_{\phi}} = z_{st_{\phi}} \cdot \mu_{\phi} = 0.567 \text{ rad}$$

where $z_{st_{\phi}} = \frac{M_{\phi}}{c_{\phi}} = 1.848$ (2.26)&(2.27).

Then the equation can be expressed as: [20, ch:10] or [13, eq:4.14]

$$\ddot{\phi} + 2\kappa_{\phi}\omega_{\phi}\dot{\phi} + \omega_{\phi}^2\phi = z_{a_{\phi}} \cos(\omega_e t - \varepsilon_{\phi}) \quad (\text{C.15})$$

$$\ddot{\phi} + 2.003\dot{\phi} + 0.387\phi = 0.567 \cos(0.628t + 3.135) \quad (\text{C.16})$$

The roots for the characteristic equation refer to (C.4).

Then the solution can be expressed as

$$\phi = A1 \exp^{\nu_{\phi} t} \sin(\omega_{d_{\phi}} t - \beta) + z_{a_{\phi}} \cos(\omega_e t - \varepsilon_{\phi}) \quad (2.54).$$

According from [20, eq:10.7A and 10.7B] the first part of the solution

$$\phi_1 = A1 \exp^{-\nu_{\phi} t} \sin(\omega_{d_{\phi}} t - \beta)$$

which is the ships natural movement. The second part

$$\theta_2 = z_{a_{\phi}} \cos(\omega_e t - \varepsilon_{2_{\phi}})$$

is the encountering movement. Hole solution: $\phi = \phi_1 + \phi_2$. The phase angle between the wave motion and the rolling motion is expressed as $\varepsilon_{\phi} = \varepsilon_{1_{\phi}} + \varepsilon_{2_{\phi}}$ where ε_1 is the phase angle between the wave motion and the exciting force caused by waves, and ε_2 is the phase angle between the exciting force and the rolling motion. Now $\varepsilon_{1_{\phi}} = -90^\circ$ [8, eq:4.12b] and from [8, page 38]

$$\varepsilon_{2_{\phi}} = \arctan \frac{2\kappa_{\phi}\Lambda_{\phi}}{1 - \Lambda_{\phi}^2} = -1.564 \text{ rad}$$

and $\varepsilon_{\phi} = -3.135 \text{ rad}$. As for (2.54) the solution to the rolling movement is as follows and will be presented only in graphical way which refer to solution (C.6) and acceleration look fig C.7: "Rolling-acceleration in beam seas".

Bow sea waves: the encountering frequency has changed: (2.5) $\omega_e = \omega_w - \frac{\omega_w^2}{g} u \cos \mu$ and probably the captain will increase speed also to $u = 5.144 \frac{m}{s}$ (10 knots). Also the exciting force has changed ($M_{0_{\phi}} = 1.337 \cdot 10^7$). Then the rolling are not in synchronization with the waves and the (C.15) equation becomes

$$\ddot{\phi} + 2.003\dot{\phi} + 0.387\phi = 0.218 \cos(0.808t + 2.281) \quad (\text{C.17})$$

As for (C.17) the solution of Bow sea rolling movement is presented only in graphical way which refer to solution (C.8) and acceleration look fig C.7: "Rolling-acceleration in beam seas".

Rolling period versus metacentric height

The ship's stability may be approximated according to Paragraph 7.6 (*Determination of ship's stability by means of rolling period tests, for ships up to 70 m in length*) of IMO Resolution A.749 (18), *Code on Intact Stability for all Types of Ships Covered by IMO Instruments*:

$$GM_0 = \left(\frac{fB}{T_r}\right)^2$$

$f = 0,8$
 $T = 8 s$ $GM_0 = 1 m$

The graph below shows this relation for breadth B=10.0 m (corresponding to a draught of 4.15 m) and different rolling coefficients.

By checking the rolling period for a loading case where GM is known, it is possible to determine the rolling coefficient, *f*.

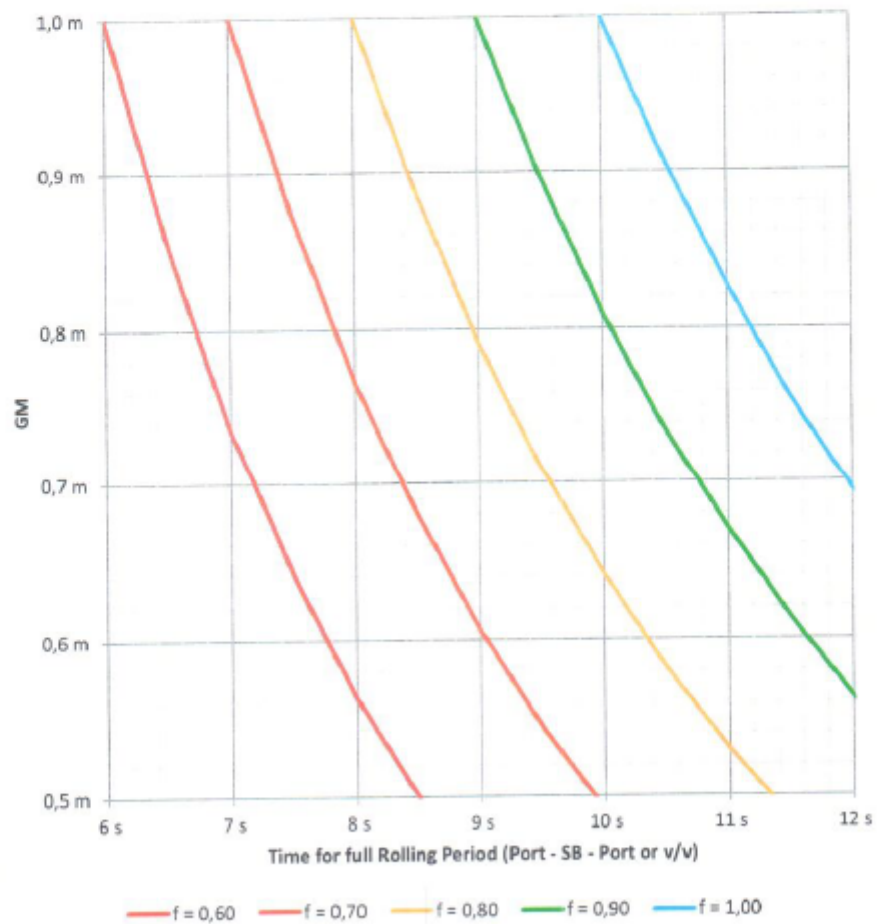


Figure C.1.: Rolling period versus metacentric height with PVL-101 crew calculation [7, Appendix 8] 115

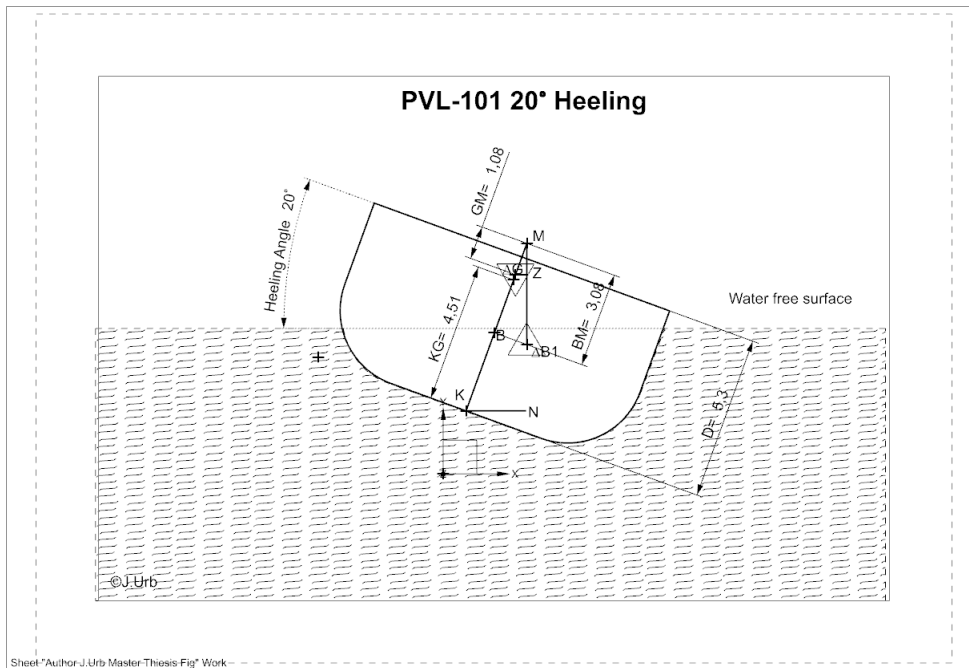


Figure C.2.: PVL-101 20° Heeling

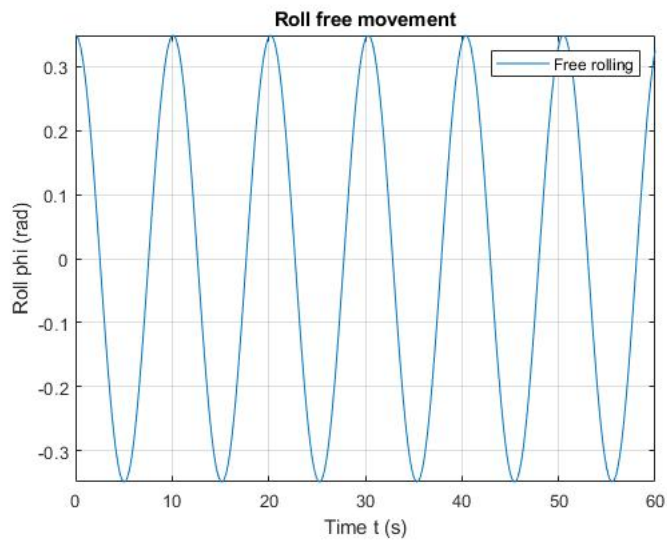


Figure C.3.: Roll Free movement without damping

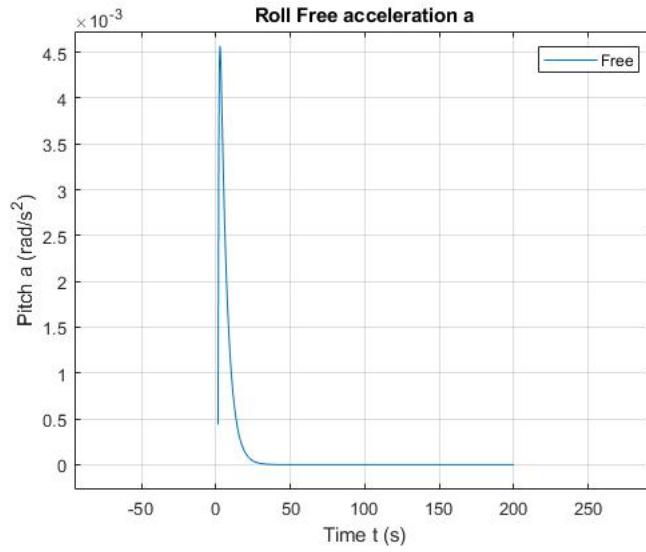


Figure C.4.: Free damped roll movement acceleration

PVL-101 20° Exciting moment due to change in buoyant force

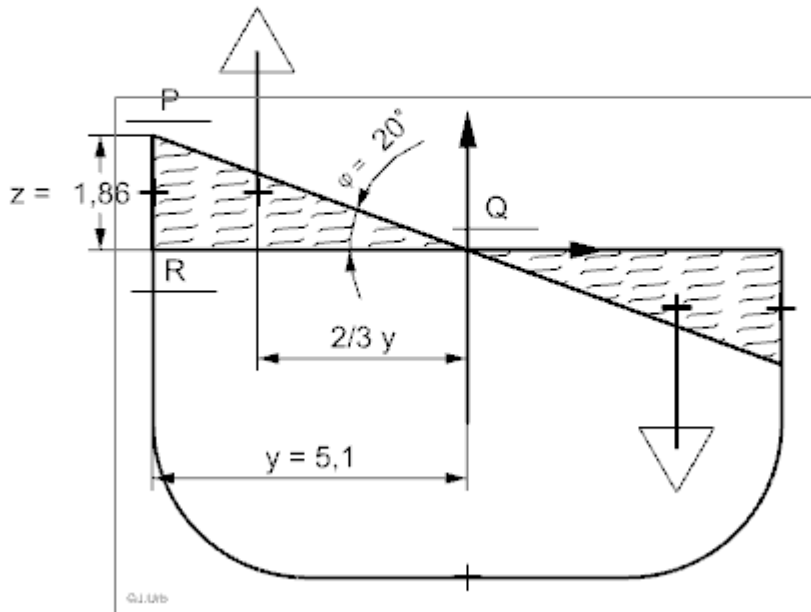


Figure C.5.: PVL-101 20° Exciting moment due to change in buoyant force

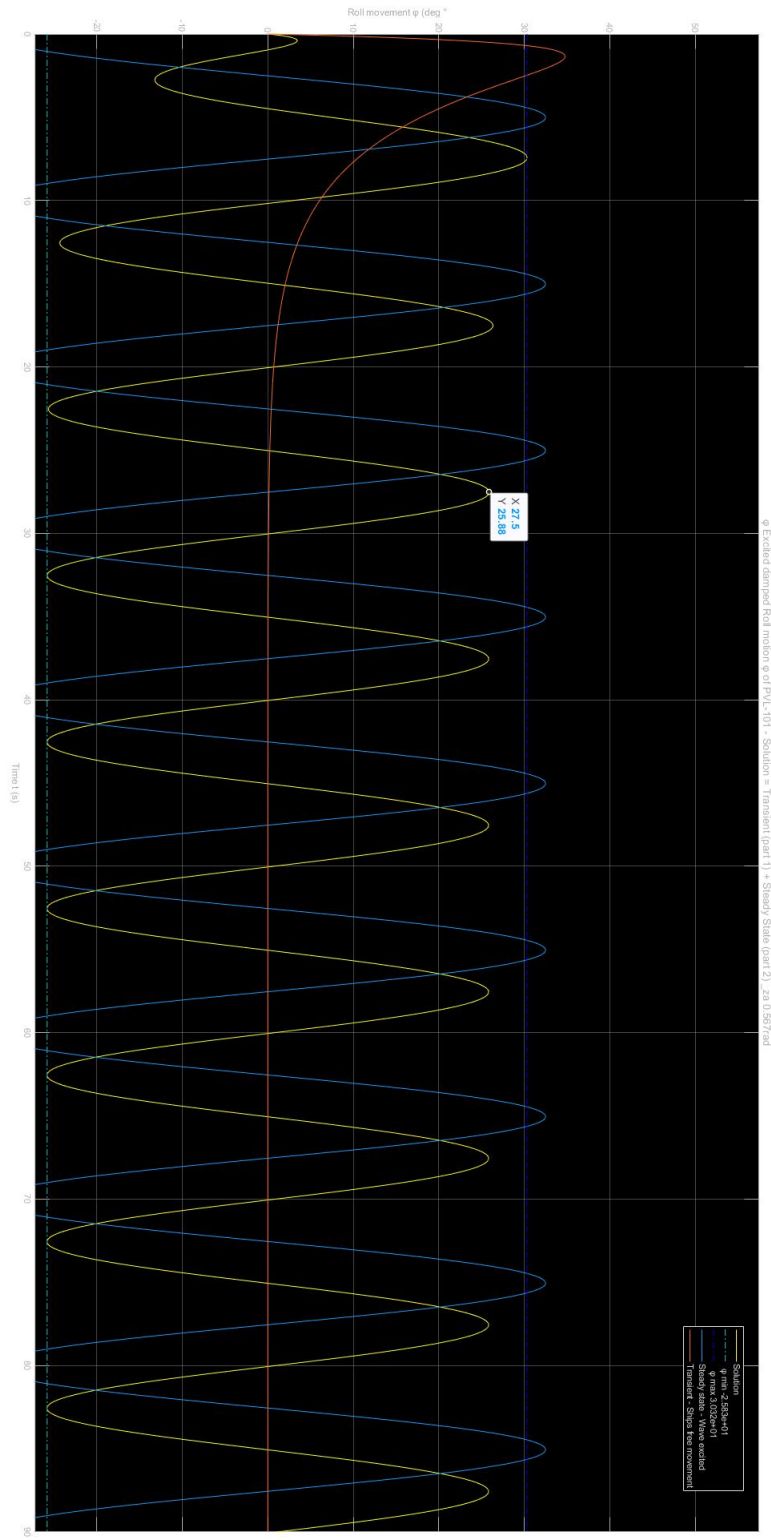


Figure C.6.: Rolling in beam seas of the PVL-101 θ

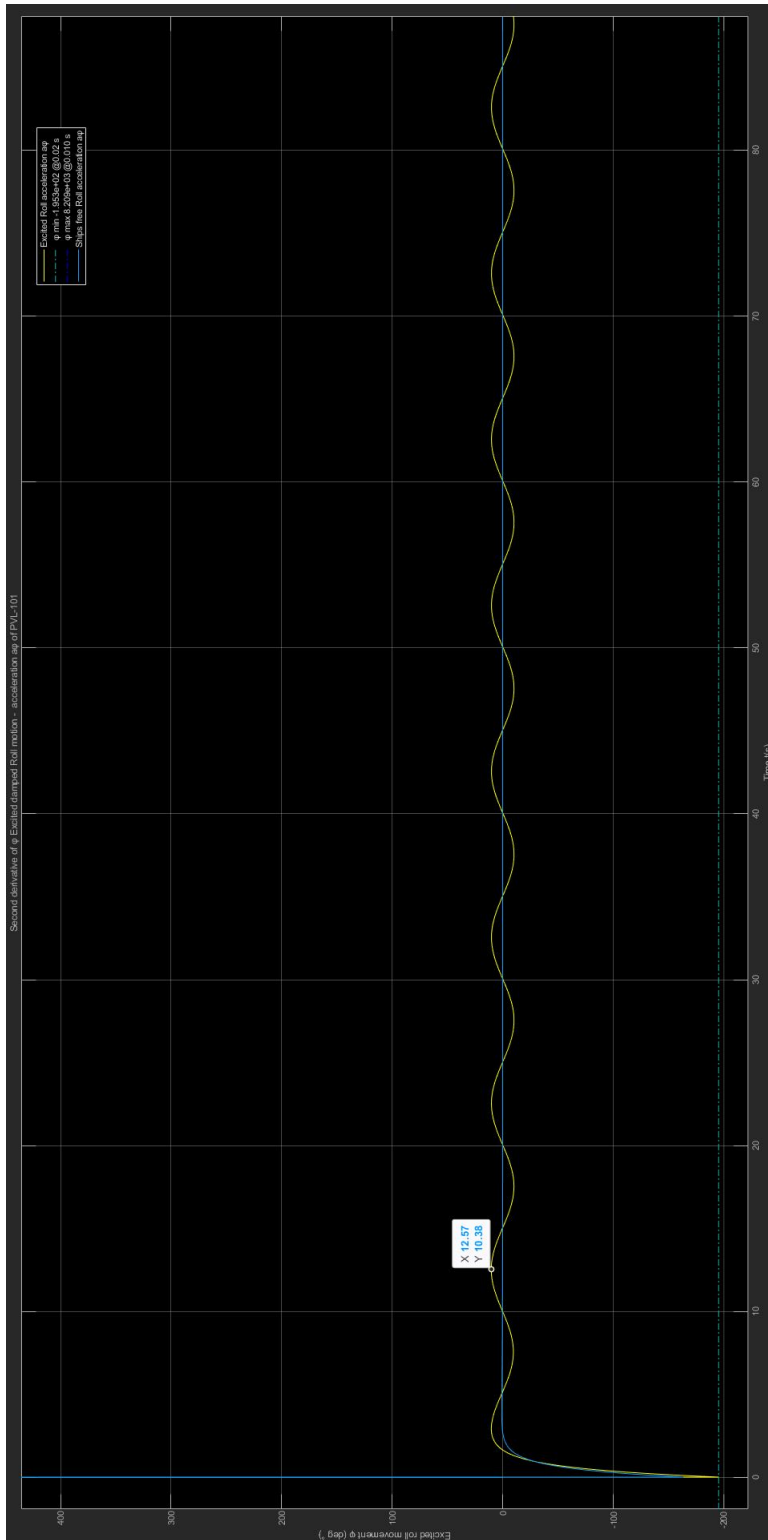


Figure C.7.: Rolling acceleration in beam seas for the PVL-101 a

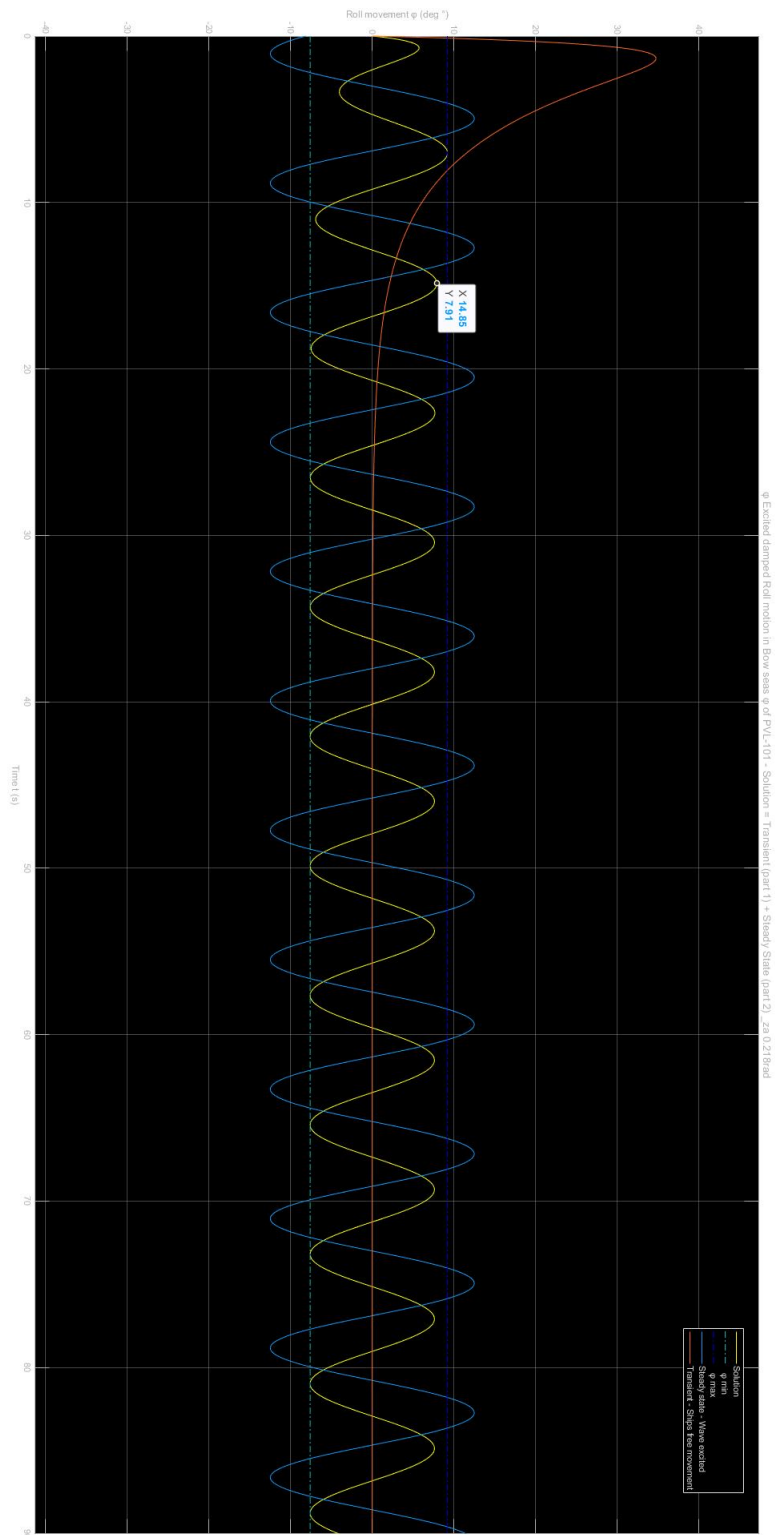


Figure C.8.: Rolling in bow seas of the PVL-101 θ

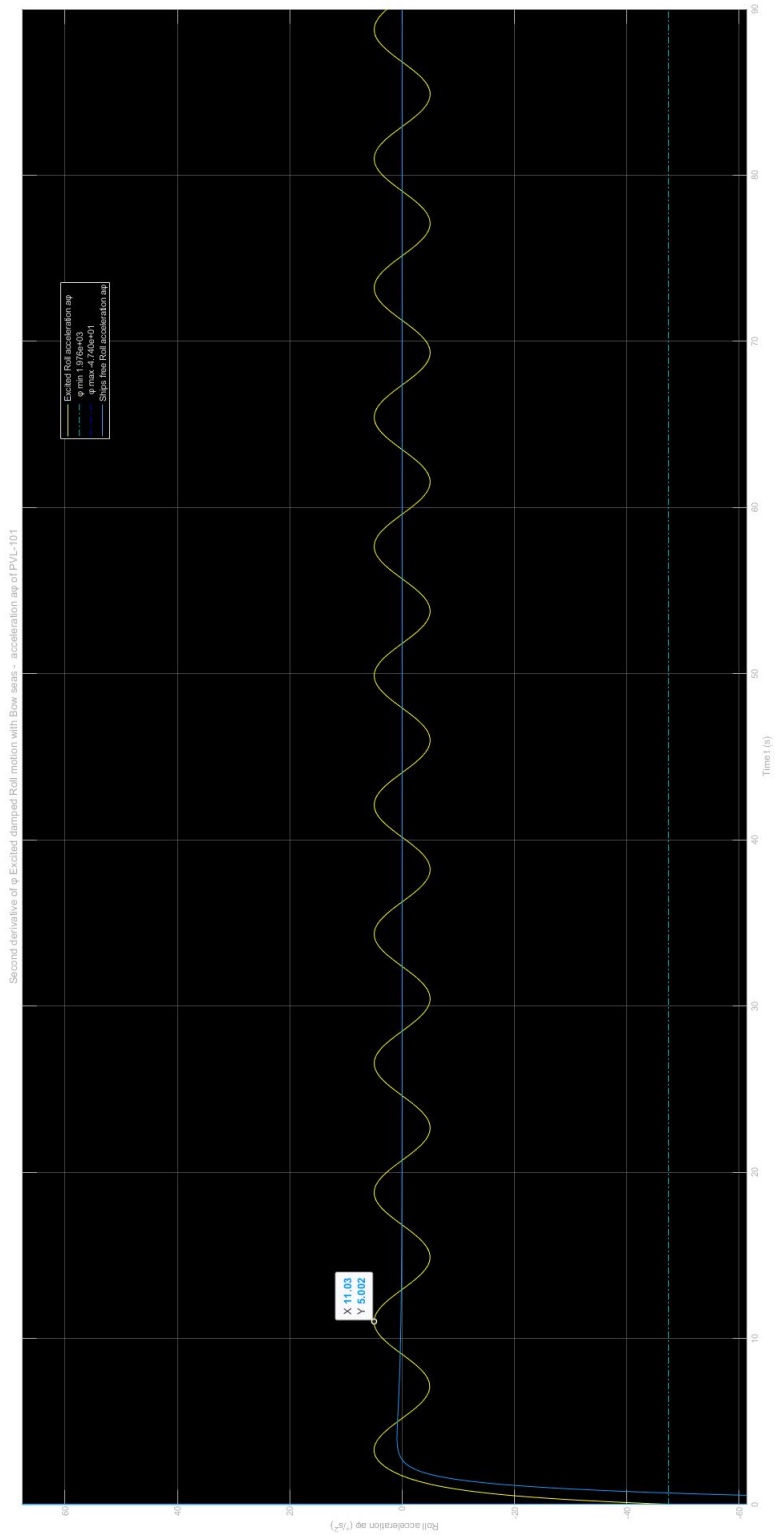


Figure C.9.: Rolling acceleration in bow seas for the PVL-101 a

D. : Appendix 4: 2 DOF mechanisms comparison and SPM calculations

**D.1. Two Degrees of Freedom parallel mechanisms
comparison**

D.2. SPM calculations


```
%%% PLATFORM KINEMATICS
```

```
% @ J.Urb 16.11.2020
```

```
% Coordinate system O-XYZ to describe 2-DOF SPM (spherical parallel  
% mechanism) DOF for this manipulator can be verified according to the  
% revised Kutzbach-Grubler formula  $M=d(n-g-1)+\sum (f_i+v-att)$ , where  $d=3$  is  
% the number of common constraints for spherical mechanism,  $n$  is the number  
% of parts,  $g$  is the number of joints,  $f_i$  is the degrees of freedom of the  
%  $i$ th joint,  $v$  is the number of redundant constraints, and  $att$  is the  
% isolated degree of freedom.  $n=6$ , joints  $g=7$ . For universal joint  $f_1=2$ ,  
% for other six revolute  $f_i=1$ . there is no redundant constraint and  
% isolated degree of freedom so  $v=0$ ,  $att=0$ .  $M=2$ .
```

```
% O-XYZ IS THE GLOBAL COORDINATE SYSTEM AND THE LOCAL SYSTEM O-XijYijZij  
% The subscript  $i$  and  $j$  represent the  $j$ th revolute joint of the  $i$ th branch,  
% where  $i=1,2$  and  $j=1,2,3$ . the center point  $O$  of the universal joint is the  
% origin of each coordinate system. In branch 1, the axis  $X_{1j}$  ( $j=1,2,3$ ) of  
% the local coordinate system constantly points to the center of the  
% revolute joint from origin  $o$ , and  $Y_{11}$  coincides with  $Y_{21}$ ,  $Y_{21}$ , and  $T_1 \times B_1$   
% are in the same direction,  $Y_{13}$  is in the same direction with the  $Y$  axis  
% of the global coordinate system, and  $Z_{1j}$  ( $j=1,2,3$ ) can be determined by  
% the right hand rule.  $O-X_{11}Y_{11}Z_{11}$  coincides with  $O-X_{21}Y_{21}Z_{21}$ .
```

```
% The position vectors of the six revolute joints in their local coordinate  
% systems are presented, respectively, as follows:
```

```
R=2; %radius of the platform
```

```
p1=[R 0 0]'; p2=[0 R 0]'; b1=[R 0 0]'; t1=[R 0 0]'; t2=[R 0 0]'; b2=[0 R 0]';
```

```
%(1)
```

representation of the joints

```
% roll angle  $\phi_x$ . Based on coordinate transformation matrices of the  
% mobile platform in Euler angle form are:
```

```
 $\phi_x=0*\pi/180$ ; % input can come from ship's differential equation
```

```
Rx22=cos( $\phi_x$ );  
Rx23=-1*sin( $\phi_x$ );  
Rx32=sin( $\phi_x$ );  
Rx33=cos( $\phi_x$ );
```

```
Rx=[1 0 0; 0 cos( $\phi_x$ ) -1*sin( $\phi_x$ ); 0 sin( $\phi_x$ ) cos( $\phi_x$ )]; %(3)
```

```
% pitch angle  $\phi_y$ . Based on coordinate transformation matrices of the  
% mobile platform in Euler angle form are:
```

```
 $\phi_y=0*\pi/180$ ; % input can come from ship's differential equation
```

```
Ry11=cos( $\phi_y$ );  
Ry13=sin( $\phi_y$ );
```

| Principal Solution | | | | |
|---|--|---|---|--|
| Functional requirement | 1 (D.1) | 2 (D.2) | 3 (D.3) | 4 (D.4) |
| Move the platform as the ship rolls and pitches or hold the top plate steady | 2 DOF Spherical Parallel manipulator (RRR-U-RRR); is developed based on the coordinate transformation approach and the cosine rule of a trihedral angle. [9] | 2 DOF parallel manipulator with fixed pole and 4 retractable poles (4STS-U). [28] | Stabilization of Platform using mechanical gyroscope: Parallel or series gyro stabilizer. [27] | 2 DOF Translational parallel manipulator with Universal joint (2RSS+U) |
| Actuation type complexity $K_A = 1 - \exp(-q_A A)$, where $q_A = 0.9$ and $A = a - a_m, a_m = 2$ | 2 rotation electric motors $K_A = 0$ | 4 linear electric actuators $K_A = 0.835$ | Actuation torques (passive or active) of their spinning wheel(s), moved by 2 rotational electric motors $K_A = 0$ | 2 linear electric actuators $K_A = 0$ |
| Complexity K_{CO} for forward kinematics 0.2 and inverse are 0.6. | Forward or inverse kinematics cosine rule of a trihedral angle or rotational transformation 0.6 | Inverse kinematics or translational transformation 0.6 | Flywheel spin. Equation of motion can be determined by momentum. Translational and rotational. Use of inverse kinematics. 0.6 | Inverse kinematics or translational transformation. 0.6 |
| Velocity and Acceleration kinematics where complexity K_{ACC} forward 0.2 and inverse are 0.6. | The angular velocity and Acceleration relates to the angular displacement, velocity and Acceleration of the actuator. 0.6 | The angular velocity and Acceleration relates to the linear displacement, velocity and Acceleration of the actuators. 0.6 | Angular displacement, velocity and acceleration of the platform relates to the flywheel spin rates velocity acc to gyroscopic precession motion. Precession control is complicated. 0.6 | The angular velocity and Acceleration relates to the linear displacement, velocity and Acceleration of the actuators 0.6 |
| Joint types K_j Two degrees of freedom mechanisms design and comparison | 0.44 | 0.33 | N/A as higher kinematic pair = 1 | 0.57 |
| Number of loops and loop complexity $K_L = 1 - \exp(-q_L L)$, where $q_L = 0.9$ and $L = l - l_m, l_m = 2$ | 2 0 | 4 0.835 | 2 0 | 2 0 |
| Joint number complexity $K_N = 1 - \exp(-q_N N)$, where $q_N = 0.9$, N is the number of joint's | 7 0.998 | 9 1 | 7 0.998 | 9 1 |
| Simplified geometric complexity of the solution K Two degrees of freedom mechanisms design and comparison | 0.444 | 0.684 | 0.5 | 0.457 |

Table D.1.: 2 DOF platform's principal solutions and functional requirements comparison [30]

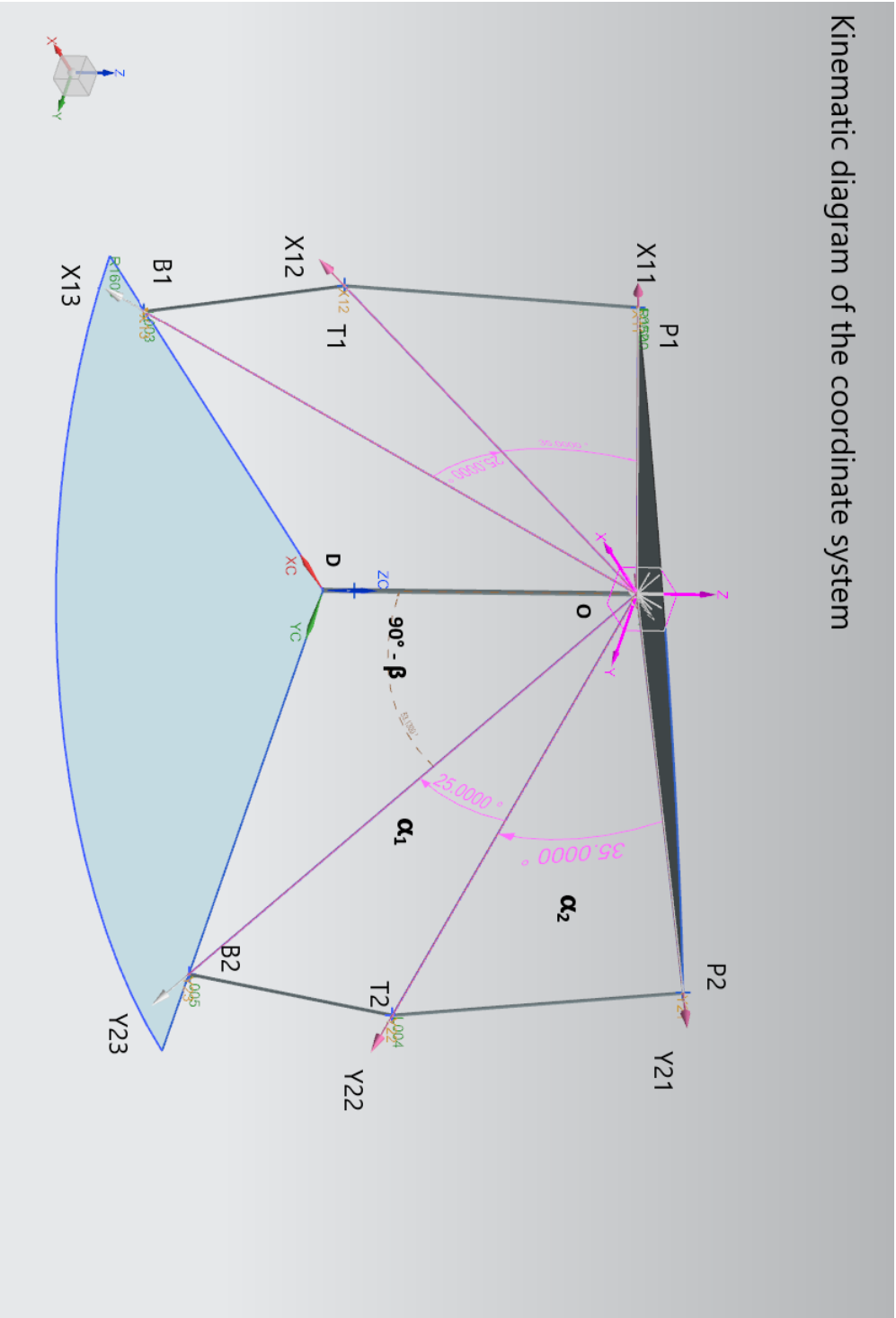


Figure D.1.: 2 DOF Spherical Parallel manipulator (RRR-U-RRR) sketch [9, Figure 2]

```

%Ry31=-sin(phiy);
%Ry33=cos(phiy);

Ry=[cos(phiy) 0 sin(phiy);0 1 0;-sin(phiy) 0 cos(phiy)]; %(2)

```

%On one hand, once the mobile platform is assumed to be in a given orientation, the representation of the position of related points such as P1,P2,T1 and T2 can be obtained. On the other hand, the angular displacement of actuators will also lead to the representation of T1 and T2. So kinematic equations can be formulated according to the equivalence of T1 and T2. Assume that the original state of the 2-DOF SPM is that the local coordinate system O-X1Y1Z1 coincides with the global coordinate system O-XYZ. FOR THE FIRST OPERATION, LET THE LOCAL COORDINATE ROTATE AROUND THE Y AXIS BY phiy to get a new coordinate system. Then for second operation let the new coordinate rotate around the X axis by phix to get the final coordinate system.

% So the resulting vectors are: P1=Ry*Rx*p1 P2=Ry*Rx*p2

```

P1=R*[cos(phiy);0;-sin(phiy)]'          %(4)

```

```

P1 = 1x3
     2   0   0

```

```

P2=R*[sin(phiy)*sin(phix);cos(phix);cos(phiy)*sin(phix)]'          %(5)

```

```

P2 = 1x3
     0   2   0

```

% Since the lower links are directly connected to the actuators, their position vectors can be represented with the input angular displacement phi1, phi2.

```

% structural parameters as shown in figure
beeta=36.87*pi/180;
alfa1=25*pi/180;
alfa2=35*pi/180;

```

```

phi1=0; % initial condition
phi2=0; % initial condition

```

% So, the resulting vectors

```

%T1=          %(6)

```

```

T1=R*[cos(beeta)*cos(alfa1)+sin(beeta)*cos(phi1)*sin(alfa1);...
      -sin(phi1)*sin(alfa1);-sin(beeta)*cos(alfa1)+...

```

```
cos(beeta)*cos(phi1)*sin(alfa1)]
```

```
T1 = 3x1
    1.9572
     0
   -0.4114
```

```
%T2=                                %(7)
```

```
T2=R*[-sin(phi2)*sin(alfa1);-cos(beeta)*cos(alfa1)+sin(beeta)*...
      cos(phi2)*sin(alfa1);-sin(beeta)*cos(alfa1)+cos(beeta)*cos(phi2)*...
      sin(alfa1)]
```

```
T2 = 3x1
     0
   -0.9429
   -0.4114
```

```
%Actuator locations in global coordinates
```

```
B1=R*[cos(beeta);0;-sin(beeta)]'                                %(8)
```

```
B1 = 1x3
    1.6000     0   -1.2000
```

```
B2=R*[0;cos(beeta);-sin(beeta)]'                                %(9)
```

```
B2 = 1x3
     0    1.6000   -1.2000
```

Inverse kinematics

```
%The inverse kinematics of a manipulator calculate the motion of actuators
%given the orientation of the mobile platform, which is the theoretical
%base for the control of the manipulator
```

```
%In branch 1, the angle between P1 and B1 is denoted as alfa31, thus ...
% P1.*B1/(abs(P1).*abs(B1))
```

```
xalfa31=cos(phiy)*cos(beeta)+sin(phiy)*sin(beeta); % cosine(alfa31) (10)
```

```
alfa31=acos(xalfa31)
```

```
alfa31 = 0.6435
```

```
%The planes related to angles alfa31, alfa2, and a1 intersect at point O.
%The angle between the planes of alfa31 and a1 is denoted as phi11. According
%to cosine rule of a trihedral angle, the geometric Equation (11)
%is obtained.
```

```
%@(alfa2,alfa1,alfa31) (cos(alfa2)-cos(alfa1).*cos(alfa31))./...
% (sin(alfa1).*sin(alfa31))
```

```
xphi11= myObjective(alfa2,alfa1,alfa31);
                                     %cosine(phi11)   (11)
phi11=acos(xphi11)
```

```
phi11 = 0.7174
```

```
%myObjective([25*pi/180;35*pi/180;1.5708])
```

```
% The angle of the plane of a31 and O-XZ is set to q12. According to
% Equation (4), P1 and B1 are in the %plane of O-XZ. Thus q12 = 0 holds.
%The input angle of the actuator in branch 1 is q1 = q11 + q12 = q11.
%In branch 2, by applying the same principle, one can obtain
% P2.*B2/(abs(P2).*abs(B2))
```

```
xalfa32=cos(phix)*cos(beeta)-cos(phiy)*sin(phix)*sin(beeta);
                                     %   cos(alfa32)   (12)
```

```
alfa32=acos(xalfa32)
```

```
alfa32 = 0.6435
```

```
xphi21= myObjective2(alfa2,alfa1,alfa32);
%
                                     cos(phi21) (13)
```

```
phi21 = acos(xphi21)
```

```
phi21 = 0.7535
```

```
%According to Equation (5), neither P2 nor B2 is in the plane of O-YZ.
%Thus, q22 not 0. In order to obtain q22 between O-P2B2 and O-YZ, the
%intermediate vector j = (0, R, 0)T is introduced.
% ((B2.*P2).*(B2.*j))/(abs(B2.*P2).*abs(B2.*j))
```

```
j=[0,R,0]';
```

```
xphi22=-sin(beeta)*(cos(beeta)*cos(phiy)*sin(phix)-sin(beeta)*cos(phix));
                                     %cos(phi22)(14)
```

```
phi22 =acos(xphi22)
```

```
phi22 = 1.2025
```

```
phi2= phi21+phi22 % the angle of actuator 2
```

```
phi2 = 1.9560
```

Forward kinematics

```
%The forward kinematics of this 2-DOF SPM calculate the orientation of the
%mobile platform, provided the angular displacement of the two actuators.
% This procedure is of great importance for the orientation sensor
%application of this SPM. More generally, the semi-closed loop control of
%the parallel mechanism also needs its forward kinematics so that the
%orientation can be obtained by reading out the feedback values of the
%actuators and a further computation. The angle between vectors T1 and P1
%is constantly equal to alfa2, which can be expressed by
```

```
% y branch
xalfa2=cos(alfa2);          %cosalfa2 - xalfa2  (15)

c1 = xalfa2
```

```
c1 = 0.8192
```

```
a1=sin(beeta).*cos(alfa1)'-cos(beeta).*cos(phi1).*sin(alfa1)
```

```
a1 = 0.2057
```

```
b1=cos(beeta).*cos(alfa1)'+sin(beeta).*cos(phi1).*sin(alfa1)
```

```
b1 = 0.9786
```

```
phiy= myObjective3(c1,a1,b1); %          (16)
```

```
% x branch
```

```
xalfa2=cos(alfa2);          %cosalfa2 - xalfa2  (17)
```

```
c2 = xalfa2 %initial condition
```

```
c2 = 0.8192
```

```
a2=-sin(phi2)*sin(alfa1)*sin(phiy)+(cos(beeta)*cos(phi2)*sin(alfa1)-...
    sin(beeta)*cos(alfa1))*cos(phiy)
```

```
a2 = -0.4631
```

```
b2=cos(beeta)*cos(alfa1)+sin(beeta)*cos(phi2)*sin(alfa1)
```

```
b2 = 0.6298
```

```
phix=myObjective3(c2,a2,b2) ; %          (18)
```

```
%From the solutions to the forward kinematics mentioned above, one can
%infer that the rotation of the mobile platform around the Y axis is only
```

%dependent on the motion of actuator 1. Compared with this conclusion, the
 %rotation of the mobile platform around X axis is dependent on the motion of
 %both actuators.

Solution to forward kinematics

phix

phix = 2.5076 - 0.3084i

phiy

phiy = -0.4037

Analysis of the velocity and Acceleration

% This section will deal with the input-output realation of the velocity
 % and acceleration of the 2-dof SPM.
 % By differeting the equations (16) and (18) with respect to time, the eq
 %

```
f11=(cos(alfa1)*sin(beeta)-cos(beeta)*cos(phi1)*sin(alfa1))*cos(phiy)-...
      (cos(alfa1)*cos(beeta)+cos(phi1)*sin(alfa1)*sin(beeta))*sin(phiy);
f21=(cos(alfa1)*sin(beeta)-cos(beeta)*cos(phi2)*sin(alfa1))*sin(phiy)*...
      sin(phix)-sin(alfa1)*sin(phi2)*cos(phiy)*sin(phix);
f22=cos(phix)*(cos(phiy)*(cos(beeta)*cos(phi2)*sin(alfa1)-cos(alfa1)*...
      sin(beeta))-sin(alfa1)*sin(phi2)*sin(phiy))-(cos(alfa1)*cos(beeta)+...
      cos(phi2)*sin(alfa1)*sin(beeta))*sin(phix);
l11=-cos(phiy)*sin(alfa1)*sin(beeta)*sin(phi1)+cos(beeta)*sin(alfa1)*...
      sin(phi1)*sin(phiy);
l22=cos(phix)*sin(alfa1)*sin(beeta)*sin(phi2)-cos(beeta)*cos(phiy)*...
      sin(alfa1)*sin(phi2)*sin(phix)-cos(phi2)*sin(alfa1)*sin(phix)*sin(phix);
```

A=[f11 0;f21 f22]

```
A = 2x2 complex
    0.5736 + 0.0000i    0.0000 + 0.0000i
   -0.3872 - 0.1574i   -0.0000 - 0.2449i
```

B=[l11 0;0 l22]

```
B = 2x2 complex
    0.0000 + 0.0000i    0.0000 + 0.0000i
    0.0000 + 0.0000i   -0.3262 + 0.0207i
```

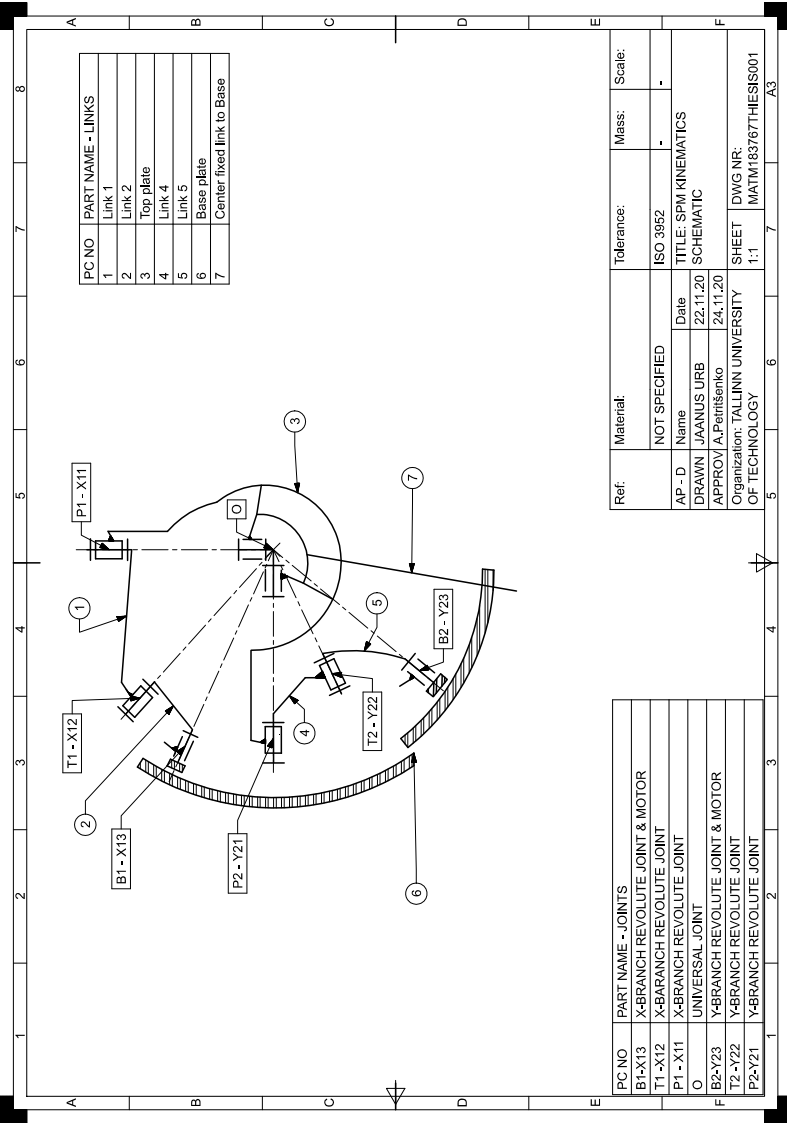
% $A*dphi(1)+B*dtheta(1)=0$ (19)

% first order rotation influence coefficient matrix on the 2 DOF rotations of
 % the mobile platform

$$G_{\text{phi}} = (\text{inv}(-A)) * B$$

Gphi = 2x2 complex
0.0000 + 0.0000i 0.0000 + 0.0000i
0.0000 + 0.0000i 0.0843 + 1.3318i

D.3. SPM kinematic schematic



| PC NO | PART NAME - LINKS |
|-------|---------------------------|
| 1 | Link 1 |
| 2 | Link 2 |
| 3 | Top plate |
| 4 | Link 4 |
| 5 | Link 5 |
| 6 | Base plate |
| 7 | Center fixed link to Base |

| PC NO | PART NAME - JOINTS |
|--------|---------------------------------|
| B1-X13 | X-BRANCH REVOLUTE JOINT & MOTOR |
| T1-X12 | X-BRANCH REVOLUTE JOINT |
| P1-X11 | X-BRANCH REVOLUTE JOINT |
| O | UNIVERSAL JOINT |
| B2-Y23 | Y-BRANCH REVOLUTE JOINT & MOTOR |
| T2-Y22 | Y-BRANCH REVOLUTE JOINT |
| P2-Y21 | Y-BRANCH REVOLUTE JOINT |

| Ref. | Material: | Tolerance: | Mass: | Scale: |
|--------|--|------------|-----------------------|---------------------|
| | NOT SPECIFIED | ISO 3952 | - | - |
| AP - D | Name | Date | TITLE: SPM KINEMATICS | |
| DRAWN | JAAANUS URB | 22.11.20 | SCHEMATIC | |
| APPROV | A.Petrisenko | 24.11.20 | SHEET | |
| | Organization: TALLINN UNIVERSITY OF TECHNOLOGY | | DWG NR: | MATM183767THESIS001 |
| | | | 1:1 | 1:1 |

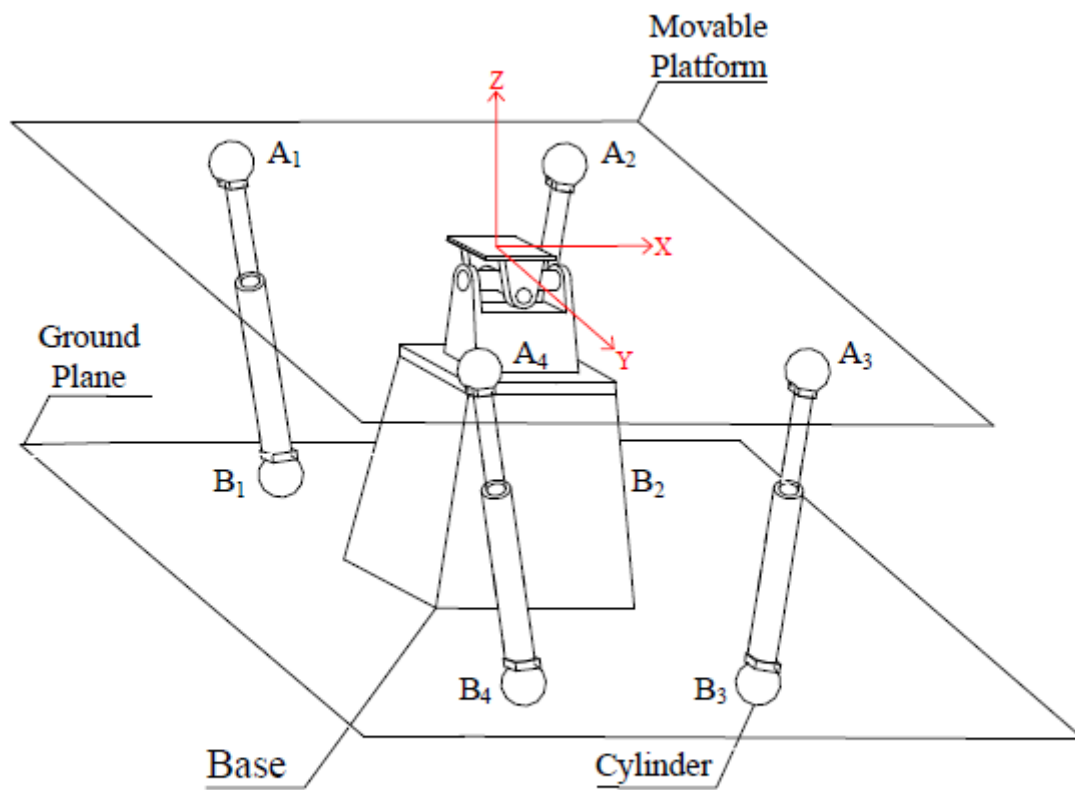


Figure 1. Skeleton drawing of 2-DOF parallel manipulator.

Figure D.2.: 2 DOF parallel manipulator with fixed pole and 4 retractable poles (4STS-U) sketch[28, Figure 1]

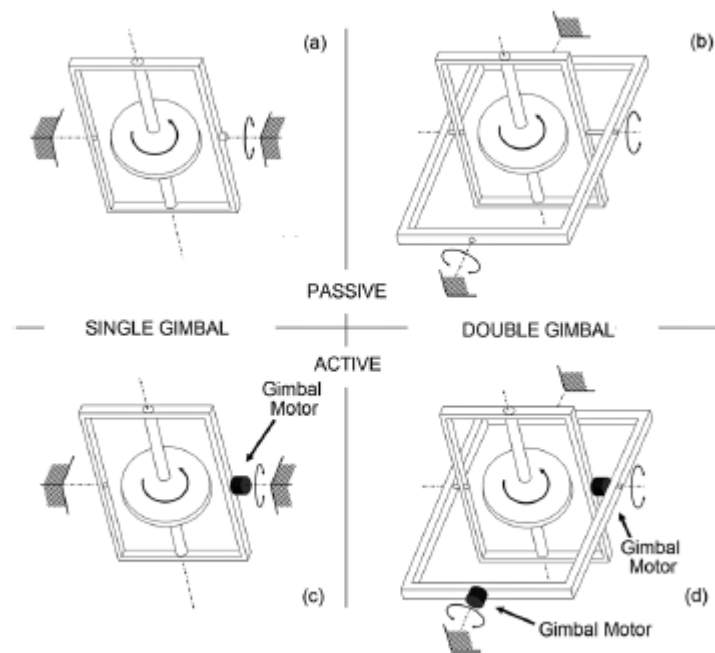


Fig. 1 Motion restrictions and actuations of a spinning wheel

Figure D.3.: Stabilization of Platform using mechanical gyroscope: Parallel or series gyrostabilizer.[27, Figure 1]

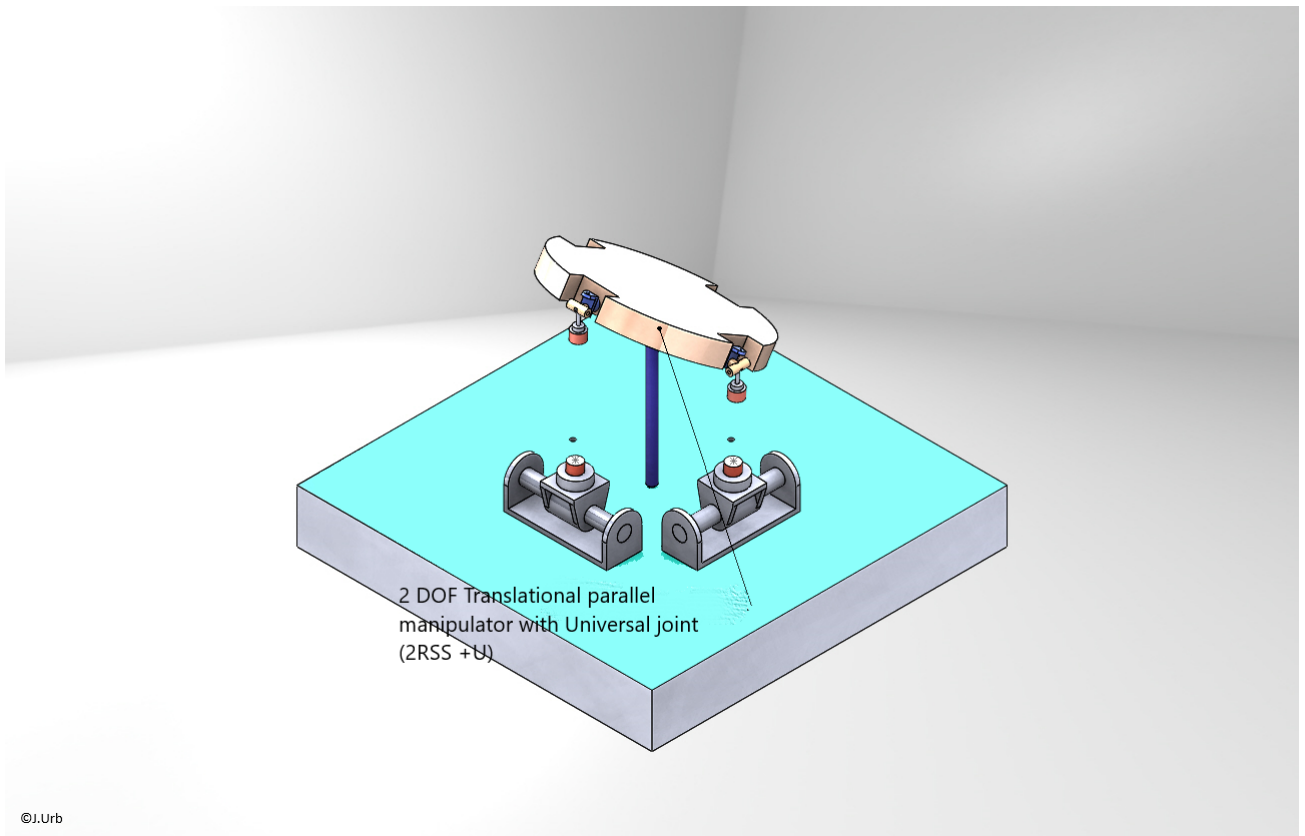


Figure D.4.: 2 DOF Translational parallel manipulator with Universal joint (2RSS+U)

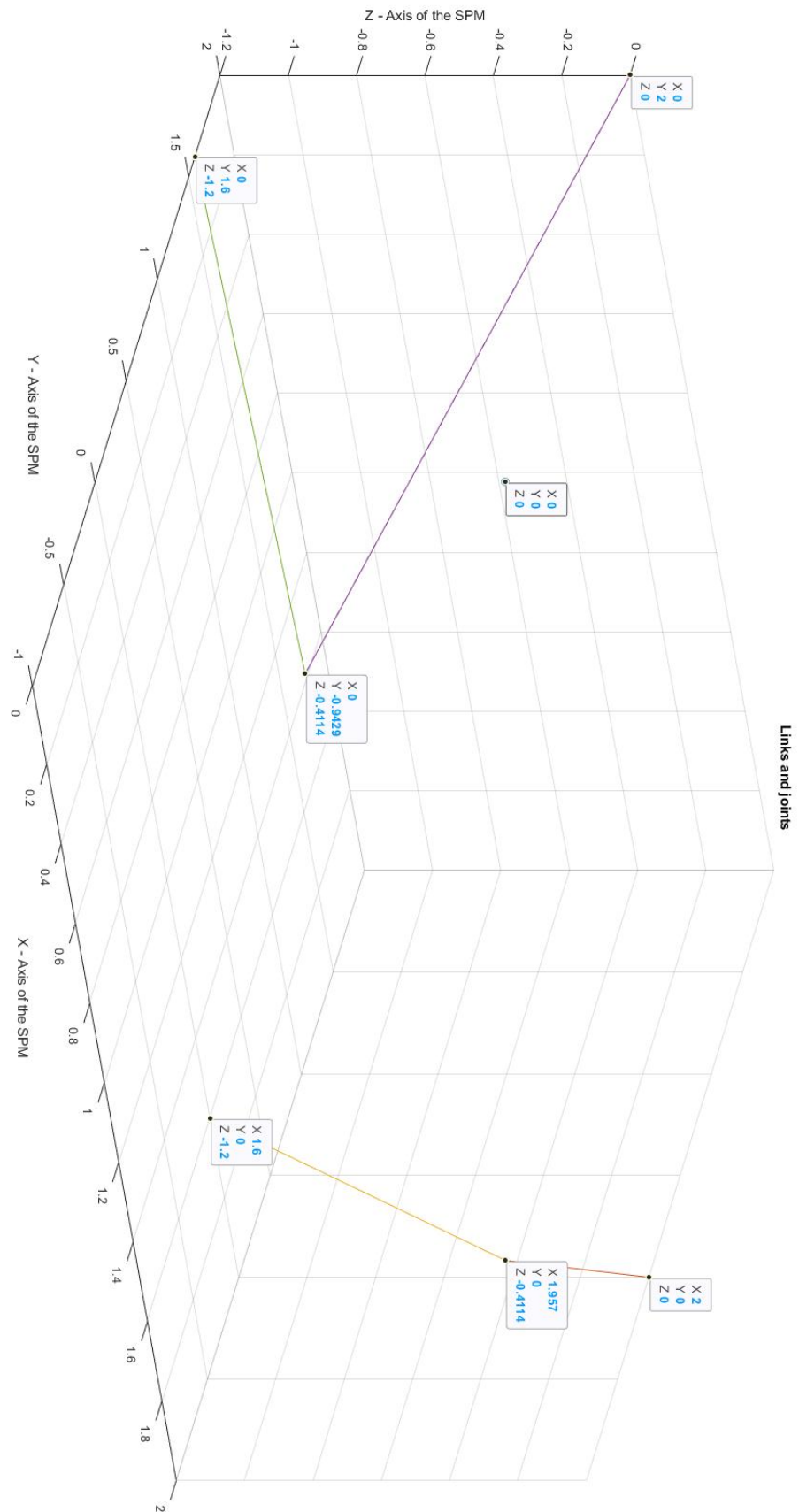
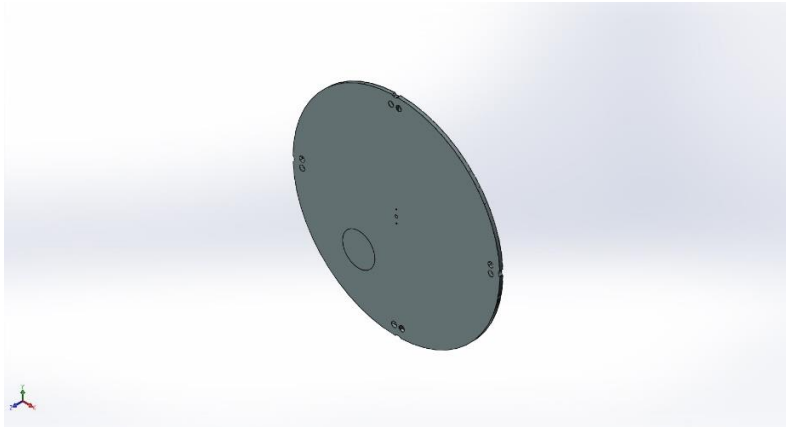


Figure D.5.: Representation of joints in initial conditions

E. : Appendix 5: 2 DOF SPM Assembly calculations

E.1. Top Plate 3 FEM



Simulation of 3 Top Plate 3 Assembly

Date: laupäev, 26. detsember 2020
Designer: Jaanus Urb, 183767MATM
Study name: Static 1
Analysis type: Static

Table of Contents

Description 1
 Assumptions 2
 Model Information 2
 Study Properties 4
 Units 4
 Material Properties 5
 Loads and Fixtures 5
 Mesh information 7
 Study Results 8
 Conclusion 11

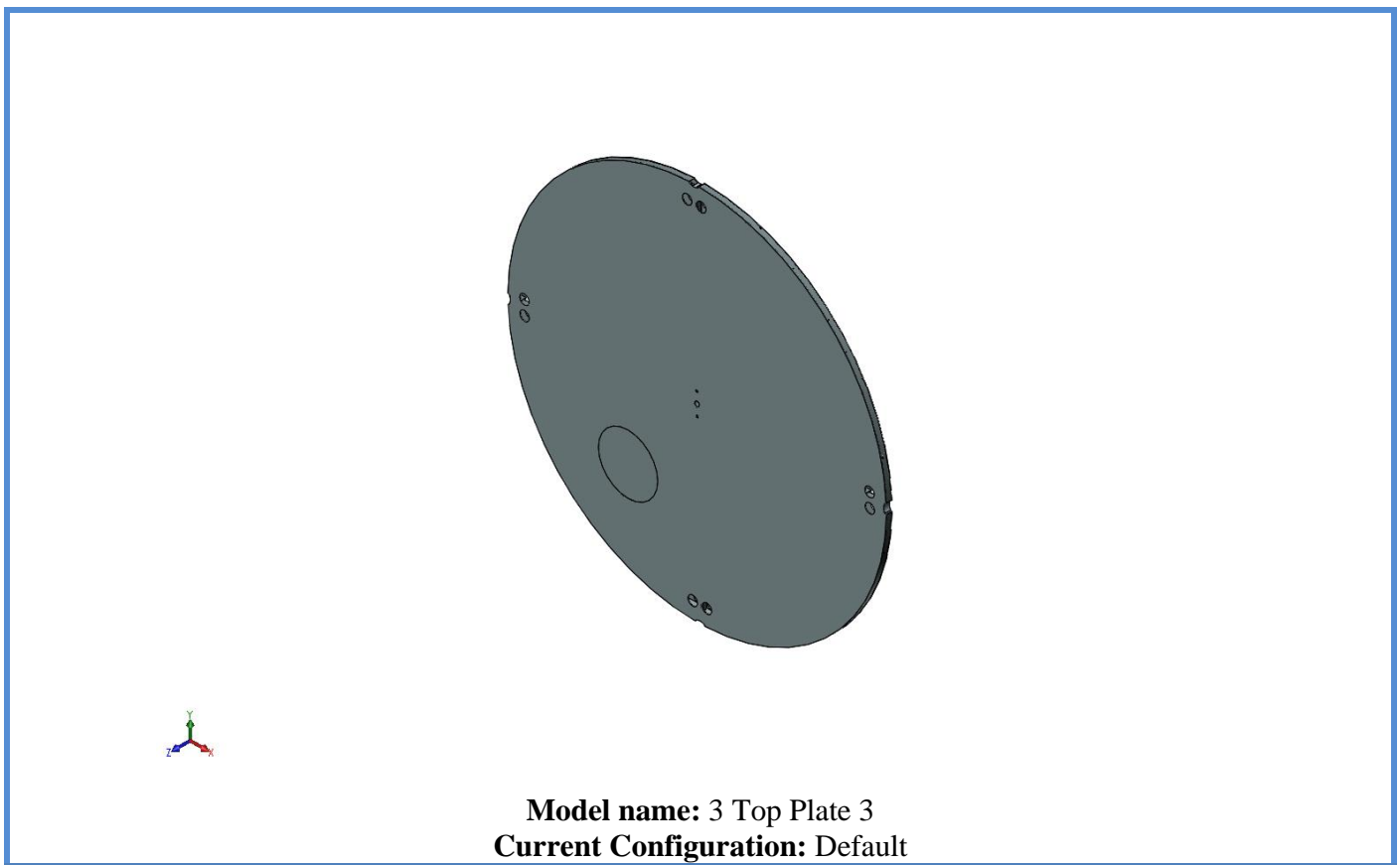
Description

Top plate stress and displacement analysis with external load 275 kg. The external load is taken from the UAV helicopter mass multiplied with 1.5 (safety factor for emergency landing). The other reaction forces are neglected due to simplicity and the joints are fixed. The reaction forces for joint P1, P2 and O from platform movement and ship movement are not considered (As dynamic loading).

Assumptions

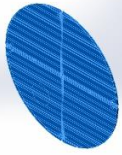
Worst case scenario, when the UAV helicopter will try to land on the opposite side of the P1 and P2 joints. I will assume that the force vector is the Top plate normal directed downwards as the gravitational force and most probable emergency landing direction.

Model Information



Solid Bodies

| Document Name and Reference | Treated As | Volumetric Properties | Document Path/Date Modified |
|-----------------------------|------------|-----------------------|-----------------------------|
|-----------------------------|------------|-----------------------|-----------------------------|

| | | | |
|--|-------------------|--|--|
| <p>Split Line1</p>  | <p>Solid Body</p> | <p>Mass:402.202 kg Volume:0.148964 m³ Density:2 700 kg/m³ Weight:3 941.58 N</p> | <p>3 Top Plate 3 Assemblyrev2step_1.SL DPRT Dec 25 03:54:57 2020</p> |
|--|-------------------|--|--|

Comments:

NX model is the original file, but due to complex geometry I did simplified the model to step file and managed to solve the FEM in Solidworks. It was the second iteration. The first one was out of the allowable stress and displacement limits, but the weight was less.

The First iteration:

Mass:257.86 kg
Volume:0.0955037 m³
Density:2 700 kg/m³
Weight:2 527.03 N

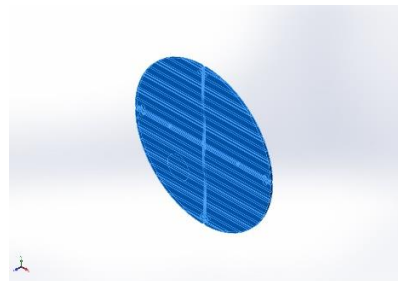
Study Properties

| | |
|---|---|
| Study name | Static 1 |
| Analysis type | Static |
| Mesh type | Solid Mesh |
| Thermal Effect: | On |
| Thermal option | Include temperature loads |
| Zero strain temperature | 298 Kelvin |
| Include fluid pressure effects from SOLIDWORKS Flow Simulation | Off |
| Solver type | FFEPlus |
| Inplane Effect: | Off |
| Soft Spring: | Off |
| Inertial Relief: | Off |
| Incompatible bonding options | Automatic |
| Large displacement | Off |
| Compute free body forces | On |
| Friction | Off |
| Use Adaptive Method: | Off |
| Result folder | SOLIDWORKS document (C:\Users\Urb\Documents\TTU\Võimalik lõputöö\MUDEL_rev0\MUDEL0_stp\Hull_pv1101+ Bottom_plate_4m) |

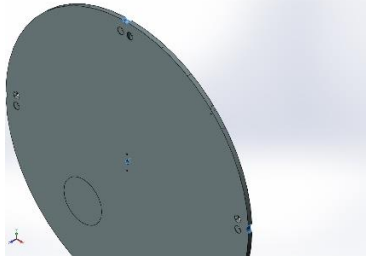
Units

| | |
|----------------------------|------------------|
| Unit system: | SI (MKS) |
| Length/Displacement | mm |
| Temperature | Kelvin |
| Angular velocity | Rad/sec |
| Pressure/Stress | N/m ² |

Material Properties

| Model Reference | Properties | Components |
|---|---|--|
|  | <p>Name: 6063-T83 Model type: Linear Elastic Isotropic Default failure criterion: Max von Mises Stress Yield strength: 2.4e+08 N/m² Tensile strength: 2.55e+08 N/m² Elastic modulus: 6.9e+10 N/m² Poisson's ratio: 0.33 Mass density: 2 700 kg/m³ Shear modulus: 2.58e+10 N/m² Thermal expansion coefficient: 2.34e-05 /Kelvin</p> | SolidBody 2(Split Line1)(3 Top Plate 3 Assemblyrev2step_1) |
| Curve Data:N/A | | |

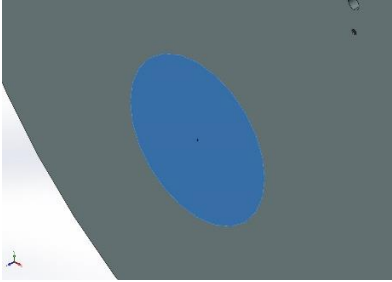
Loads and Fixtures

| Fixture name | Fixture Image | Fixture Details |
|--------------|---|---|
| Fixed-1 |  | <p>Entities: 9 edge(s), 2 face(s) Type: Fixed Geometry</p> |

Resultant Forces

| Components | X | Y | Z | Resultant |
|----------------------|----------|-----------|----------|-----------|
| Reaction force(N) | 0.191872 | -0.107716 | 2 699.49 | 2 699.49 |
| Reaction Moment(N.m) | 0 | 0 | 0 | 0 |

| Load name | Load Image | Load Details |
|-----------|------------|--------------|
|-----------|------------|--------------|

| | | |
|----------------|---|---|
| <p>Force-1</p> |  | <p>Entities: 1 face(s) Type: Apply normal force Value: 2 700 N</p> |
|----------------|---|---|

Resultant Forces from External Load

Reaction forces

| Selection set | Units | Sum X | Sum Y | Sum Z | Resultant |
|---------------|-------|----------|-----------|----------|-----------|
| Entire Model | N | 0.191872 | -0.107716 | 2 699.49 | 2 699.49 |

Reaction Moments

| Selection set | Units | Sum X | Sum Y | Sum Z | Resultant |
|---------------|-------|-------|-------|-------|-----------|
| Entire Model | N.m | 0 | 0 | 0 | 0 |

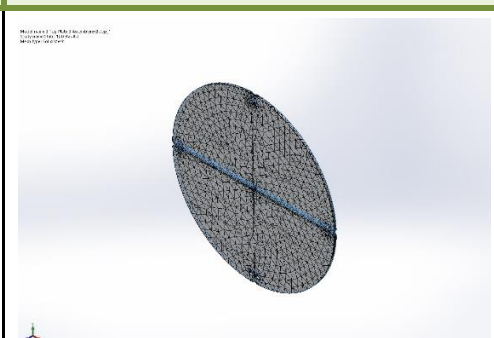
Mesh information

| | |
|----------------------|------------------------------|
| Mesh type | Solid Mesh |
| Mesher Used: | Blended curvature-based mesh |
| Jacobian points | 4 Points |
| Maximum element size | 158.241 mm |
| Minimum element size | 31.6482 mm |
| Mesh Quality Plot | High |

Mesh information - Details

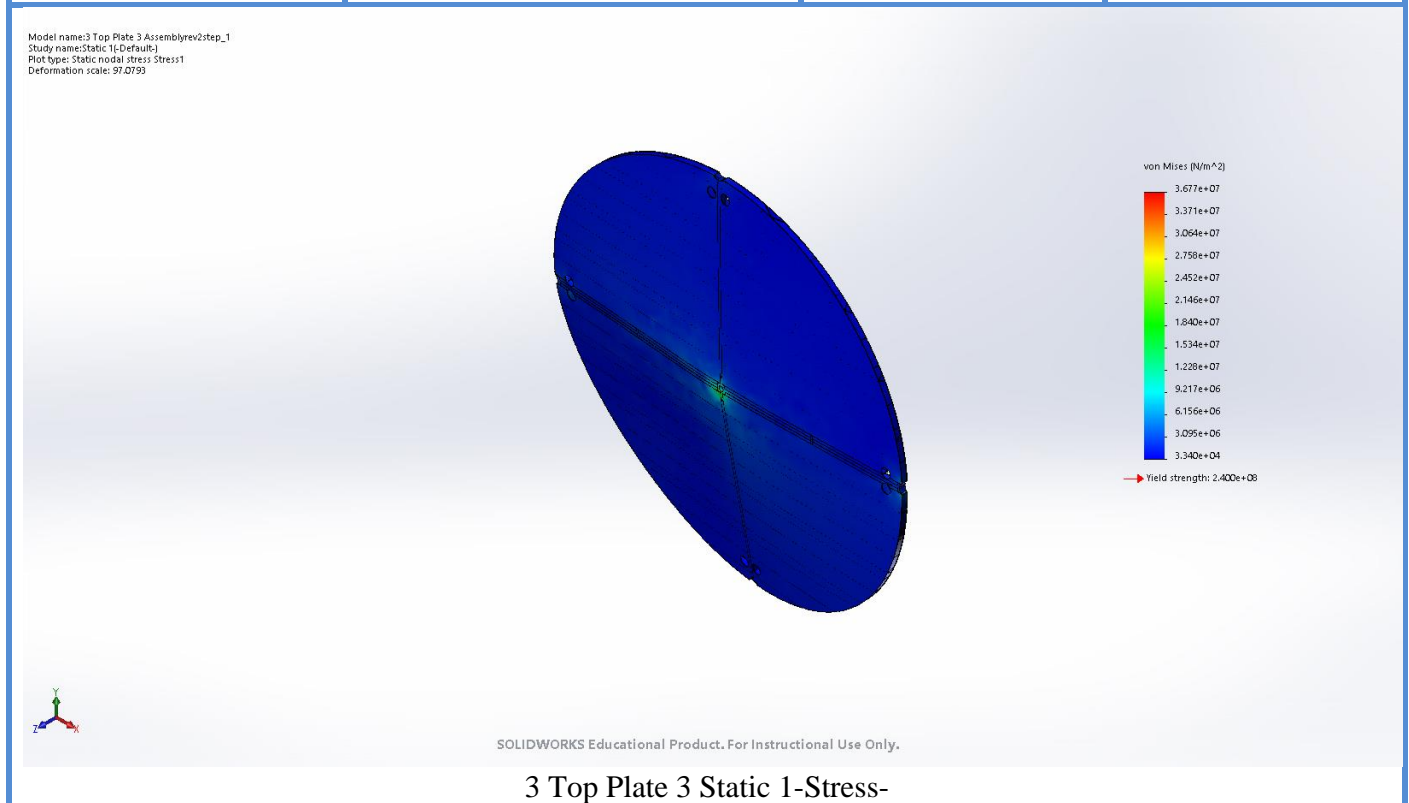
| | |
|--------------------------------------|----------|
| Total Nodes | 84764 |
| Total Elements | 48589 |
| Maximum Aspect Ratio | 3 840.8 |
| % of elements with Aspect Ratio < 3 | 0.331 |
| % of elements with Aspect Ratio > 10 | 93.3 |
| % of distorted elements(Jacobian) | 0 |
| Time to complete mesh(hh:mm:ss): | 00:00:43 |
| Computer name: | URB |

Mesh Control Information:

| Mesh Control Name | Mesh Control Image | Mesh Control Details |
|-------------------|---|---|
| Control-1 |  | Entities: 1 face(s) Units: mm Size: 71.2084 Ratio: 71.2084 |

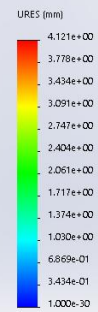
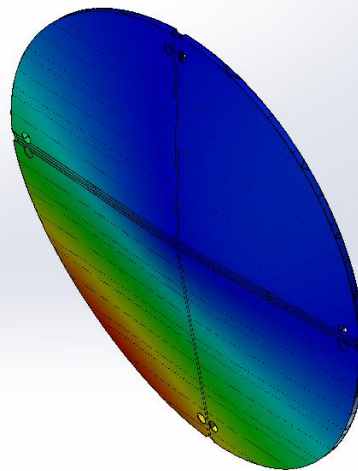
Study Results

| Name | Type | Min | Max |
|---------|-----------------------|---|---|
| Stress1 | VON: von Mises Stress | 3.340e+04 N/m ² Node: 22480 | 3.677e+07 N/m ² Node: 22878 |



| Name | Type | Min | Max |
|---------------|------------------------------|-------------------------|----------------------------|
| Displacement1 | URES: Resultant Displacement | 0.000e+00 mm Node: 2 | 4.121e+00 mm Node: 1714 |

Model name: 3 Top Plate 3 Assemblyrev2step_1
Study name: Static 1 (Default)
Plot type: Static displacement Displacement1
Deformation scale: 97.0793

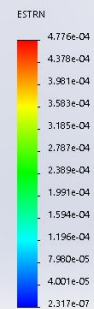
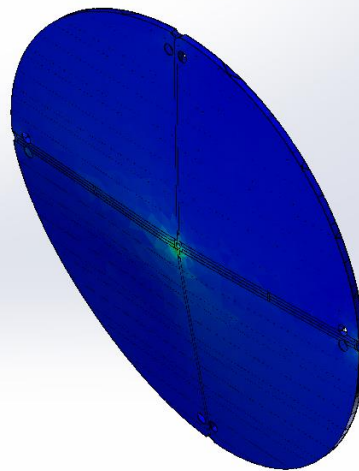


SOLIDWORKS Educational Product. For Instructional Use Only.

3 Top Plate 3 Assemblyrev2step_1-Static 1-Displacement-Displacement1

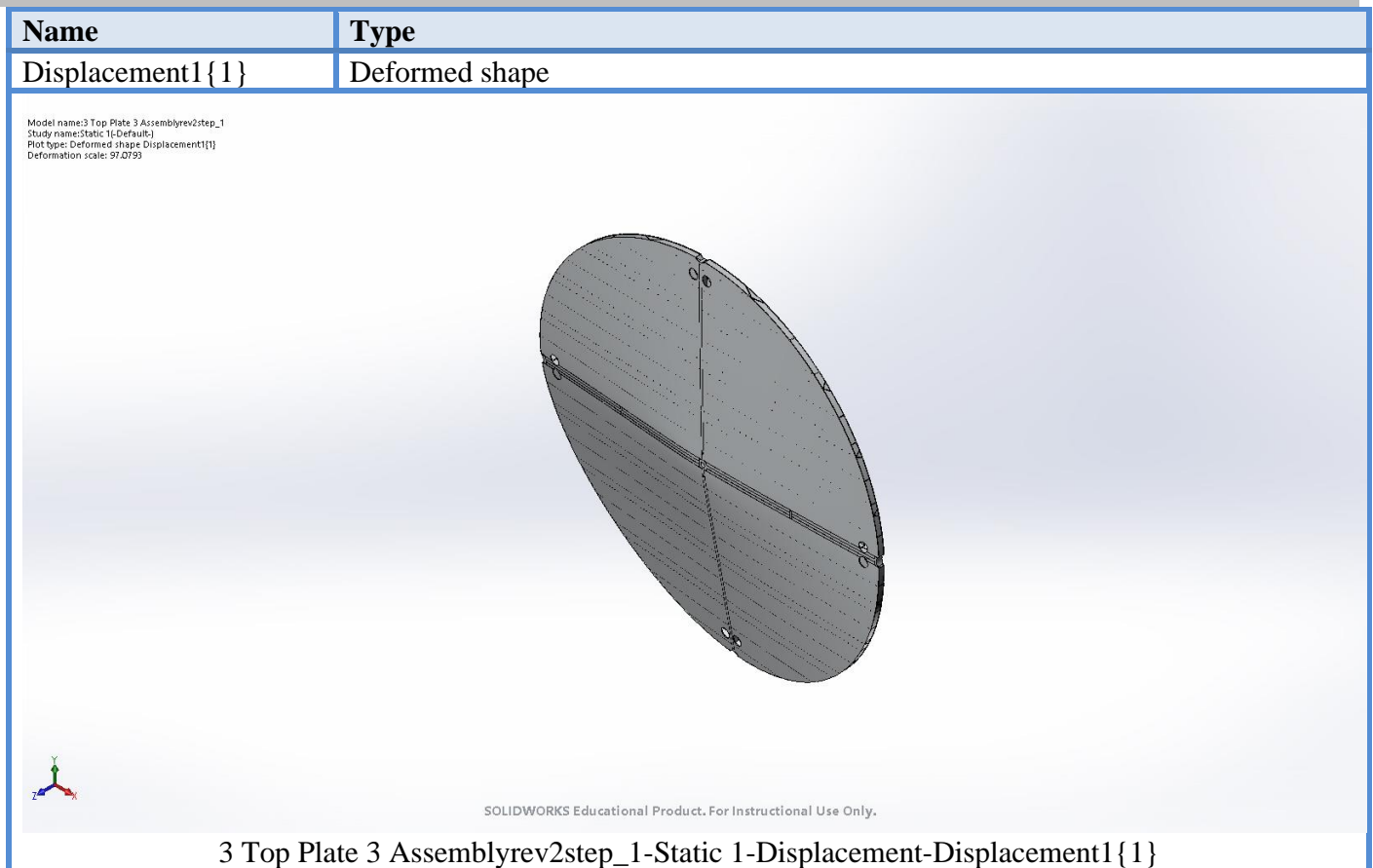
| Name | Type | Min | Max |
|---------|--------------------------|-----------------------------|-----------------------------|
| Strain1 | ESTRN: Equivalent Strain | 2.317e-07 Element: 31235 | 4.776e-04 Element: 33300 |

Model name: 3 Top Plate 3 Assemblyrev2step_1
Study name: Static 1 (Default)
Plot type: Static strain Strain1
Deformation scale: 97.0793



SOLIDWORKS Educational Product. For Instructional Use Only.

3 Top Plate 3 Assemblyrev2step_1-Static 1-Strain-Strain1



Conclusion

The original model was modeled in the NX and I was not able to solve the FEM in NX. Due to complex geometry I did simplify the model to step file and managed to solve the FEM in Solidworks. The structure loads are carried mainly by the two cross beams which are connected with author designed profile structure (look for the drawings). I tried to solve the Top plate Assembly in NX with mid-surface and 2D mesh, but due to my computer limitations, I did not get a solution. This solution is satisfactory as the maximum stress ($3.677 \cdot 10^7 \frac{N}{m^2}$) are below the material yield strength $2.400 \cdot 10^8 \frac{N}{m^2}$.

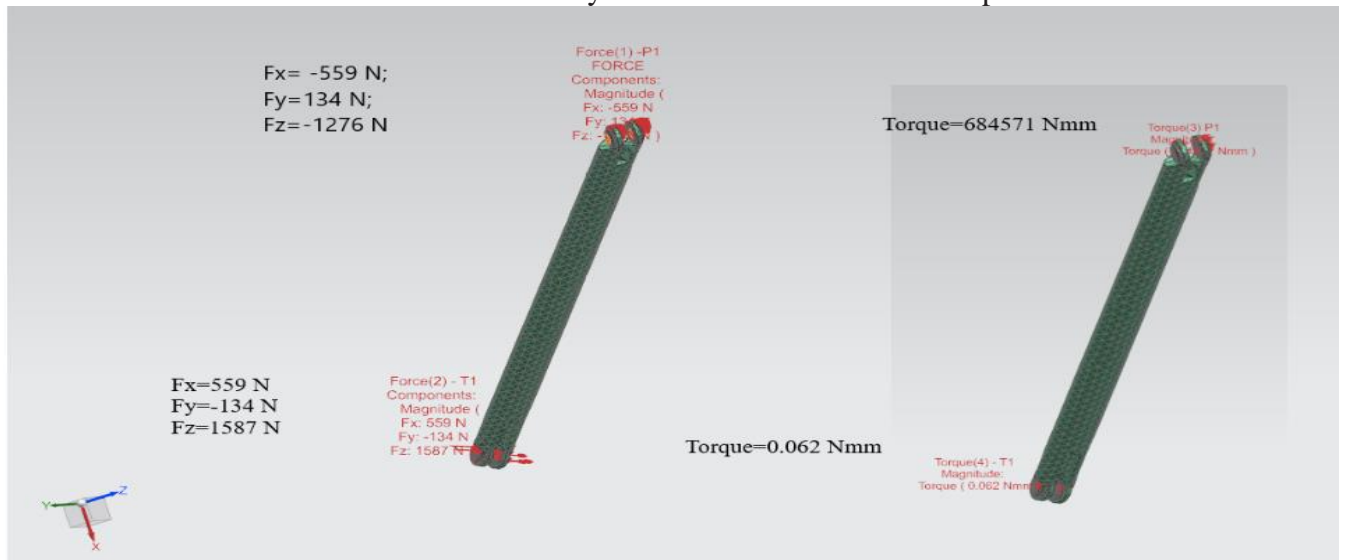
E.2. Link 1 Assembly FEM

| | | | |
|---|-------------------------------|----------------------|------------|
| Discipline or report series | Document number Appendix 5 | Report number E.2 | Issue 0 |
| Title Tallinn University of Technology, Master Thesis Appendix 5: E.2: Link 1 Assembly FEM Analysis | | | |
| Author(s) Jaanus Urb, 183767MATM | Telephone: | Date 27.12.2020 | |

Summary

Assembly is the moving link to the platform to position the Top plate according to the elevation.

Link 1 assembly stress and displacement analysis with external load 275 kg. The external load is taken from the UAV helicopter mass multiplied with 1.5 (safety factor for emergency landing). The reaction forces for joints are calculated with NX motion analysis and the the initial loading on time 0 s will be considered as the heaving will be downward as the gravity and the z component for the reaction force are then maximum. The reaction forces components will differ on time, but in the initial state it is maximum. The conclusion of the motion analysis will be covered in the Chapter 4. Joint are T1 and P1.



| | |
|---------------------|----------|
| Additional keywords | Category |
|---------------------|----------|

Circulation:

Approved by:

| | | | |
|-------------------------------|------------|--|-------------|
| Document number Appendix 5 | Issue 0 | | Page 1 of 5 |
|-------------------------------|------------|--|-------------|



| Project | Sub-system | Process | Part number |
|--|------------|---------|-------------|
| 2 DOF SPM FOR PVL- | X-Branch | | |
| Material Bend Link and Bushing link 1 MIDDLE x 4 - ALUMINIUM 6082 or 6062, Sleeve Bearing-XSM-3034-16 - Bronze | | | File/folder |

TABLE OF CONTENTS

| | | |
|----------|---------------------------|----------|
| 1 | INTRODUCTION | 3 |
| 1.1 | HEADER | 3 |
| 1.2 | MODEL CONSTRUCTION | 3 |
| 1.3 | MODEL SUMMARY:..... | 3 |
| 1.4 | MESHES..... | 3 |
| 1.5 | MATERIALS..... | 3 |
| 1.6 | CONSTRAINTS | 4 |
| 1.7 | MODEL RESULTS | 4 |

| | | | |
|-------------------------------|------------|--|-------------|
| Document number Appendix 5 | Issue 0 | | Page 2 of 5 |
|-------------------------------|------------|--|-------------|

1 INTRODUCTION

1.1 Header

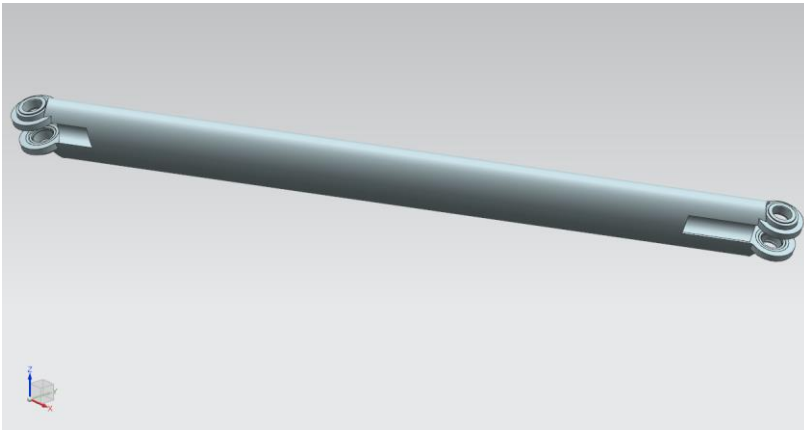
Critical part to move the X-Branch of the manipulator.

1.2 Model Construction

The version of Product used to create this model was [NX 12](#).

1 Link 1_Assembly.prt

1.3 Model Summary:



Weight data was calculated

Density = 0.000002736 kg/mm³
 Area = 335123.608440610 mm²
 Volume = 4093655.965090800 mm³
 Mass = 11.198293167 kg

1.4 Meshes

| | |
|---------------|-----|
| Node Count | 282 |
| Element Count | 706 |

Element type CTETRA(4)

Element Size : 7.29 mm

1.5 Materials

Aluminum_6061

| | | | |
|-------------------------------|------------|--|-------------|
| Document number Appendix 5 | Issue 0 | | Page 3 of 5 |
|-------------------------------|------------|--|-------------|

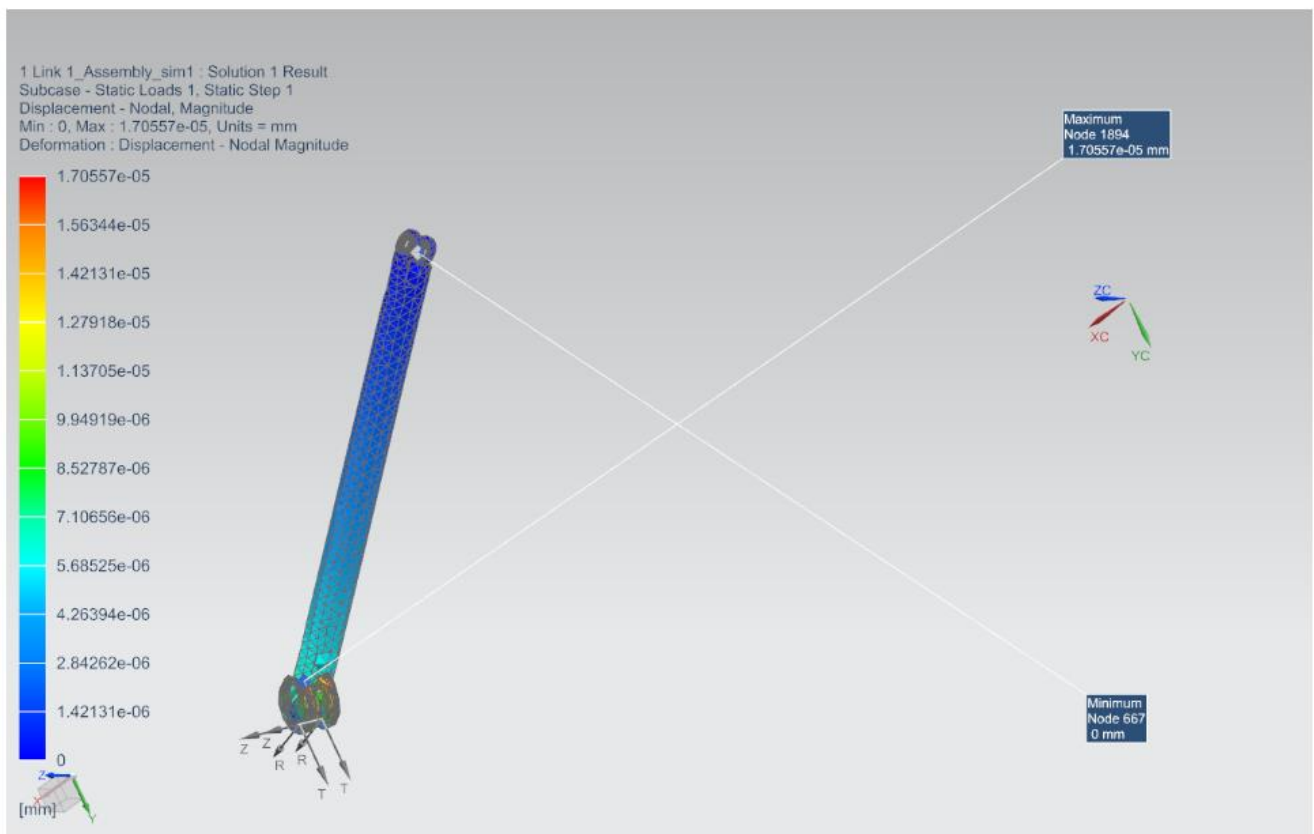
1.6 Constraints

Pinned constraint in the T1 and fixed in the P1. Buchings and bearings are glued to Bend link.

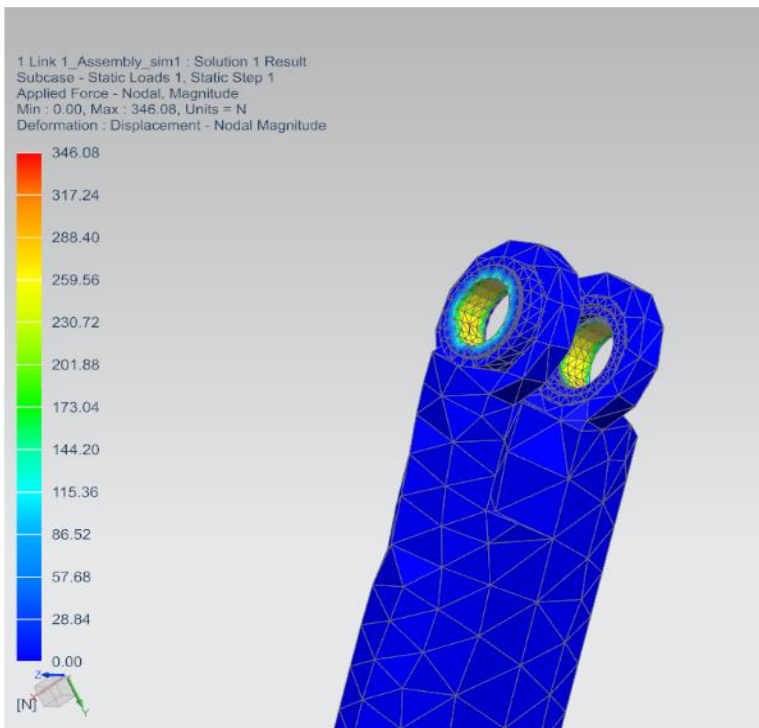
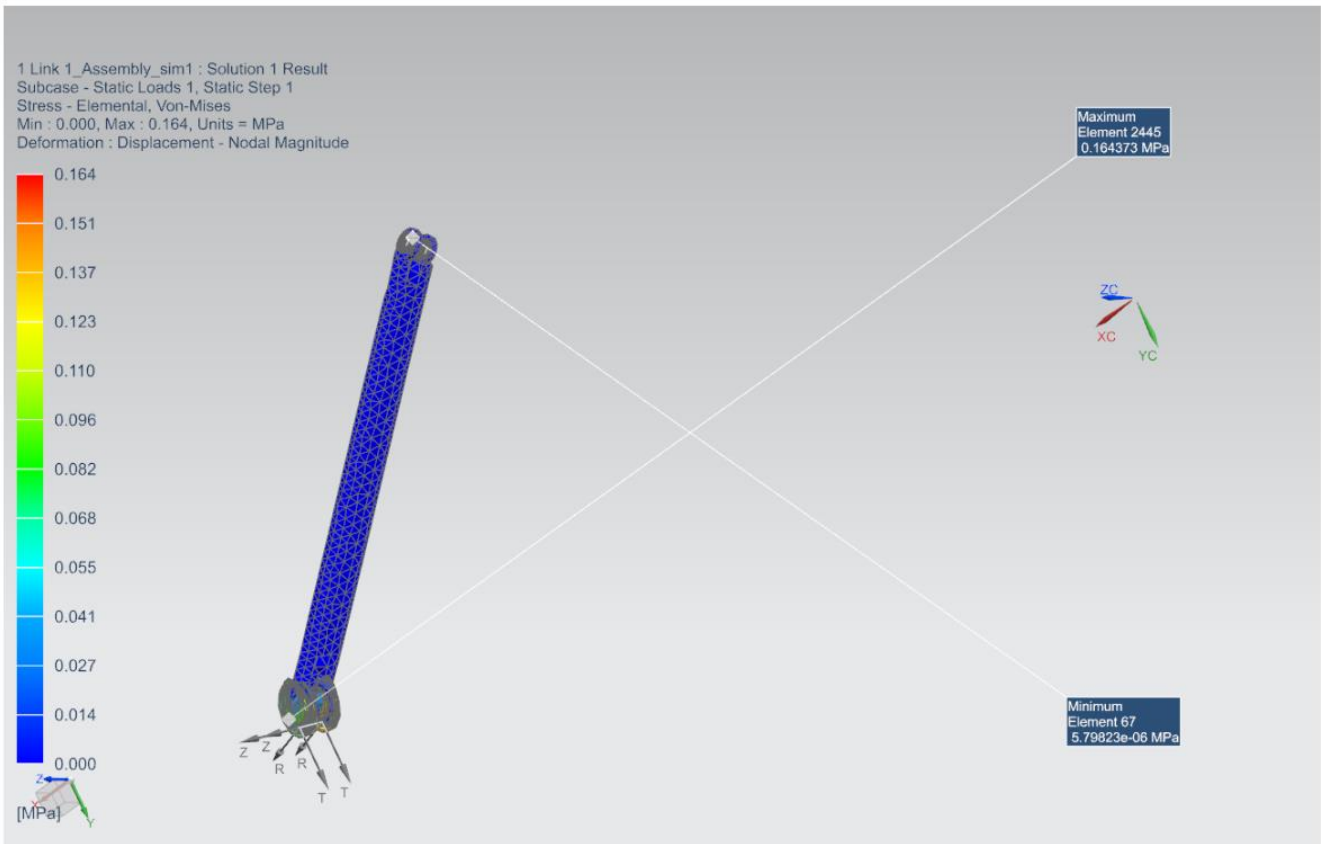
1.7 Model Results

Solver Name and version NX Nastran Design Linear Statics.

Maximum displacement $1.7 \cdot 10^{-5}$ mm. Maximum stress 0.164373 MPa.



| | | | |
|-------------------------------|------------|--|-------------|
| Document number Appendix 5 | Issue 0 | | Page 4 of 5 |
|-------------------------------|------------|--|-------------|



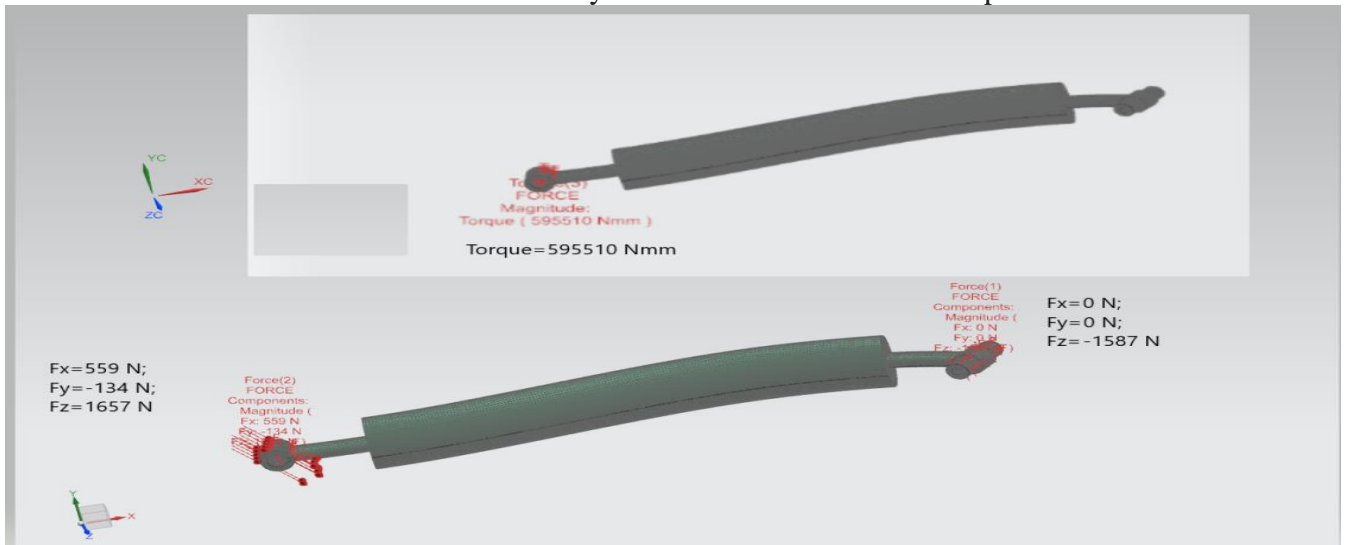
E.3. Link 2 Assembly FEM

| | | | |
|---|-------------------------------|----------------------|------------|
| Discipline or report series | Document number Appendix 5 | Report number E.3 | Issue 0 |
| Title Tallinn University of Technology, Master Thesis Appendix 5: E.3: Link 2 Assembly FEM Analysis | | | |
| Author(s) Jaanus Urb, 183767MATM | Telephone: | Date 27.12.2020 | |

Summary

Assembly is the driving link to the platform to position the Link 1 and Top plate according to the elevation.

Link 2 assembly stress and displacement analysis with external load 275 kg. The external load is taken from the UAV helicopter mass multiplied with 1.5 (safety factor for emergency landing). The reaction forces for joints are calculated with NX motion analysis and the the initial loading on time 0 s will be considered as the heaving will be downward as the gravity and the z component for the reaction force are then maximum. The reaction forces components will differ on time, but in the initial state it is maximum. The conclusion of the motion analysis will be covered in the Chapter 4. Joint are T1 and B1.



| | |
|---------------------|----------|
| Additional keywords | Category |
|---------------------|----------|

Circulation:

Approved by:

| | | | |
|-------------------------------|------------|--|-------------|
| Document number Appendix 5 | Issue 0 | | Page 1 of 5 |
|-------------------------------|------------|--|-------------|



| Project | Sub-system | Process | Part number |
|---|------------|---------|-------------|
| 2 DOF SPM FOR PVL- | X-Branch | | |
| Material 2 Link 2 Bend and SHAFT - ALUMINIUM 6082 or 6062 | | | File/folder |

TABLE OF CONTENTS

| | | |
|-----|--------------------------|---|
| 1 | INTRODUCTION | 3 |
| 1.1 | HEADER | 3 |
| 1.2 | MODEL CONSTRUCTION | 3 |
| 1.3 | MODEL SUMMARY:..... | 3 |
| 1.4 | MESHES..... | 3 |
| 1.5 | MATERIALS..... | 4 |
| 1.6 | CONSTRAINTS | 4 |
| 1.7 | MODEL RESULTS | 4 |

| | | | |
|-------------------------------|------------|--|-------------|
| Document number Appendix 5 | Issue 0 | | Page 2 of 5 |
|-------------------------------|------------|--|-------------|

1 INTRODUCTION

1.1 Header

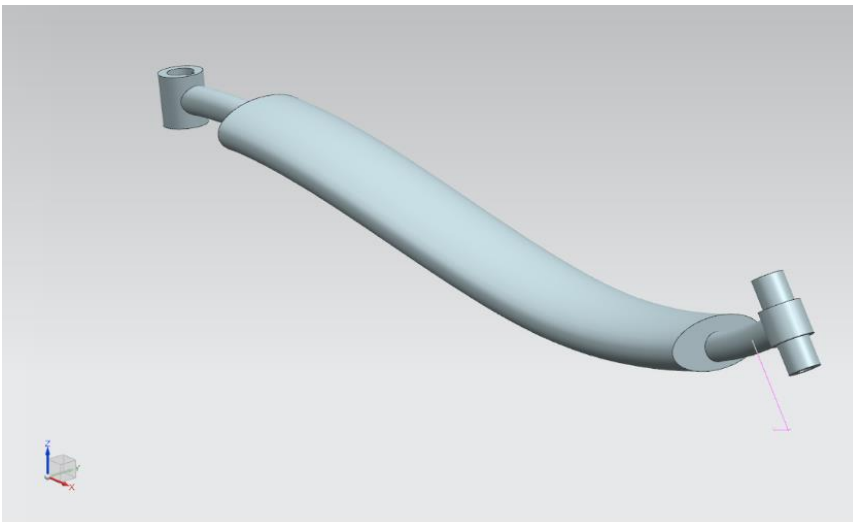
Critical part to move the X-Branch of the manipulator as a driving link that takes the motor torque and transfers it to the Top Plate.

1.2 Model Construction

The version of Product used to create this model was [NX 12](#).

2 Link 2_Assembly.prt

1.3 Model Summary:



Weight data was calculated

Density = 0.000002711 kg/mm³
 Area = 210707.694061730 mm²
 Volume = 2708215.017310600 mm³
 Mass = 7.341970912 kg

1.4 Meshes

| | |
|---------------|---------------|
| Node Count | 193984 |
| Element Count | 126123 |

Element type PSOLID

Element Size : 4 mm

| | | | |
|--------------------------------------|------------|--|-------------|
| Document number Appendix 5 | Issue 0 | | Page 3 of 5 |
|--------------------------------------|------------|--|-------------|

1.5 Materials

Aluminum_6061

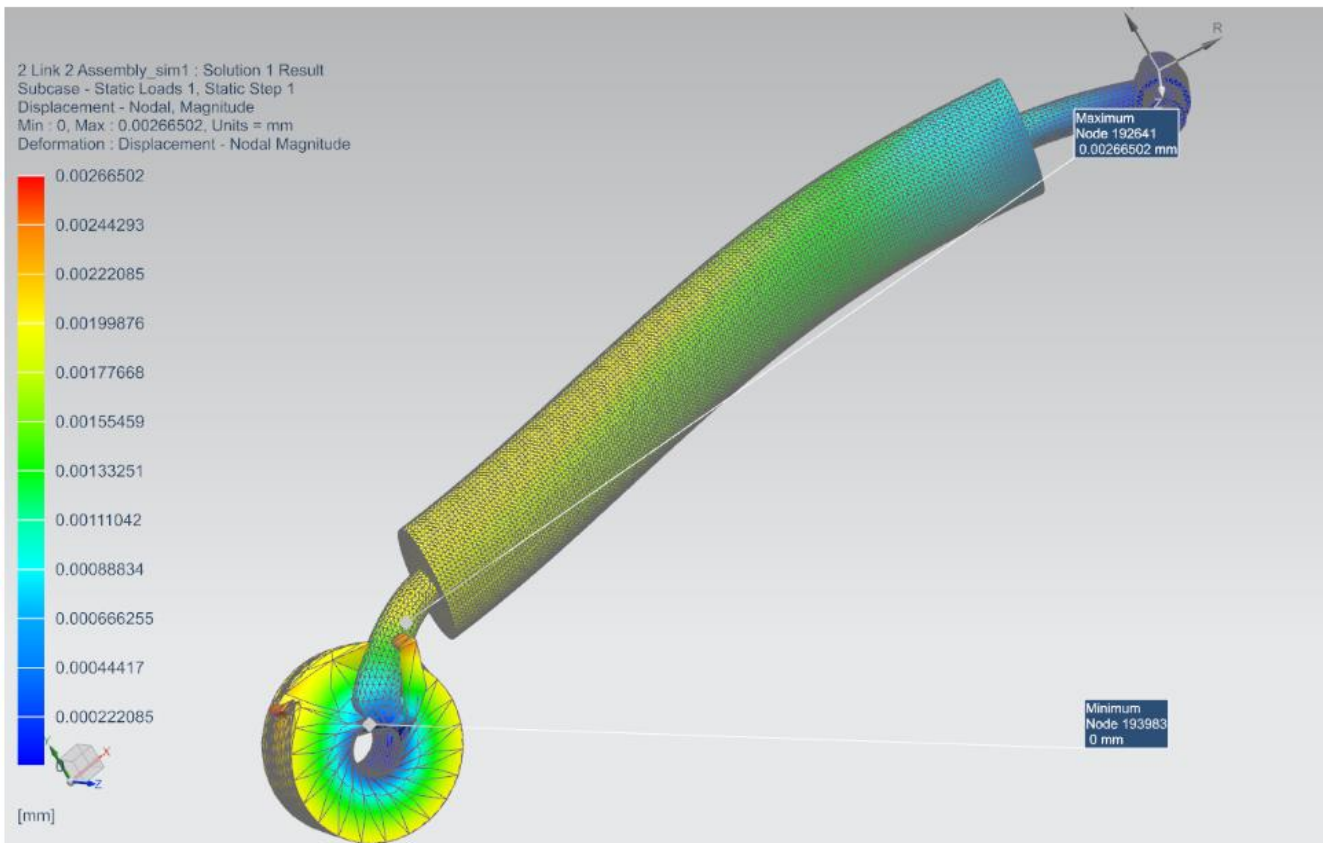
1.6 Constraints

Pinned constraint in the T1 and fixed in the B1.

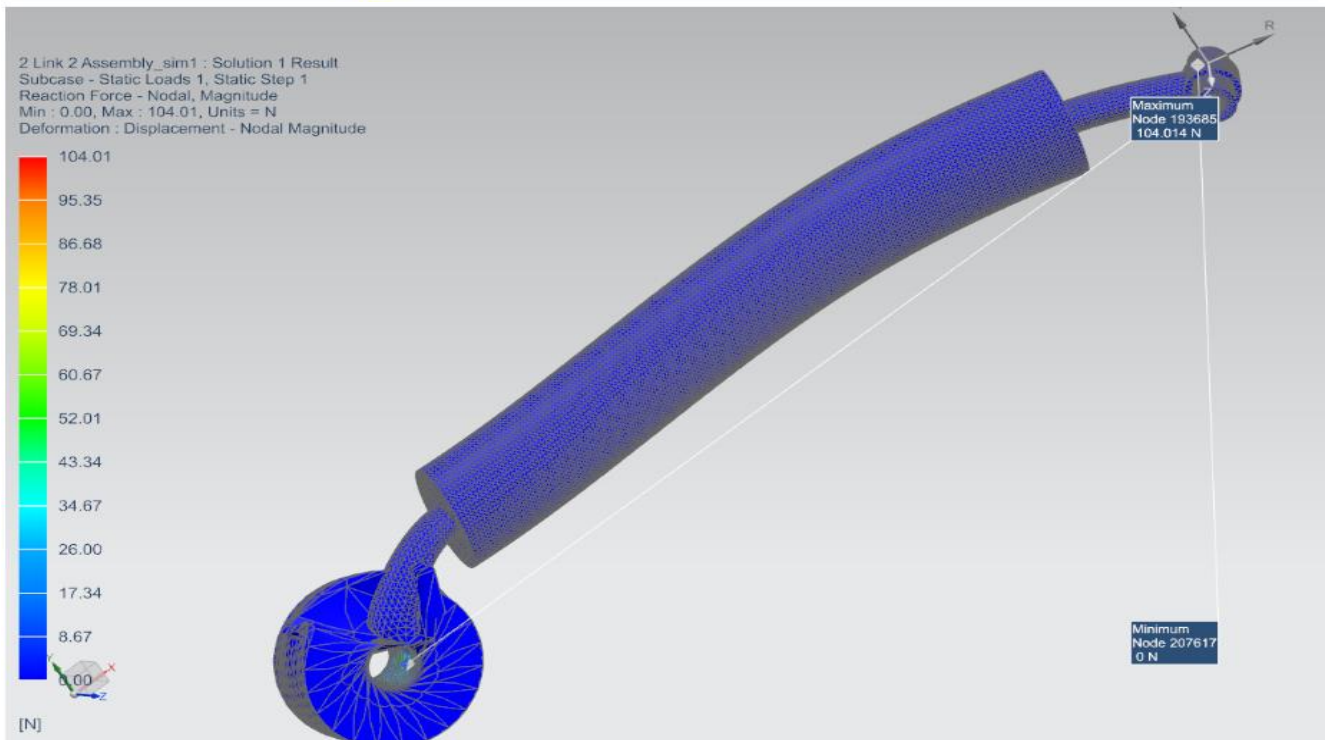
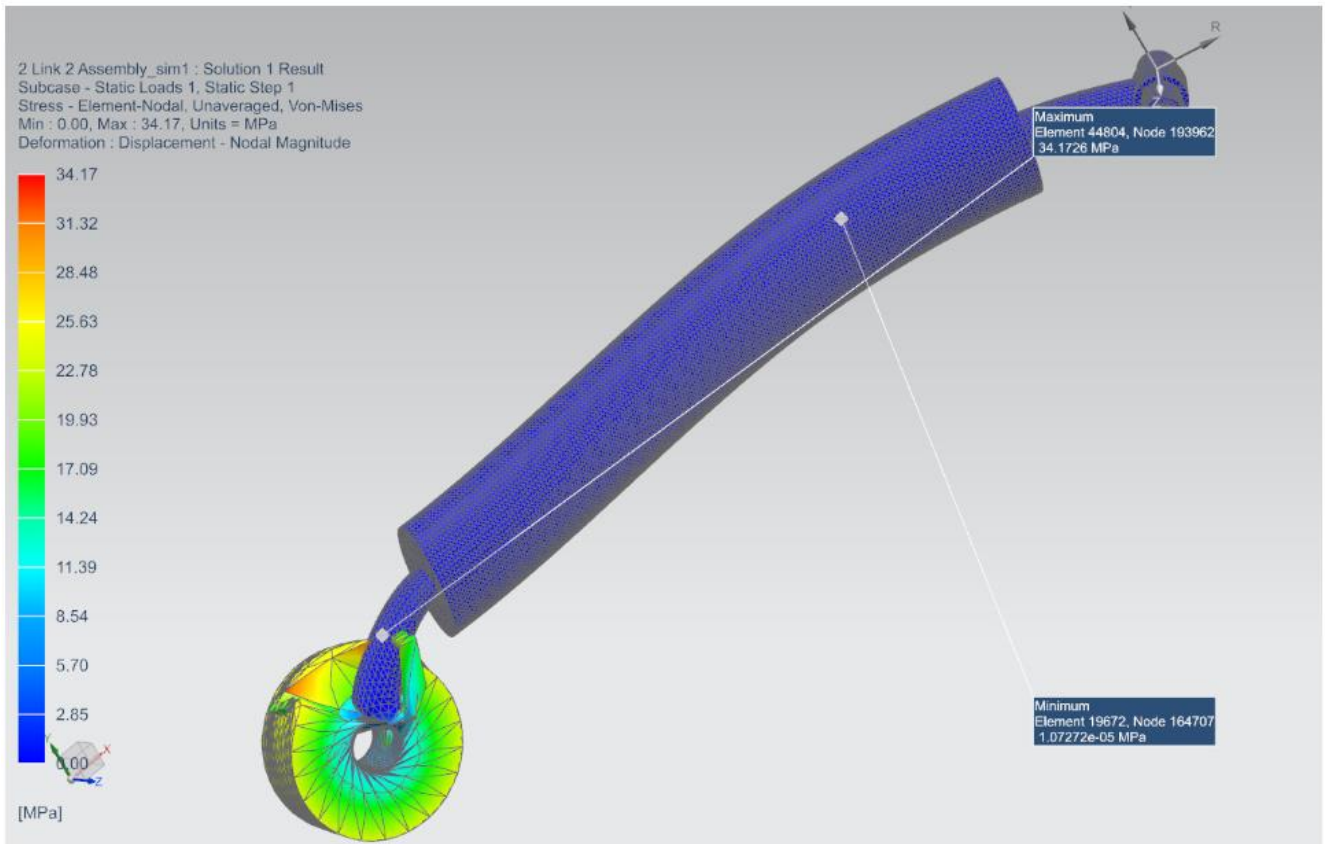
1.7 Model Results

Solver Name and version NX Nastran Design Linear Statics – Single Constraint.

Maximum displacement $2.7 \cdot 10^{-3} \text{ mm}$. Maximum stress 34.17 MPa.



| | | | |
|-------------------------------|------------|--|-------------|
| Document number Appendix 5 | Issue 0 | | Page 4 of 5 |
|-------------------------------|------------|--|-------------|



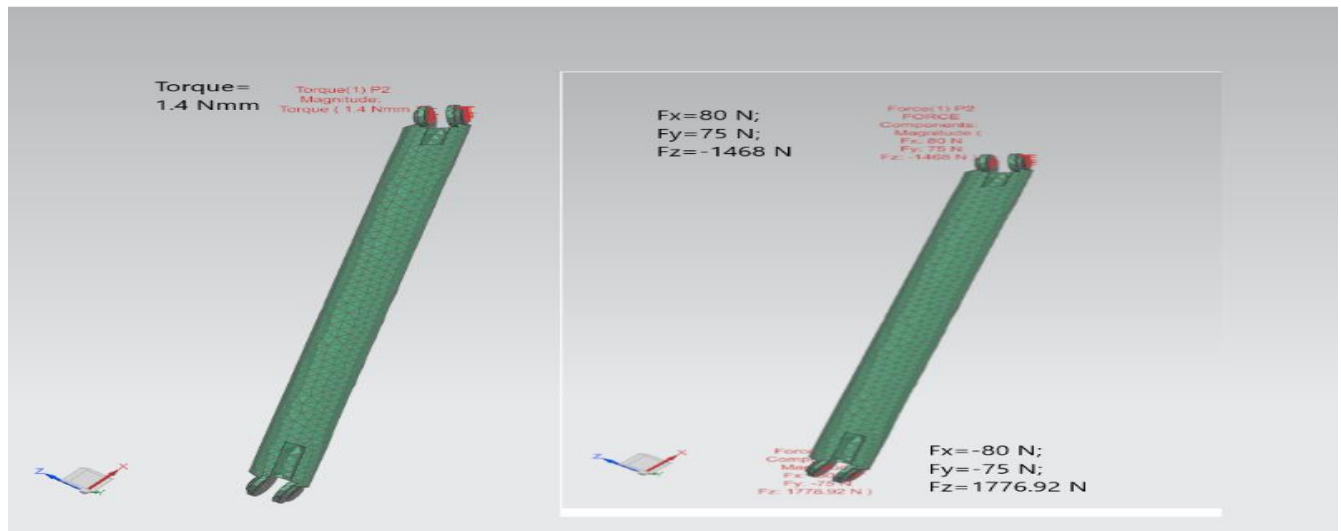
E.4. Link 4 Assembly FEM

| | | | |
|---|-------------------------------|----------------------|------------|
| Discipline or report series | Document number Appendix 5 | Report number E.4 | Issue 0 |
| Title Tallinn University of Technology, Master Thesis Appendix 5: E.4: Link 4 Assembly FEM Analysis | | | |
| Author(s) Jaanus Urb, 183767MATM | Telephone: | Date 27.12.2020 | |

Summary

Assembly is the moving link to the platform to position the Top plate according to the elevation.

Link 1 assembly stress and displacement analysis with external load 275 kg. The external load is taken from the UAV helicopter mass multiplied with 1.5 (safety factor for emergency landing). The reaction forces for joints are calculated with NX motion analysis and the the initial loading on time 0 s will be considered as the heaving will be downward as the gravity and the z component for the reaction force are then maximum. The reaction forces components will differ on time, but in the initial state it is maximum. The conclusion of the motion analysis will be covered in the Chapter 4. Joints are T2 and P2.



| | |
|---------------------|----------|
| Additional keywords | Category |
|---------------------|----------|

Circulation:

Approved by:

| | | | |
|-------------------------------|------------|--|-------------|
| Document number Appendix 5 | Issue 0 | | Page 1 of 5 |
|-------------------------------|------------|--|-------------|



| Project | Sub-system | Process | Part number |
|--|------------|---------|-------------|
| 2 DOF SPM FOR PVL- | Y-Branch | | |
| Material Bend Link and Bushing link 1 MIDDLE x 4 - ALUMINIUM 6082 or 6062, Sleeve Bearing-XSM-3034-16 - Bronze | | | File/folder |

TABLE OF CONTENTS

1 INTRODUCTION3

1.1 HEADER3

1.2 MODEL CONSTRUCTION3

1.3 MODEL SUMMARY:.....3

1.4 MESHES.....3

1.5 MATERIALS.....3

1.6 CONSTRAINTS4

1.7 MODEL RESULTS4

1 INTRODUCTION

1.1 Header

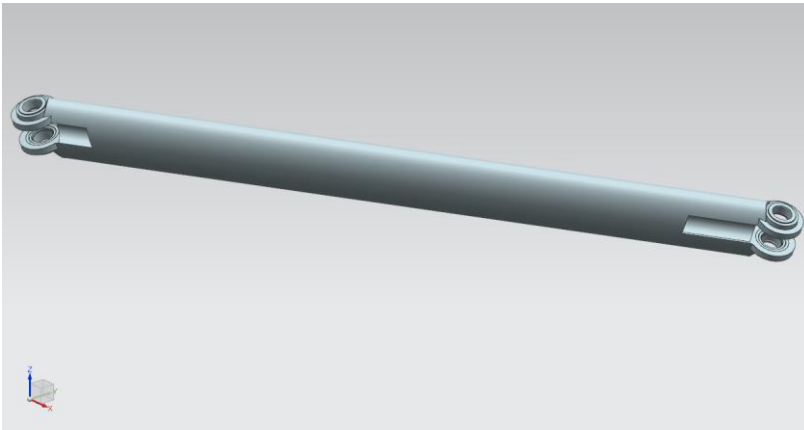
Critical part to move the Y-Branch of the manipulator.

1.2 Model Construction

The version of Product used to create this model was [NX 12](#).

4 Link 4_Assembly.prt

1.3 Model Summary:



Weight data was calculated

Density = 0.000002736 kg/mm³
 Area = 335123.608440610 mm²
 Volume = 4093655.965090800 mm³
 Mass = 11.198293167 kg

1.4 Meshes

| | |
|---------------|-----|
| Node Count | 282 |
| Element Count | 706 |

Element type CTETRA(4)

Element Size : 7.29 mm

1.5 Materials

Aluminum_6061

| | | | |
|-------------------------------|------------|--|-------------|
| Document number Appendix 5 | Issue 0 | | Page 3 of 5 |
|-------------------------------|------------|--|-------------|

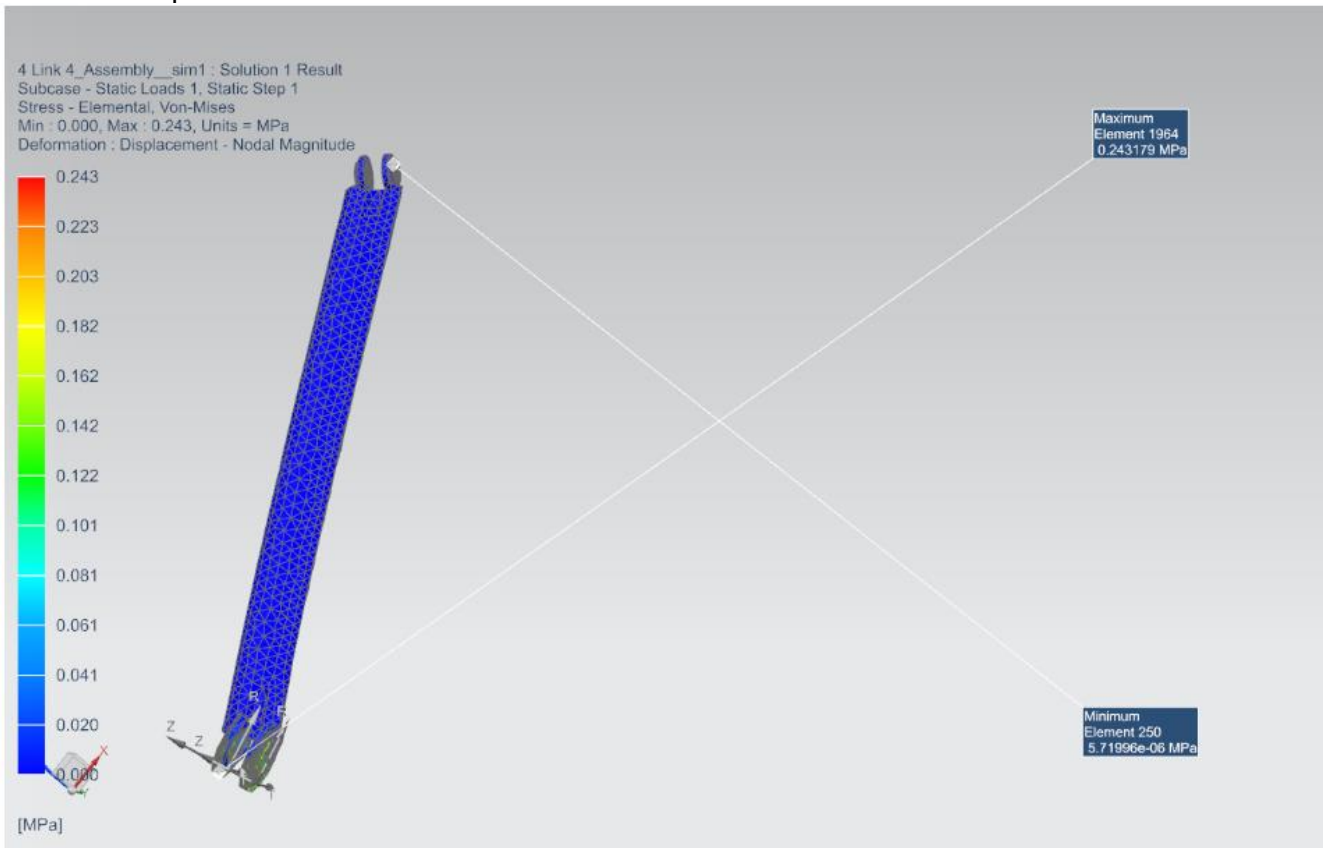
1.6 Constraints

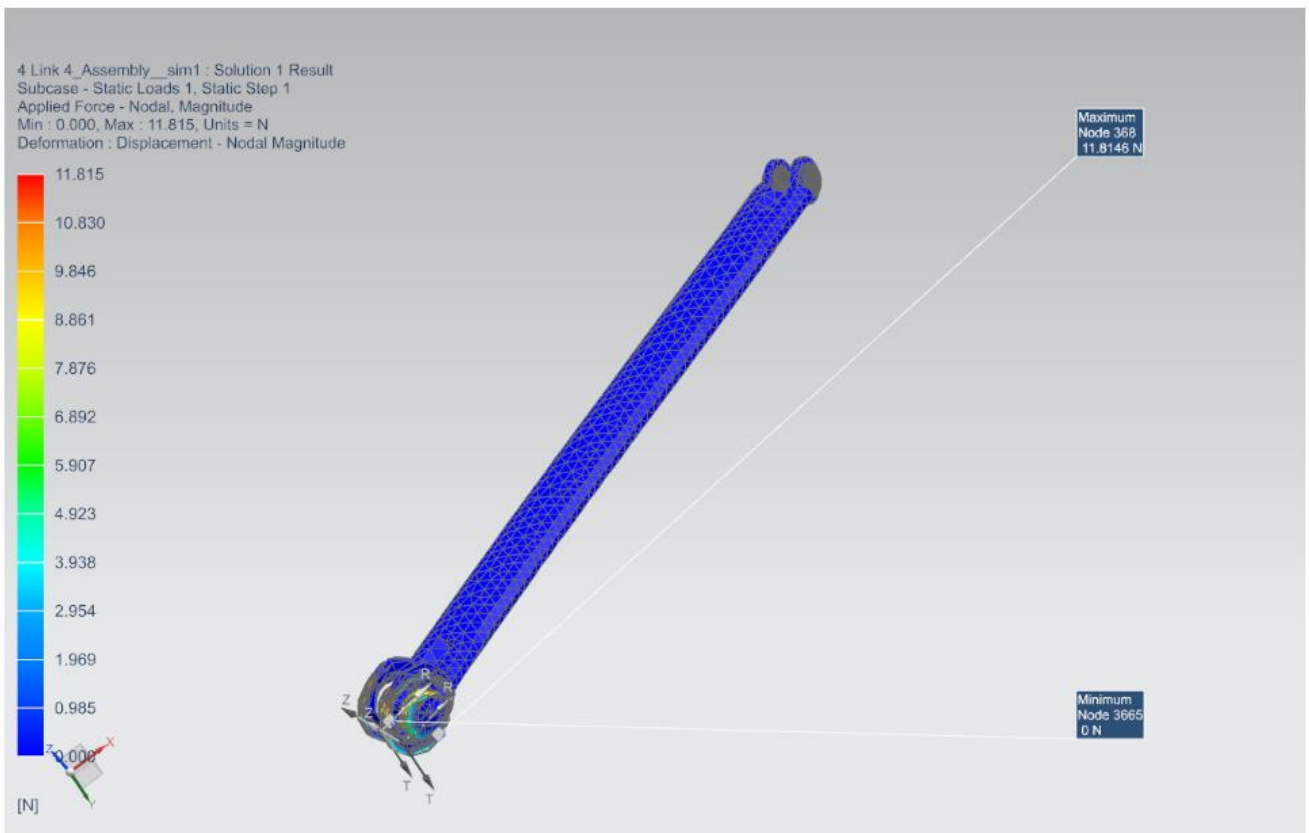
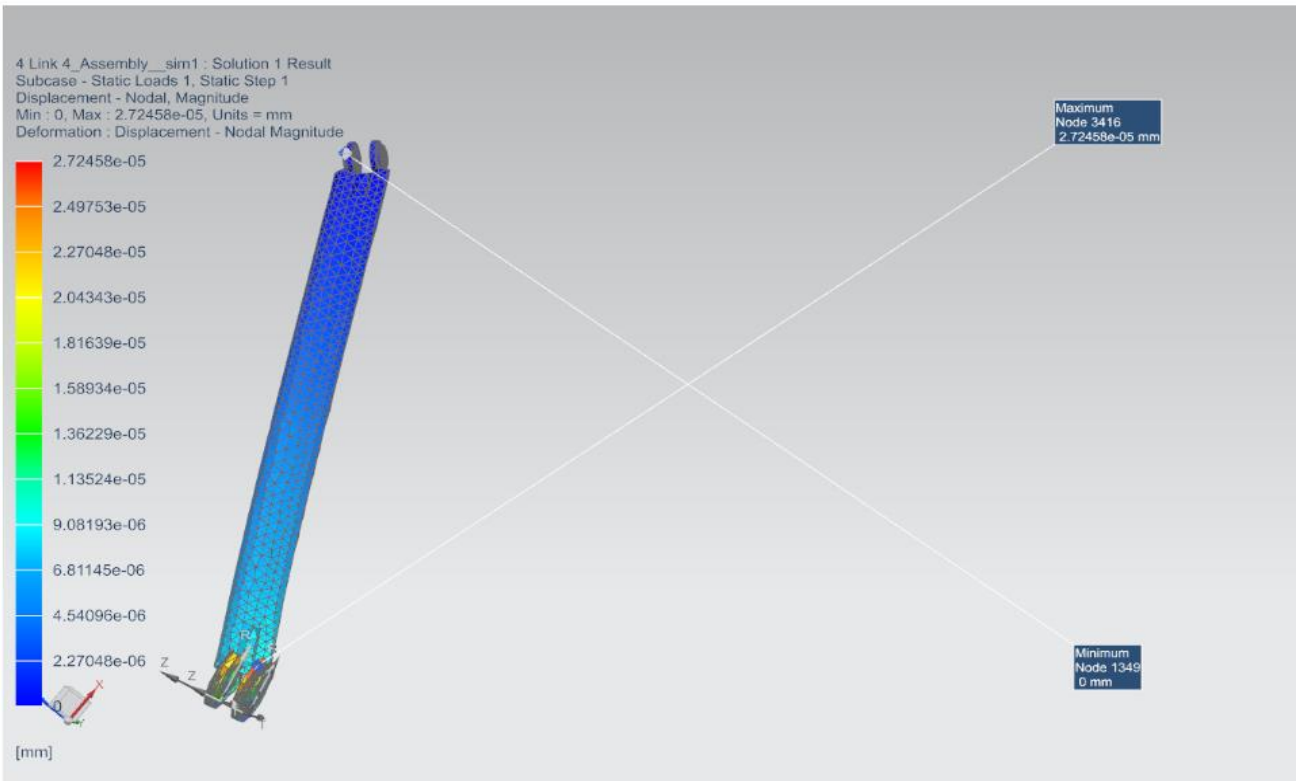
Pinned constraint in the T2 and fixed in the P2. Buchings and bearings are glued to Bend link.

1.7 Model Results

Solver Name and version NX Nastran Design Linear Statics.

Maximum displacement $2.7 \cdot 10^{-5} \text{ mm}$. Maximum stress 0.243 MPa.





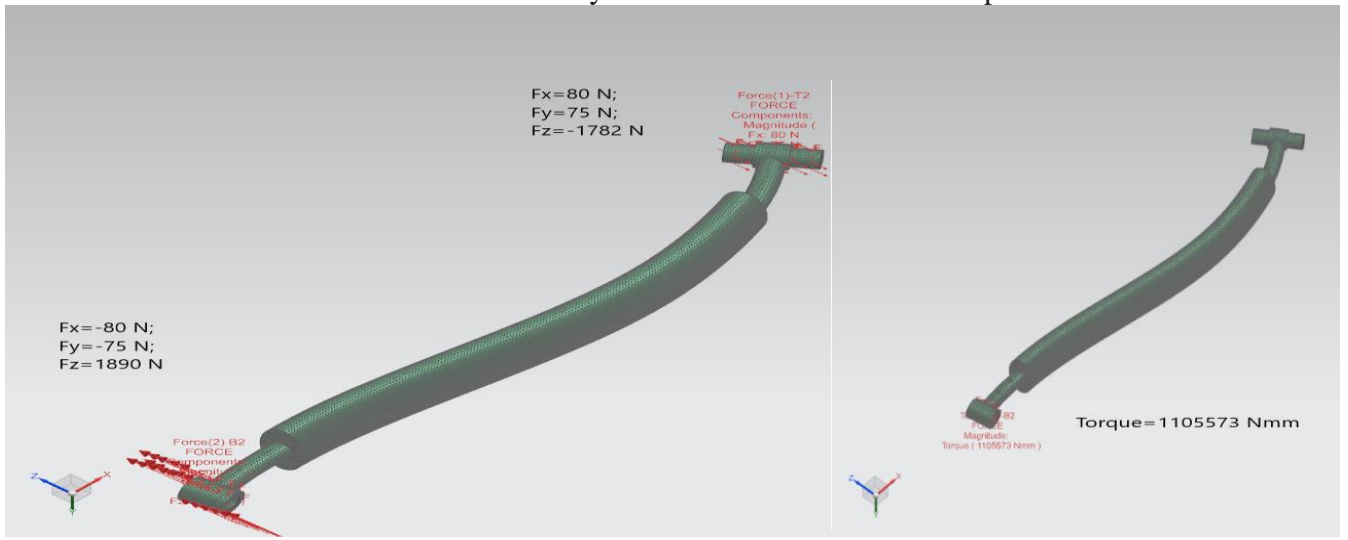
E.5. Link 5 Assembly FEM

| | | | |
|---|-------------------------------|----------------------|------------|
| Discipline or report series | Document number Appendix 5 | Report number E.5 | Issue 0 |
| Title Tallinn University of Technology, Master Thesis Appendix 5: E.5: Link 5 Assembly FEM Analysis | | | |
| Author(s) Jaanus Urb, 183767MATM | Telephone: | Date 27.12.2020 | |

Summary

Assembly is the driving link to the platform to position the Link 4 and Top plate according to the elevation.

Link 5 assembly stress and displacement analysis with external load 275 kg. The external load is taken from the UAV helicopter mass multiplied with 1.5 (safety factor for emergency landing). The reaction forces for joints are calculated with NX motion analysis and the the initial loading on time 0 s will be considered as the heaving will be downward as the gravity and the z component for the reaction force are then maximum. The reaction forces components will differ on time, but in the initial state it is maximum. The conclusion of the motion analysis will be covered in the Chapter 4. Joint are T2 and B2.



| | |
|---------------------|----------|
| Additional keywords | Category |
|---------------------|----------|

Circulation:

Approved
by:

| | | | |
|-------------------------------|------------|--|-------------|
| Document number Appendix 5 | Issue 0 | | Page 1 of 5 |
|-------------------------------|------------|--|-------------|



| Project | Sub-system | Process | Part number |
|---|------------|---------|-------------|
| 2 DOF SPM FOR PVL- | Y-Branch | | |
| Material 5 Link 5 Bend and SHAFT - ALUMINIUM 6082 or 6062 | | | File/folder |

TABLE OF CONTENTS

1 INTRODUCTION3

1.1 HEADER3

1.2 MODEL CONSTRUCTION3

1.3 MODEL SUMMARY:.....3

1.4 MESHES.....3

1.5 MATERIALS.....4

1.6 CONSTRAINTS4

1.7 MODEL RESULTS4

1 INTRODUCTION

1.1 Header

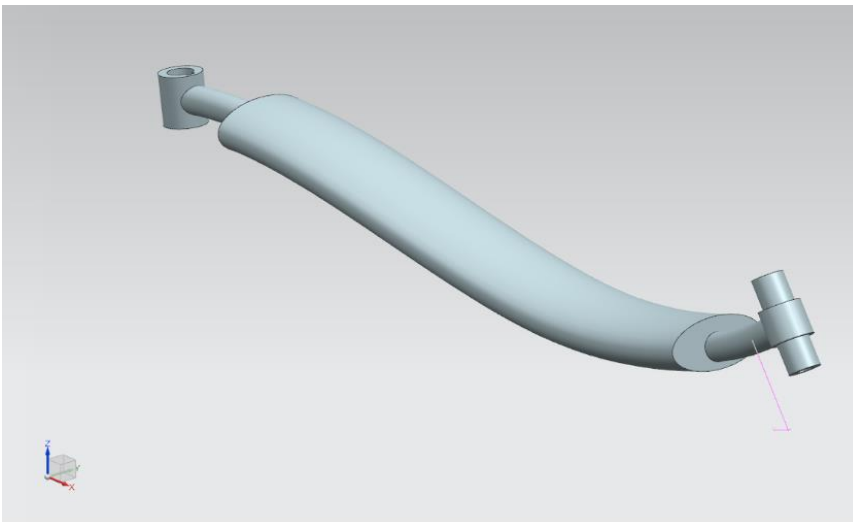
Critical part to move the Y-Branch of the manipulator as a driving link that takes the motor torque and transfers it to the Top Plate.

1.2 Model Construction

The version of Product used to create this model was [NX 12](#).

5 Link 5_Assembly.prt

1.3 Model Summary:



Weight data was calculated

Density = 0.000002711 kg/mm³
 Area = 210707.694061730 mm²
 Volume = 2708215.017310600 mm³
 Mass = 7.341970912 kg

1.4 Meshes

| | |
|---------------|---------------|
| Node Count | 193984 |
| Element Count | 126123 |

Element type PSOLID

Element Size : 4 mm

| | | | |
|--------------------------------------|------------|--|-------------|
| Document number Appendix 5 | Issue 0 | | Page 3 of 5 |
|--------------------------------------|------------|--|-------------|

1.5 Materials

Aluminum_6061

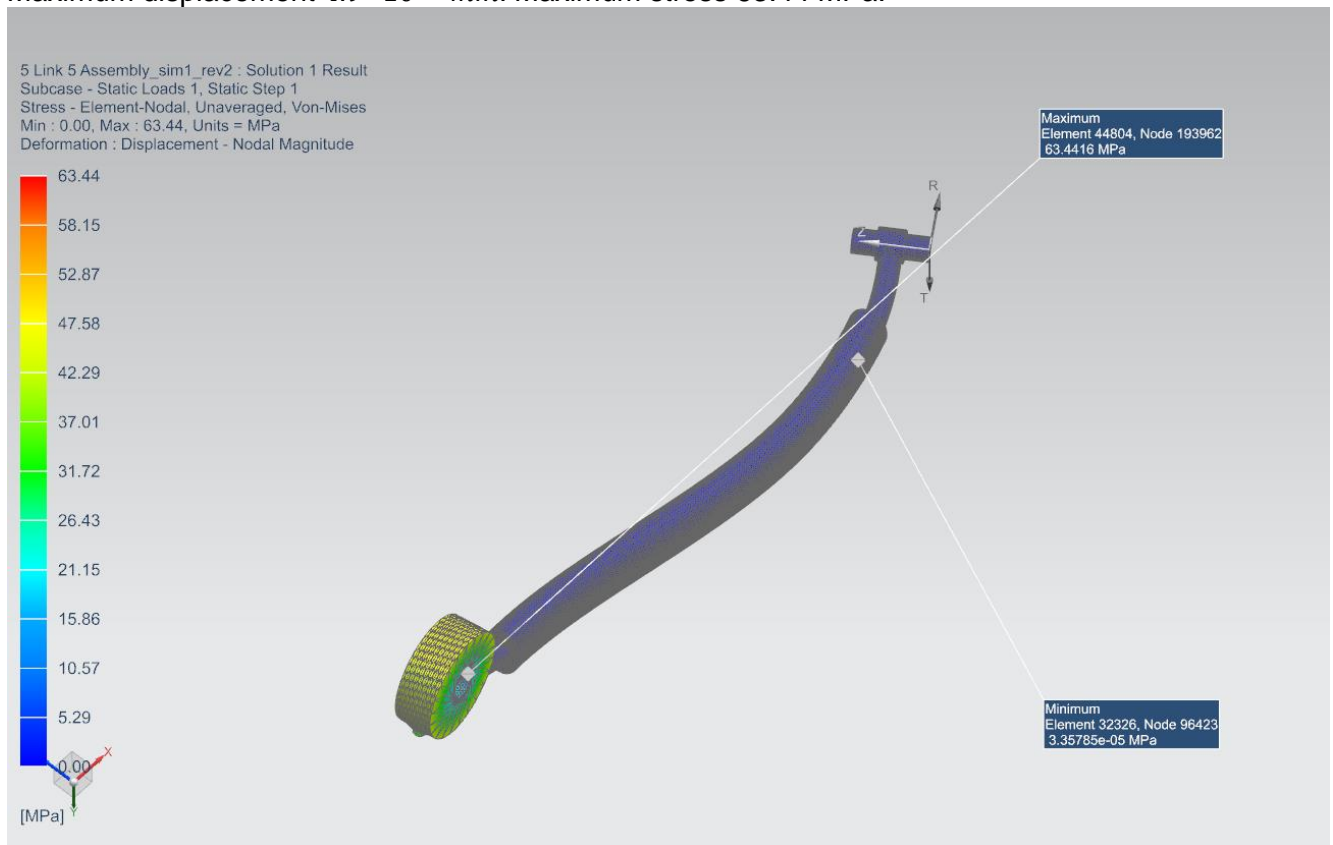
1.6 Constraints

Pinned constraint in the T2 and fixed in the B2.

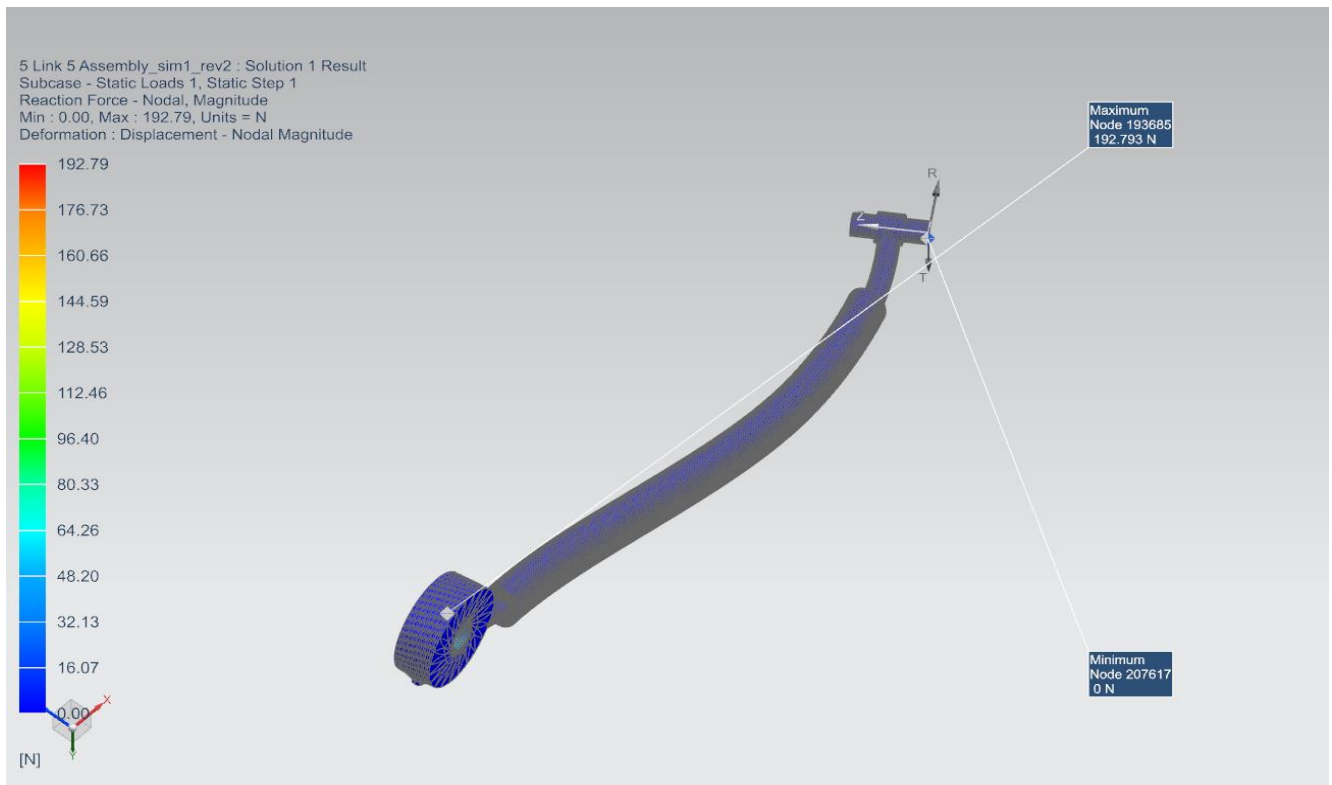
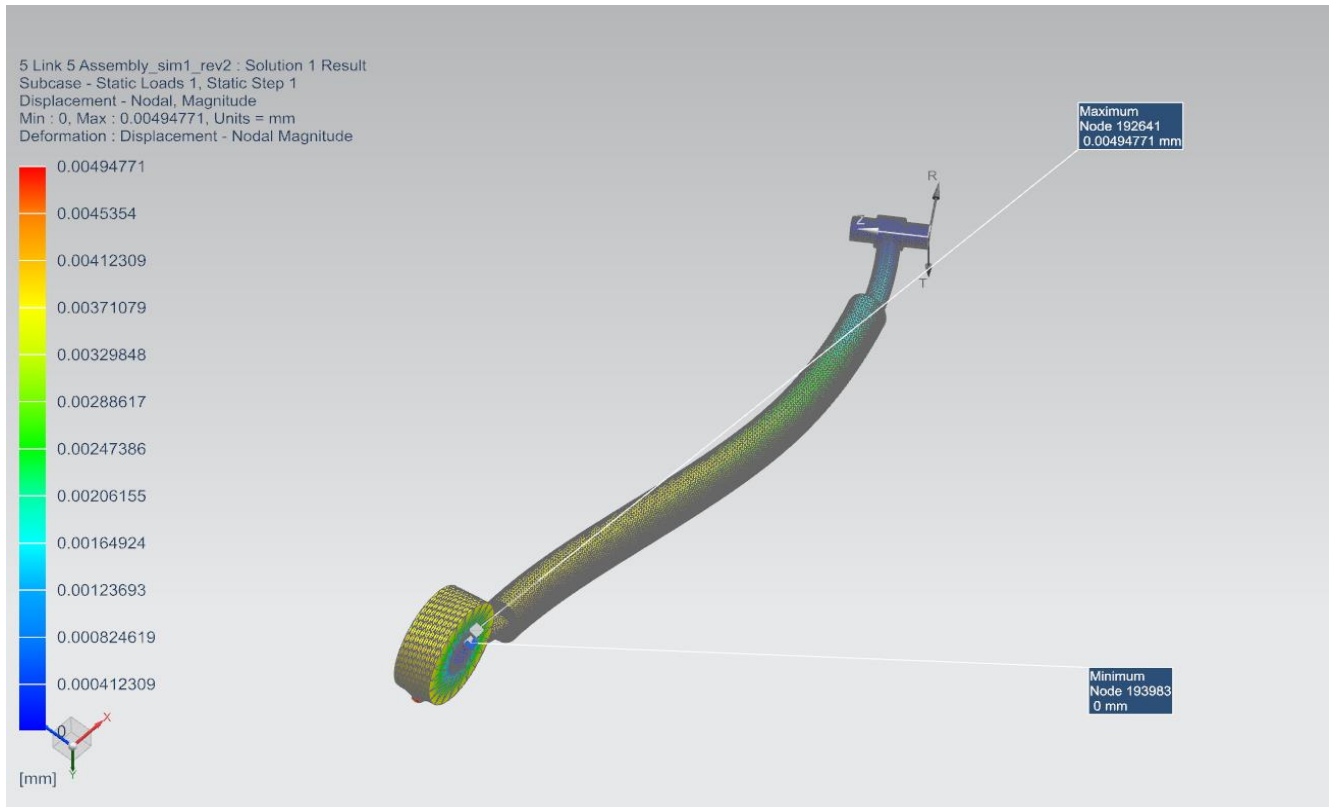
1.7 Model Results

Solver Name and version NX Nastran Design Linear Statics – Single Constraint.

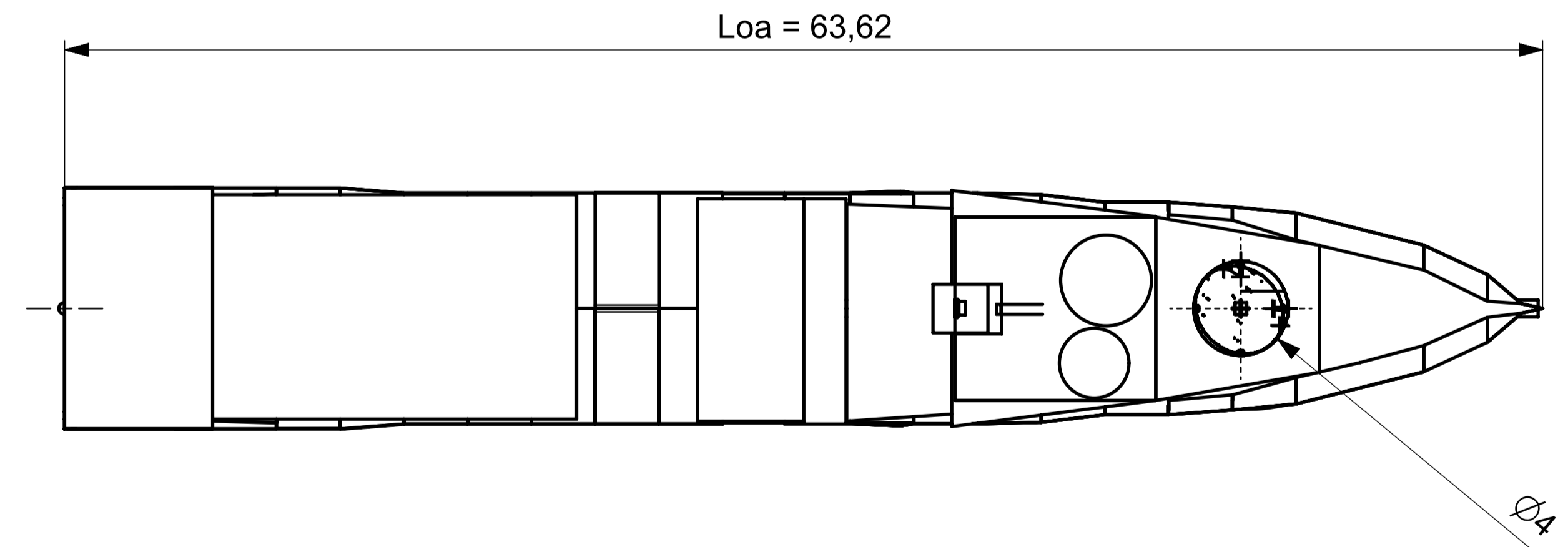
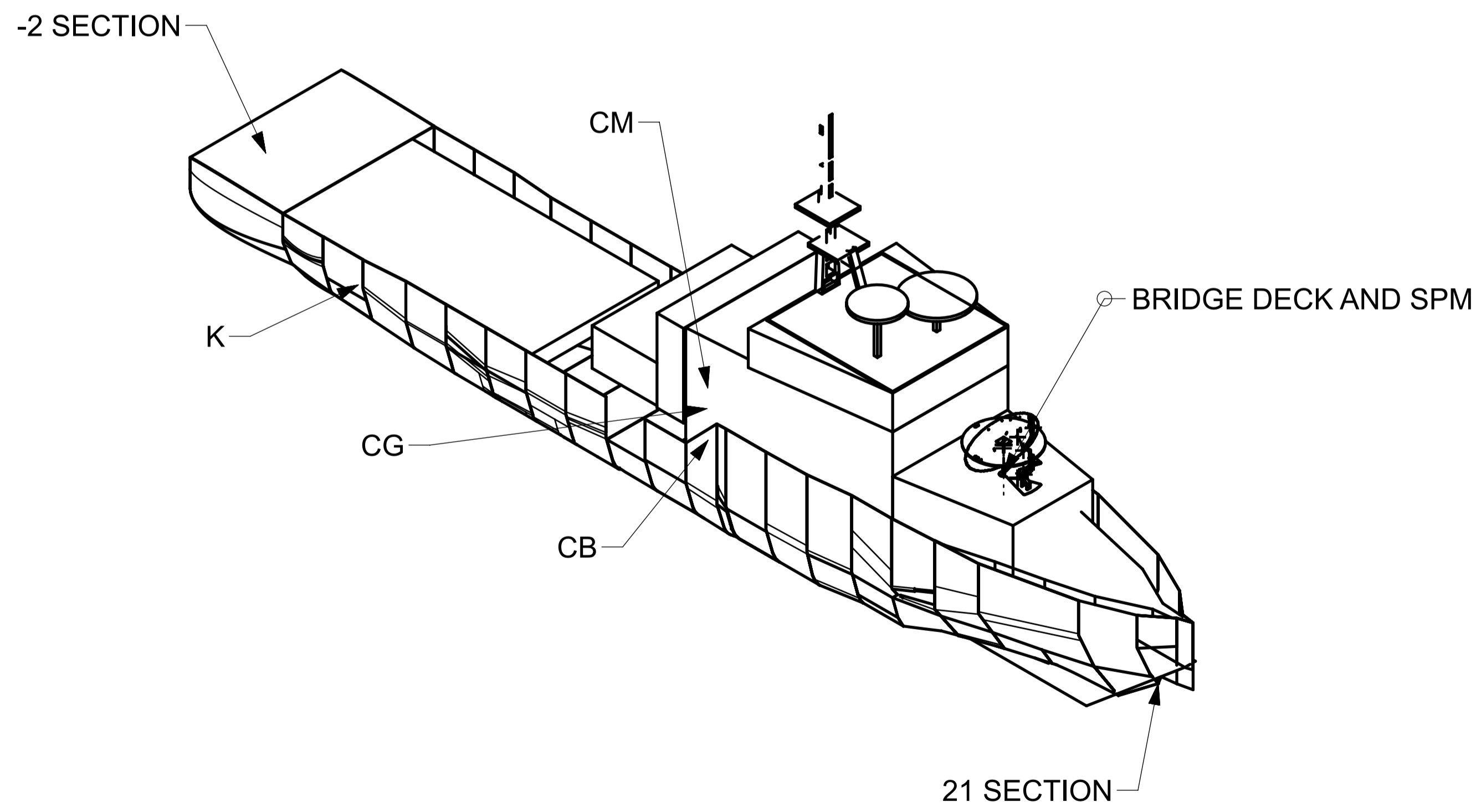
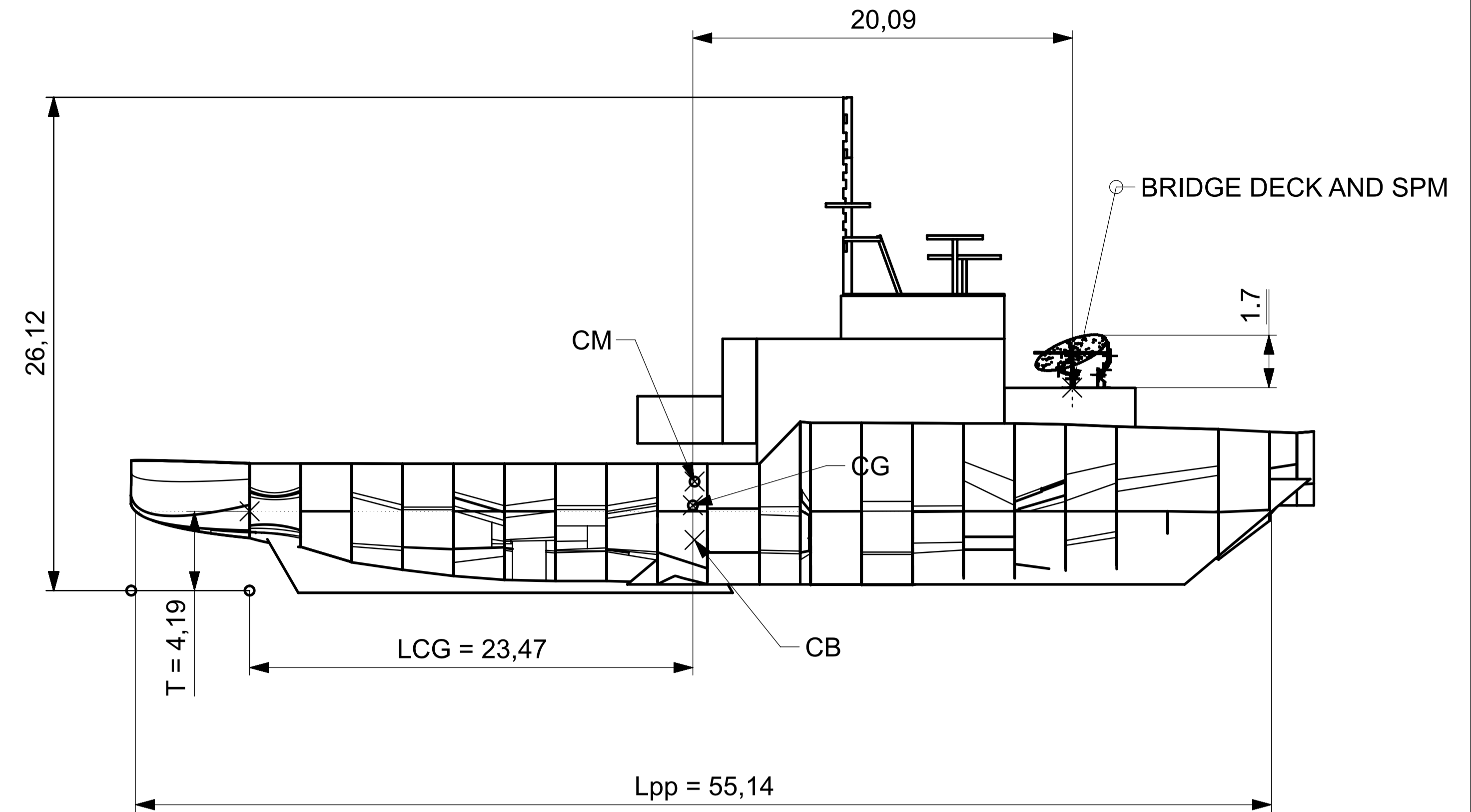
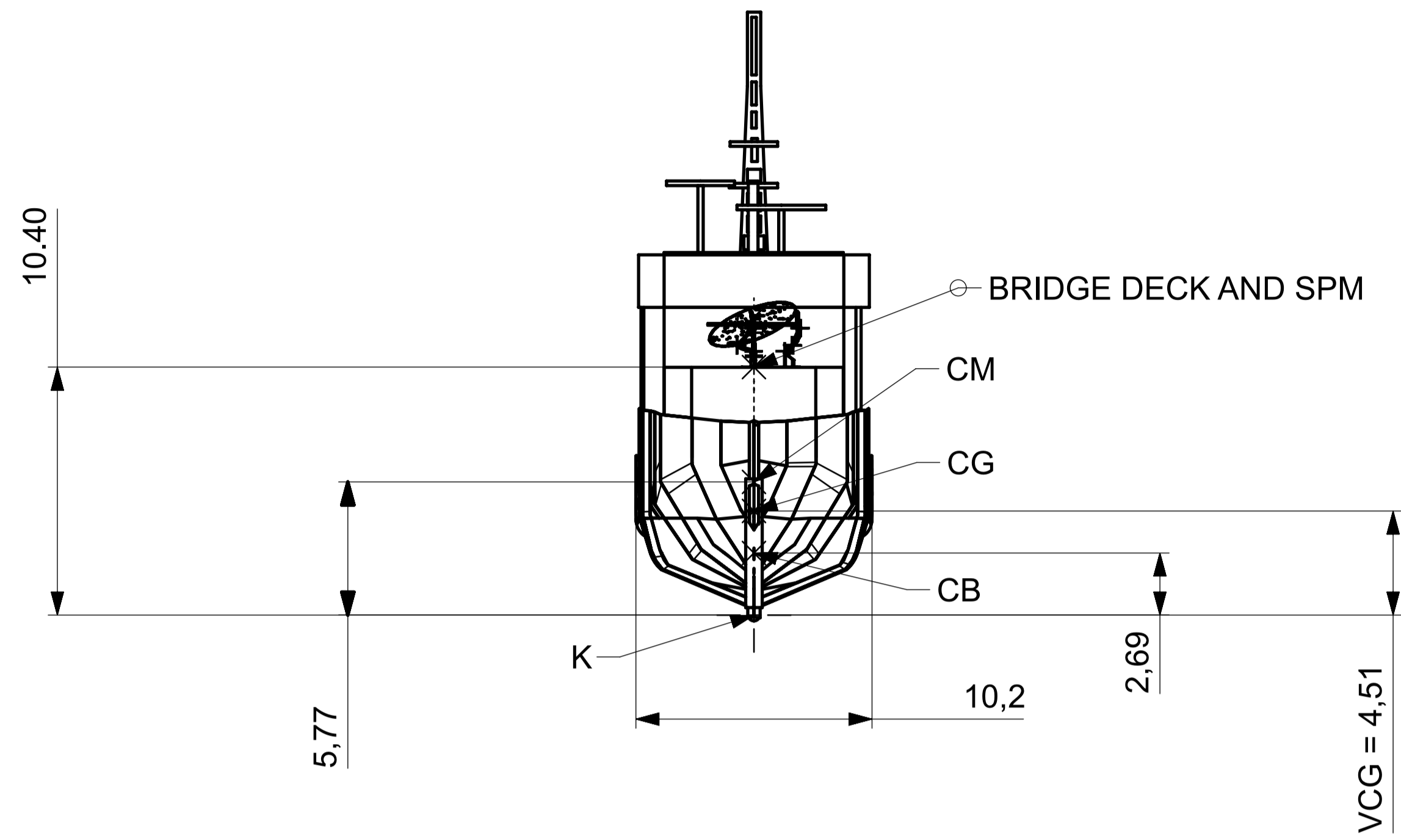
Maximum displacement $4.9 \cdot 10^{-3} \text{ mm}$. Maximum stress 63.44 MPa.



| | | | |
|-------------------------------|------------|--|-------------|
| Document number Appendix 5 | Issue 0 | | Page 4 of 5 |
|-------------------------------|------------|--|-------------|



F. Appendix 6: Preliminary- project drawings

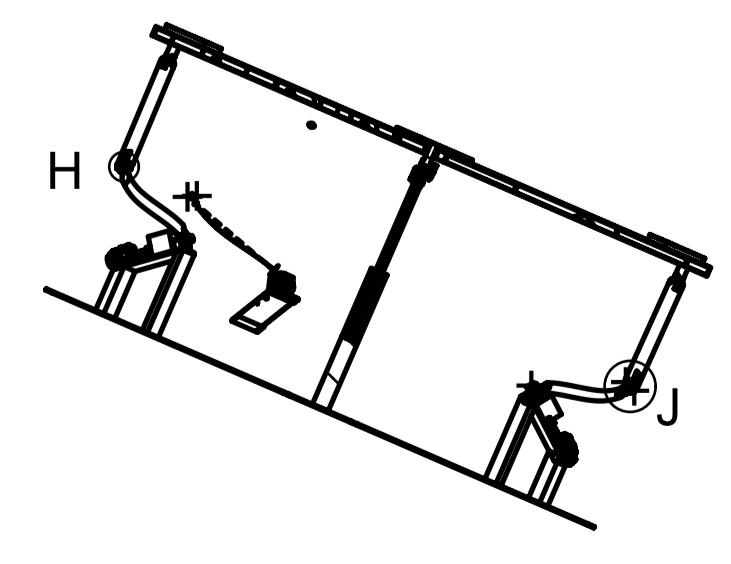
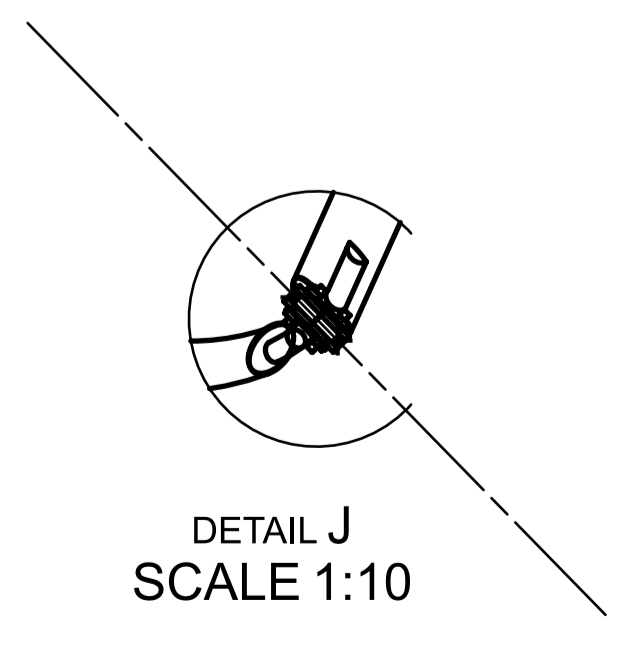
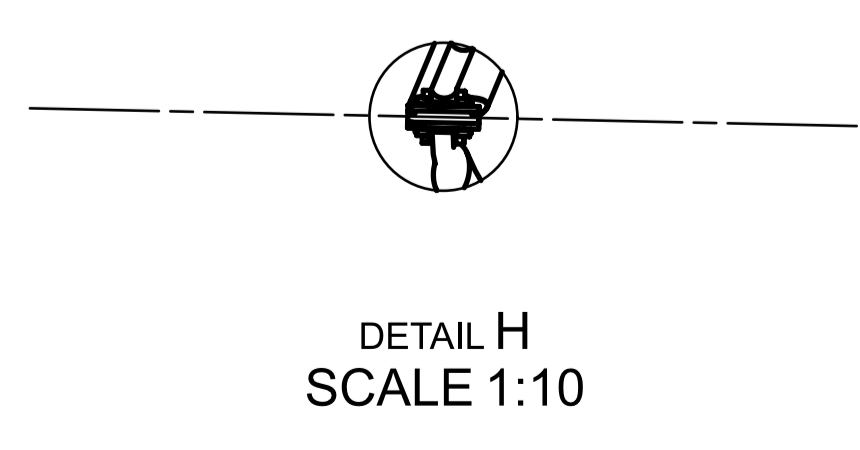
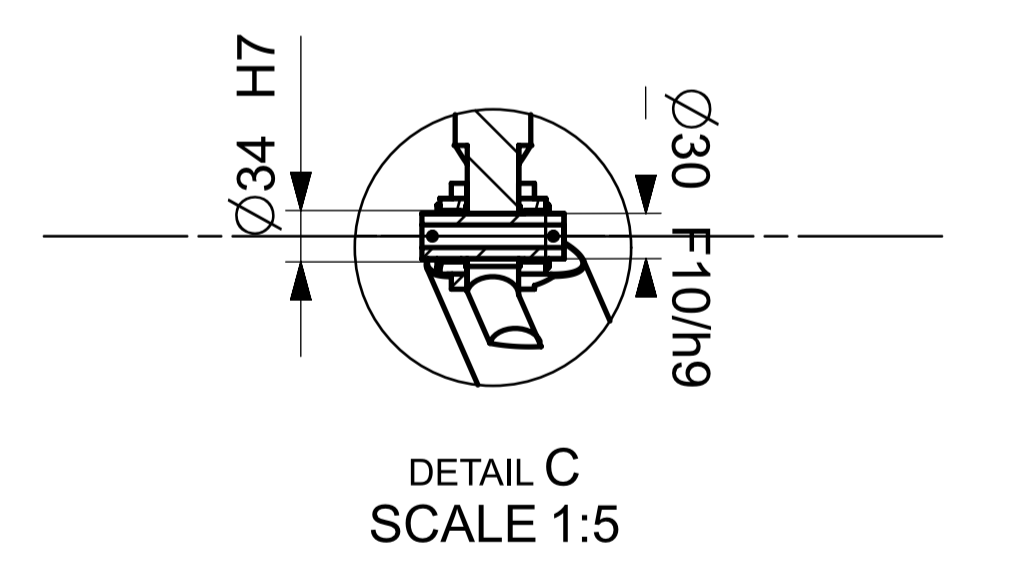
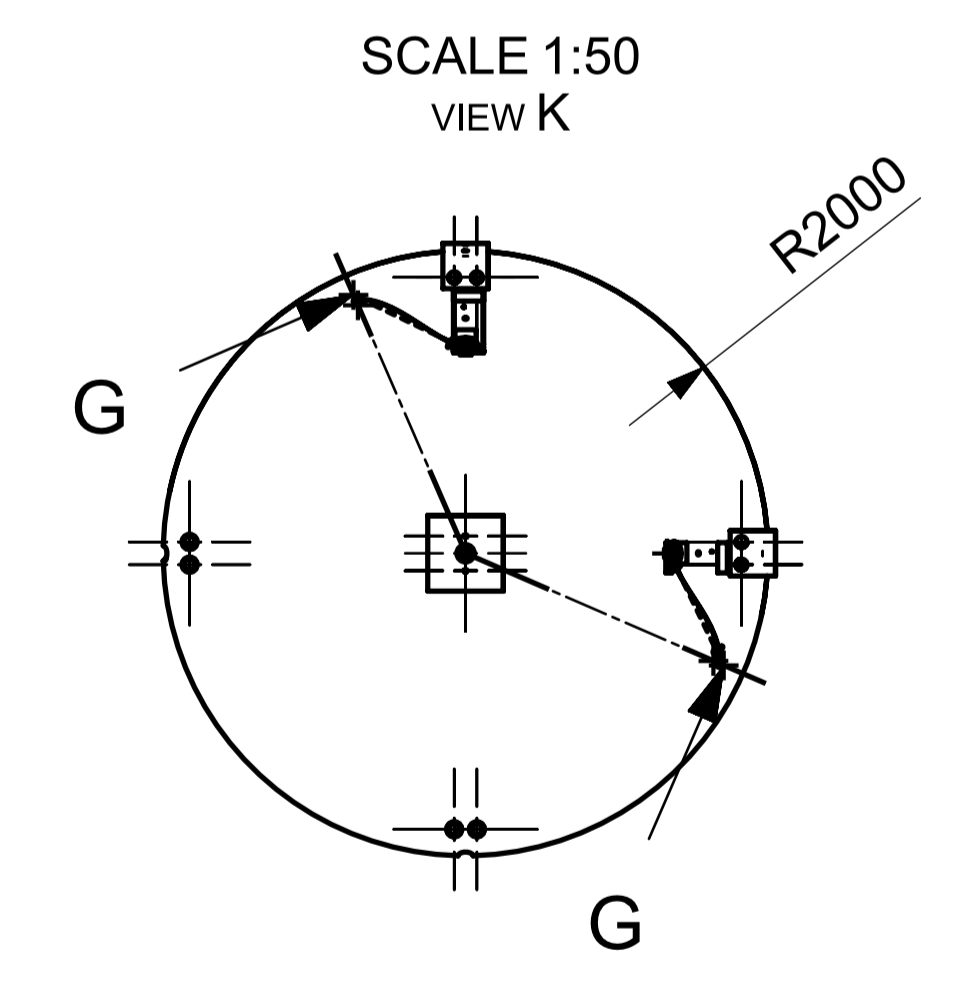
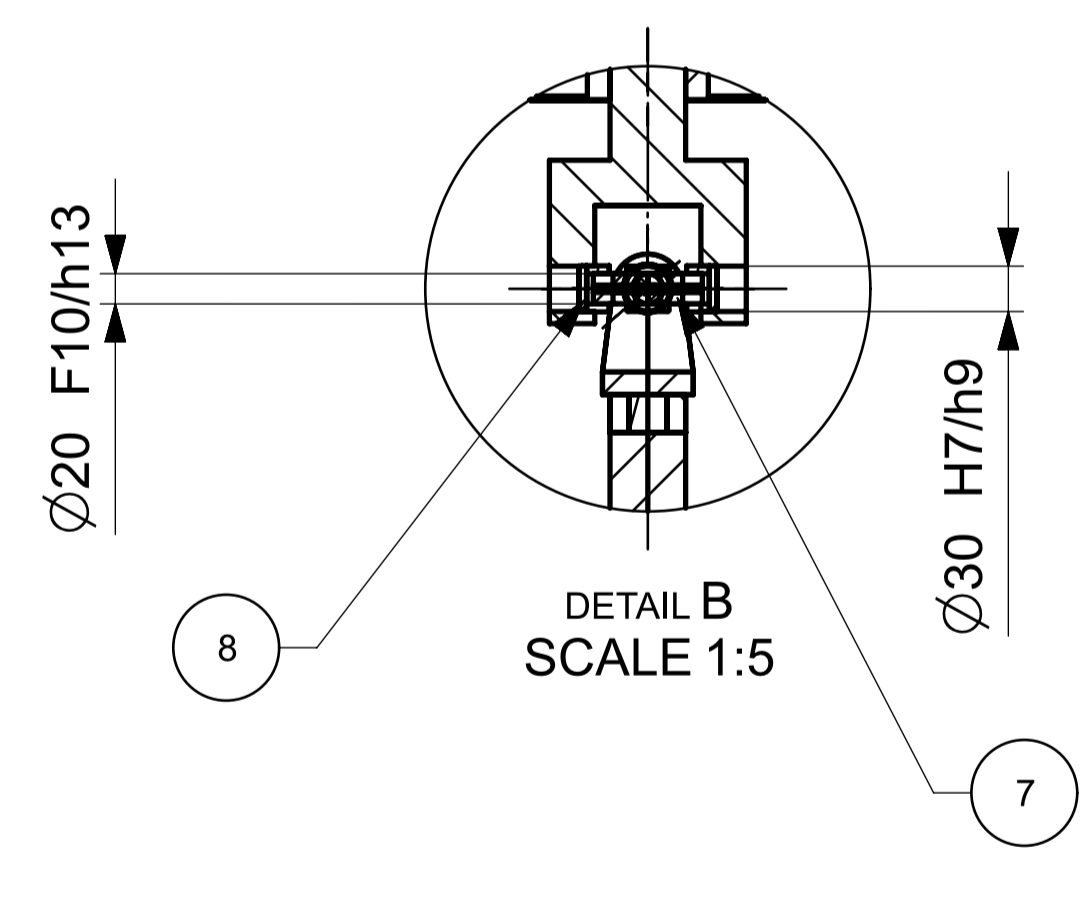
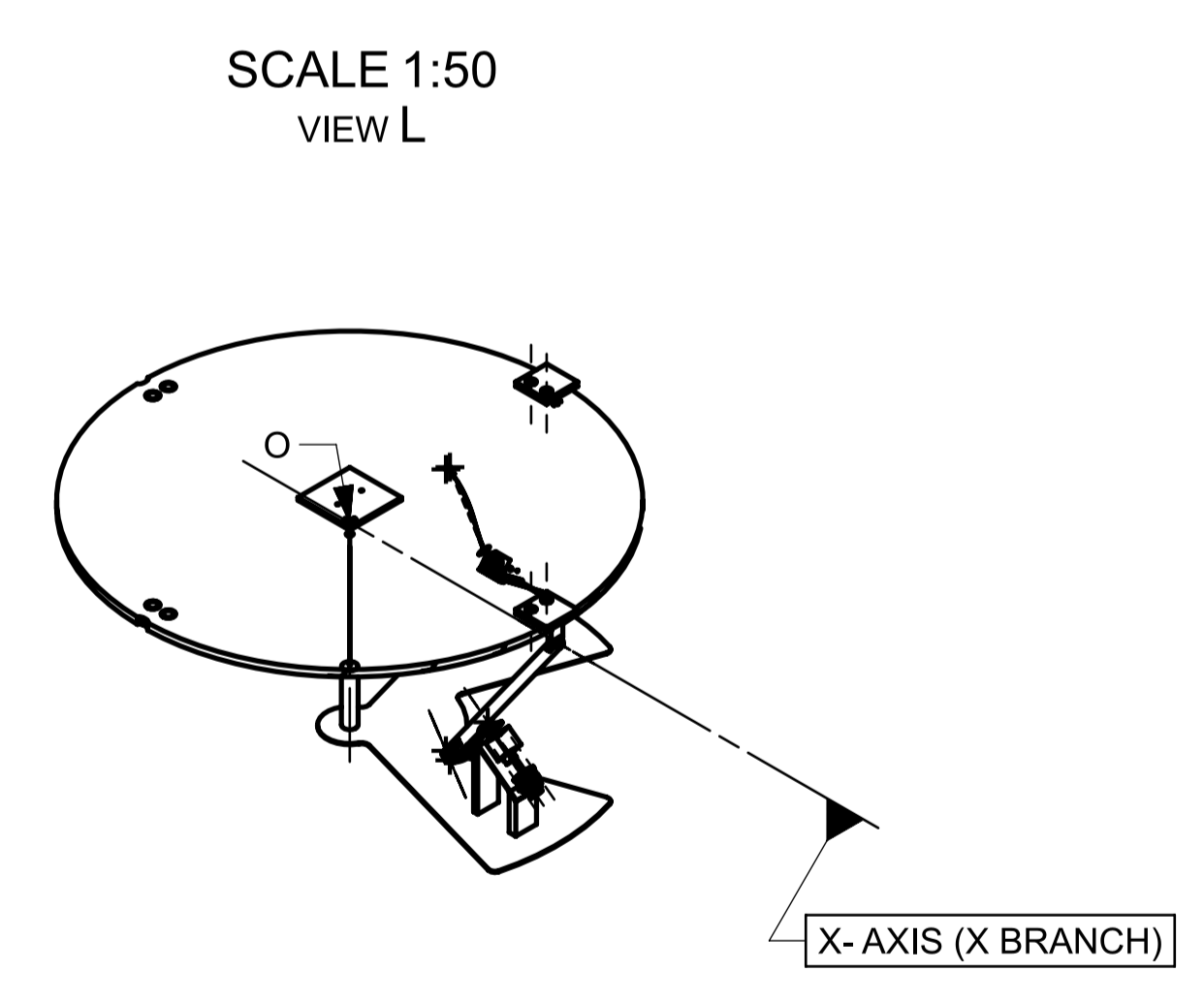
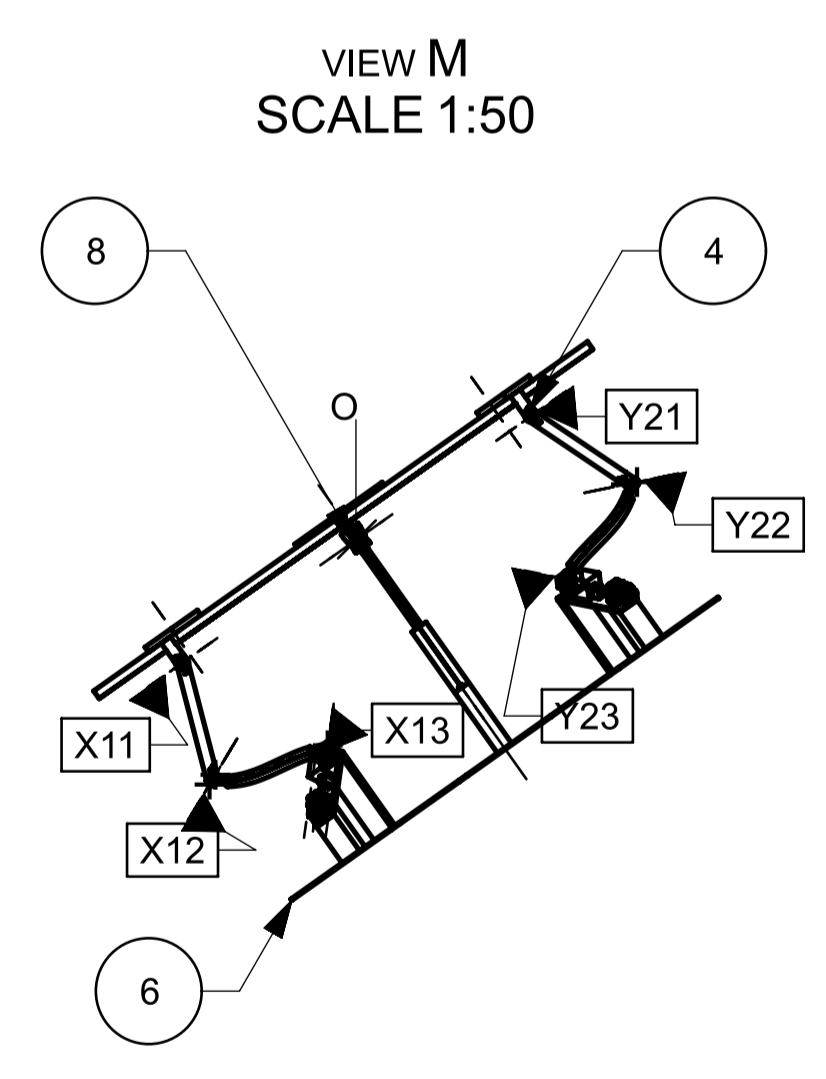
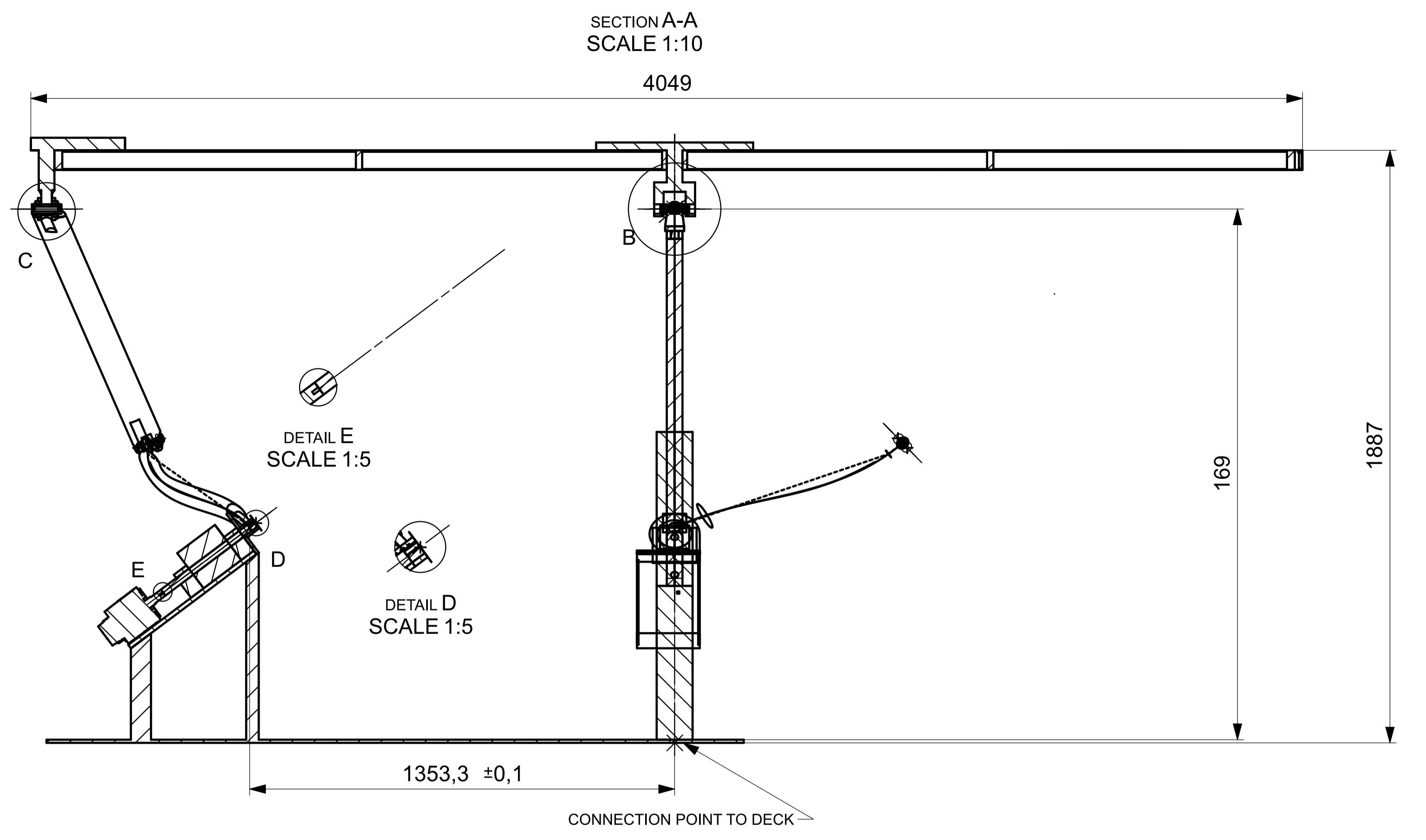
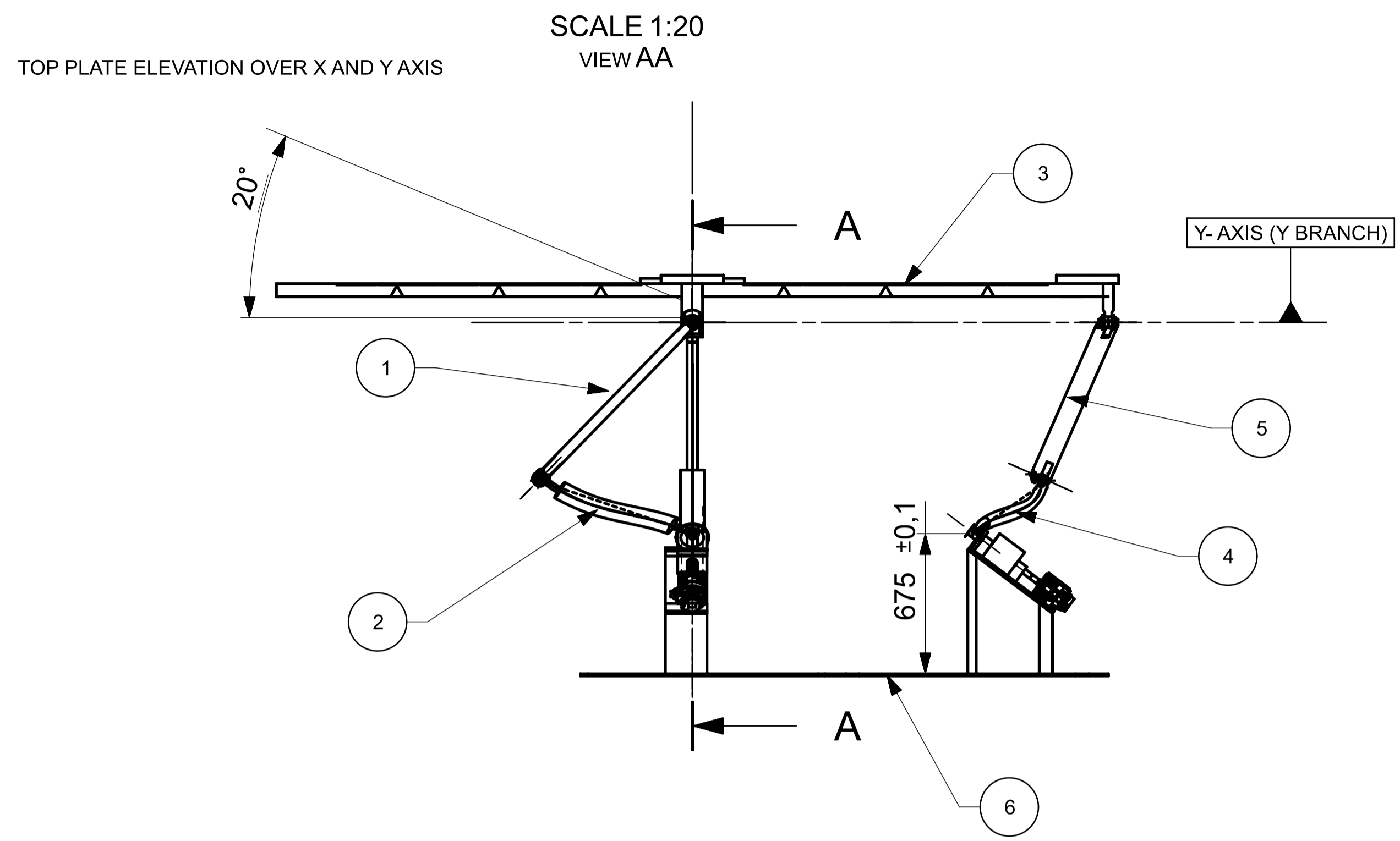


| | |
|-----|---------------------------------|
| CM | METACENTER |
| CG | CENTER OF GRAVITY |
| CB | CENTR OF BUOYANCY |
| K | KEEL |
| SPM | SPHEARICAL PARALLEL MANIPULATOR |

| | | | | | |
|----------------------------------|-------------------|------------|--|---------------------|--------|
| EM70LT - APPENDIX 6 | Material: | | Tolerance: | Mass: | Scale: |
| | N/A | | DIMENSIONS IN METER | N/A | 1:200 |
| F.0 | Name | Date | TITLE: GENERAL LAYOUT OF THE PVL-101 SPM ASSEMBLY LOCATION | | |
| DRAWN | JAAANUS URB | 30.12.2020 | | | |
| APPROV | ANDRES PERITŠENKO | 4.01.2021 | | | |
| TALLINN UNIVERSITY OF TECHNOLOGY | | | SHEET 1:2 | DWG NR: GL-SPM-0000 | |

F.1. SPERICAL PARALLEL MANIPULATOR ASSEMBLY DWG NR-SPM0000

Master Assembly.

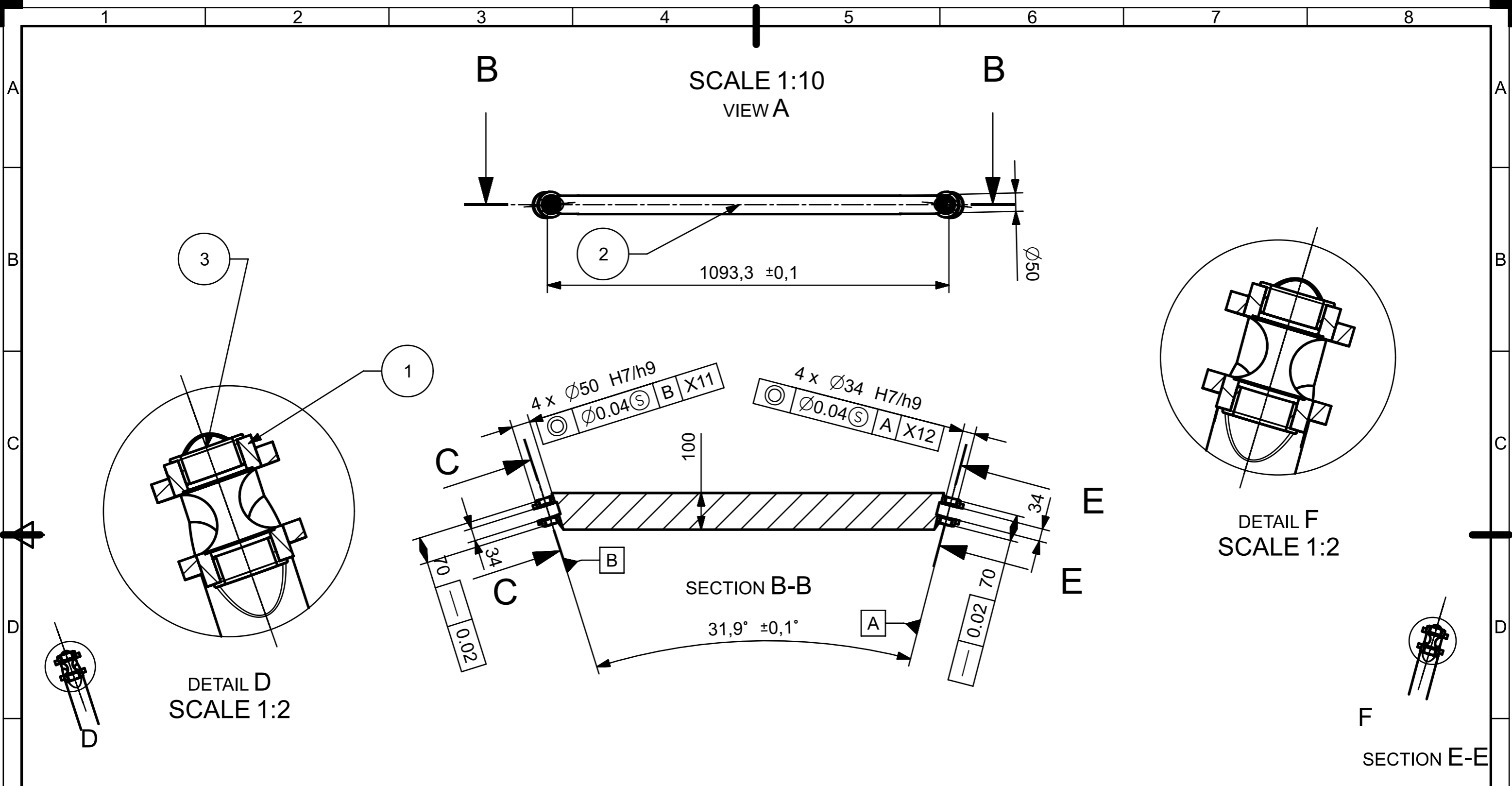


| | | | | | |
|-------|------------------------|-----|---------|--------------|--------------|
| 8 | UJ BEARING CUP | 4 | | | |
| 7 | UJ BEARING CROSS | 1 | N/A | β31D | MOOD |
| 6 | 6 BASE PLATE ASSEMBLY | 1 | SPM600D | N/A | N/A |
| 5 | 5 LINK 5 ASSEMBLY | 1 | SPM100D | N/A | N/A |
| 4 | 4 LINK 4 ASSEMBLY | 1 | SPM200D | N/A | N/A |
| 3 | 3 TOP PLATE 3 ASSEMBLY | 1 | SPM300D | N/A | N/A |
| 2 | 2 LINK 2 ASSEMBLY | 1 | SPM200D | N/A | N/A |
| 1 | 1 LINK 1 ASSEMBLY | 1 | SPM100D | N/A | N/A |
| PC NO | PART NAME | QTY | DWG NR | STANDARD P/N | MANUFACTURER |

| | | | | | | | | |
|----------------------------------|-------------------|---------------------|------------|---------------------------------|---|------------------|--------|--|
| EM70LT - APPENDIX 6 | Material: | | Tolerance: | | Mass: | | Scale: | |
| | | AA6082-T651 OR 5083 | | ISO 286-2F; ISO 19901-3; CAP437 | 750 | | 1:20 | |
| F.1 | Name | | Date | | TITLE: SHERICAL PARALLEL MANIPULATOR ASSEMBLY | | | |
| DRAWN | JAAANUS URB | | 30.12.2020 | | | | | |
| APPROV | ANDRES PERITŠENKO | | 4.01.2021 | | | | | |
| TALLINN UNIVERSITY OF TECHNOLOGY | | | | | SHEET 1:1 | DWG NR: SPM-0000 | | |

F.2. LINK 1 ASSEMBLY & LINK 5 ASSEMBLY DWG NR-SPM1000

Moving Links. sleeve bearings, bushings.

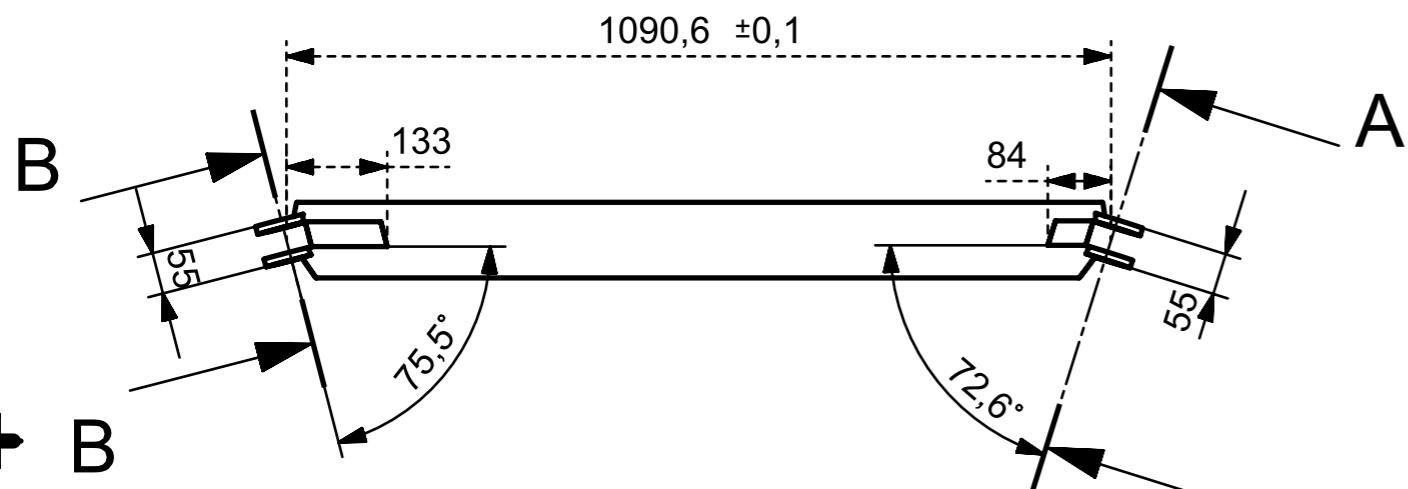
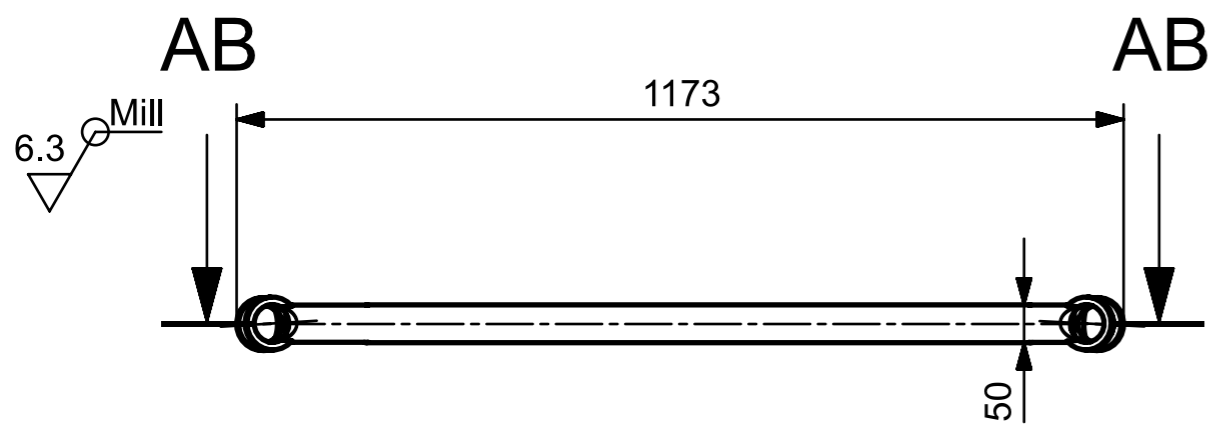


| PC NO | PART NAME | QTY | STANDARD P/N OR DWG NR | Manufacturer |
|-------|-------------------------------------|-----|------------------------|--------------|
| 3 | SLEEVE BEARING_XSM-3034_D1_30_B2-34 | 4 | XFM-3034-1d | IGUS |
| 2 | BEND LINK | 1 | SPM110d | N/A |
| 1 | BUSHING_LINK 1_MIDDLE | 4 | SPM120d | N/A |

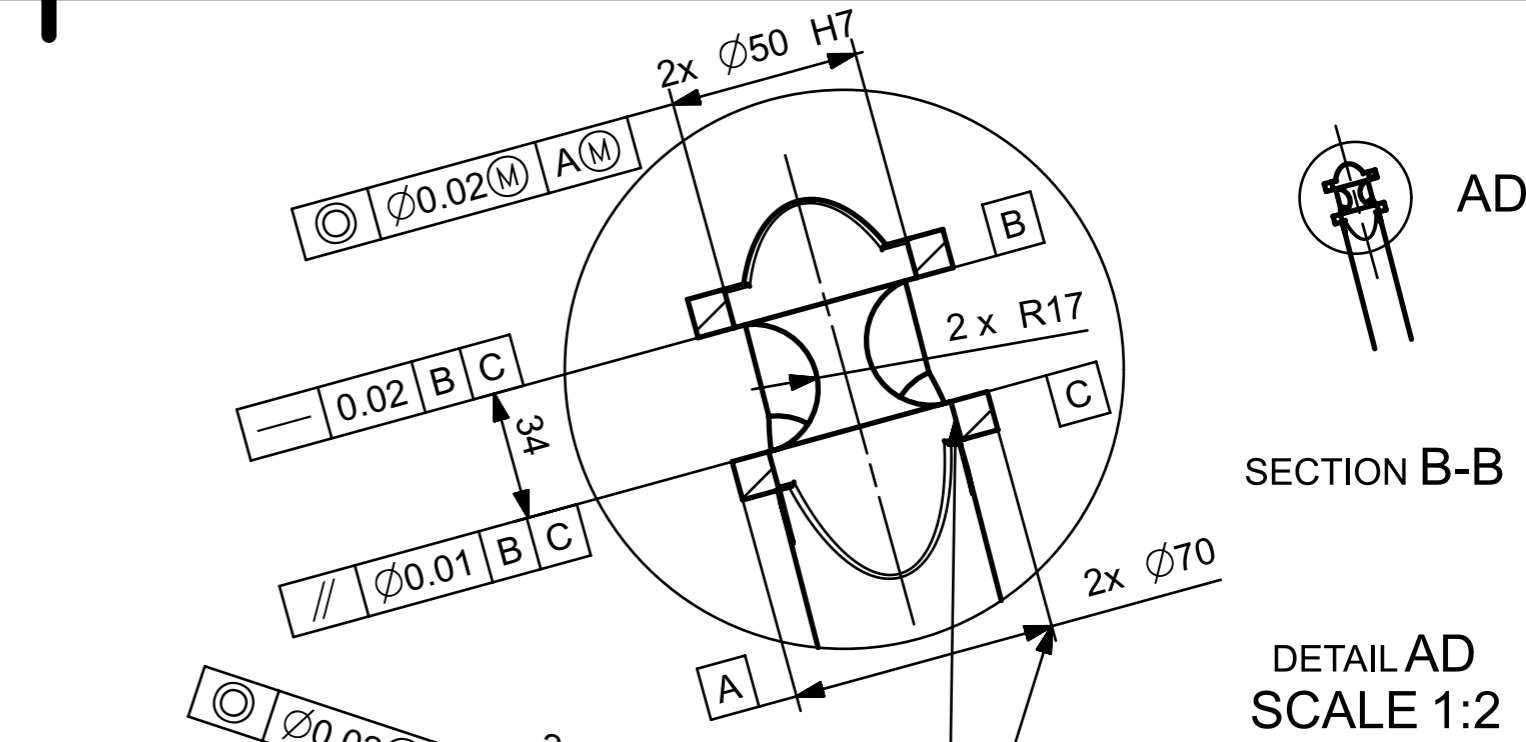
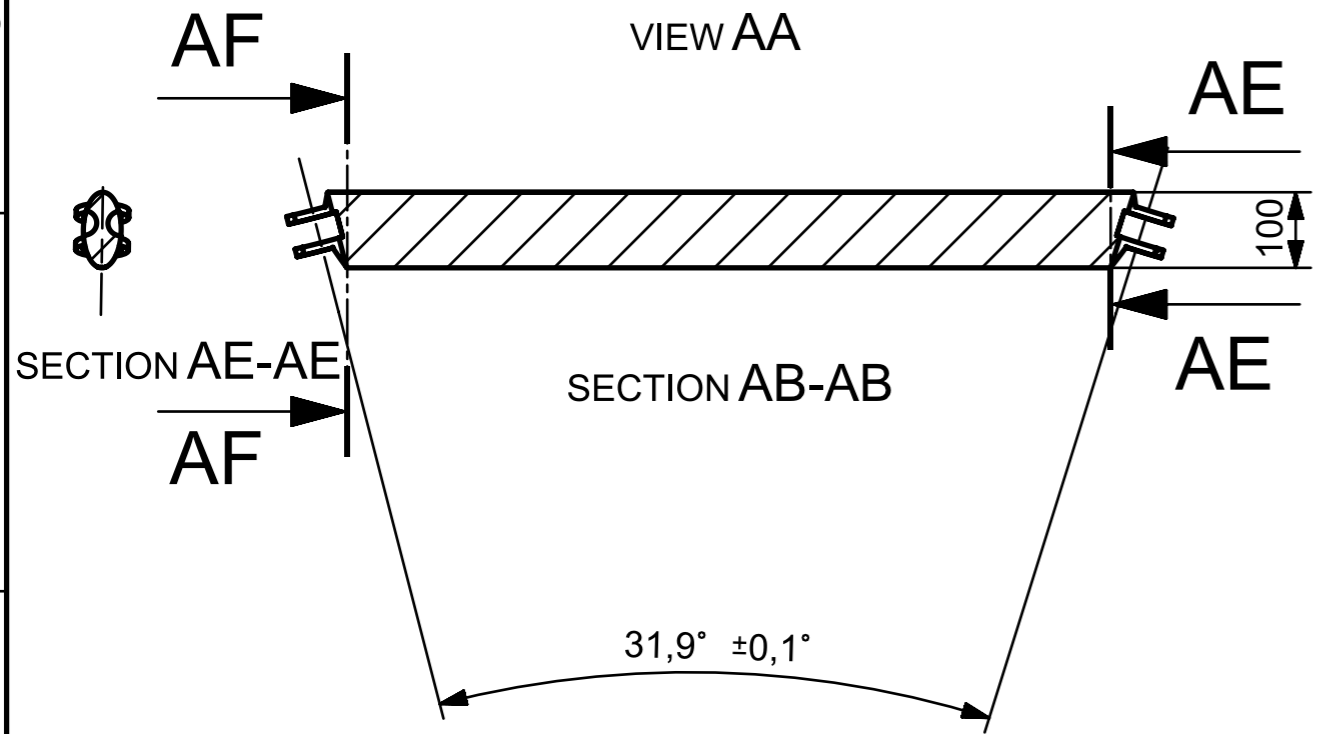
| | | | | | |
|---|-----------------------------|------------|--|---------|--------|
| EM70LT - APPENDIX 6 | Material: | | Tolerance: | Mass: | Scale: |
| F.2 | ALYMINIUM ALLOY AA6082-T651 | | ISO 286; ISO 19901-3; ISO 3547-1 | 11.2 KG | 1:10 |
| DRAWN | Name | Date | TITLE: LINK 1 ASSEMBLY & LINK 5 ASSEMBLY | | |
| APPROV | JAANUS URB | 30.12.2020 | | | |
| | | | SHEET 1:1 | | |
| | | | DWG NR: SPM1000 | | |
| TALLINN UNIVERSITY OF TECHNOLOGY | | | | | |

F.3. BEND LINK DWG NR-SPM1100

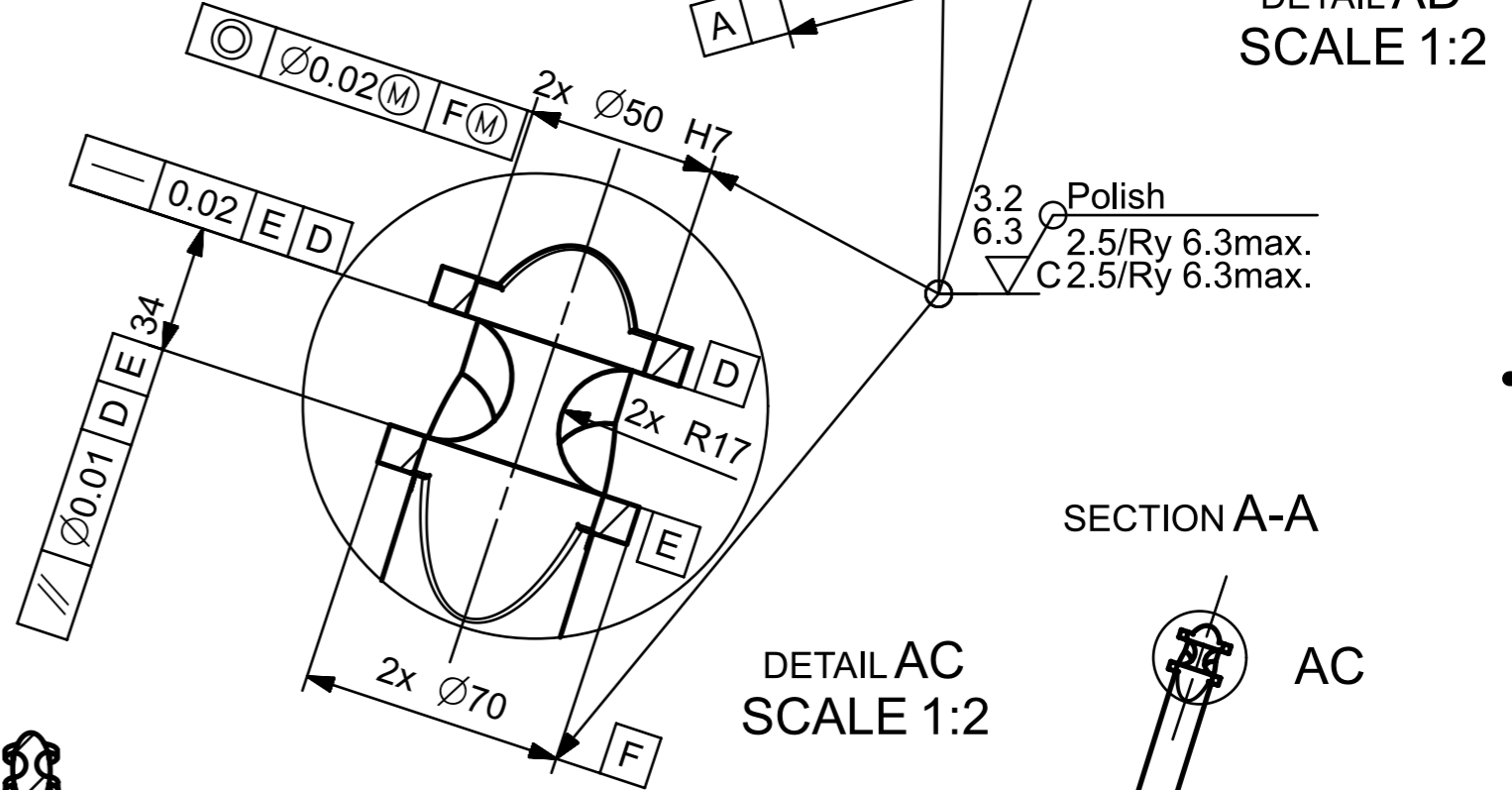
Driven Links.



SCALE 1:10
VIEW AA



SECTION B-B
DETAIL AD
SCALE 1:2



SECTION A-A
DETAIL AC
SCALE 1:2

SECTION AF-AF

| | | | | | |
|----------------------------------|-------------------------------------|------------|----------------------------------|---------|--------|
| EM70LT - APPENDIX 6 | Material: | | Tolerance: | Mass: | Scale: |
| | ALYMINIUM ALLOY AA6082-T651 OR 5083 | | ISO 286; ISO 19901-3; ISO 3547-1 | 11.2 KG | 1:10 |
| F.3 | Name | Date | TITLE: BEND LINK | | |
| DRAWN | JAANUS URB | 30.12.2020 | | | |
| APPROV | ANDRES PERITŠENKO | 4.01.2021 | SHEET 1:1 DWG NR: SPM1100 | | |
| TALLINN UNIVERSITY OF TECHNOLOGY | | | | | |

F.4. MIDDLE BUSHING DWG SPM1200

Details.

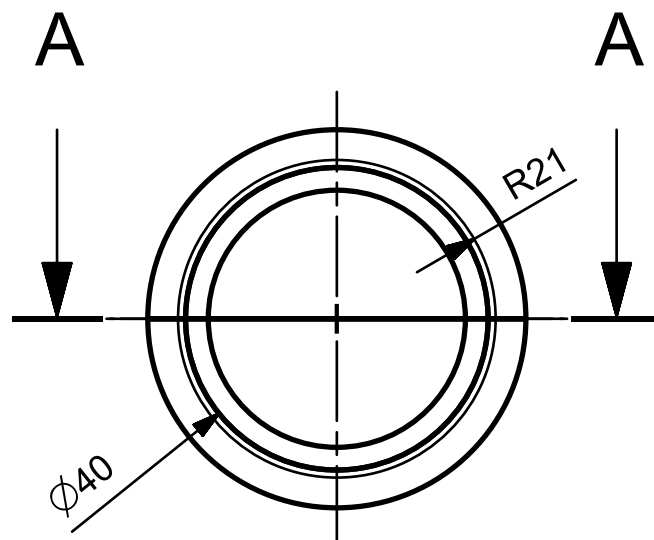
1

2

3

4

75 HB



3.2 Polish
 6.3 2.5/Ry 6.3max.
 5,9 - 6,1 C 2.5/Ry 6.3max.

$\phi 50 \pm 0,1$

\textcircled{C} $\phi 0.02 \textcircled{M}$ $A \textcircled{M}$

$\phi 1$

$\phi 18$

$\phi 34 \text{ H7}$

A

SECTION A-A

| | | | | |
|----------------------------------|-------------------|---------------------|-----------------------|-----------------|
| EM70LT - APPENDIX 6 | MATERIAL | TOLERANCE | MASS | SCALE |
| | AA6082-T651 | ISO 286; ISO 3547-1 | 50 g | 1:1 |
| F.4 | NAME | DATE | TITLE: MIDDLE BUSHING | |
| DRAWN | JAANUS URB | 30.12.2020 | | |
| APPROV | ANDRES PERITŠENKO | 4.01.2021 | | |
| TALLINN UNIVERSITY OF TECHNOLOGY | | | SHEET 1:1 | DRW NR: SPM1200 |

1

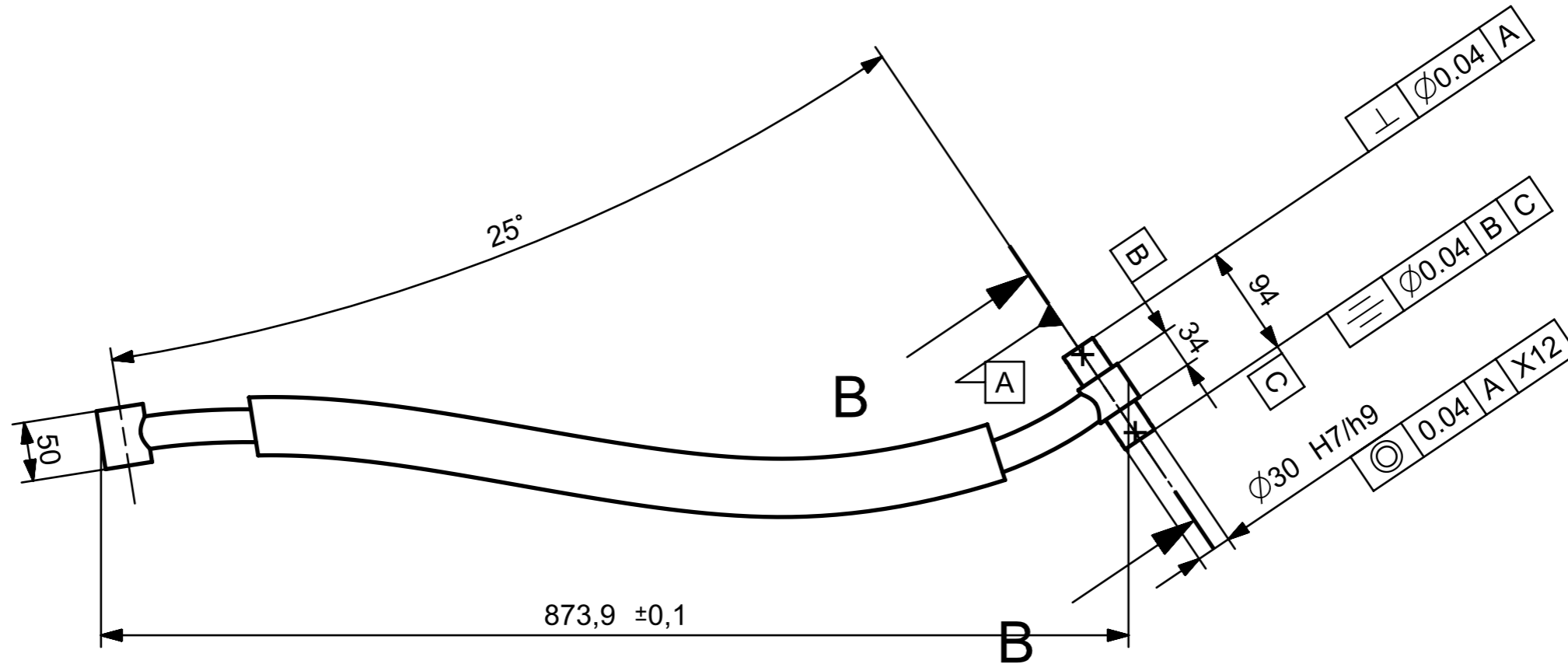
2

3

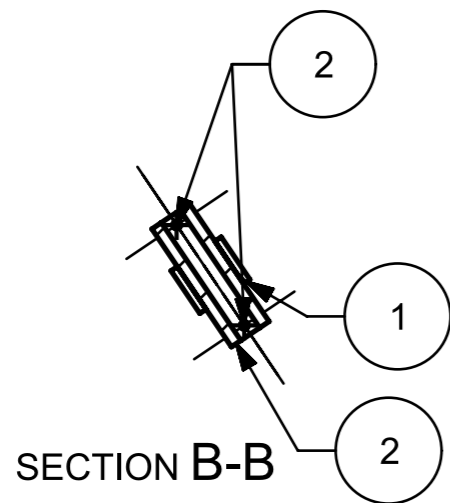
4

F.5. LINK 2 ASSEMBLY & LINK 4 ASSEMBLY DWG NR-SPM2000

Driving Links, shaft.



VIEW A
SCALE 1:5



| PC NO | PART NAME | QTY | DWG NR | NOTE |
|-------|---------------|-----|---------|-----------|
| 2 | SHAFT | 1 | SPM210d | WITH PINS |
| 1 | 2 LINK 2_BEND | 1 | SPM220d | |

| | | | | | |
|----------------------------------|-------------------------|------------|--|---------|--------|
| EM70LT - APPENDIX 6 | Material: | | Tolerance: | Mass: | Scale: |
| | AA6082-T651; EN AW 6061 | | ISO 286; ISO 19901-3; ISO 3547-1 | 11.2 KG | 1:5 |
| F.5 | Name | Date | TITLE: LINK 2 ASSEMBLY & LINK 4 ASSEMBLY | | |
| DRAWN | JAANUS URB | 30.12.2020 | | | |
| APPROV | ANDRES PERITŠENKO | 4.01.2021 | SHEET 1:1 DWG NR: SPM2000 | | |
| TALLINN UNIVERSITY OF TECHNOLOGY | | | | | |

F.6. SHAFT DWG NR SPM2100

Details.

1 2 3 4

75 HB

A

A

B

B

C

C

D

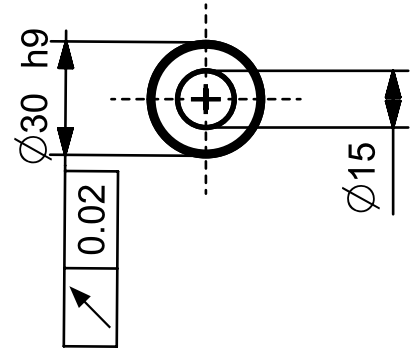
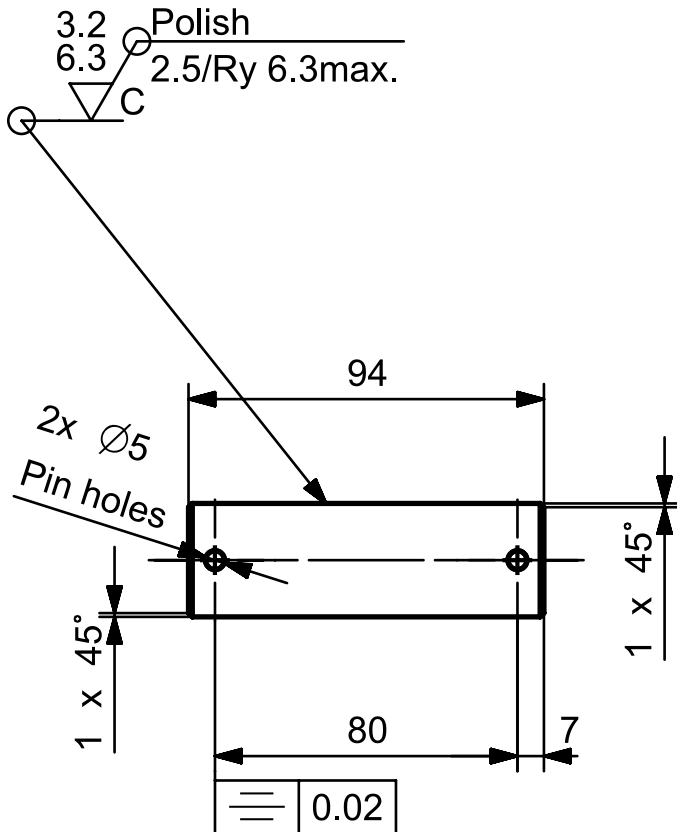
D

E

E

F

F



FOR FASTENING USE SPRING PIN (REFER TO DIN 1481) OR
 FLAT HEAD CYLINDRICAL PIN WITH HOLE (REFER TO DIN1444)
 USE STAINLESS STEEL SAFETY WIRE (0.51 mm)

| | | | | |
|----------------------------------|-------------------|---------------------|--------------|-----------------|
| EM70LT - APPENDIX 6 | MATERIAL | TOLERANCE | MASS | SCALE |
| | AA6082-T651 | ISO 286; ISO 3547-1 | 133 g | 1:1 |
| F.6 | NAME | DATE | TITLE: SHAFT | |
| DRAWN | JAANUS URB | 3.01.2020 | | |
| APPROV | ANDRES PERITŠENKO | 4.01.2021 | | |
| TALLINN UNIVERSITY OF TECHNOLOGY | | | SHEET 1:1 | DRW NR: SPM2100 |

1

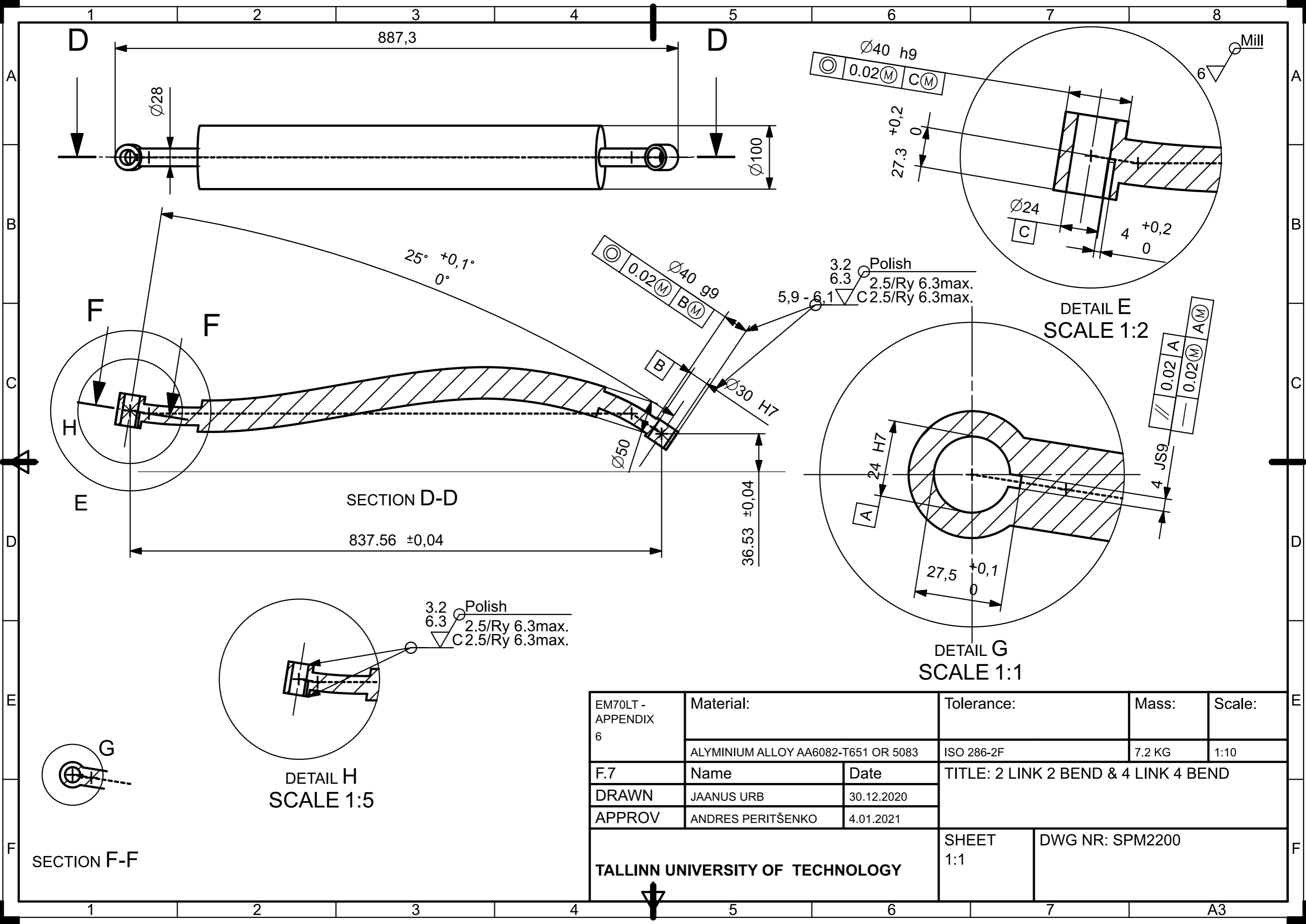
2

3

4

F.7. 2 LINK 2 BEND & 4 LINK 4 BEND DWG NR-SPM2200

Driving Links and connection to Drive.



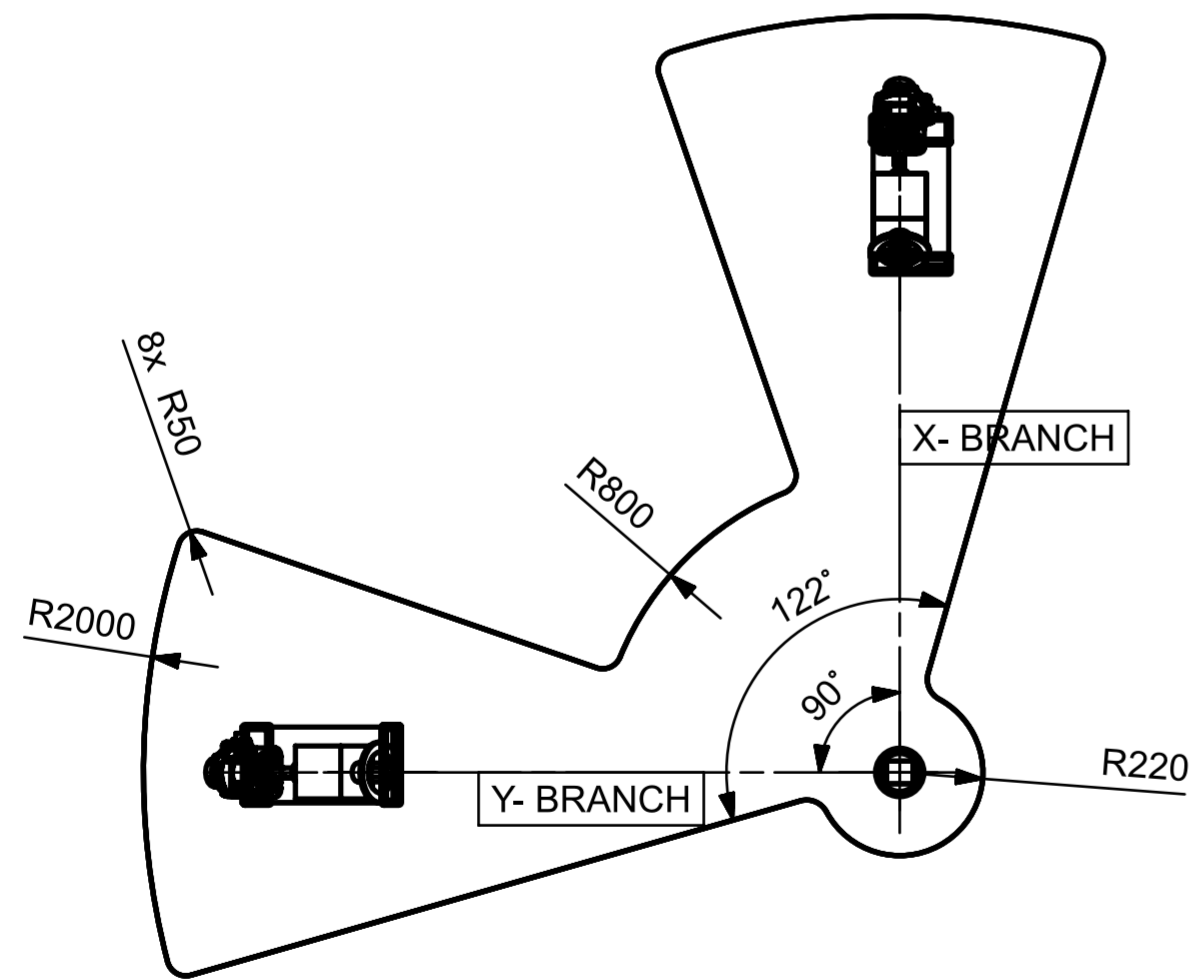
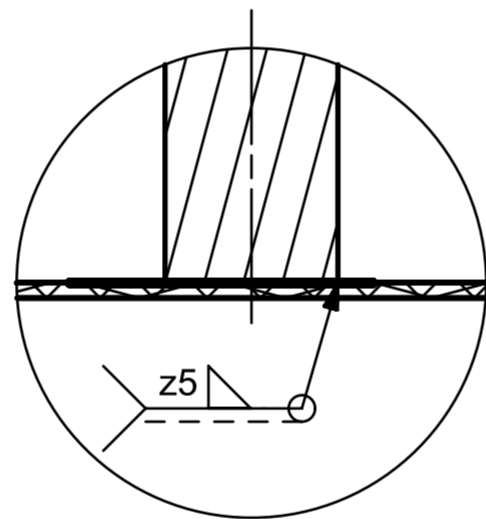
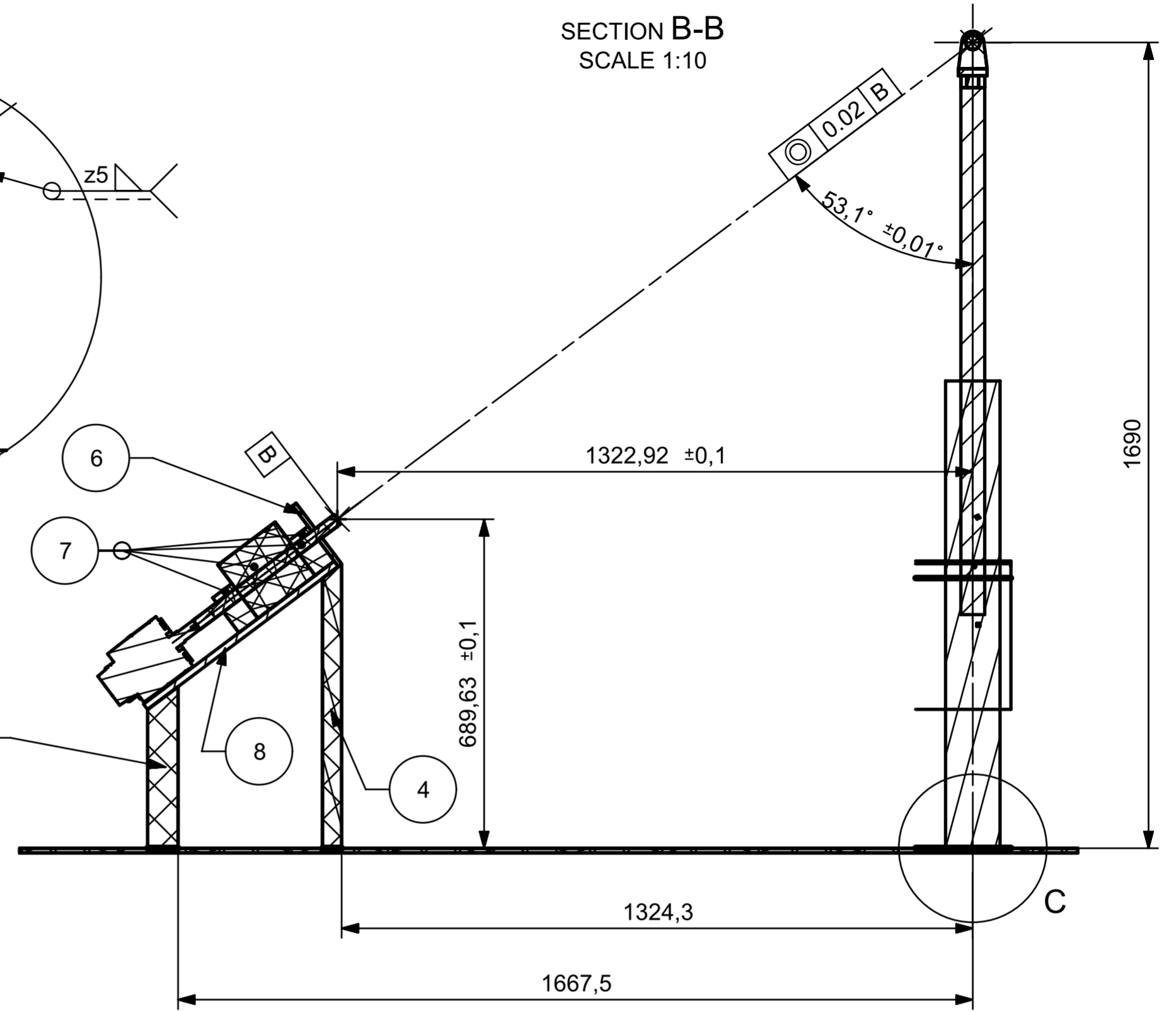
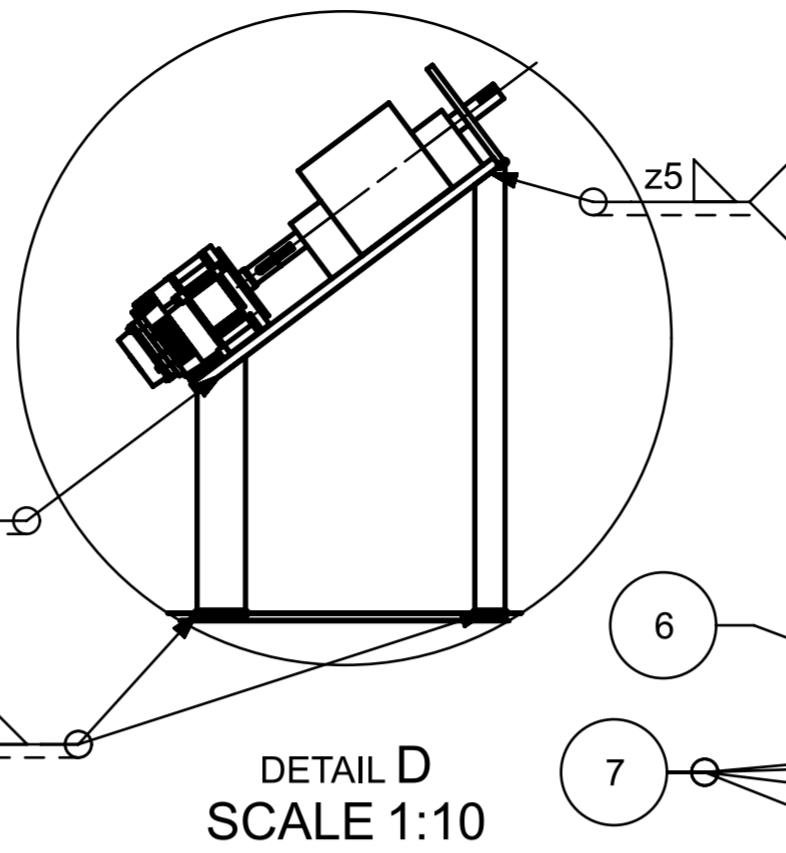
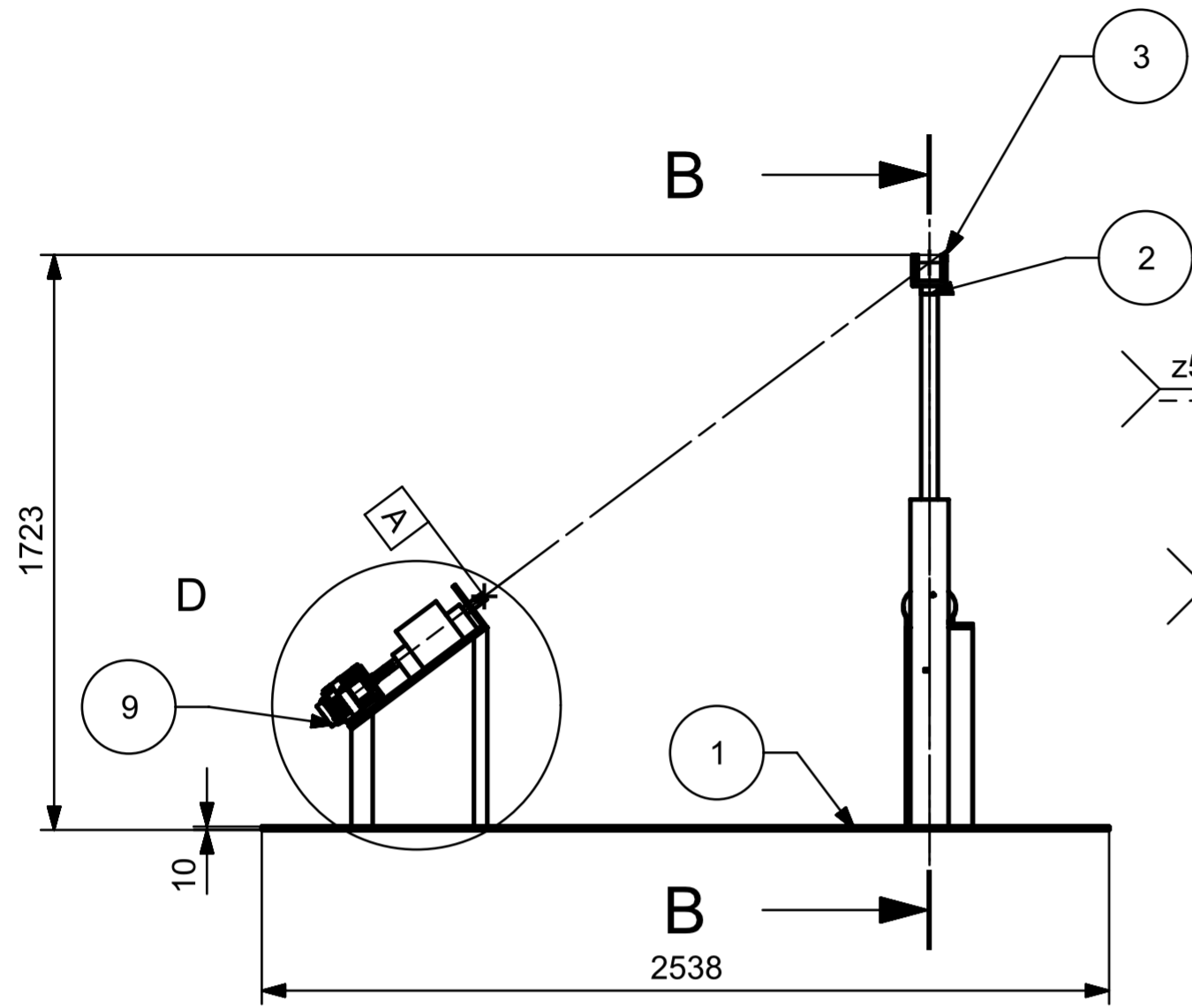
| | | | | | |
|----------------------------------|-------------------------------------|------------|--------------------------------------|-----------------|--------|
| EM70LT - APPENDIX 6 | Material: | | Tolerance: | Mass: | Scale: |
| | ALYMINIUM ALLOY AA6082-T651 OR 5083 | | ISO 286-2F | 7.2 KG | 1:10 |
| F.7 | Name | Date | TITLE: 2 LINK 2 BEND & 4 LINK 4 BEND | | |
| DRAWN | JAANUS URB | 30.12.2020 | | | |
| APPROV | ANDRES PERITŠENKO | 4.01.2021 | | | |
| TALLINN UNIVERSITY OF TECHNOLOGY | | | SHEET 1:1 | DWG NR: SPM2200 | |

F.8. 6 Base Plate Assembly DWG SPM6000

Fixed plate, drive stand, center post and fixed yoke.

SCALE 1:20
VIEW A

SECTION B-B
SCALE 1:10



| PC NO | PART NAME | QTY | DWG NR | STANDARD P/N | MANUFACTURER | NOTES |
|-------|--------------------------|-----|----------|----------------------------------|-----------------------------------|--|
| 9 | DRIVE-BASE | 2 | N/A | N/A | YASKAWA, ABB, SIEMENS OR BECKHOFF | [1200 Nm] |
| 8 | MOTOR STAND PLATE | 2 | SPM6800 | | | |
| 7 | MOTOR TO LINK CONNECTION | 2 | N/A | N/A | YASKAWA, ABB, SIEMENS OR BECKHOFF | max speed 3.3 rpm; max acceleration 0.28 rad/s^2 |
| 6 | MOTOR STAND PLATE 2 | 2 | SPM6600 | | | |
| 5 | MOTOR STAND LEG 2 | 2 | SPM6500 | | | |
| 4 | MOTOR STAND LEG 1 | 2 | SPM6400 | | | |
| 3 | FIXED YOKE | 1 | N/A | DRIVESHAFT SLIP YOKE; 3730235050 | [SYTH TOYOTA] | [MAY NEED SOME MODIFICATION FOR THE CENTER POST] |
| 2 | CENTER POST | 1 | SPM6200 | | | |
| 1 | 6 BASE PLATE | 1 | SPM61000 | | | |

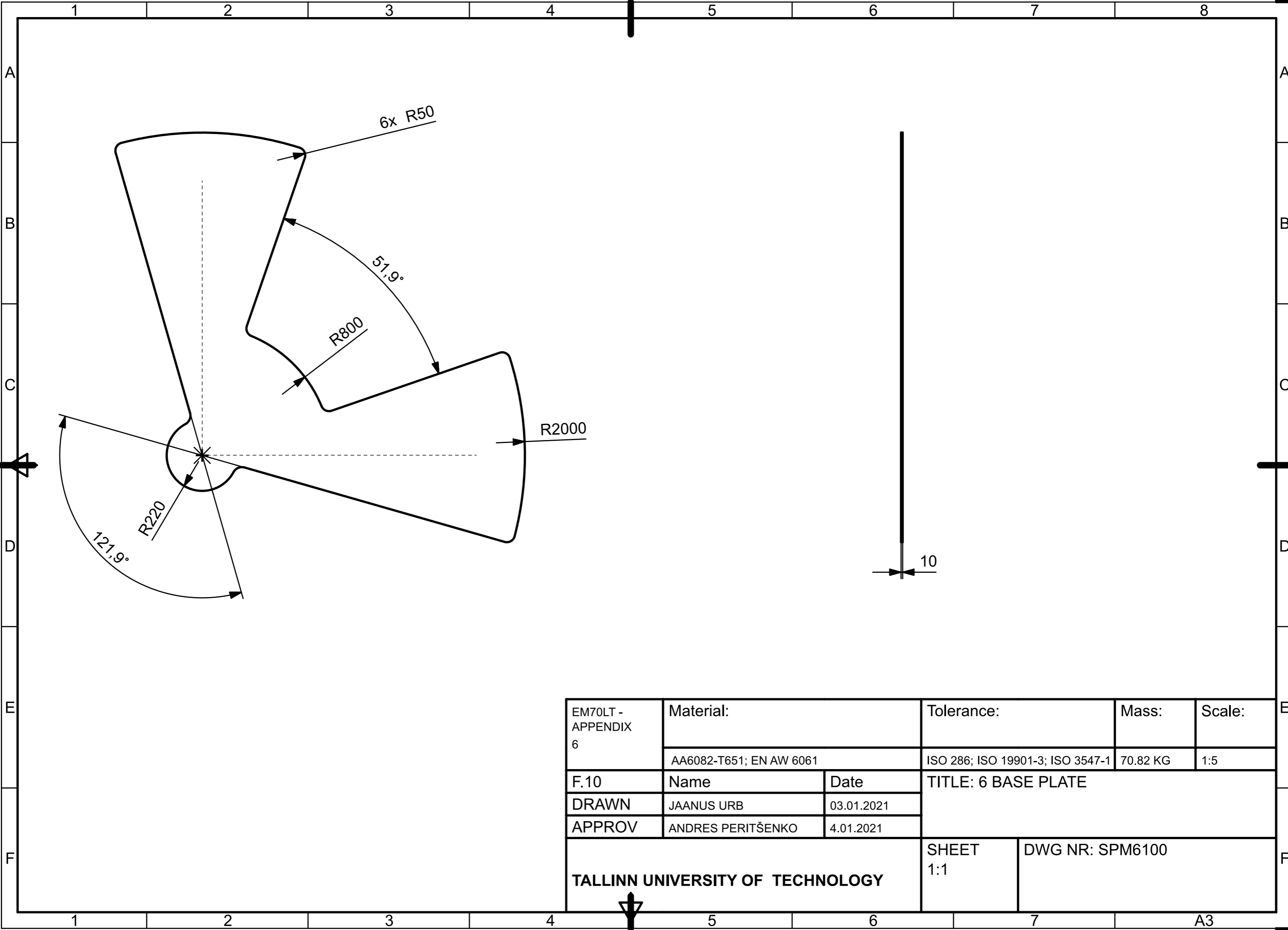
DETAIL C
SCALE 1:5

| | | | | |
|----------------------------------|-----------------------------|-------------------------------|------------------------------|-----------------|
| EM70LT - APPENDIX 6 | Material: | Tolerance: | Mass: | Scale: |
| F.8 | ALYMINIUM ALLOY AA6082-T651 | ISO 286; ISO 19901-3; CAP 437 | 251 KG | 1:20 |
| DRAWN | Name | Date | TITLE: 6 BASE PLATE ASSEMBLY | |
| APPROV | JAANUS URB | 3.01.2020 | | |
| | ANDRES PERITŠENKO | 4.01.2021 | SHEET 1:1 | DWG NR: SPM6000 |
| TALLINN UNIVERSITY OF TECHNOLOGY | | | | |

X-BRANCH AND Y BRANCH MOTOR STAND PLATES AND LEGS (LEG 1, LEG 2, PLATE, PLATE 2) WILL BE WELDED TOGETHER. NO EXTRA REQUIREMENTS FOR WELDING (REFER TO ISO 19902 FOR WELDING REQUIREMENTS). CENTER POST WILL BE WELDED ACCORDING TO THE ISO 19902. NO CORROSION ARE ALLOWED ON THE WELDED STRUCTURE (WELDED AREA HEAT TREATMENT IS REQUIRED).

F.9. 6 Base Plate DWG SPM6100

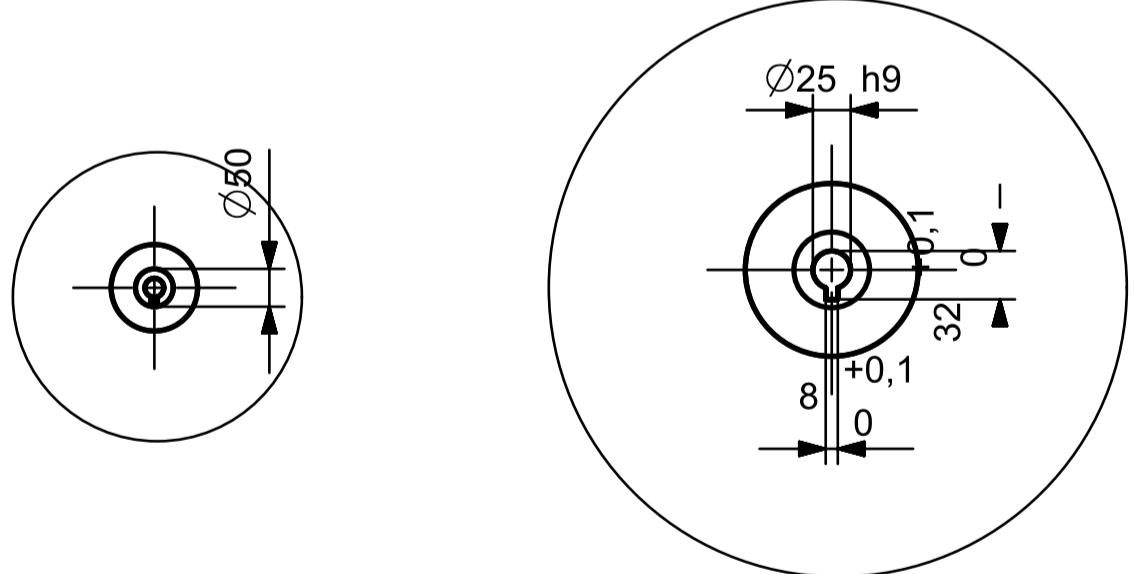
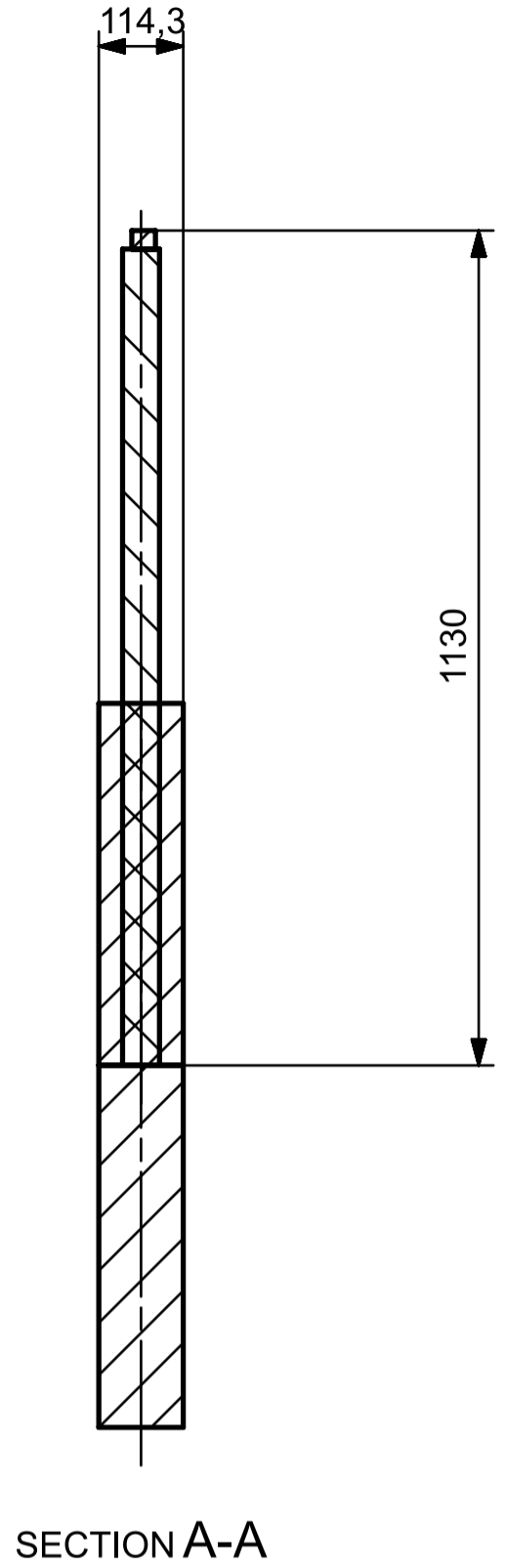
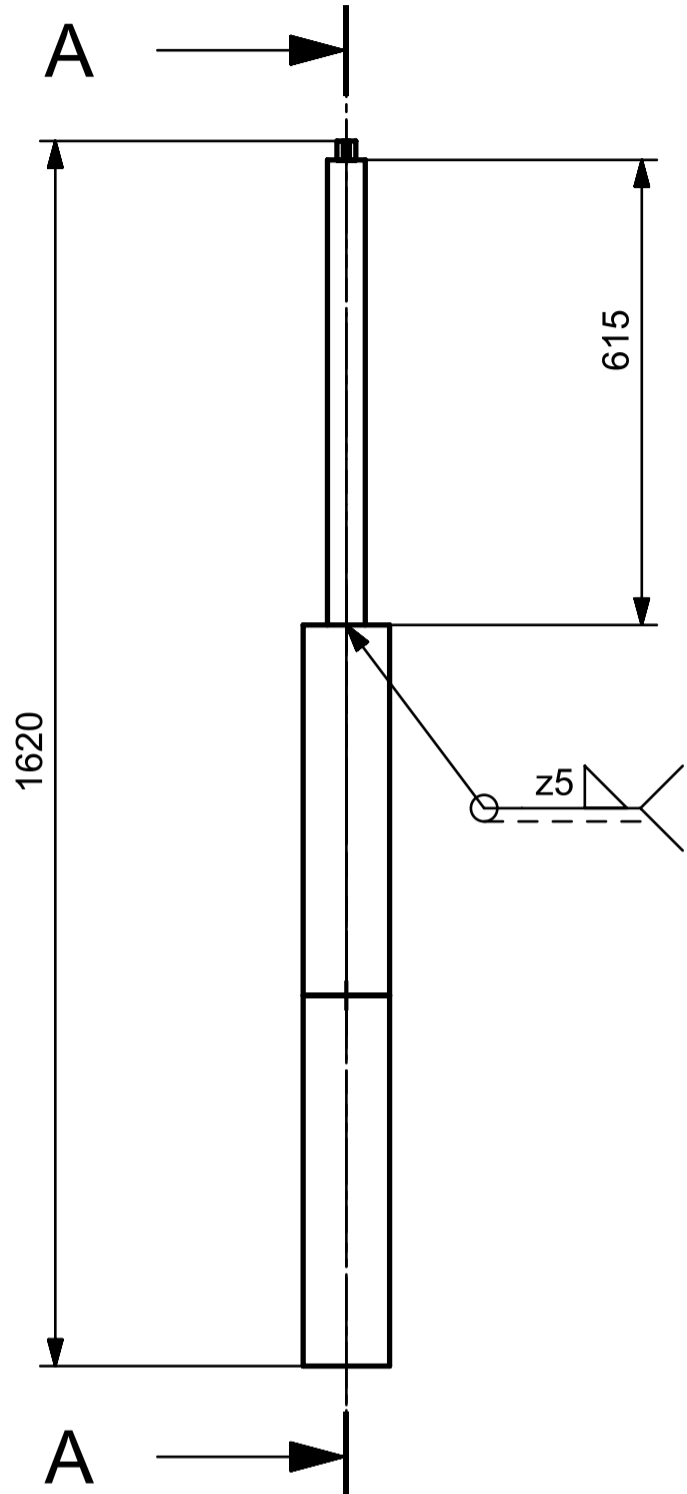
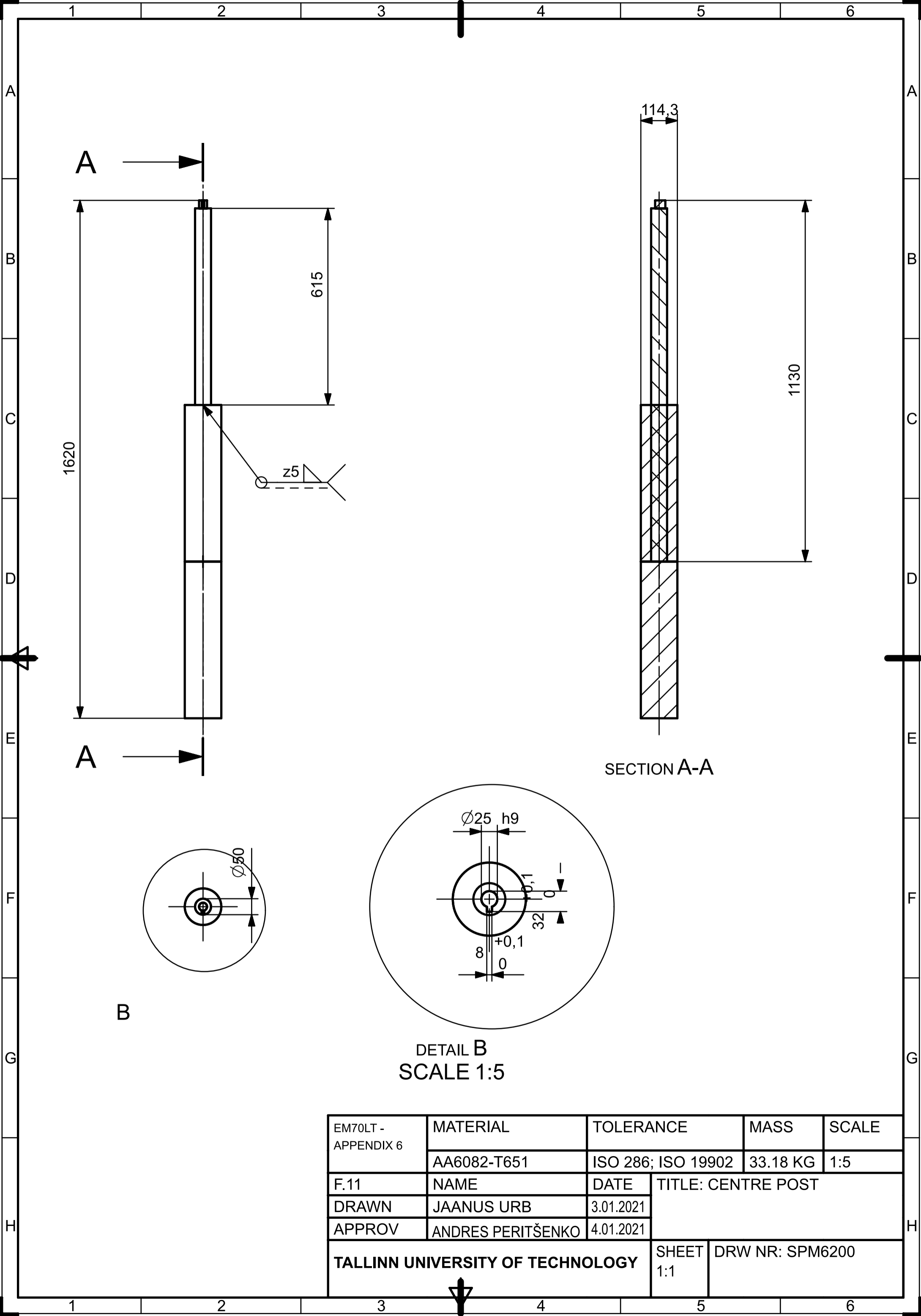
Plate 6.



| | | | | | |
|----------------------------------|-------------------------|------------|----------------------------------|-----------------|--------|
| EM70LT - APPENDIX 6 | Material: | | Tolerance: | Mass: | Scale: |
| | AA6082-T651; EN AW 6061 | | ISO 286; ISO 19901-3; ISO 3547-1 | 70.82 KG | 1:5 |
| F.10 | Name | Date | TITLE: 6 BASE PLATE | | |
| DRAWN | JAANUS URB | 03.01.2021 | | | |
| APPROV | ANDRES PERITŠENKO | 4.01.2021 | | | |
| TALLINN UNIVERSITY OF TECHNOLOGY | | | SHEET 1:1 | DWG NR: SPM6100 | |

F.10. CENTRE POST DWG SPM6200

Post and yoke.



DETAIL B
SCALE 1:5

| | | | | |
|----------------------------------|-------------------|--------------------|--------------------|-----------------|
| EM70LT - APPENDIX 6 | MATERIAL | TOLERANCE | MASS | SCALE |
| | AA6082-T651 | ISO 286; ISO 19902 | 33.18 KG | 1:5 |
| F.11 | NAME | DATE | TITLE: CENTRE POST | |
| DRAWN | JAANUS URB | 3.01.2021 | | |
| APPROV | ANDRES PERITŠENKO | 4.01.2021 | | |
| TALLINN UNIVERSITY OF TECHNOLOGY | | | SHEET 1:1 | DRW NR: SPM6200 |

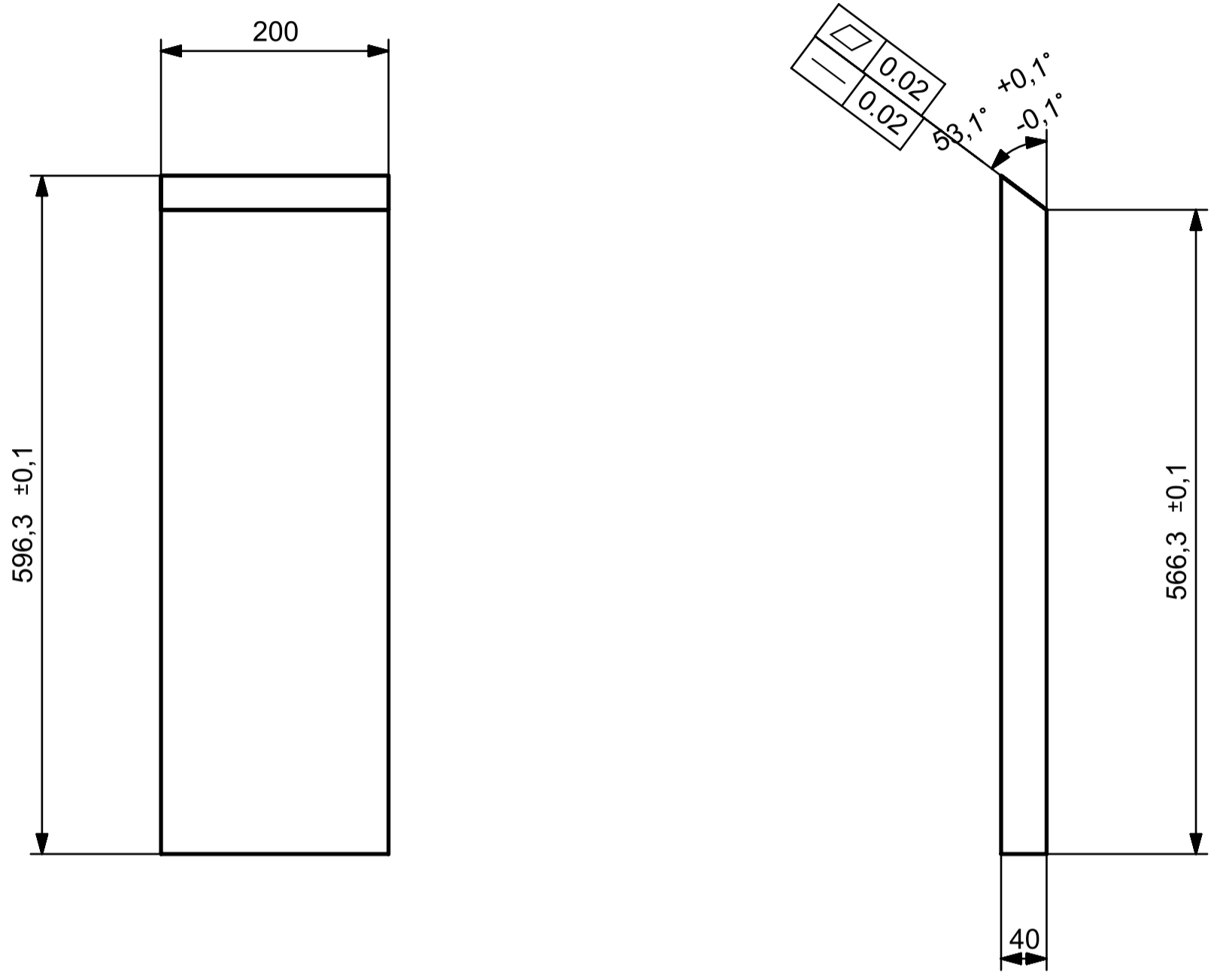
F.11. Fixed yoke - N/A

Future design.

F.12. Motor Stand Leg 1 DWG SPM 6400

Leg 1.

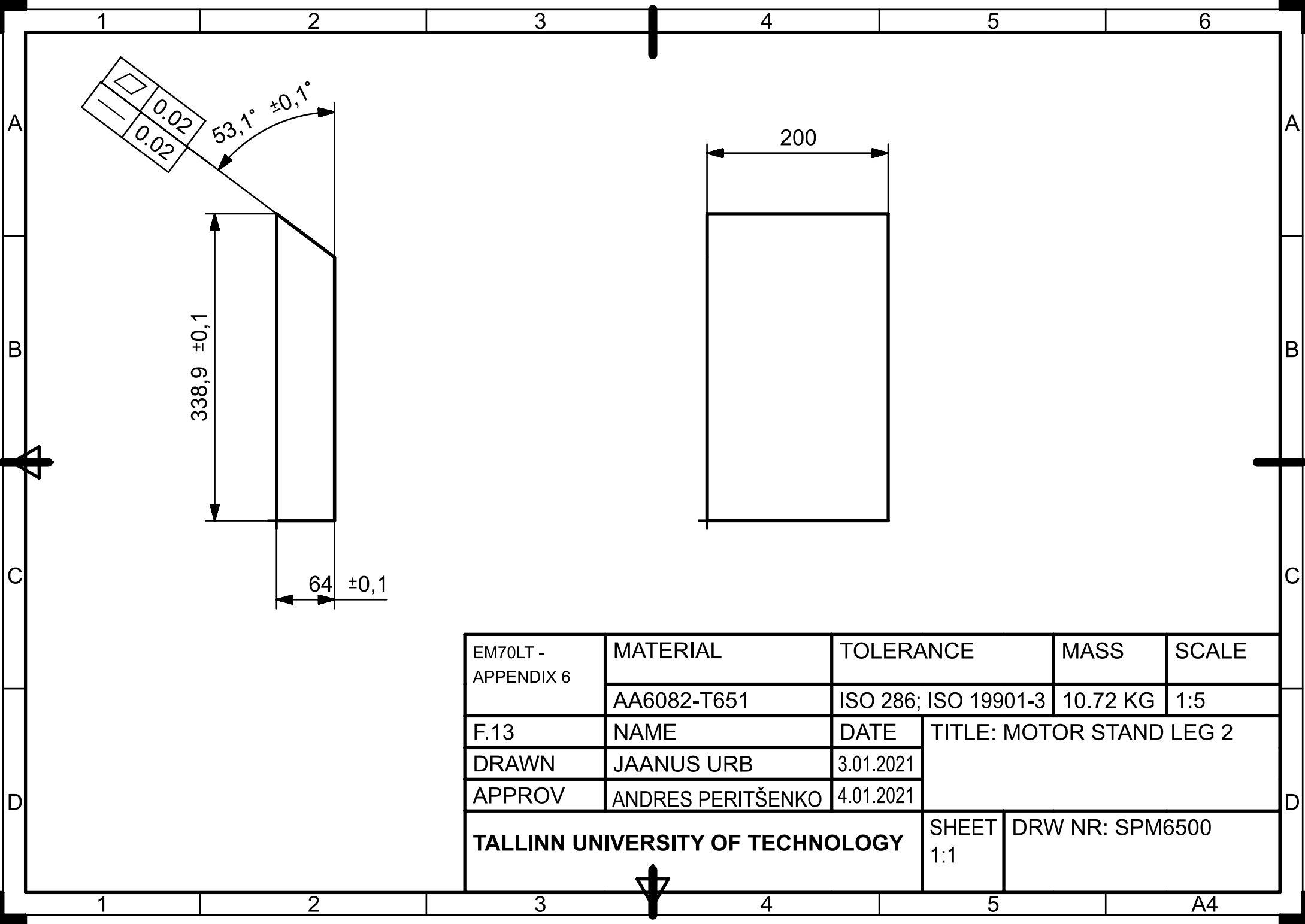
3.2 Polish
6.3



| | | | | |
|----------------------------------|-------------------|----------------------|--------------------------|-----------------|
| EM70LT - APPENDIX 6 | MATERIAL | TOLERANCE | MASS | SCALE |
| | AA6082-T651 | ISO 286; ISO 19901-3 | 18.18 KG | 1:5 |
| F.12 | NAME | DATE | TITLE: MOTOR STAND LEG 1 | |
| DRAWN | JAANUS URB | 3.01.2021 | | |
| APPROV | ANDRES PERITŠENKO | 4.01.2021 | | |
| TALLINN UNIVERSITY OF TECHNOLOGY | | | SHEET 1:1 | DRW NR: SPM6300 |

F.13. MOTOR STAND LEG 2 DWG SPM6500

Leg 2.



| | | | | |
|---|-------------------|----------------------|--------------------------|-----------------|
| EM70LT - APPENDIX 6 | MATERIAL | TOLERANCE | MASS | SCALE |
| | AA6082-T651 | ISO 286; ISO 19901-3 | 10.72 KG | 1:5 |
| F.13 | NAME | DATE | TITLE: MOTOR STAND LEG 2 | |
| DRAWN | JAANUS URB | 3.01.2021 | | |
| APPROV | ANDRES PERITŠENKO | 4.01.2021 | | |
| TALLINN UNIVERSITY OF TECHNOLOGY | | | SHEET 1:1 | DRW NR: SPM6500 |

1 2 3 4 5 6

A

A

B

B

C

C

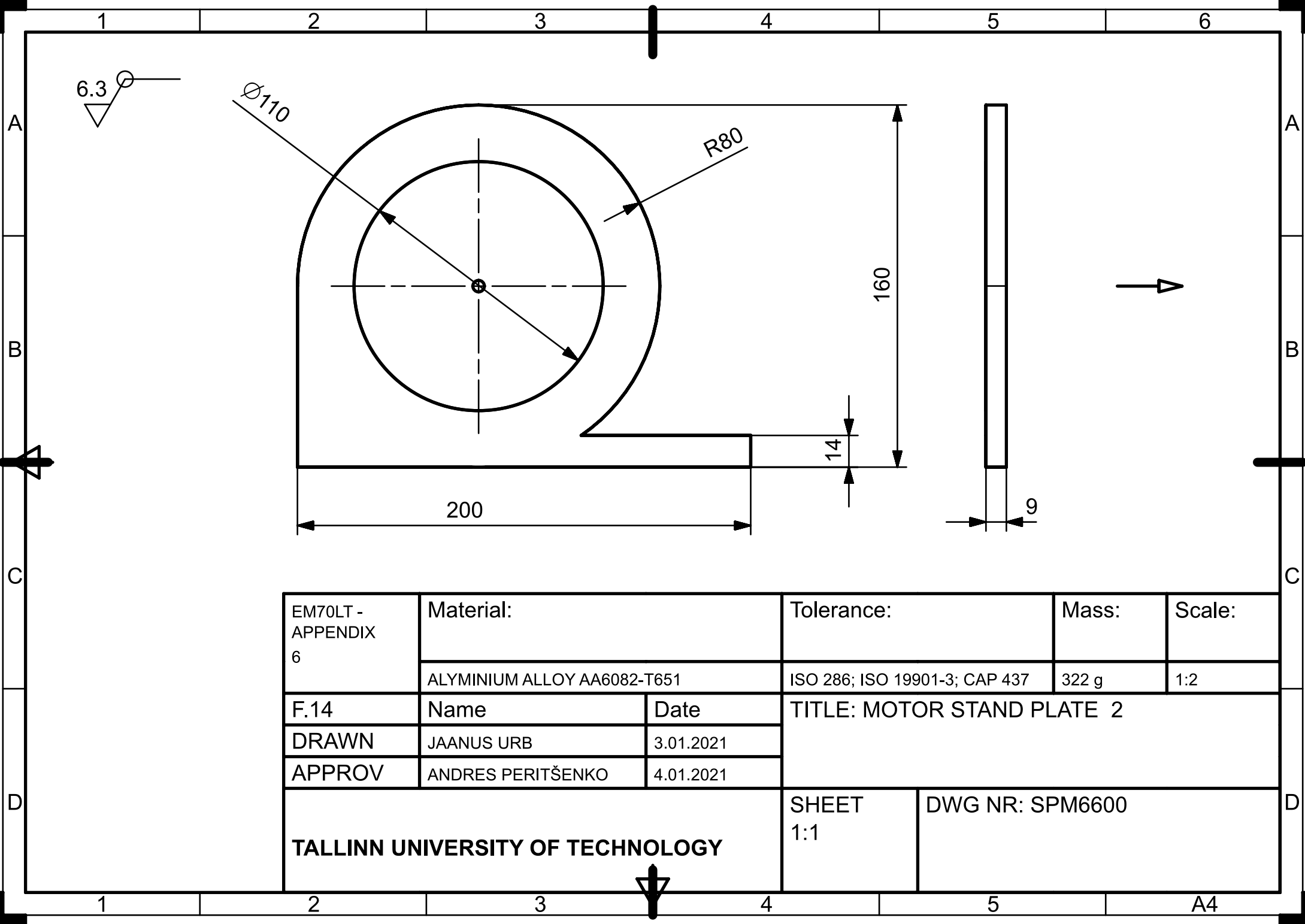
D

D

1 2 3 4 5 A4

F.14. MOTOR STAND PLATE 2 DWG SPM6600

Plate 2.



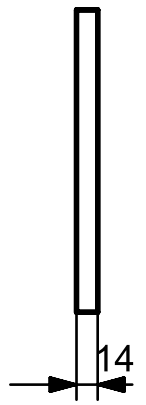
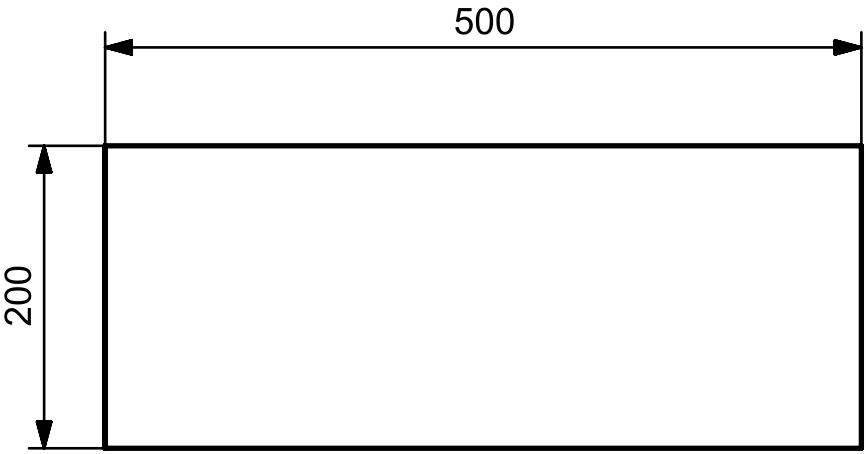
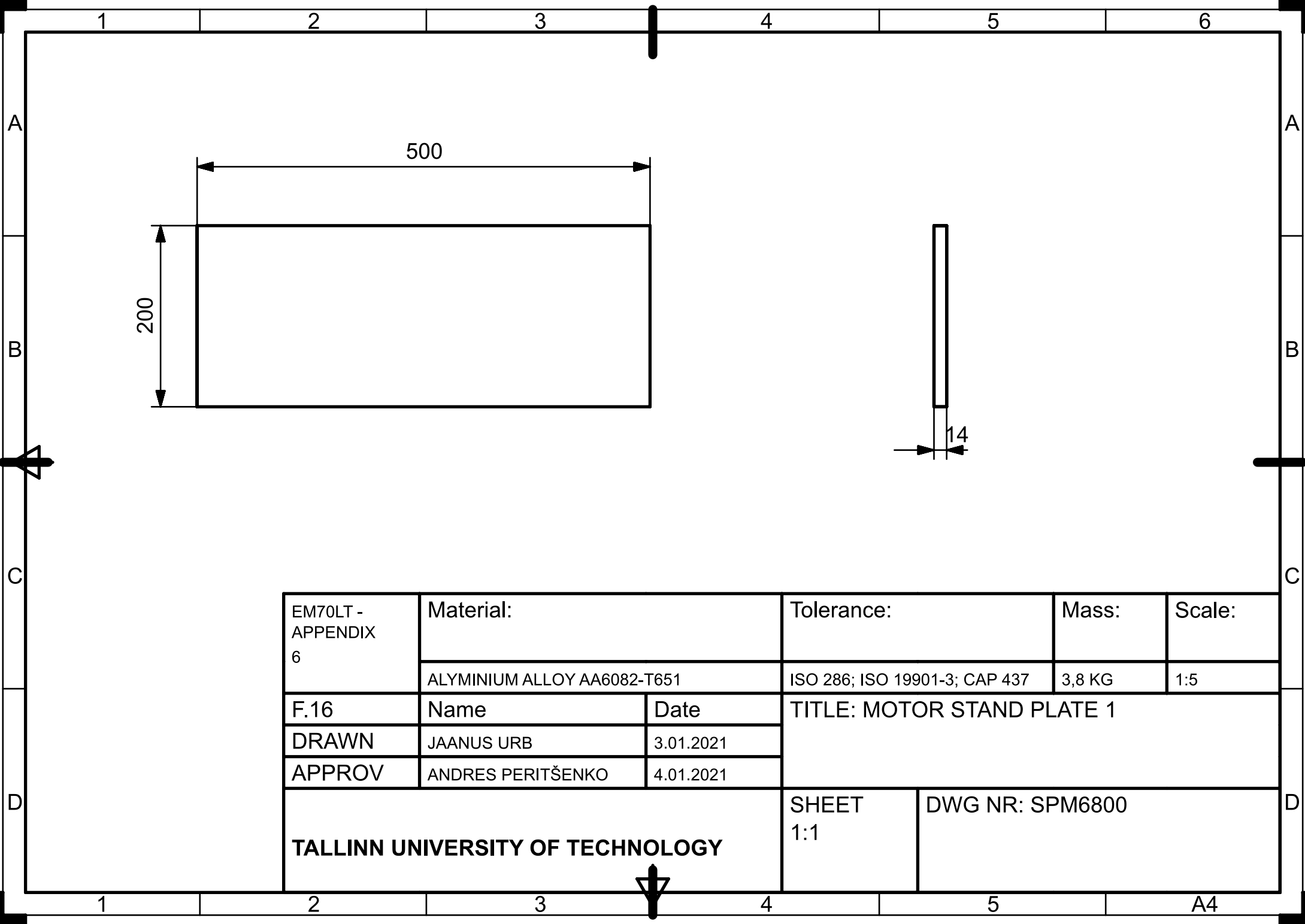
| | | | | | |
|----------------------------------|-----------------------------|-----------|-------------------------------|-----------------|--------|
| EM70LT - APPENDIX 6 | Material: | | Tolerance: | Mass: | Scale: |
| | ALYMINIUM ALLOY AA6082-T651 | | ISO 286; ISO 19901-3; CAP 437 | 322 g | 1:2 |
| F.14 | Name | Date | TITLE: MOTOR STAND PLATE 2 | | |
| DRAWN | JAANUS URB | 3.01.2021 | | | |
| APPROV | ANDRES PERITŠENKO | 4.01.2021 | | | |
| TALLINN UNIVERSITY OF TECHNOLOGY | | | SHEET 1:1 | DWG NR: SPM6600 | |

F.15. Motor to Link 1 and 5 connection -N/A

Future development.

**F.16. F.16 MOTOR STAND PLATE 1 DWG
SPM6800**

Plate 1.



| | | | | | |
|----------------------------------|-----------------------------|-----------|-------------------------------|-----------------|--------|
| EM70LT - APPENDIX 6 | Material: | | Tolerance: | Mass: | Scale: |
| | ALYMINIUM ALLOY AA6082-T651 | | ISO 286; ISO 19901-3; CAP 437 | 3,8 KG | 1:5 |
| F.16 | Name | Date | TITLE: MOTOR STAND PLATE 1 | | |
| DRAWN | JAANUS URB | 3.01.2021 | | | |
| APPROV | ANDRES PERITŠENKO | 4.01.2021 | | | |
| TALLINN UNIVERSITY OF TECHNOLOGY | | | SHEET 1:1 | DWG NR: SPM6800 | |

1 2 3 4 5 6

A

A

B

B

C

C

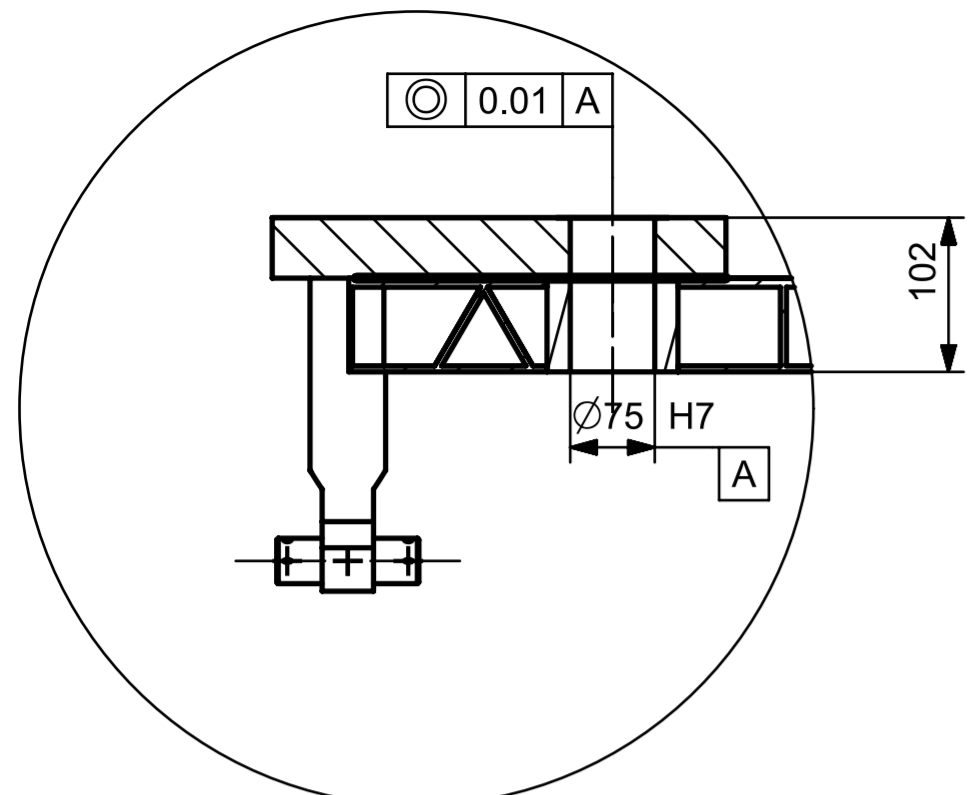
D

D

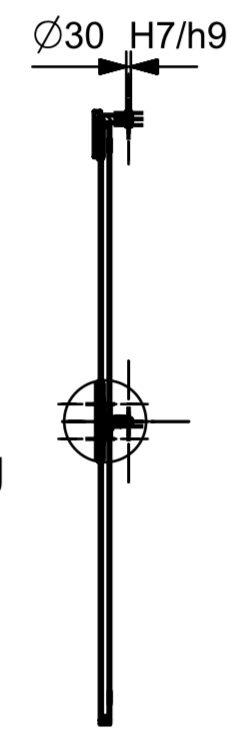
1 2 3 4 5 A4

F.17. 3 TOP PLATE ASSEMBLY 3 DWG SPM3000

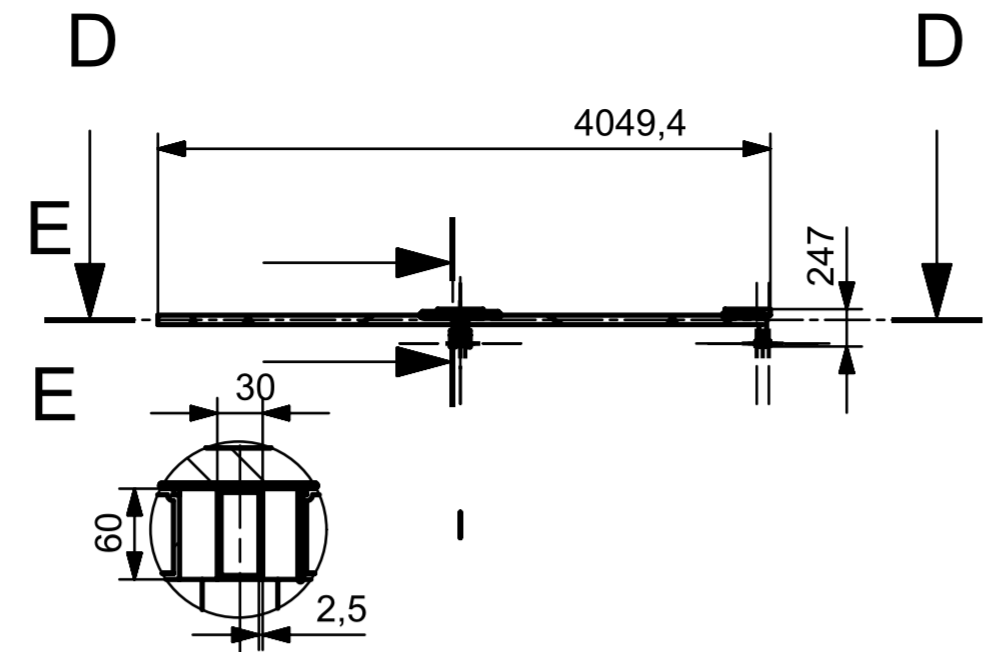
Top plate parts and connection to links.



DETAIL F
SCALE 1:5

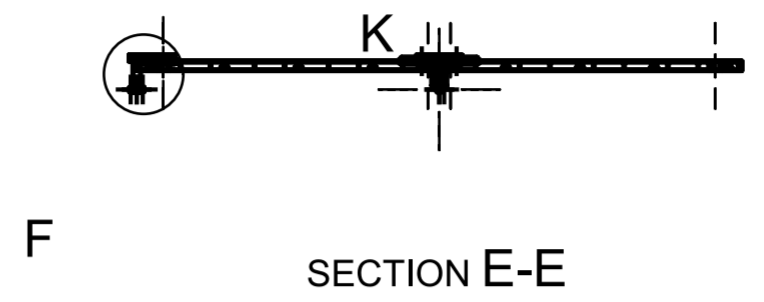


SECTION A-A

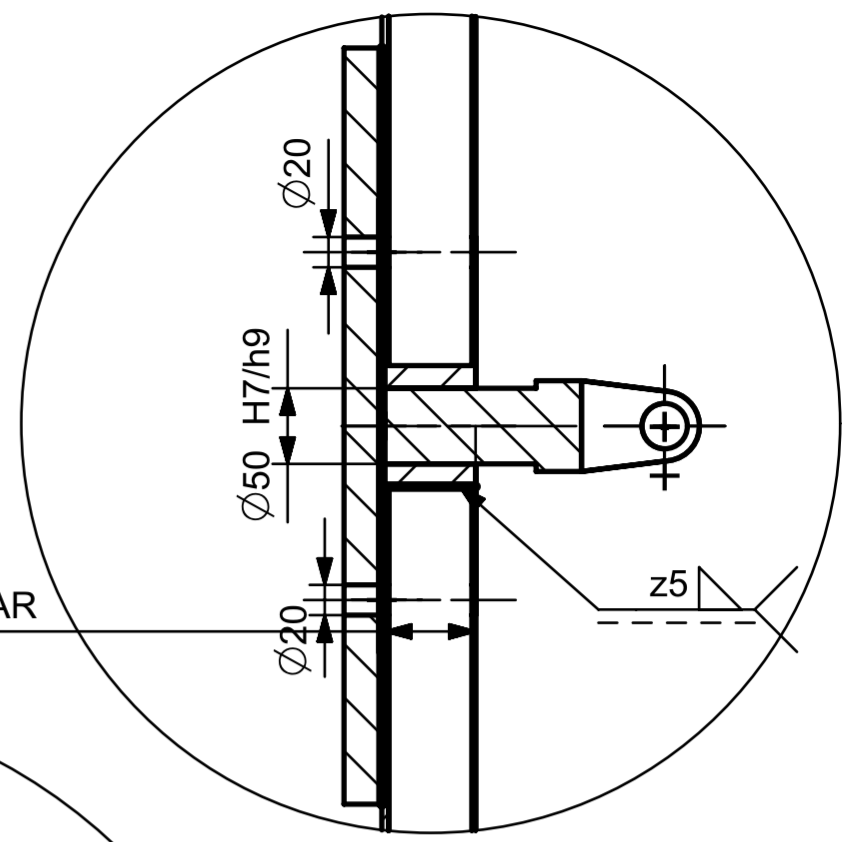


DETAIL K
SCALE 1:5

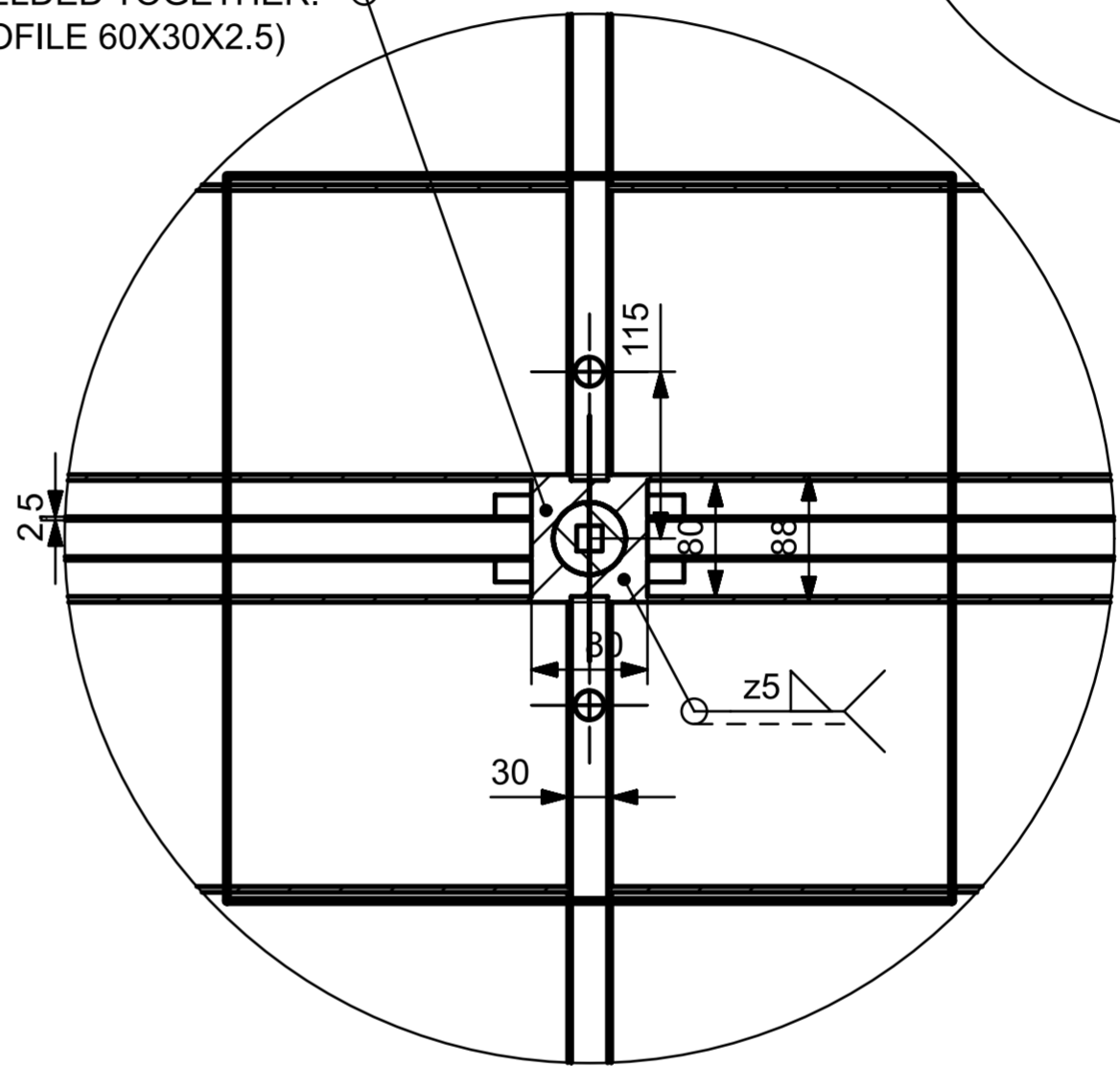
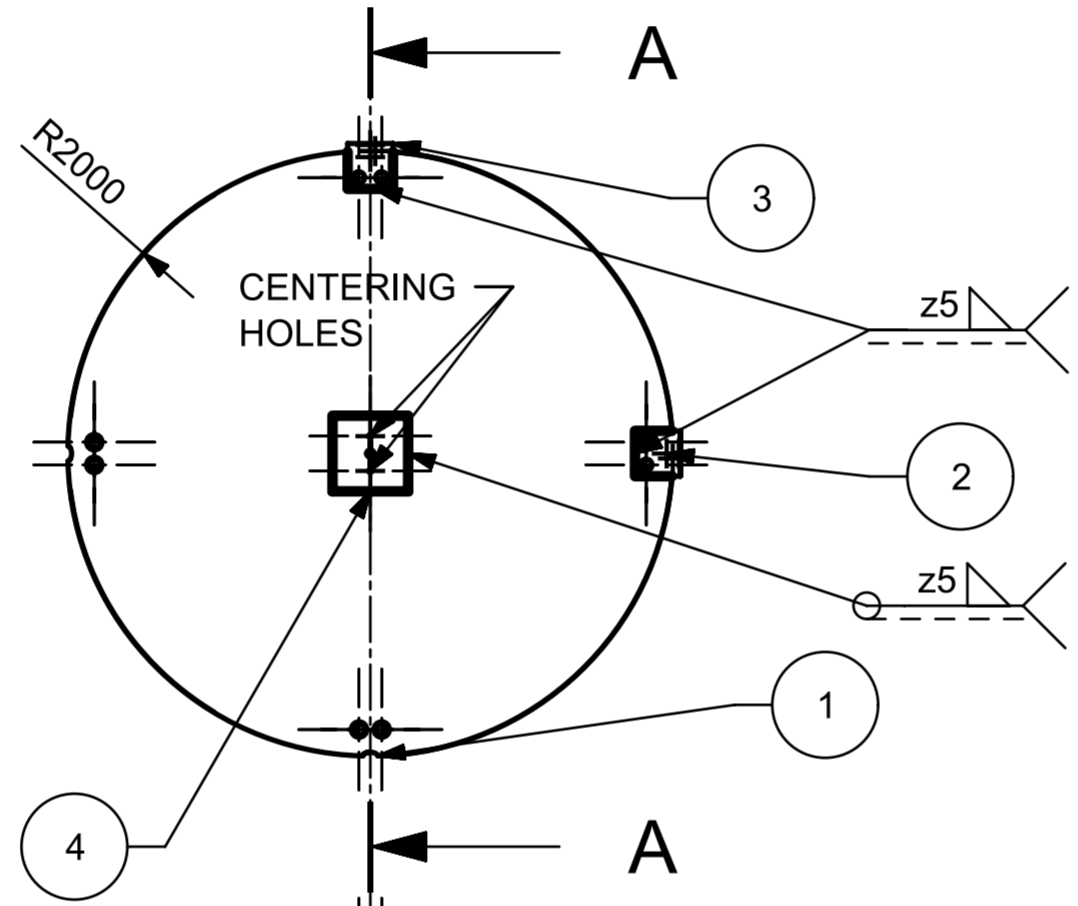
CENTER BAR (80X80X60). ALL WELDED TOGETHER.
X-AXIS AND Y AXIS (SQUARE PROFILE 60X30X2.5)



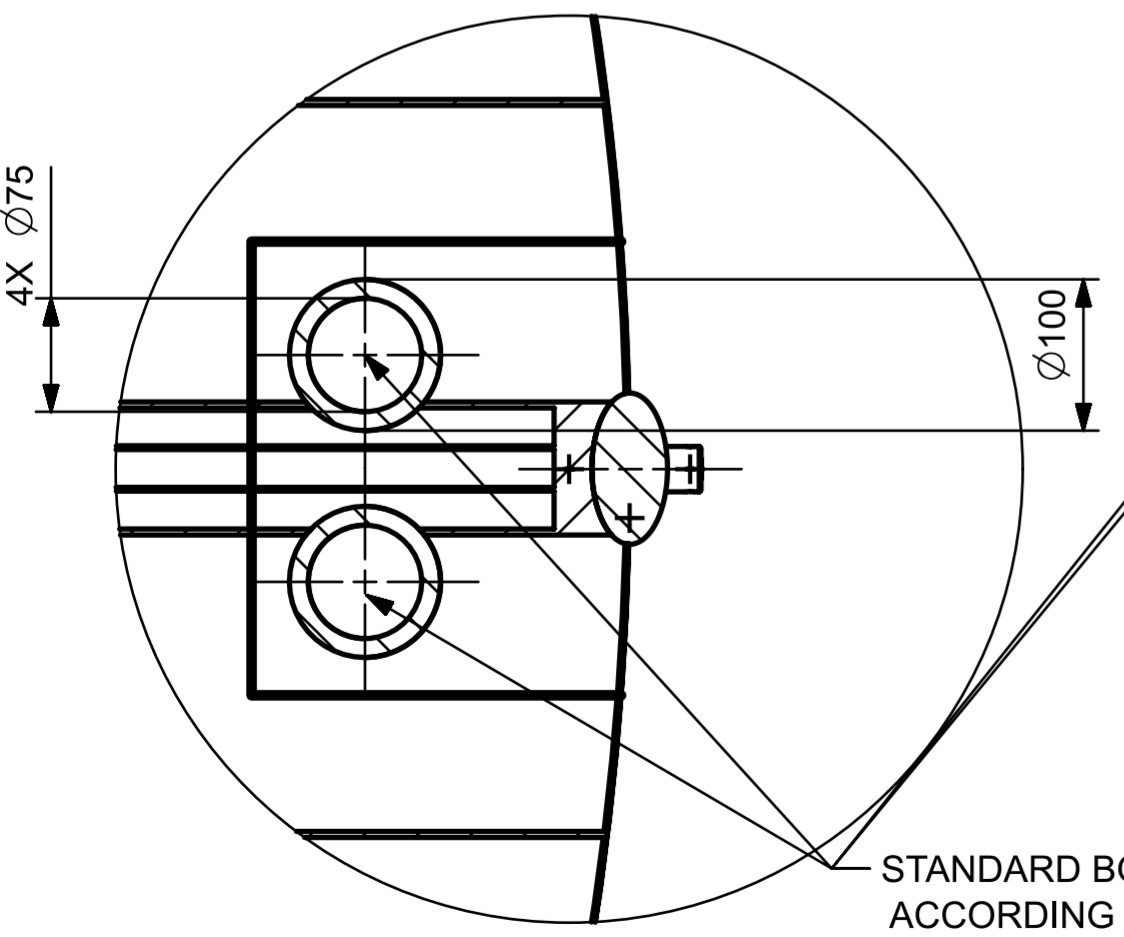
SECTION E-E



DETAIL J
SCALE 1:5

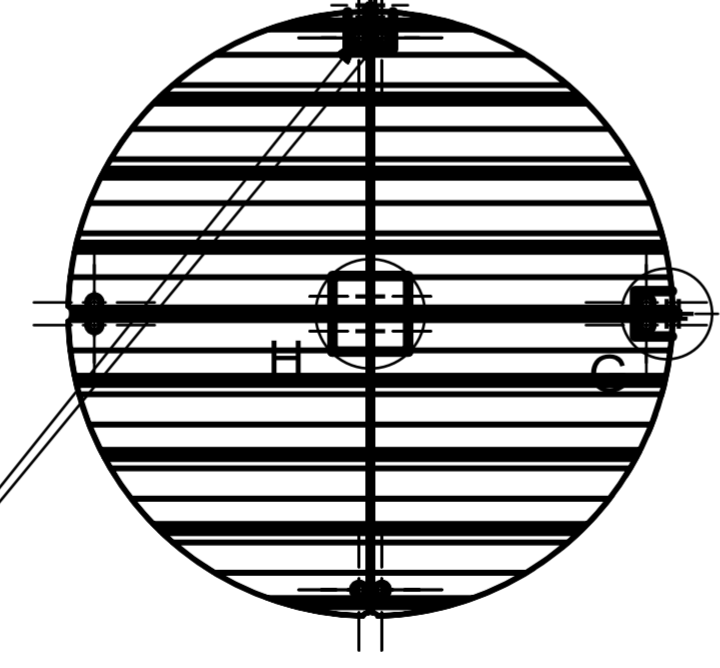


DETAIL H
SCALE 1:5



DETAIL G
SCALE 1:5

STANDARD BOLT CONNECTION M75
ACCORDING TO THE ISO 724 THREADS
X4 (XBRANCH AND Y BRANCH)



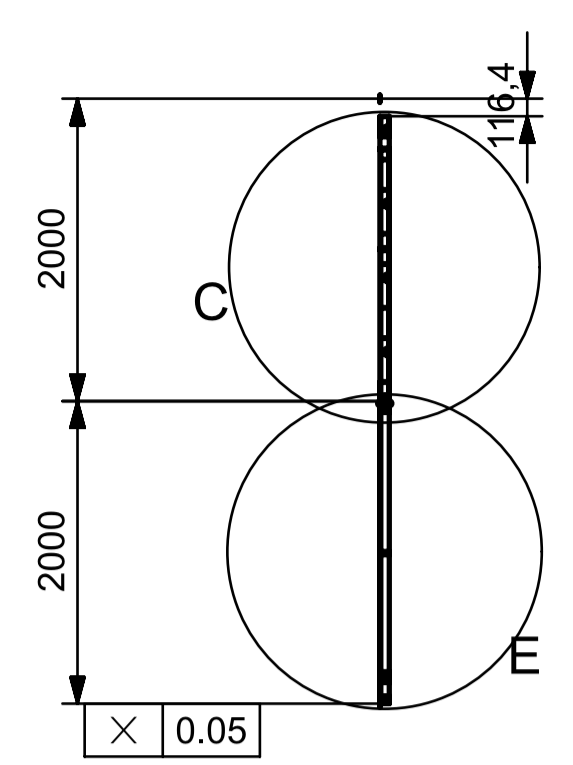
SECTION D-D

| | | | |
|-------|-----------------------------|-----|---------|
| 4 | TOP PLATE CENTER CONNECTION | 1 | ▣ |
| 3 | TOP PLATE CONNECTION LINK | 2 | ▣ |
| 2 | SHAFT | 2 | SPM2100 |
| 1 | 3 TOP PLATE 3 | 1 | SPM3100 |
| PC NO | PART NAME | QTY | DWG NR |

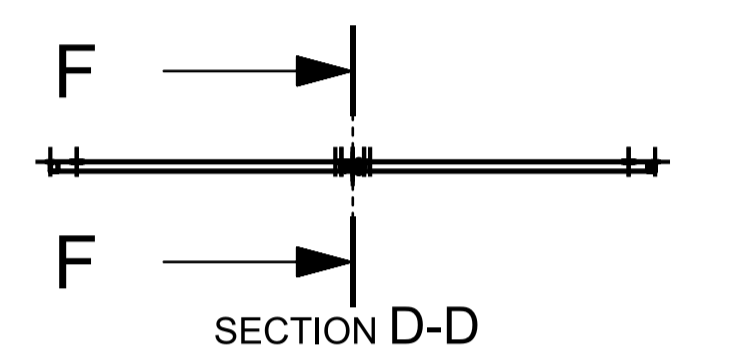
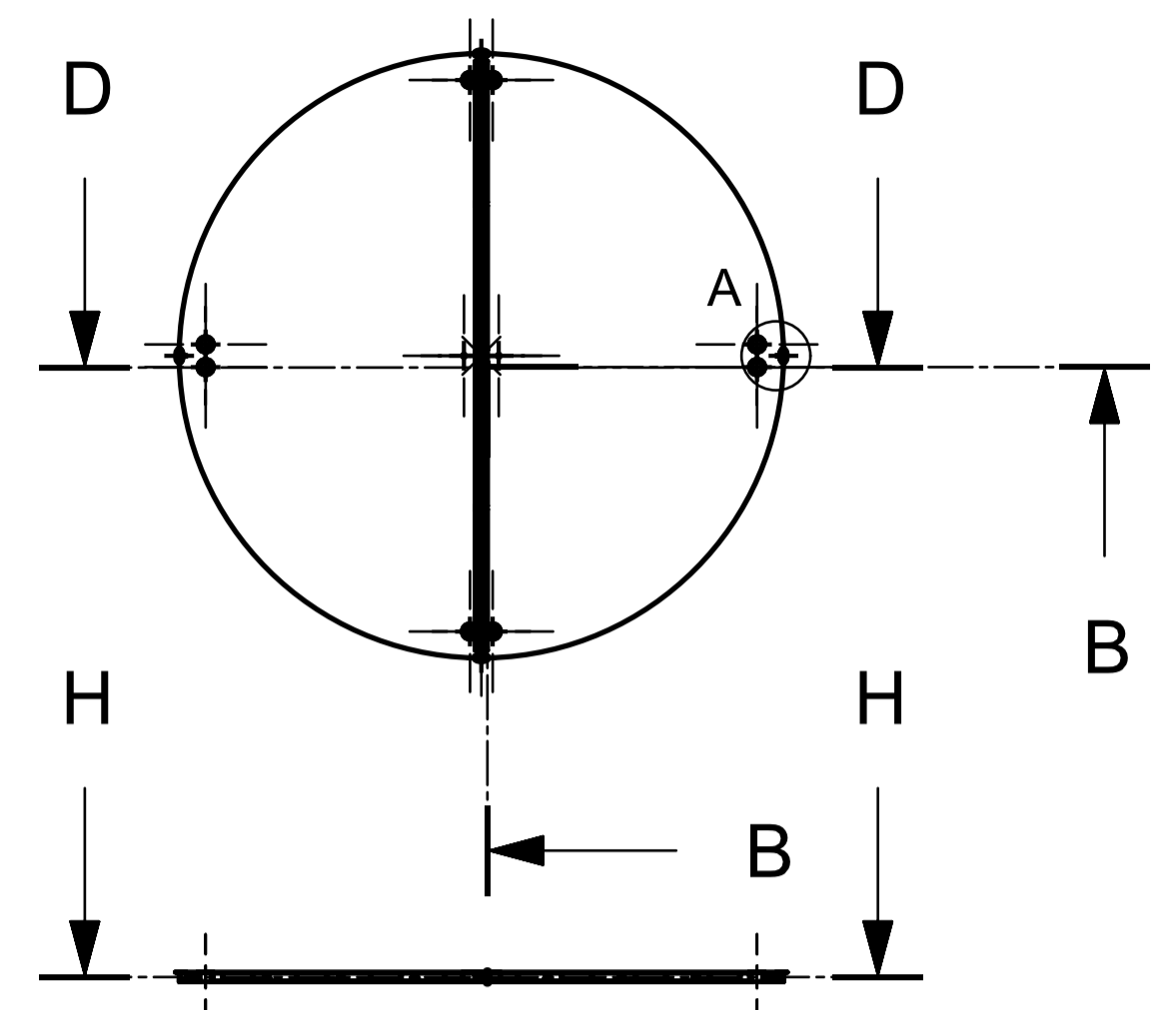
| | | | | |
|----------------------------------|-----------------------------|-------------------------------|------------------------------|--------|
| EM70LT - APPENDIX 6 | Material: | Tolerance: | Mass: | Scale: |
| | ALYMINIUM ALLOY AA6082-T651 | ISO 286; ISO 19901-3; CAP 437 | 251 KG | 1:20 |
| F.17 | Name | Date | TITLE: 6 BASE PLATE ASSEMBLY | |
| DRAWN | JAANUS URB | 3.01.2020 | | |
| APPROV | ANDRES PERITŠENKO | 4.01.2021 | SHEET 1:1 DWG NR: SPM3000 | |
| TALLINN UNIVERSITY OF TECHNOLOGY | | | | |

F.18. F.18 3 TOP PLATE 3 DWG SPM3100

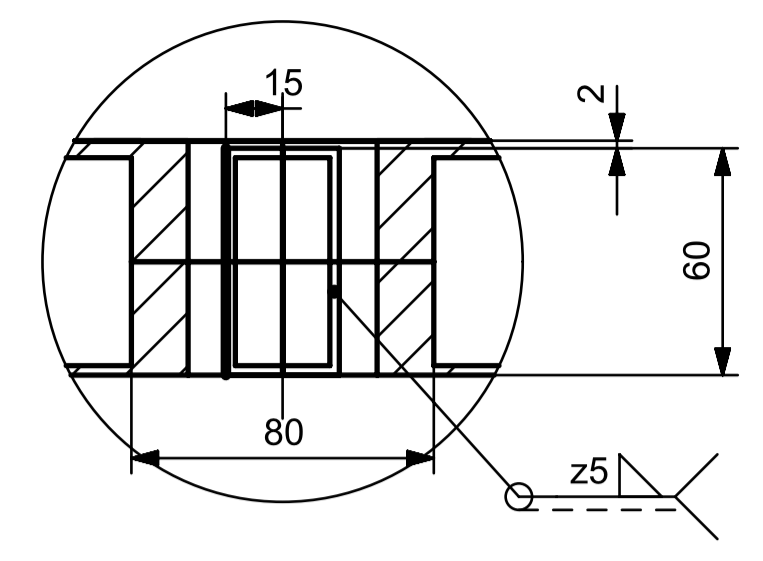
Top plate.



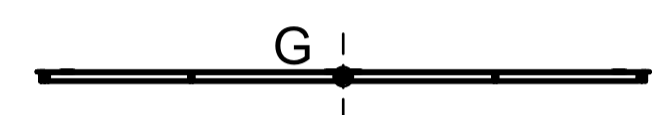
SECTION B-B



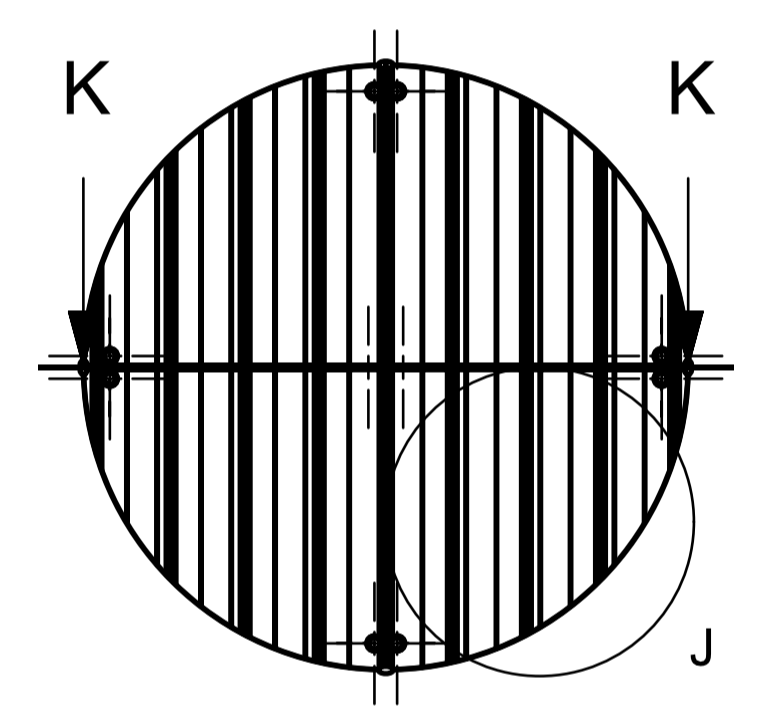
SECTION D-D



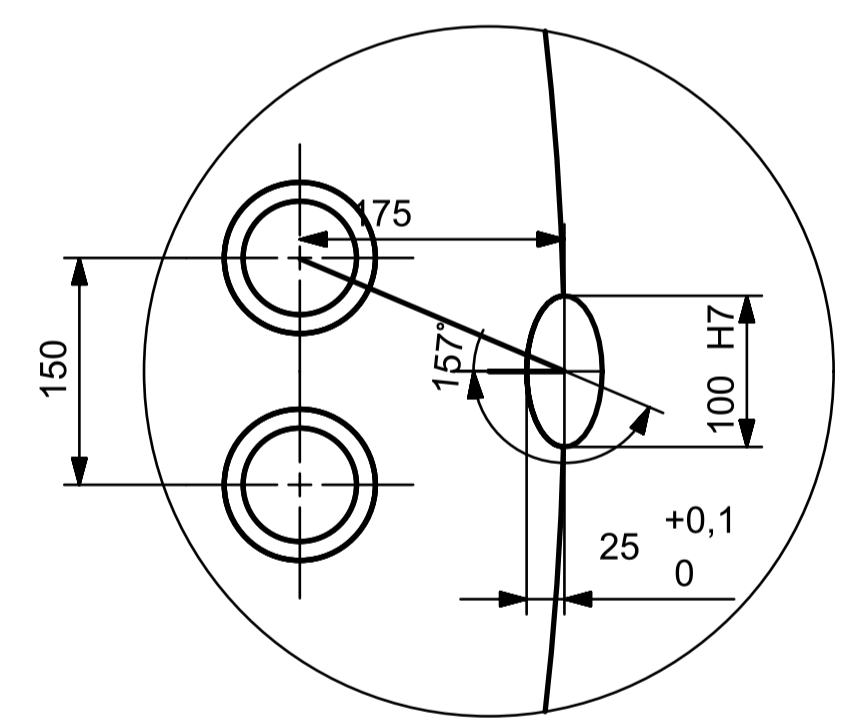
DETAIL G
SCALE 1:2



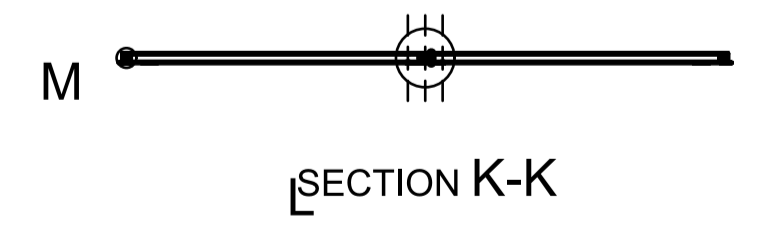
SECTION F-F



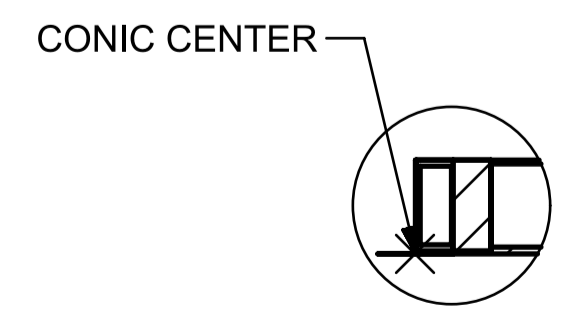
SECTION H-H



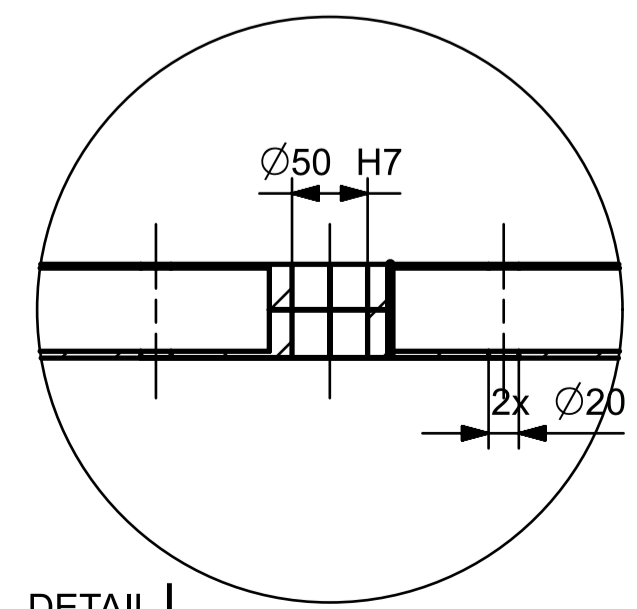
DETAIL A
SCALE 1:5



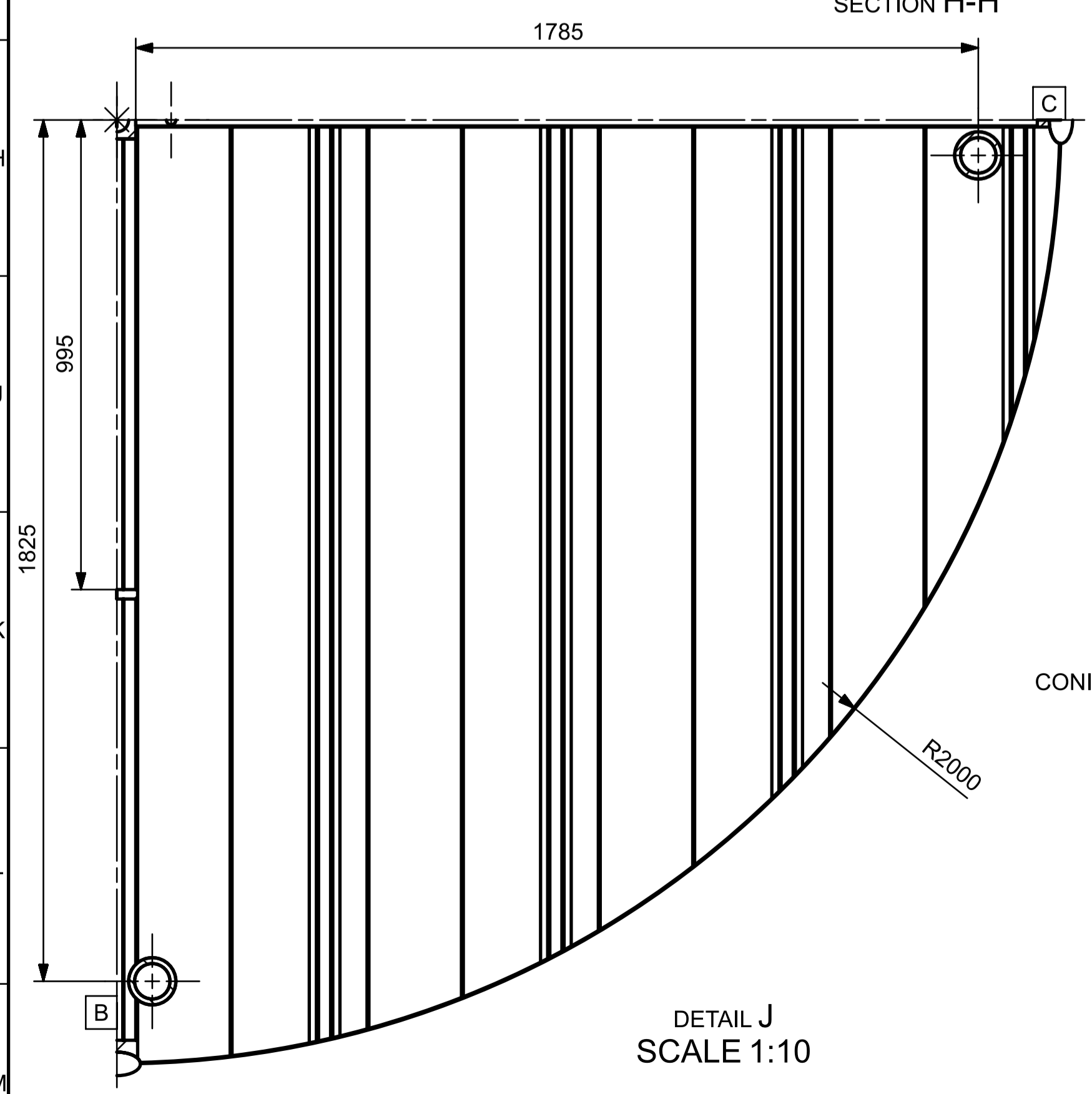
SECTION K-K



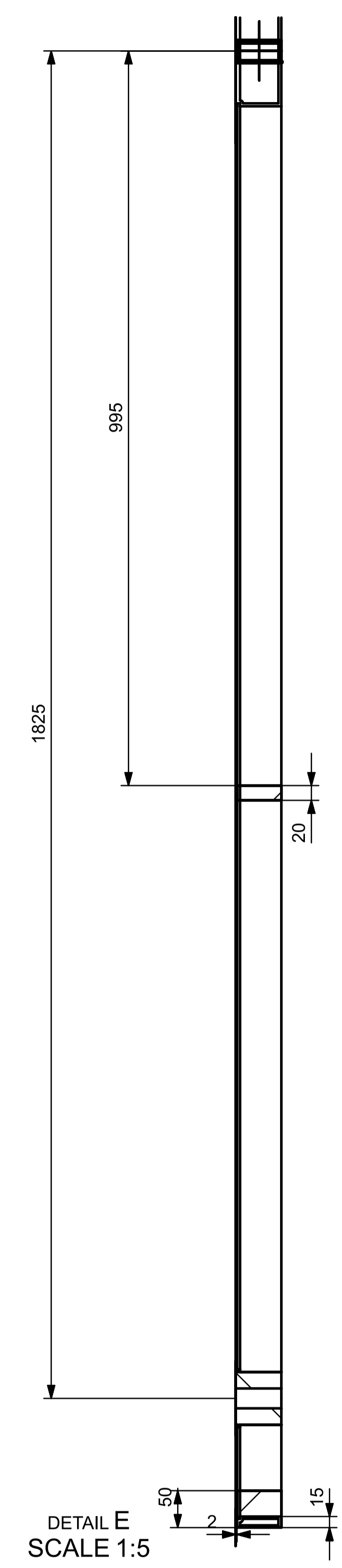
DETAIL M
SCALE 1:5



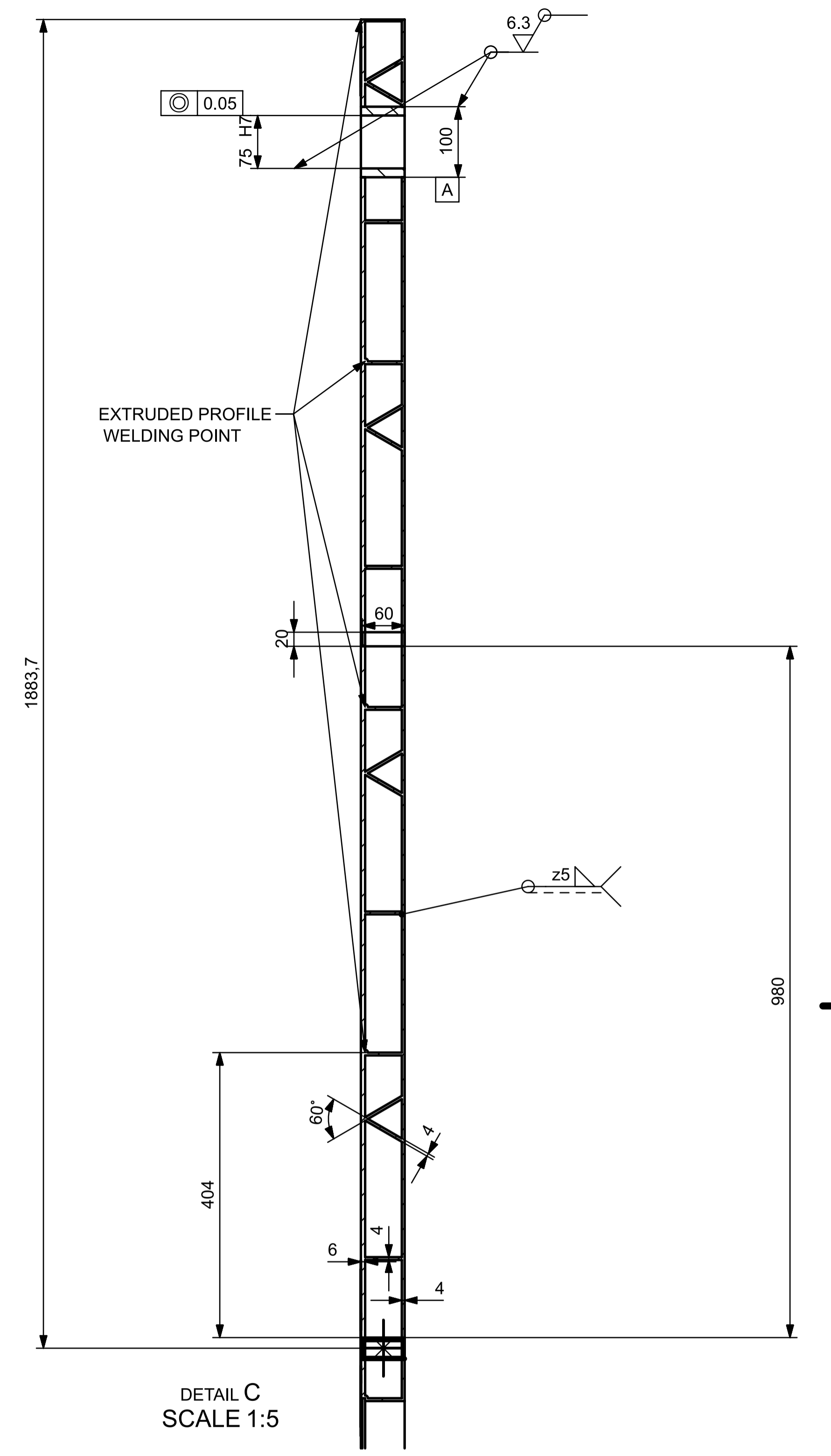
DETAIL L
SCALE 1:5



DETAIL J
SCALE 1:10



DETAIL E
SCALE 1:5



DETAIL C
SCALE 1:5

| | | | | |
|----------------------------------|---------------------|---------------------------------|--------------------|------------------|
| EM70LT - APPENDIX 6 | Material: | Tolerance: | Mass: | Scale: |
| | AA6082-T651 OR 5083 | ISO 286-2F; ISO 19901-3; CAP437 | 408 KG | 1:20 |
| F.18 | Name | Date | TITLE: TOP PLATE 3 | |
| DRAWN | JAAANUS URB | 4.01.2021 | | |
| APPROV | ANDRES PERITŠENKO | 4.01.2021 | | |
| TALLINN UNIVERSITY OF TECHNOLOGY | | | SHEET 1:1 | DWG NR: SPM-3100 |

Bibliography

- [1] <https://ec.europa.eu>
- [2] <https://en.wikipedia.org>
- [3] <https://alphaunmannedsystems.com/a900>
- [4] <https://sciebel.net/support-form/>
- [5] <https://schibel.net/videos>
- [6] Christopher A. Brown. *Industry 4.0 for SMEs Challenges, Opportunities and Requirements - Chapter 13*. Palgrave Macmillan, 2020.
- [7] ASCE AB Ltd. 210200-1530-001-1D EESTI PIIRIVALVE PVL-101 STABILITY BOOKLET (Loading Manual) FOR SEA WATER DENSITY = 1.005 T/M³. *Norra Esplanadgatan 4, AX - 22100, Mariehamn, Finland*, 2012.
- [8] Rameswar Bhattacharya. *Dynamics of Marine Vehicles*. A Wiley-Interscience Publication; John Wiley Sons, 1978.
- [9] Xuechao, Duan; Yongzhi, Yang; Bi Cheng. Modeling and Analysis of a 2-DOF Spherical Parallel Manipulator. *Sensors*, 2016, 16, 1485, 2016.
- [10] Bristow babcock CHC NHV HCA UK Civil Aviation Authority. *Standard Measuring Equipment for Helideck Monitoring System (HMS) and Weather Data Rev 9b 2020 11 01*. HCA, UK CAA, Bristow Group, Babcock International, CHC, NHV, 2020.
- [11] Chein-Shan Liu Wun-Sin Jhao. The power series method for a long term solution of Duffing oscillator. *ISPACS Communications in Numerical Analysis*, Volume 2014(cna-00214):14, 2014.
- [12] Claude Archer; F,G, Daalen; S, Dobberschutz; M, Godeau; J, Grasman; M, Gunsing; M, Muskulus; A, Pischansky; M, Wakker. *Proceedings of the Sixty-Seventh European Study Group Mathematics with Industry*, chapter 1 "Dynamical Models of Extreme Rolling of Vessels in Head Waves". Ecole Royale Militaire, Belgium; MARIN, Wageningen, The Netherlands; Delft University of Technology, The Netherlands; Universitat Bremen, Germany; Wageningen University and Research Centre, The Netherlands; Leiden University, The Netherlands; Delft University of Technology, The Netherlands, 2009.
- [13] Bill Goodwine. *Engineering Differential Equations Theory and Applications*. Springer, 2011.

- [14] Harold V. Thurman. *Introductory Oceanography*. Wresterville, Ohio, 1988.
- [15] Hisham Moiden. Prediction of Parametric roll of Ships in regular and Irregular sea. Master's thesis, Texas AM University, 2010.
- [16] I.C.Clarc. *Ship Dynamics for Mariners*. The Nautical Insitute, 2004.
- [17] Intelligence, Strategy Policy, Safety Airspace Regulation Group. Standards for offshore helicopter landing areas published in CAP 437. Published by the Civil Aviation Authority, 2018.
- [18] INTERNATIONAL ORGANIZATION for STANDARDIZATION. Petroleum and natural gas industries - Specific requirements for Offshore structures - Part 3: topsides structure (EVS-EN ISO 19901-3:2014). EESTI STANDARD-IKESKUS, 2014.
- [19] Carolyn Q. Judge. USNA EN455 Seakeeping and Maneuvering - <https://www.usna.edu/NAOE/academics/en455.php>. USNA Course Catalog:, 2019.
- [20] Kirs, J. *Mehaanikaliste Susteemide Vonkumised*. TTU, 1998.
- [21] Edward V. Lewis, editor. *Principles of Naval Architecture Second Revision - Volume I * stability and strength*. The Society of Naval Architects and Marine Engineers, 1988.
- [22] Edward V. Lewis, editor. *Principles of Naval Architecture Second Revision - Volume III * Motions in Waves and Controllability*. The Society of Naval Architects and Marine Engineers, 1989.
- [23] Frank M. Lewis. The inertia of the water surrounding a vibrating ship. In *Webb Institute of Naval Architecture, New York, USA, 37th Meeting of The Society of Naval Architects and Marine Engineers, SNAME*, 1929.
- [24] Latifah NURAHMI. Conceptual Design and Analysis of 2 Degrees of Freedom Translational Manipulators. Master's thesis, Ecole Centrale de Nantes, 2012.
- [25] PAFA Consulting Engineers. Helideck structural requirements offshore technology report. techreport 072, UK Health and Safety Executive, 2001.
- [26] Wojciech Wawrzyński Przemysław Krata. Prediction of The Natural Frequency of Ship's Roll with Regard to Various Models of Roll Dapming. *Journal of KONES Powertrain and Transport, Vol. 23, No. 3*, 2016.
- [27] Nicholas C. Townsend and Ramanand A. Sheno. Gyrostabilizer Vehicular Technology. *Applied Mechanics Reviews*, 64(1), 09 2011. 010801.
- [28] Quanzhao Tu, Xiafu Peng, Jiehua Zhou, and Xunyu Zhong. Kinematics Simulation and Analysis of 2-DOF Parallel Manipulator with Highly Redundant Actuation. 2012.
- [29] K. J. Rawson; E. C. Tupper. *Basic Ship Theory Fifth edition Volume 2*, volume 2. Butterworth-Heinemann, 2001.

- [30] Waseem Ahmad Khan Stephane Caro Jorge Angeles Damiano Pasini. A Formulation of Complexity-Based rules for the Preliminary Design stage of robotic Architectures. *INTERNATIONAL CONFERENCE ON ENGINEERING DESIGN, ICEDâ07, 28 - 31 AUGUST 2007, CITE DES SCIENCES ET DE L'INDUSTRIE, PARIS, FRANCE, 2007.*
- [31] William E. Boyce Richard C. DiPrima. *Elementary Differential Equations and Boundary Value Problems.* Laurie Rosatone, 2012.
- [32] William J. Palm III. *System Dynamics - 2nd ed.* Raghathan Srinivasan McGraw-Hill, 2010.
- [33] Wojciech WawrzyÅski PrzemysÅaw Krata. Method for Ship's Rolling Period Prediction with regard to Non-Linearity of GZ curve. *Journal of Theoretical and Applied Mechanics* 54, 4, pp. 1329-1342, Warsaw, 2016.
- [34] Inga Zaitseva-Parnaste. *Wave Climate and its Decadal Changes in the Baltic Sea Derived from Visual Observation.* PhD thesis, Tallinn University of Technology, 2013.